國立臺灣大學生命科學院動物學研究所

博士論文

Graduate Institute of Zoology

College of Life Science

National Taiwan University

Doctoral Dissertation

大鼠視丘腹基核轉接神經元的

興奮性突觸傳導與可塑性

Excitatory Synaptic Transmission and Plasticity

of Relay Neurons in The Ventrobasal Nucleus of

Rat Thalamus

徐 經 倫

Ching-Lung Hsu

指導教授： 閔 明 源 博士

Ming-Yuan Min, Ph.D.

中華民國100年7月

July, 2011

國立臺灣大學（碩）博士學位論文
口試委員會審定書

大鼠視丘腹基核轉接神經元的
興奮性突觸傳導與可塑性

Excitatory Synaptic Transmission And Plasticity of Relay Neurons in The Ventrobasal Nucleus of Rat Thalamus

本論文係徐經倫君（F95B41015）在國立臺灣大學動物學研究所完成之博士學位論文，於民國一百年六月二十九日承下列考試委員審查通過及口試及格，特此證明

口試委員：

_____（簽名）

（指導教授）

_____

_____

_____

_____

動物學研究所所長 _____（簽名）

誌　　　謝

　　從第一步踏進台大動物系那一天起，到拿到台大動物所博士為止，對我來說是一段難以言喻的奇妙旅程。台大動物系(今生科系)是孕育我、啟蒙我的地方，對我有再造之恩，對於所有與這個系有關的人、事、物，我都有無盡的感謝。我本來就不是一個很聰明的人，看到的世界越大，越感覺到自己的矮小。我只是憑著一個對科學的夢想和與收獲不成比例的努力，撐到今天。在這條路上無怨無悔扶持著我的人們，才是我生命中的全部意義。

　　我首先要感謝我的指導教授閔明源老師。閔老師可以說是我學術起點的一切。因老師的博學、付出與包容，我才得以一窺細胞神經生理學的美麗與堂奧。老師總是為學生設想，在我迷途的時候與我分享，在我徬徨的時候指點我最好的路，我在博士結束後可以立刻銜接西北大學的博士後研究工作，也是靠老師多方的指點與支持。我永遠難以忘懷老師親手帶著我吸破第一個細胞的那個下午，也難忘老師在晚上十點實驗室讀書會結束後，站在白板前，愉快地與我們分享從前在英國的研究經驗與奇妙的神經電纜理論(cable theory)。老師對我的恩情太深，一句謝謝實在顯得微不足道。

　　我要感謝台大動物所嚴震東老師。嚴老師是我心目中的學者典範，溫文中充滿了思想的睿智。如果沒有老師在視丘腦切片研發上的幫助，沒有老師所發起、既深且廣的《視丘》(〈The Thalamus〉)讀書會，我絕不能走到今天。我要感謝陽明神研所連正章老師。老師的視野、博學與氣度，是我在學術領域的一盞明燈，也在生涯規劃的十字路口上，給了我重要的助力。我要感謝台大生理所湯志永老師。老師開的突觸生理學是我在醫學院修課最美好的回憶之一。我要感謝中山醫學大學生醫系楊琇雯老師。老師對我們在實驗技術細節上的要求讓我養成了嚴謹的態度，到了國外，我更感受到其中的可貴。我要感謝台大動物所陳瑞芬老師。老師總像家人一樣地溫暖，老師的動物學教學實習對我有很大的啟發。

　　我要特別感謝自我進入動物系開始，擔任我的導師前後長達十年的台大動物

中文摘要

大鼠視丘腹基核轉接神經元的興奮性突觸傳導與可塑性

　　視丘腹基核(Thalamic ventrobasal nucleus)是體感覺訊息由脊髓上行之內側蹄系路徑(medial lemniscal pathway, ML pathway)傳往大腦皮質的主要轉運站，同時也接受皮質-視丘路徑(corticothalamic pathway, CT pathway)的皮質回饋。儘管這是一個感覺與知覺生理學中樞處理研究中的重要模式系統，許多興奮性突觸傳導與可塑性的基本性質卻付之闕如。此外，視丘轉接神經元(relay neuron)會依據生理條件的不同，放射不同模式的動作電位，在現象上，平行於視丘-皮質系統依據個體意識狀態的不同，呈現出不同的計算特性。動作電位模式的二元性一直被猜測是這種系統狀態相關(state-dependent)的感覺訊息處理的細胞學基礎，但是在突觸與細胞生理層次，不同的神經元活化模式對於其突觸強度動態調節的了解仍然非常不足。

　　本研究採用標準的全細胞膜片箝制記錄(whole-cell patch-clamp recording)與細胞組織化學呈色法，以系統性的方法與比較性的觀點探討腹基核皮質(CT)與感覺(蹄系)(ML)突觸的突觸傳導與可塑性。皮質與感覺突觸在興奮性突觸後電流(EPSC)大小對電刺激強度的關係與短期可塑性(short-term plasticity)上相當不同：皮質 ESPC 表現出線性的輸入-輸出關係，其強度在成對的高頻率刺激時增強(paired-pulse facilitation)；感覺 EPSC 則表現出全有全無(all-or-none)的輸入-輸出關係，其強度在成對高頻率刺激時則衰減(paired-pulse depression)。更有趣的是，離子通道型麩氨酸受體(ionotropic glutamate receptor)的組成有很大的不同。皮質路徑的 NMDA 受體電流與非 NMDA 受體電流的比值較高，同時也選擇性地表現透鈣性 AMPA 受體(CaP-AMPAR)。許多研究顯示，這些受體的活化在

長期突觸可塑性的引發(induction)與表現(expression)上扮演重要的角色，促使我們進一步比較突觸可塑性在這兩個路徑上的不同。皮質突觸可以表現依賴 NMDA 受體的長期增益(long-term potentiation, LTP)以及依賴 L 型電壓閘控鈣離子通道(L-type voltage-gated calcium channel)的長期衰減(long-term depression, LTD)；相對而言，同樣的實驗條件無法在感覺突觸誘發長期可塑性的表現。在不同的實驗誘發條件同時被滿足的情況下，皮質突觸的連結強度則能對多重興奮性活動進行整合性的回應。我們接著嘗試運用實驗與雜訊分析(noise analysis)技術探討離子通道型麩氨酸受體在皮質突觸長期可塑性中扮演的角色。我們發現，NMDA 受體與透鈣性 AMPA 受體皆未參與皮質突觸長期衰減的引發與表現。我們的證據更進一步顯示其表現機制主要牽涉突觸前機制的變化。

為了對突觸可塑性引發的生理條件有更深刻的了解，我們測試了數種不同的神經元放電(spiking)與配對(pairing)模式對突觸連結強度的影響。我們發現轉接神經元連續型的動作電位放電(continuous spiking)能夠誘發皮質突觸依賴於 L 型鈣離子通道的長期突觸衰減，但高頻率爆炸式的動作電位放電(burst spiking)則無法誘發其可塑性。儘管如此，若以特定時序(時間差)對突觸前輸入與突觸後神經元進行重覆性、低頻率的配對活化，爆炸式的放電模式則能誘發皮質突觸的長期增益，且該現象依賴於低閾值電位(low threshold potential)的存在，顯示 T 型電壓閘控鈣離子通道(T-type voltage-gated calcium channel)對於此種可塑性的重要性。

根據上述發現，我提出了一個視丘訊息處理與傳遞的動態模型，並據此提出可驗證的假設與值得繼續研究的方向。縱觀而言，本研究詳細探討了視丘轉接神經元上感覺與皮質突觸的基本差異，並指出皮質突觸連結強度有強烈的傾向回應不同的經驗而產生相應的變化，此種變化可能是個體調節視丘感覺訊息處理的生

理與細胞學基礎。這些基礎知識在我們對於活體感覺訊息處理時,視丘-大腦皮質交互作用的深入理解與其相關的應用上是不可或缺的。

關鍵詞:皮質-視丘突觸、T 型鈣離子通道、NMDA 受體、透鈣性 AMPA 受體、長期突觸增益、長期突觸衰減、L 型鈣離子通道

Abstract

Thalamus is regarded as the gateway for sensory information relay from periphery to higher cortical areas, and has been suggested to play pivotal roles in state-dependent information processing and several different types of neurological disorders. Relay neurons in the ventrobasal nucleus (VBN) of the thalamus transmit somatosensory information to the cerebral cortex and receive sensory and cortical (feedback) synaptic inputs via, respectively, medial lemniscal (ML) and corticothalamic (CT) fibres. Despite an invaluable model for studying central processes of sensation and perception, this system has not been well characterized in terms of basic details of the excitatory synaptic transmission and plasticity. With more functional relevance, changes of the synaptic transmission, especially in response to physiological patterned activities, have critical implications for the computation of the thalamo-cortico-thalamic network, but this aspect is rarely studied. For example, the duality of spiking modes, burst and continuous, was thought to underlie state dependence of thalamic information transfer, but the impact of different firing patterns on synaptic weight is not explored.

Our work applies standard whole-cell patch-clamp electrophysiology and cellular histochemistry to study the fast excitatory synaptic transmission and plasticity of relay neurons in the ventrobasal nucleus of rat thalamus in a systematic and comparative manner. CT and ML synapses had distinct properties in terms of stimulus-response

relationships and short-term plasticity: CT excitatory postsynaptic current (EPSC) had linear input-output relationship and paired-pulse facilitation, while ML EPSC all-or-none and paired-pulse depression. More interestingly, the compositions of ionotropic glutamate receptors differed. CT synapses showed higher NMDAR / non-NMDAR peak current ratio than ML synapses, and preferentially expressed calcium-permeable AMPA receptors (CaP-AMPARs). Activation of these receptors has been widely implicated in the induction and / or expression of synaptic plasticity, which motivated the comparison of synaptic plasticity between these two synapses. NMDAR-dependent long-term potentiation (LTP) and L-type voltage-gated calcium channel(VGCC)-dependent long-term depression (LTD) were readily induced at CT synapses, but not ML synapses, under the induction protocols tested. In addition, CT synaptic strength could be modulated in response to pre- and postsynaptic activities in an integrative manner while multiple induction conditions were met concurrently. Efforts were then made to elucidate the role of ionotropic glutamate receptors in long-term plasticity of CT synapses by experimental and analytical approaches. We found that activation of CaP-AMPARs and NMDARs contributed to neither induction nor expression of LTD at CT synapses, and evidence further suggested that the expression of LTD mainly involves presynaptic modification.

In order to get insights into the physiological conditions for induction of synaptic

plasticity, several protocols involving different spiking and pairing patterns were tested under current-clamp recording. Intriguingly, LTD was induced at CT synapses in response to repetitive continuous spiking, rather than burst spiking, of VBN relay neuron. Furthermore, we showed that LTP at CT synapses could be induced by repetitive, low-frequency pairing of CT EPSP with burst spiking of relay neuron, but not by pairing of CT EPSP with high-frequency spiking (without LTS) which mimicked the fast Na^+ action potentials riding on the LTS of natural burst spiking, suggesting a critical role of T-type VGCCs in the induction of STDP at CT synapses.

In light of our discovery, I propose a working model of dynamic thalamic information relay, and generate testable ideas for future research. Taken together, this study unveils the fundamental functional differences between sensory and cortical inputs onto thalamic relay neurons, and shows that the strength of corticothalamic pathway is preferentially subjected to use-dependent modifications, which can be a cellular substrate for dynamic regulation of thalamic information relay, and therefore instrumental to our in-depth interpretation and understanding of the ongoing *in-vivo* sensory processes within the thalamocortical system at synaptic and cellular levels.

Keywords: corticothalamic synapse, T-type calcium channel, NMDA receptor, calcium-permeable AMPA receptor, long-term potentiation, long-term depression, L-type calcium channel

Contents

Chapter 1　　Introduction

Chapter 2　　Properties of fast excitatory synaptic transmissions of relay

neurons in the ventrobasal nucleus of rat thalamus

Chapter 3   Differential induction of synaptic plasticity between

corticothalamic and medial lemniscal synapses

Chapter 4   The role of ionotropic glutamate receptors in long-term plasticity

of corticothalamic synapses

List of Figures

List of Tables

Chapter 1

Introduction

A. Ventrobasal nucleus (VBN) of thalamus and somatosensory system

a1. Thalamus: a major gateway of sensory information

Thalamus has been viewed as a major gateway of sensory information from periphery to higher cortical areas (Jones, 2007; Sherman and Guillery, 2004). Based on previous physiological and anatomical literature, the sensory information of vision, audition, gustation, olfaction, touch, pressure, pain, temperature perception, and proprioception is transmitted to higher cortex through it (Sherman and Guillery, 2004; Bear et al., 2001). Historically, it was suggested that thalamus play its major role as a passive relay in the mammalian central nervous system, and the principal neurons of thalamus are referred to as relay neurons (Jones, 2007; Sherman and Guillery, 2004), although many lines of evidence have emphasized the active role of thalamus in information transfer, indicating that thalamus is more than a simple relay station of sensory signals (Briggs and Usrey, 2008; Nicolelis, 2005; Nicolelis and Fanselow, 2002;

Jones, 2007). Sensation and perception are of indispensible importance to survival of animals, and the detailed anatomical, physiological, biochemical and biophysical knowledge of thalamus is crucial to our in-depth understanding of its operational and functional principles in various physiological and pathological states.

a2. VBN as the first-order relay of somatosensory information of rodents

VBN is one of the most clearly defined nuclei of thalamus because of its large size and lobulated appearance, which is imposed on it by penetrating bundles of myelinated fibers (Jones, 2007). Cytoarchitectonically, the division of ventral posterior medial nucleus (VPM) and ventral posterior lateral nucleus (VPL) is very distinct; VPM tends to be composed of relatively closely packed cells, whereas VPL cells usually arranged in clusters (Jones, 2007) (Fig. 1.1).

The terms ventral posterolateral / ventral posteromedial nuclei, and ventrobasal complex were first introduced by Clark (1930) and Rose (1935), respectively (Jones, 2007). In addition to VPL and VPM, two additional zones of smaller cells distinguished by weak cytochrome oxidase (CO) staining can be identified in primates (Jones, 2007). One is characterized by closely-packed small- and medium-sized neurons, which

represents the thalamic termini for taste and other visceral afferents and can be quite

distinct and relatively large in rodents, termed parvocellular part of ventral posterior

nucleus (VPPC; Paxinos and Watson, 2007) or basal ventral medial nucleus (VMb;

Jones, 2007). The other subnucleus dominated by neuroglial cells but containing many

small neurons as well, which is traversed by medial lemniscus (*ml*) as it enters the

thalamus, called ventral posterior inferior nucleus (VPI), is commonly not separately

identified in rodents (Jones, 2007; Paxinos and Watson, 2007). In this study, we used the

term "VBN" simply referring to VPL and VPM, but not VPPC (VMb).

Besides transmitting gustatory information from central taste pathway (VPM),

VBN is well-established to play vital roles for relaying somatosensory information in a

somatotopically-organized manner. Dorsal column-medial lemniscal pathway and

trigeminal nerve pathway transmit touch, vibration, two-point discrimination, and

proprioception information upwards via VBN. Spinothalamic pathway and trigeminal

pathway also send pain, temperature, and some touch signals via VBN (Bear et al.,

2001). Vibrissal information is one of the most important survival cues for rodents. The

ascending trigeminal system of rodents contains clear structural representations of the

whisker pads in the brainstem ("barrelettes") (Ma and Woolsey, 1984), thalamus

("barreloids" of VPM) (Haidarliu and Ahissar, 2001; Land et al., 1995; Van der Loos,

1976), and cortex ("barrels") (Woolsey and Van der Loos, 1970). Because of this morphologically demonstrable arrangement, the vibrissal system of rodents has become one of the most valuable models in sensory physiology (Deschênes, 2009).

The medial lemniscus, at its entry into the thalamus, consists of fibers arising from the contralateral dorsal column nuclei (and some of their satellite nuclei) (Fig. 1.2), trigeminal nuclei, and lateral cervical nuclei of spinal cord (reviewed by Jones, 2007). These terminals end on the proximal portions of the dendrites of relay cells. These afferent connections are summarized as follows: (1) Among the dorsal column system, the cuneate and gracile nuclei project to the contralateral VPL. (2) The trigeminothalamic inputs to VPM arise from the principal (PrV) and spinal trigeminal (SpV) nuclei of the contralateral side. The PrV and all the subdivisions of SpV contribute axons to the trigenimothalamic tract. (3) The lateral cervical nucleus of the spinal cord, after a period of uncertainty, is now thought to be represented in most mammals. Fibers from lateral cervical nucleus ascend to contralateral VPL and certain other thalamic nuclei. In VPL, they have been described in physiological studies to project to the "deep shell" region (see below) in monkeys, cats, and possibly in rats, but this point is controversial (Jones, 2007). Neurons in the lateral cervical nucleus respond to movement of hairs, to pressure or pinch, including noxious pinch, and have large

4

receptive fields on the limbs.

Spinothalamic afferents arising from both sides of spinal cord, with a contralateral preponderance, terminate in VPL (Fig. 1.2). Spinal trigeminothalamic projections arise mainly from the contralateral caudal subnucleus of the SpV (SpVc), although there are also contributions from the oral subnucleus (SpVo) in rats and especially from the interpolar subnucleus (SpVi) (Pierret et al., 2000; reviewed by Jones, 2007). The fibers leaving the SpV ascend with the spinothalamic tract. For spinothalamic and spinal trigeminothalamic fibers in cats, it is shown thin preterminal branches that lack the concentrated large boutons typical of lemniscal fibers; for the relay neurons of rat VBN, Ma et al. (1987) also showed that lemniscal terminals frequently contact somata and dendrites more proximally than spinothalamic projections (but see Lavallée et al., 2005, which showed that SpVir axons make large synaptic contacts with the proximal dendrites of relay neurons in the dorsomedial aspect of VPM). These may indicate the existence of some basic differences between lemniscal and spinothalamic / spinal trigeminothalamic systems.

By the mid-1990s, only two central pathways of vibrissal information processing in rodents are known: *lemniscal pathway*, which transmits signals from PrV to layer IV

of barrel cortex (primary somatosensory cortex, S1) via VPM, and *paralemniscal pathway*, whose origin was uncertain (now it is known as the multiwhisker cells in SpVir; Williams et al., 1994), which transmits signals to cortical regions surrounding the barrels through the whisker responsive part of posterior complex (posterior thalamic nuclear group; POm) (Deschênes, 2009; the nomenclature POm used here is, in reality, incorrect, since the "whisker responsive part" also includes the most lateral portion of posterior complex; the usage of this term in this paragraph is following the terminology of Deschênes, 2009). Since then, combined tracing and electrophysiological approaches have revealed two additional pathways (Fig. 1.3). It was shown that relay neurons of rat VPM have further target-specific segregation, namely the "core" (dorsal medial division of VPM, VPMdm) and "tail" (ventral lateral division of VPM, VPMdl) compartments of the barreloids, the former of which receive monowhisker input from PrV and project to single barrel column of S1 (i.e. *lemniscal pathway*), and the latter of which receive multiwhisker input from SpVi (SpVic according to Deschênes, 2009) and project to dysgranular zones of primary (S1) and secondary (S2) somatosensory cortices (i.e. *extralemniscal pathway*) (Pierret et al., 2000). Furthermore, the lemniscal pathway can be divided into two subdivisions, as additional "head" (VPMh) and "core" (VPMc) sub-compartments can be distinguished in the barreloids within VPMdm (Fig. 1.3), which features neurons with large multiwhisker and small monowhisker receptive fields,

6

respectively (Veinante and Deschênes, 1999). It has been proposed that the lemniscal and extralemniscal pathways transiting via core and tail of rat VPM respectively, and the paralemniscal pathway transiting through POm, altogether constitute the parallel thalamic streams for processing the "what" (object identity), "where" (object location), and whisking signals, all of which are important for object identification using active-touch information (Yu et al., 2006).

a3. Synaptic organization of VBN

Primary sensory information is transmitted to cerebral cortex through thalamus, which also receives reciprocal feedback from cortex. It is widely accepted that CT synapses outnumber the subcortical terminations on relay neurons, although Jones (2007) argued that the quantitative estimation of an order of magnitude more by Sherman and Koch (1986) was erroneous. In the lateral geniculate nucleus (LGN; the visual thalamus), it was estimated that sensory inputs account for 10% of synapses onto TC relay neurons, whereas cortical inputs account for more than 50% (Erisir et al., 1997; Latawiec et al., 2000).

Getting insights from the synaptic organization of LGN, Sherman proposed the concept that thalamic afferents can be divided into two categories, namely driver and modulator, which also applies to VBN (Sherman, 2005). Lemniscal input belong to driver, which forms large, glomerular presynaptic elements contacting proximal dendrites of VBN relay neurons (Špacek and Lieberman, 1974), providing powerful synaptic drive as well as major receptive properties to them. On the other hand, non-lemniscal inputs, such as the corticothalamic fibers from cortical layer VI, belonging to modulator, which can contact widespread over on the dendritic arbors and affect properties of neuronal receptive field only subtly. In Sherman's proposition, drivers provide major information streams, whereas modulators play modulatory roles for information relay.
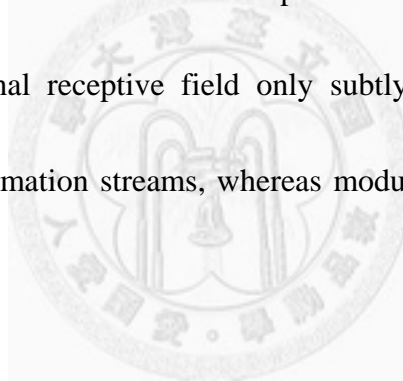
As an extension of the driver / modulator concept, it was further suggested that corticothalamic feedbacks can also fall into either category based on the morphological and electrophysiological characteristics, and, according to the types of corticothalamic connections received, thalamic nuclei can be classified as first-order or higher-order relay (Llano and Sherman, 2009; Reichova and Sherman, 2004; Sherman, 2005; Van Horn and Sherman, 2004). Two types of corticothalamic cells, with distinct electrophysiological properties and local network connectivity (Llano and Sherman,

2009), give projections from S1 to thalamus: it was previously shown that the upper and lower portions of layer VI cells send projection to VBN and POm, respectively (Bourassa et al., 1995), while CT axons originating in layer V cells only project to POm. The thin axons arising from layer VI neurons, the modulator, terminate in small boutons on distal dendrites of relay neurons; the fibers arising from layer V neurons, the driver, form giant synaptic boutons on proximal dendrites (Hoogland et al., 1987; Jones, 2007). The view of differential projection of large terminals between POm and VBN has been, however, recently modified, because of the discovery of large terminal-projected zones within the caudal and surrounding "shell" regions of VBN in rats and mice (Liao et al., 2010).

As a corollary inferred from the correlation of presynaptic morphology and information modality being transmitted in the primary sensory thalamic nuclei, driver CT feedbacks are considered feedforward and responsible for transmitting sensory-related information, whereas modulator CT feedbacks are suggested to serve to modulate this process. All thalamic nuclei receive input from cortical layer VI, but only those also receive layer V projections are termed higher-order relay, since they therefore retain the major sensory signals coming from previous thalamo-cortical transmission to relay further; on the contrary, those receive only layer VI inputs are first-order relay. In

view of the fact that the particular subzones of VBN are also innervated by large terminals, Liao et al. (2010) proposed that VBN may simultaneously coordinate first- and higher-order relays and therefore play multiple roles in the thalamocortical relay function.

Despite being composed of a single type of principle neuron, VBN still have functional and anatomical segregations. In cats, monkeys, and humans, it is the "deep shell" and "cutaneous core" which form modality-specific compartmentalization within VPL (Jones, 2007). In these compartments, neurons are clustered according to their peripheral principal inputs, i.e. sensory receptors in the skin or in deep tissues such as muscles and joints. The neurons of the anterodorsal "deep shell" respond to movements of joints, stretching of tendons, and manipulation of muscle bellies; the most are, in fact, driven by discharges of primary afferent fibers innervating muscle spindles. This functional segregation actually reflects the differential spatial distributions of lemniscal fiber terminals arising from different subdivisions of dorsal column nuclei and lateral cervical nucleus.

Lemniscal and spinothalamic pathways engage neurons located in separate compartments of VBN, although they are grossly converging (for rats, see Peschanski

and Besson, 1986). The evidence is most convincing in monkeys (Jones, 2007): anterograde labeling studies show that the parvalbumin-positive, cytochrome oxidase (CO)-rich "core" is dominated by terminations of dorsal column-medial lemniscus (in VPL) or principal trigeminal afferents (the rod-like structures in VPM), whereas the calbindin-positive, CO-weak "matrix" is dominated by terminations of spinothalamic afferents (the isolated patches within VPL) or spinal trigeminothalamic afferents (between and outside the rod-like structures within VPM). The matrix forms a strip along the medial border of VPM, intervenes between the rod-like structures, aggregates into islands within VPL, and extands to VMb and VPI even further beyond into adjacent nuclei. These two compartments have their cortical lamina-specific thalamocortical projections: the matrix projects diffusively to the superficial layers, while the core projects to the middle layers of somatosensory cortex. For rats, the principle of calcium binding proteins -- histochemical compartments of calcium binding proteins correspond to those of different projecting classes of relay neurons -- cannot apply well; nevertheless, the lamina-specific segregation of relay neurons in the somatosensory thalamus still exists (Rubio-Garrido et al., 2007). It is noteworthy that, Diamond (1995) suggested POm correspond to the "matrix" of the trigeminal somatosensory thalamus in rodents, whose projecting terminations are distributed throughout layers I – VI in the perigranular areas between the granular islands and barrels of somatosensory

cortex.

a4. Thalamic firing modes and state-dependent information relay

Since the first intracellular recording of mammalian thalamic neurons was obtained (Deschênes et al., 1982; Llinás and Jahnsen, 1982), electrophysiologists have been obsessed with their striking spiking properties for decades: relay neurons fire in continuous (tonic / regular) mode at relatively depolarized membrane potential (V_m), while in burst mode at relatively hyperpolarized V_m (Bal and McCormick, 1993; Jahnsen and Llinás, 1984a) (Fig. 1.4). This duality originates from the voltage-dependent inactivation property of T-type voltage-gated calcium channels (VGCCs) (Suzuki and Rogawski, 1989) in that the steady-state half-inactivation potential is very hyperpolarized (~ -96.8 mV for the relay neurons of rat VBN) (Kuo and Yang, 2001). At hyperpolarized V_m, low threshold spike (LTS) is triggered upon activation of T-type VGCCs, which drives high-frequency bursts of Na^+ action potential firing; on the contrary, T-type VGCCs are inactivated at depolarized V_m, and the action potentials fire in a continuous fashion instead (Bal and McCormick, 1993; Jahnsen and Llinás, 1984b; Luthi and McCormick 1998a, 1998b; Sherman, 2001; Suzuki and

12

Rogawski, 1989). Recent findings (most of them were performed in cats) indicated the firing repertoire of thalamic relay neurons can be even richer than previously recognized (Fig. 1.4B): in addition to the continuous firing and classical LTS-burst firing (which contributes to the sleep spindles and delta oscillation), relay neurons can express slow oscillation (contingent on the opening of a small fraction of non-inactivating T-type VGCCs) and high-threshold burst (HTB) (which contributes to sleep theta rhythm and is contingent on activation of putative dendritic T-type VGCCs), both of which are revealed upon the activation of type 1a metabotropic glutamate receptors (mGluR1a) (note: VBN relay cells may not have HTB mode) (Hughes et al., 2002; Zhu et al., 2006).

Historically, the state-dependent firing properties of thalamic relay neurons have facilitated the conceptual linkage between firing mode and thalamic relay function, especially when researchers considered the flexibility of central sensory processes dictated by global conscious states. Continuous spiking mode is typically observed in the thalamus of awake and vigilant animals, while rhythmic burst spiking is mostly associated with inattentive, drowsy, anesthetized states or slow-wave sleep, which prompted the suggestion that, in the burst mode, thalamus is functionally disconnected from its afferent input (Jones, 2007; Le Masson et al., 2002; Livingstone and Hubel,

1981; McCormick and Bal, 1997; McCormick and Feeser, 1990; Steriade and Llinas, 1988); emerging evidence has, however, indicated that bursting also occurs in awake animals and can serve as a powerful mode of thalamocortical information transfer (Crick, 1984; Fanselow et al., 2001; Guido et al., 1992; Guido et al., 1995; Guido and Weyand, 1995; Lu et al., 1992; Mukherjee and Kaplan, 1995; Ramcharan et al., 2000; Reinagel et al., 1999; Swadlow and Gusev, 2001; Weyand et al., 2001).

Recent studies have indicated that, from the recordings of slightly anaesthetized or even awake animals, one can still observe un-synchronous burst firing without pacemaking activities in thalamic relay neurons. Under this condition, relay neurons are responsive to sensory inputs, and probably encode information in terms of burst spiking (Fanselow et al., 2001; Nicolelis and Fanselow, 2002; Sherman, 2001; theoretical study see Babadi, 2005). Moreover, Fanselow (2001) et al. proposed that during the twitching of rat whiskers, a descending signal from S1 triggers thalamic bursting that primes the thalamocortical loop for enhanced signal detection. Therefore, at least three different responsive states (continuous, rhythmic burst spiking, and unsynchronous burst firing) can be distinguished for the operation of thalamic relay neurons, probably corresponding to different brain-mind conditions for information processing.

Burst activities are also intrinsic to many other systems such as hippocampal pyramidal neurons (O'Keefe and Recce, 1993; Ranck, 1973) and neocortical pyramidal neurons (Connors et al., 1982; Llinás, 1988; McCormick et al., 1985; Williams and Stuart, 1999), which is often considered as a qualitatively distinct signaling unit with a great variety of functional impacts, such as providing higher reliability of synaptic activation, enhancing stimulus detectability (Babadi, 2005; Beierlein et al., 2002; Fanselow et al., 2001; Guido et al., 1995; Guido and Weyand, 1995; Lisman, 1997; Sherman, 2001; Swadlow and Gusev, 2001; Williams and Stuart, 1999), induction of synaptic plasticity, reorganization of cortical circuits, synaptic downscaling, memory consolidation, and gene expression (Birtoli and Ulrich, 2004; Clark and Normann, 2008; Fields et al., 1997; Frank et al., 2001; Lanté et al., 2011; Paulsen and Sejnowski, 2000; Pick et al., 1999; Remy and Spruston, 2007; Steriade, 2006; Thomas et al., 1998), to name a few.

It has been widely appreciated that conscious states can significantly influence the processes of sensation and perception. Descending corticothalamic input is considered to be an essential determinant for the gating of thalamic information relay (Destexhe, 2000; Jones, 2007; Sherman, 2005; Steriade and Paré, 2007). Neuromadulators are also proposed to dominate the transition of thalamic operation modes between different

15

conscious states, one of the potential mechanisms for which is by switching the spiking

modes of relay neurons via modulation of membrane potential (Castro-Alamancos,

2002; Castro-Alamancos and Calcagnotto, 2001; Steriade et al., 1990; Steriade and Paré,

2007).

B. Excitatory fast synaptic transmission and homosynaptic long-term plasticity

b1. Ionotropic non-NMDA glutamate receptors and calcium permeability

Three families of mammalian ionotropic glutamate receptors, the AMPA (GluR1-4

or A-D), kainate (GluR5-7, KAR1-2), and NMDA (NR1, NR2A-D), have been

identified, based on their primary sequences, biophysical and pharmacological

characteristics (Wisden and Seeburg, 1993). Of these, AMPA receptors mediate the

majority of fast excitatory transmission in the CNS (Cull-Candy et al., 2006). Their

functional properties are dictated by subunit composition and auxiliary proteins

(Hollmann et al., 1991; Hume et al., 1991). The mRNA encoding each subunit is also

subject to post-transcriptional modification, in the form of alternative splicing or RNA

editing. For example, alternative splicing generates "flip" and "flop" slice variants for

each of the GluR1-4 subunits, with distinct desensitization kinetics (Blakemore and

Trombley, 2003).

Transcripts of AMPA and kainite receptor subunits, each of which contains an

RNA editing site in an axon encoding part of the pore-lining (M2) region, have been

shown to undergo oxidative deamination of adenosine to inosine at this site (Sommer et

al., 1991). It causes the substitution of an arginine (R) for glutamine (Q) residue in the

GluR2, GluR5 and GluR6 subunits, which leads to profound functional influences,

including calcium permeability, rectification, sensitivity to external polyamines, single

channel conductance, receptor assembly and trafficking (Cull-Candy et al., 2006; Hume

et al., 1991; Washburn et al.,1997). For GluR2 and GluR5, the extent of editing is also

found to be regulated in a tissue and developmentally specific pattern, implying a

general regulatory mechanism for the function of non-NMDARs (Bowie and Mayer,

1995).

The AMPA receptors that lack GluR2 subunits are permeable to calcium ions (Iino

et al., 1990), exhibit a high single-channel conductance, are blocked by endogenous

(intracellular) polyamines in a voltage-dependent manner, giving rise to an

inward-rectifying current-voltage (I-V) relationship (Cull-Candy et al., 2006), and show

use-dependent relief from polyamine block (Rozov and Burnashev, 1999), providing

activity-dependent short-term modulation of receptor efficacy (McBain, 1998). In the

model accounting for the dependence of calcium permeability and rectification

properties on GluR2, Washburn et al. (1997) proposed that, incorporaton of arginines

into the Q/R site replaces the negatively charged ring of carbonyl oxygens of glutamines

by the positively charged guanidinium groups, which also neutralizes the negatively

charged carboxyl groups of aspartates near the cytoplasmic mouth of the channel by

formation of a salt bridge, Because the carbonyl oxygens of glutamines and carboxyl

groups of aspartates contribute to or form a binding site for calcium ion and polyamine,

incorporation of GluR2 would confer the calcium impermeability and linear I-V

relationship to AMPA receptors; on the other hand, GluR2-lacking AMPA receptors are

calcium-permeable and inward-rectifying.

Although the majority of AMPA receptors in CNS are GluR2-containing,

calcium-impermeable, significant expression of calcium-permeable AMPA receptors

(CaP-AMPARs) is found in subpopulation of hippocampal interneurons (Iino et al.,

1990), hippocampal CA3 pyramidal neurons (Ho et al., 2007), neocortical interneurons

(Rozov and Burnashev, 1999), cerebellar granule cells (Kamboj et al., 1995), cerebellar

stellate cells (Liu and Cull-Candy, 2000), olfactory bulb neurons (Blakemore et al.,

2006; Ma and Lowe, 2007), dopamine neurons of ventral tegmental area (VTA) (Bellone and Lüscher, 2005), and Bergmann glial cells (Burnashev et al., 1992). Native calcium-permeable kainate receptors are less well characterized, but strong inwardly rectifying responses characteristic of the unedited form of GluR6 have been described in embryonic hippocampal neurons and glial progenitor cells (Lerma et al., 1993).

CaP-AMPARs have been proposed to play a great variety of roles in normal physiological functions or neuropathology, such as precise control of spike timing (Geiger et al., 1995; Geiger et al., 1997; Lawrence et al., 2004; Walker et al., 2002), induction / expression / consolidation / maintenance of activity-dependent, homeostatic, or drug-induced long-term synaptic plasticity, learning and fear memory erasure (Asrar et al., 2009; Bellone and Lüscher, 2005; Bellone and Lüscher, 2006; Clem and Barth, 2006; Clem and Huganir, 2010; Derkach et al., 1999; Desai et al., 2002; Goel et al., 2006; Guire et al., 2008; Ju et al. 2004; Kakegawa et al., 2004; Laezza et al., 1999; Liu and Cull-Candy, 2000; Manhanty and Sah, 1998; Mameli et al., 2007; Oh and Derkach, 2005; Pelkey et al., 2005; Plant et al., 2006; Sutton et al., 2006; Thiagarajan et al., 2005; Toth et al., 2000; Watt et al., 2000; Wiltgen et al., 2010), a postsynaptic form of short-term plasticity (Bowie et al., 1998; McBain, 1998; Rozov et al., 1998; Rozov and Burnashev, 1999), neurodevelopment (Ho et al., 2007; Kumar et al., 2002; Monyer et al.,

1991; Shin et al., 2005; Smith et al., 1999; Smith et al., 2000; Whitney et al., 2008; Wisden and Seeburg, 1993), and activity- and pathophysiology-dependent synaptic modulation through the regulation of endogenous polyamines (Aizenman et al., 2002; Aizenman et al., 2003; Hayashi et al., 1993; Shin et al., 2005). Therefore, the physiological significance of CaP-AMPARs is more profound and widespread in the native CNS.

b2. The discovery of homosynaptic LTP and LTD

Synaptic plasticity is usually defined as the upregulation or downregulation of synaptic efficacy (Martin and Morris, 2002). In 1940s, Canadian psychologist Donald Hebb first laid down the theoretical foundation of learning in neural systems by articulating the potential mechanisms of synaptic plasticity. In his pioneering book, 《The Organization of Behavior》 (1949), it was proposed that increments in synaptic efficacy occur during learning when firing of one neuron repeatedly or persistently produces firing in another neuron to which it connects. That is, temporal correlation (or association) of pre- and postsynaptic activities induces structural and / or chemical (metabolic) processes, subsequently eliciting the strengthening of synaptic connections.

This is well-known as a principle in the form of "neurons that fire together wire together" (Bear et al., 2001; Maren and Baudry, 1995). In 1973, Tim Bliss and Terje Lømo successfully demonstrated the existence of such a phenomenon at synaptic level. In the experiments on the dentate gyrus of anesthetized rabbits, they showed that brief tetanic (high-frequency) stimulation of perforant-path axons produced an increase in the amplitude of field excitatory synaptic potentials that last for hours, or even for days, which was termed long-term potentiation (LTP). Since then, a huge body of knowledge has burgeoned regarding the induction conditions and properties of long-term synaptic plasticity. In 1977, Lynch, Dunwiddie, and Gribkoff reported a seemingly inverse version of LTP — long-term depression (LTD) — at the synapses of Schaffer collateral input to CA1 pyramidal neurons in hippocampus. Cerebellar LTD was then identified by Masao Ito et al. in 1982, which immediately received extensive attention because of its rich implications on motor learning. Studying the requirement for temporal specificity in associative synaptic plasticity of dentate gyrus, Levy and Steward (1983) discovered the temporal order of pre- and postsynaptic spiking is crucial to the induction of long-term synaptic modification. In cortical pyramidal neurons of rats, Markram et al. (1997) further elegantly demonstrated that precise temporal structure of pre- and postsynaptic activation is an important determinant for the sign (potentiation or depression) of synaptic plasticity. Bell et al. (1997) also found that induction of synaptic

21

plasticity is dependent on the timing for pairing EPSP with dendritic Na$^+$ spike in the electrosensory lobe of mormyrid electric fish. This is now referred to as spike-timing-dependent plasticity (STDP), a cellular correlate for timing-based causal learning.

b3. Molecular mechanisms underlying early-phase long-term synaptic plasticity

After decades of experimental studies on the properties and mechanisms of long-term synaptic plasticity, it now appears that there are various forms of LTP and LTD, which share some common characteristics but vary in many details (Malenka and Bear, 2004). Therefore, when the mechanisms underlying LTP or LTD are considered, it is necessary to point out the specific type of synapse, the developmental phase, and the induction protocol used. Here we limit our discussion to the molecular mechanisms of early-phase, monosynaptic synaptic plasticity, especially in the hippocampus, which has been received extensive and systematic analyses. On the contrary, the studies of synaptic plasticity in thalamus are extremely limited (see Bright and Brickley, 2008; Castro-Alamancos and Calcagnotto, 1999).

The locus of induction and expression of synaptic plasticity has invoked fierce

debate over the last two decades (especially in the 1990's), with the main battlefield in

the hippocampus. We take NMDAR-dependent LTP at Schaffer collateral (SC)-CA1

pyramidal neuron synapses for most of the discussion as an example to highlight the

experimental and theoretical challenges as well as our current understanding regarding

the molecular mechanisms of early-phase synaptic plasticity. Arguably, the classical

model of synaptic plasticity induction, with postsynaptic NMDA receptors (NMDARs)

as a coincidence detector for correlated pre- and postsynaptic activities, was established

in series of classical studies done on SC-CA1 synapses of hippocampus. It was showed

that postsynaptic depolarization (Kelso et al., 1986; Gustafsson et al., 1987), activation

of postsynaptic NMDARs (Collingridge et al., 1983; Mayer et al., 1984; Nowak 1984),

the accompanying calcium influx, and the resultant rise in intracellular calcium

concentration (Cummings et al., 1996; Lynch et al., 1983; MacDermott et al., 1986;

Zalutsky and Nicoll, 1990) are necessary initial events for inducing LTP. Similar events

can also account for LTD induction, while calcium-induced calcium release (CICR) is

also involved (Malenka and Bear, 2004).

Theories were proposed to explain how activation of single molecular entity, which

conducts the same type of intracellular messenger (calcium), can lead to entirely
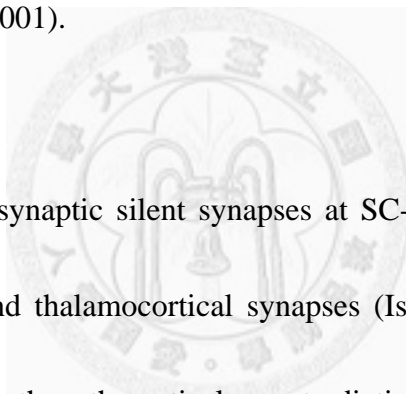
different functional outcomes. The calcium hypothesis for plasticity induction (Artola and Singer, 1993; Malenka and Nicoll, 1993) and BCM theory (Bienenstock et al., 1982) articulate that the magnitude of postsynaptic calcium influx determines the polarity and strength of synaptic modification: with respect to a threshold calcium level, more calcium influx leads to LTP, while modest calcium influx leads to LTD. This formulation has acquired direct experimental support, such as in rat neocortical system (Hansel et al., 1996). Wu et al. (2001) showed a sigmoid relationship between synaptic modification and the charge transfer via NMDARs, corresponding to the proposed biphasic relationship between synaptic plasticity and calcium influx. It is noteworthy that the time course of postsynaptic calcium concentration was also proposed to be involved in the induction of synaptic plasticity (Rubin et al., 2005).

Following the calcium influx, the initiation of downstream signaling cascades for LTP induction can involve calcium / calmodulin-dependent protein kinase II (CaMKII), cAMP-dependent protein kinase (PKA), protein kinase C (PKC, especially the atypical PKC isozyme protein kinase M ξ, PKM ξ), mitogen-activated protein kinase (MAPK), extracellular signal-regulated kinases (ERKs), phosphatidylinositol 3-kinase (PI3 kinase), or Src-family tyrosine kinase (Malenka and Bear, 2004), depending on different experimental paradigms. These signaling can engage the cellular effectors which lead to

functional alterations of synaptic strength, such as presynaptic modification of the

probability of neurotransmitter release or / and postsynaptic modification of AMPAR

number, conductance, or trafficking (Malenka and Bear, 2004). For LTD induction, the

most well-characterized downstream enzyme is calcineurin or protein phosphatase 1

(PP1), which dephosphorylates PKC and PKA substrates, thus leading to

posttranslational modification and internalization of AMPARs (Malenka and Bear,

2004). LTD of the excitatory synapses on MSNs of striatum and the synapses between

layer V neurons of visual cortex were shown to be dependent on endocannabinoid

signaling (Malenka and Bear, 2004; Sjöström et al., 2003).

The locus of LTP expression at SC-CA1 synapses has been very controversial. It

was proposed that LTP is mediated by an persistent increase in the release probability of

presynaptic neurotansmitter (Malinow et al., 1989). Two research groups, Bekkers and

Stevens (1990), and Malinow and Tsien (1990), independently reported that the

coefficient of variation (CV) of EPSC amplitude decreases following LTP induction,

which, under certain assumptions (see Chapter 4), reflects presynaptic quantal

parameters (quantal content) are changed. Moreover, Kullmann and Nicoll (1992)

showed that the probability of failure (failure rate) in evoking measurable synaptic

responses is reduced after LTP induction. Stevens and Wang (1994) also showed that

amplitude of unitary synaptic responses does not change after LTP is induced. On the

contrary, several lines of evidence also suggested that LTP can be accounted for by

functional modification of postsynaptic AMPARs. For example, phosphorylation of

AMPARs is enhanced after LTP induction (Lee et al., 2000), which was found to

increase open probability (Banke et al., 2000) and single-channel conductance (Derkach

et al., 1999) of AMPARs. In addition, insertion of AMPAR subunit GluR1 into dendritic

memebranes occurs after experimental requirements for LTP induction are fulfilled (Lu

et al., 2001; Pickard et al., 2001).

The discovery of postsynaptic silent synapses at SC-CA1 synapses (Isaac et al.,

1995; Liao et al., 1995) and thalamocortical synapses (Isaac et al., 1997) seemed to

successfully compromise the theoretical contradictions between experimental

interpretations. In these systems, some proportion of excitatory synapses were shown to

be *functionally silent* (at the experimentally measurable level) postsynaptically. It was

proposed that they express functional NMDARs, but not functional AMPARs, therefore

are unable to contribute to synaptic response around resting membrane potential in

normal slice conditions. Most intriguingly, silent synapses can be converted to

functional ones through incorporation of functional AMPARs (which does not

necessarily correspond to a physical insertion of receptors) into postsynaptic sites by an

LTP induction protocol which activates NMDARs (Liao et al., 1995). At thalamocortical

synapses, the critical period in which an NMDAR-dependent LTP can be successfully

induced elegantly matches the developmental window in which postsynaptically silent

synapses are present (Isaac et al., 1997). Isaac et al. (1996) showed that, by recruiting

putative single synapses with minimal stimulation technique, release probability of

neurotransmitter release does not change, whereas amplitude of EPSC in successful

trials ("potentcy") increases following LTP induction. Therefore, the results of change in

CV and failure rate, as mentioned above, can be reinterpreted as reflecting an equivalent

functional upregulation of the number of release sites because of incorporating

functional synaptic AMPARs (Malenka and Nicoll, 1997). However, it should be noted

that, potential spillover of glutamate released from neighboring synaptic sites, and the

accompanying preferential activation of synaptic NMDARs due to higher glutamate

binding affinity (relative to AMPARs), may complicate this interpretation (Kullmann,

1996; Kullmann et al., 1996).

At mossy fiber (MF)-CA3 pyramidal neuron synapses of hippocampus, the locus

of LTP induction has also remained controversial, partly due to a considerable body of

conflicting experimental results and interpretations. These contractions appeared to be

partly resolved by the finding that different inducing paradigms engage distinct

induction mechanisms (Urban and Barrioneuvo, 1996), and the requirement for the

retrograde signaling mediated by interactions of postsynaptic EphB receptors and

presynaptic ephrins (Contractor et al., 2002) might to some extent explain the sensitivity

of LTP induction to both pre- and postsynaptic interventions in experiments.

Nevertheless, there is consensus over the presynaptic locus of LTP expression at

MF-CA3 synapses (Reid et al., 2004; Zalutsky and Nicoll, 1990).

As more different types of synaptic plasticity were discovered and characterized,

our knowledge of the mechanistic repertoire for synaptic plasticity is enriched.

Metabotropic glutamate receptor (mGluR)-dependent LTP or LTD can be induced at

SC-CA1 synapses of hippocampus (Malenka and Bear, 2004; Oliet et al., 1997), parallel

fiber-Purkinje cell synapses of cerebellum (Ito, 1982), and the excitatory synapses on

the medium spiny neurons (MSNs) of dorsal and ventral striatum (Malenka and Bear,

2004). More interestingly, induction of LTD at the synapses between layer V neurons of

visual cortex requires coincident activation of presynaptic NMDARs and cannabinoid

type 1 receptors (CB1Rs) (Sjöström et al., 2003), and induction of LTD at layer

IV-layerII/III synapses of primary somatosensory cortex requires coincident activation

of presynaptic NMDARs, mGluRs and retrograde cannabinoid signaling (Bender et al.,

2006). The only study on the long-term plasticity of excitatory synaptic transmission in

thalamus is done by Castro-Alamancos and Calcagnotto (1999). They reported an

NMDAR-independent LTP at corticothalamic synapses of VBN relay neurons in mice,

and proposed a presynaptic locus of expression.

b4. Functional significance of long-term synaptic plasticity

Memory is usually appreciated as the experience-dependent changes in the

behavior, or the stored knowledge upon which changes in behavior are dependent

(Martin and Morris, 2002). The idea that memory is stored by modifications of neuronal

connections was perhaps first proposed in the 19th century by Alexander Bain (1855)

and Ramón y Cajal (Andersen et al., 2007). From a modern perspective of view, the

striking parallelisms between classical characteristics of LTP and that of declarative

memory have made it a very appealing cellular model of learning and memory (see

Bliss and Collingridge, 1993). For example, formations of different memorial entities

are separable, which parallels the property of *specificity* (*selectivity*) (Andersen et al.,

1977; Lynch et al., 1977); input information has to be robust (e.g. strong and / or

important) enough to be remembered, which parallels the property of *cooperativity*

(Levy and Steward, 1979; McNaughton et al., 1978); critical facts or events can make

other less noteworthy ones to be memorized in concert, which parallels the property of *associativity* (Levy and Steward, 1979; McNaughton et al., 1978). Moreover, LTP has been demonstrated in a number of brain regions believed to be critically involved in learning and memory, including hippocampus (Jarrard, 1993), cerebellum (Crepel and Jaillard, 1991), and prefrontal cortex (Laroche and Lynch, 1986; Laroche et al., 1990).

"Synaptic plasticity and memory (SPM) hypothesis", formulated by Martin and Morris (2002), is a good example illustrating contemporary theoretical basis for the neurobiology of learning and memory in terms of synaptic mechanisms. It states that "activity-dependent synaptic plasticity is induced at appropriate synapses during memory formation, and is both necessary and sufficient for the information storage underlying the type of memory mediated by the brain area in which that plasticity is observed." Some theoretical considerations such as *timing contiguity* and *contingency* (the ability of the conditioned stimulus to predict the unconditioned stimulus) were also provided. More importantly, they further suggested experiment-based criteria regarding the assessment and testability of SPM hypothesis, i.e. detectability, mimicry, anterograde alteration, and retrograde alteration (Martin and Morris, 2002). There has been compelling experimental evidence supporting the function of synaptic plasticity as a underlying mechanism for learning. For instance, several reports indicated that there

are changes in synaptic strength occurring as a consequence of certain forms of learning (reviewed by Malenka and Bear, 2004; Maren and Baudry, 1995, Martin and Morris, 2002; Massey and Bashir, 2007). In addition, the pharmacological agents that block LTP induction are capable of impairing learning acquisition (Stanton, 1996).

C. Specific aims

Despite the fact that ventrobasal thalamus of rodents is taken as a classical model system for studying sensory processing in higher mammals, systematic analysis of basic properties of synaptic transmission at corticothalamic (CT) and lemniscal (ML) synapses, the two major inputs onto VBN relay neurons, is so far very limited. State-dependent, top-down influences of higher cortical origins on sensory processes have been widely appreciated, especially via the actions of corticothalamic pathways (e.g. Briggs and Usrey, 2008; Fanselow et al., 2001; Krupa et al., 1999; Sherman, 2005; Wolfart et al., 2005); however, one of the most important questions in this field remains: what kinds of cellular and synaptic mechanisms, and how these mechanisms, underlie the dynamic nature of corticothalamic modulation in response to variable internal and external stimuli? In this work, I tried to address these issues by applying standard

whole-cell patch clamp recording to compare the basic synaptic properties and composition of ionotropic glutamate receptors of CT and ML pathways, test their ability to expressing different forms of long-term synaptic plasticity, and investigate the underlying induction and expression mechanisms. The physiological conditions required for plasticity induction, the functional significance of long-term plasticity, and the relations between receptor composition and synaptic transmission properties of VBN relay neurons will also need more investigation to get insight of the operational principle of thalamocortical and corticothalamic systems.

Specific Aim 1   **Morphological and electrophysiological identification of rat VBN relay neurons**

Combining standard whole-cell recording with *post hoc* ABC histochemistry, we will confirm the identity of recorded cells by established anatomical, morphological, and electrophysiological criteria.

Aim 1a   Anatomical and morphological characteristics of VBN relay neurons

Aim 1b   Basic firing properties of VBN relay neurons

Specific Aim 2　Comparison of basic properties of evoked CT and ML EPSCs

Properties of evoked responses will be characterized to reveal basic differences between CT and ML EPSCs.

Aim 2a　Kinetic properties of CT and ML EPSCs

Aim 2b　Stimulus-response relationships of CT and ML EPSCs

Aim 2c　Short-term plasticity of CT and ML EPSCs

Specific Aim 3　Examining the composition of ionotropic glutamate receptors at

　　　　　　CT and ML synapses

Basic characteristics of CT and ML EPSCs will be examined, including NMDAR- / non-NMDAR peak current ratio and current-voltage (I-V) relationship of the non-NMDAR-mediated EPSCs. Rrectification index (**Aim 3b, c**), sensitivity to selective pharmacological agencies (**Aim 3d**), voltage dependence of paired-pulse ratio (**Aim 3e**), and weighted mean single-channel conductance revealed by peak-scaled non-stationary noise analysis (Traynelis et al., 1993) (**Aim 3f**) will be used as supporting evidence for the expression of calcium-permeable non-NMDARs.

**Aim 3a**   NMDAR- and non-NMDAR-mediated components of CT and ML EPSCs

Aim 3b   I-V relationship of the non-NMDAR-mediated components of CT and ML

EPSCs

Aim 3c   Dependence of rectification properties of CT and ML EPSCs on polyamines

Aim 3d   Sensitivity of non-NMDAR-mediated EPSCs to selective antagonists of

CaP-AMPARs

Aim 3e   Use-dependent relief of ionotropic glutamate receptors from polyamine block

at CT and ML synapses

Aim 3f   Weighted mean single-channel conductance of non-NMDARs at CT and ML

synapses
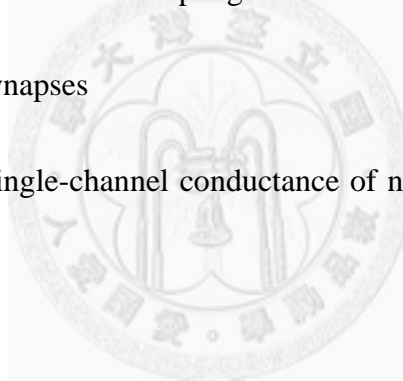
<u>Specific Aim 4</u>   Comparison of long-term plasticity of CT and ML EPSCs

Differential contribution of NMDAR and calcium-permeable non-NMDAR would

imply distinct ability to expressing long-term plasticity of CT and ML EPSCs. We will

try to induce NMDAR-dependent plasticity by conjunctive pairing extracellular

stimulation with membrane depolarization, and test the role of VGCCs, especially

T-type and L-type ones, in the induction of plasticity. Phamocological tools, analysis of

CV (coefficient of variation) of EPSCs and input resistance will be applied to elucidate

the induction and expression mechanisms of the long-term plasticity

.

Aim 4a   Induction of NMDAR-dependent plasticity of CT and ML EPSCs

Aim 4b   Testing the role of VGCCs in the induction of synaptic plasticity

Aim 4c   Induction of VGCC-dependent plasticity of CT and ML EPSCs

Aim 4d   Induction and expression mechanisms of synaptic plasticity of CT and ML

   EPSCs

Specific Aim 5   **Examining the role of CaP-AMPARs in long-term synaptic**

   plasticity of CT EPSC

CaP-AMPARs have been reported to involve the induction (Lamsa et al., 2007; Liu

and Cull-Candy, 2000) and expression (Ho et al., 2007) of long-term plasticity. By

assessing the rectification of EPSCs (**Aim 5a**), the effect of selective CaP-AMPAR

antagonists (**Aim 5b**), and weighted mean single-channel conductance (**Aim 5c**), roles

of CaP-AMPARs in expression of plasticity can be identified. Furthermore, we can test

the potential of CaP-AMPARs in inducing synaptic plasticity by conjuctive pairing

high-frequency stimulation with membrane hyperpolarization (an "anti-Hebbian"

pairing protocol; **Aim 5d**), which potentially maximizes activation of CaP-AMPARs.

Aim 5a Rectification of EPSCs before and after induction of synaptic plasticity

Aim 5b Effect of selective CaP-AMPAR antagonists on synaptic plasticity

Aim 5c Weighted mean single-channel conductance before and after induction of

 synaptic plasticity

Aim 5d Induction of "anti-Hebbian" long-term plasticity of CT EPSCs

<u>Specific Aim 6</u>   Identifying the physiological activity patterns required for

long-term synaptic plasticity of VBN relay neurons

Next, in current-clamp recording, we will induce synaptic plasticity by repetitively

triggering physiologically relevant firing patterns, i.e. regular / continuous mode or

burst mode, to see whether synaptic plasticity can be induced in a firing-mode

dependent manner. The roles of T-type VGCCs and back-propagating action potentials

(bAPs) for the induction of synaptic plasticity are also assessed under the framework of

spike-timing-dependent plasticity (STDP).

Aim 6a Firing pattern dependence of long-term plasticity in current-clamp mode

Aim 6b Induction mechanism of firing-induced long-term plasticity

Aim 6c Dependence of STDP on activation of T-type VGCCs

Figures

Figure 1.1 Gross anatomy of the ventrobasal nucleus (VBN, including VPM and VPL) of rat thalamus

Comparison of the rat brain atlas (Paxinos & Watson, 2007) (**A**) and a representative bright-field image of coronal thalamic slices (**B**); the dark spot within VPM is the recorded cell stained by *post hoc* biocytin-DAB histochemistry.

Please note the lobulated appearance of VBN, imposed on it by penetrating bundles of myelinated fibers, and the clearly identifiable border between ventral posterior medial nucleus (VPM) and ventral posterior lateral nucleus (VPL). Rt, reticulat nucleus.
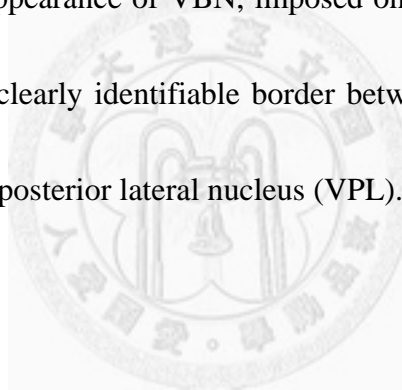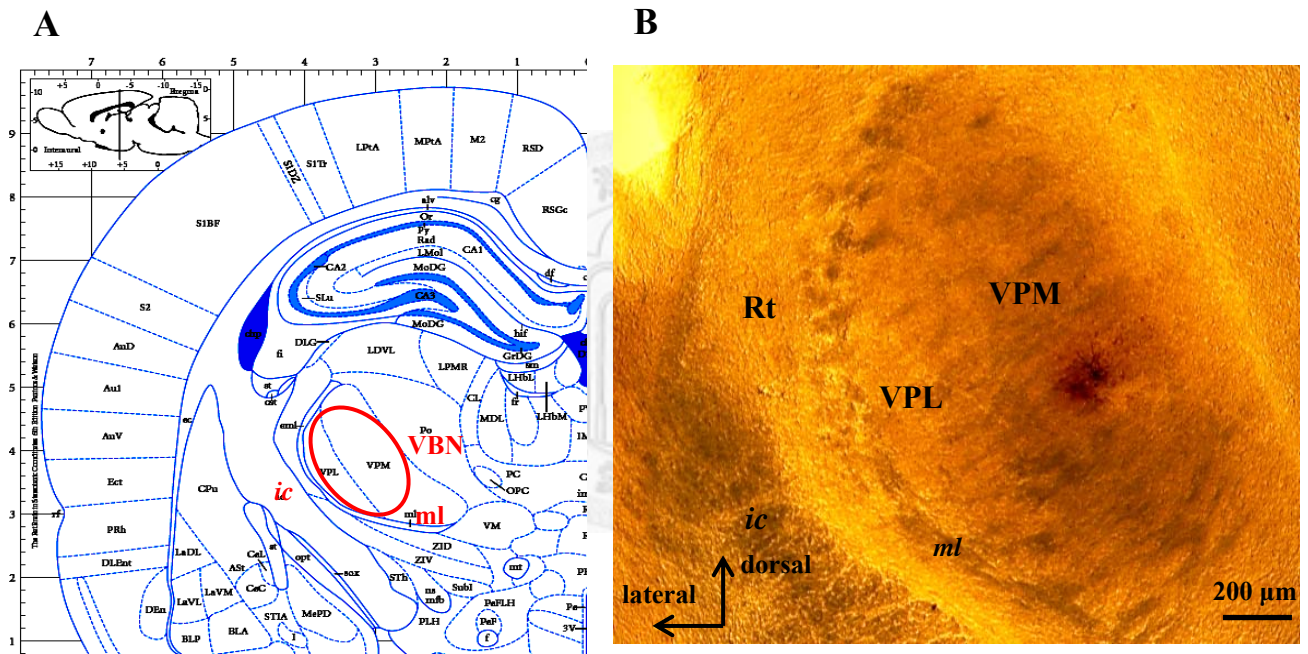
Figure 1.1

A

B

Figure 1.2 Anatomical organization of dorsal column-medial lemniscal pathway and spinothalamic (anterolateral) pathway

Tactile and proprioceptive information is transmitted to the VBN of thalamus by dorsal column-lemniscal pathway, ascending ipsilaterally in spinal cord, while pain and thermal sensations are by spinothalamic (anterolateral) pathway, ascending contralaterally; the second-order neurons are located in the dorsal column nuclei and the dorsal horn of spinal cord, respectively. As the axons originating from dorsal column nuclei ascend through brain stem, they shift laterally and join spinothalamic tract in the midbrain, forming medial lemniscus (*ml*). Spinothalamic fibers terminate in other thalamic nuclei are not illustrated. Filled circles represent soma of neurons, and Y shape represents presynaptic terminals of axons. Adapted from Kandel et al. (2000). VPL, ventral posterior lateral nucleus of thalamus; VPM, ventral posterior medial nucleus of thalamus.

Figure 1.2

Dorsal Column-medial lemniscal system

Anterolateral (spinothalamic) system

Somatosensory cortex
(postcentral gyrus in human)

Somatosensory cortex
(postcentral gyrus in human)

cerebral cortex

dorsal anterior
insular cortex

Ventrobasal nucleus
(VPM and VPL)

thalamus

Ventrobasal nucleus
(VPM and VPL)

midbrain

spinomesencephalic tract

medial lemniscus

pons

sensory decussation

spinoreticular tract

gracile nucleus, cuneate nucleus
(dorsal column nuclei)

medulla

gracile fascicle,
cuneate fascicle

spinal cord dorsal horn

spinal cord

dorsal root ganglion

dorsal root ganglion

tactile /
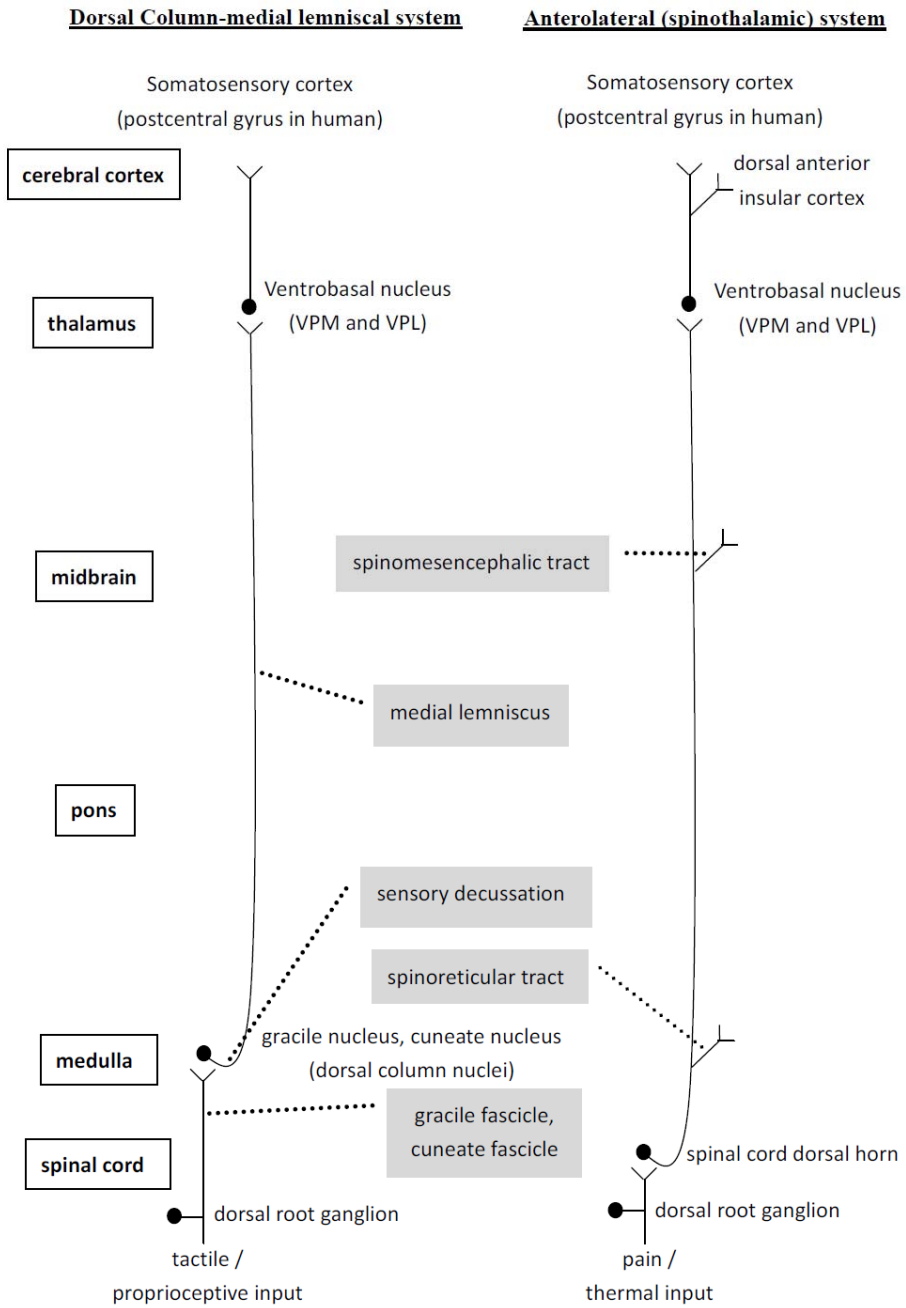proprioceptive input

pain /
thermal input

Figure 1.3 Anatomical organization of trigeminothalamic pathway and spinal trigeminothalamic pathway

Trigeminal ganglion cells (GV) that innervate a vibrissa project to various trigeminal subnuclei; each pathway arises from different subnucleus and cell type, transits through a particular thalamic region and projects to specific cortical areas or layers. These include lemniscal pathway (red and brown), extralemniscal pathway (green) and paralemniscal pathway (blue). Adapted from Deschênes (2009). Pom, medial portion of posterior complex of thalamus; PrV, principal trigeminal nucleus (pincipalis); SpV, spinal trigeminal nucleus; SpVc, caudal subnucleus of SpV (caudalis); SpVi, interpolar subnucleus of SpV (interpolaris); SpVic, interpolar subnucleus of SpV, caudal territory; SpVir, interpolar subnucleus of SpV, rostral territory; SpVo, oral subnucleus of SpV (oralis); VPM, ventral posterior medial nucleus; VPMc, core subdivision of the barreloid in VPMdm; VPMdm, dorsal medial division of VPM; VPMh, head subdivision of the barreloid in VPMdm; VPMvl, ventral lateral division of VPM; ZIv, ventral division of zona incerta.
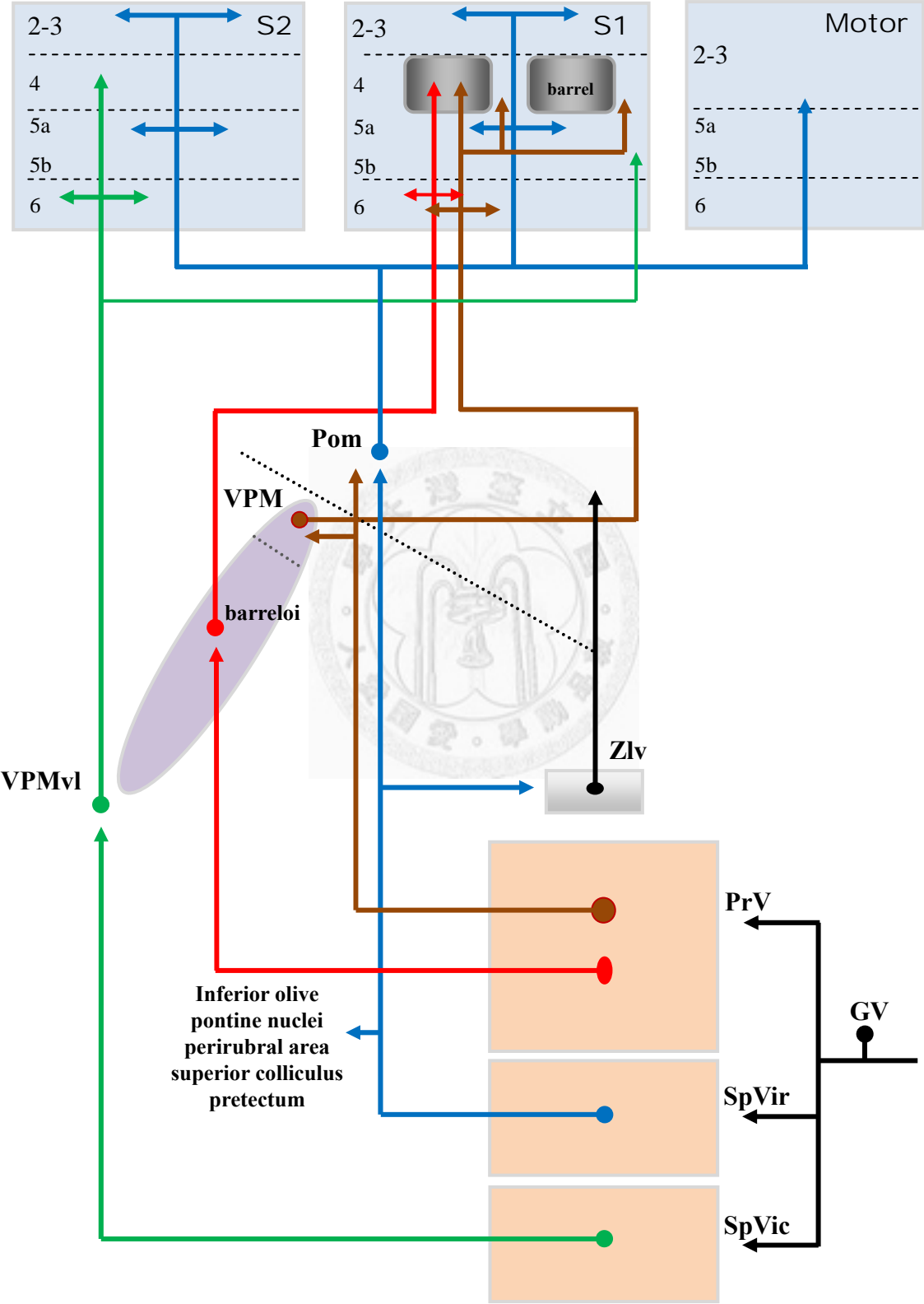
Figure 1.3

Figure 1.4 Firing modes of thalamic neurons

A, Ionic basis of thalamic burst spiking. A hyperpolarizing current injection de-inactivate T-type voltage-gated calcium channels (T-type VGCCs), which are activated by the subsequent cessation of the current injection, resulting in a rebound low threshold spike (LTS). LTS activates a high-frequency burst of action potentials mediated by the transient Na^+ current (I_{Na}), various K^+ currents (I_K), and high-threshold voltage-gated calcium currents (I_{Ca}). The entry of calcium activates Ca^{2+}-dependent K^+ current ($I_{K,Ca}$) and therefore an after-hyperpolarization (AHP), and Ca^{2+}-activated nonselective cation current (I_{CAN}) which results in a slow afterdepolarization (ADP), which is responsible for the generation of continuous / tonic discharge following the oscillatory burst spiking. Adapted from Bal and McCormick (1993). **B**, Firing repertoire of thalamic relay neurons. Thalamic relay neurons have membrane potential (V_m)-dependent duality of firing modes, which is dependent on the availability of T-type VGCCs. Upon activation of postsynaptic type 1a metabotropic glutamate receptors (mGluR1a) preferentially expressed at CT synapses by high-frequency stimulation (Hughes et al., 2002) or exogenous application of non-specific group I/II mGluR agonist *trans*-ACPD (Zhu et al., 2006), additional T-type VGCCs can be unmasked, and the repertoire of firing patterns is expanded. These include: high-threshold burst (HTB) mediated by transient opening of putative dendritic T-type VGCCs, and slow oscillation

44

(at the frequency of < 1Hz) mediated by activation of non-inactivating T-type VGCCs at

the $V_m \sim$ -60 mV. Adapted from Crunelli et al. (2006).
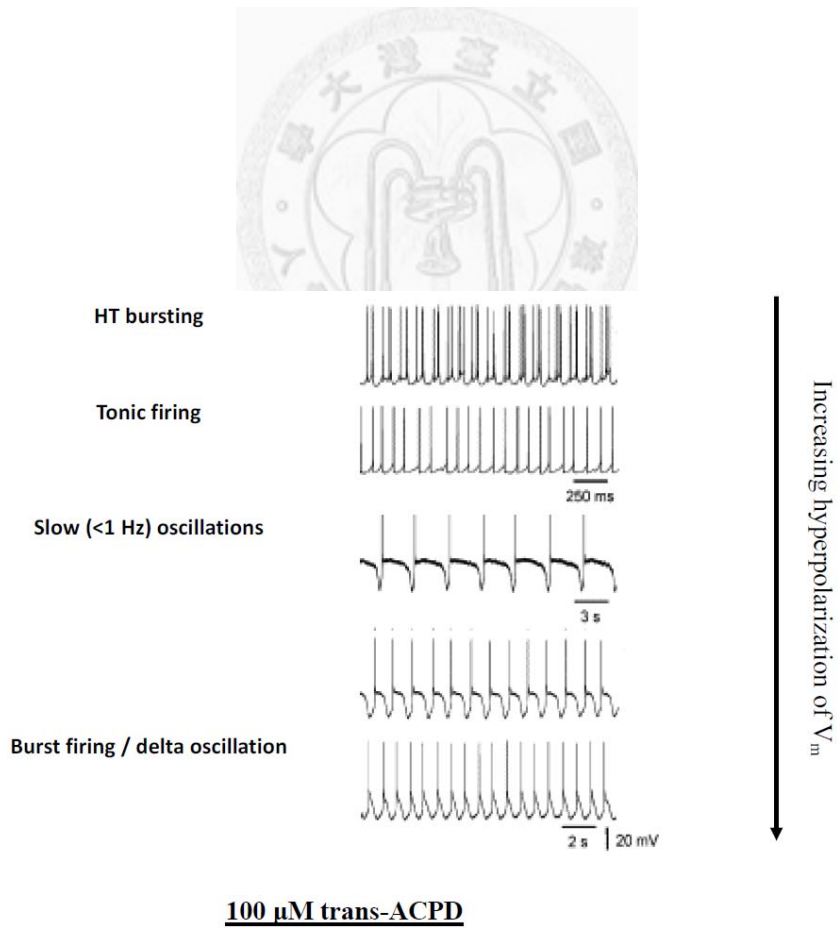
Figure 1.4

A
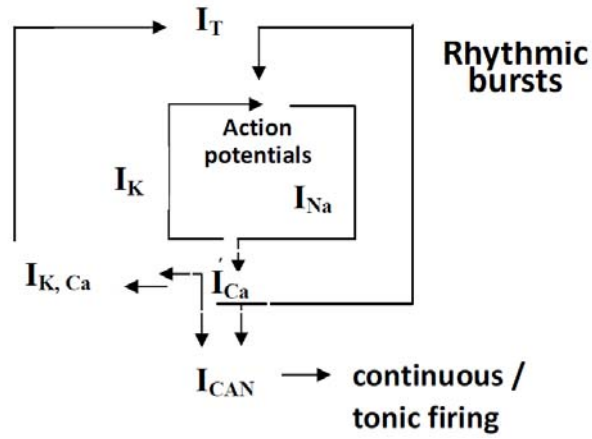
B

100 μM trans-ACPD

Chapter 2

Properties of fast excitatory synaptic transmissions of relay neurons in the ventrobasal nucleus of rat thalamus
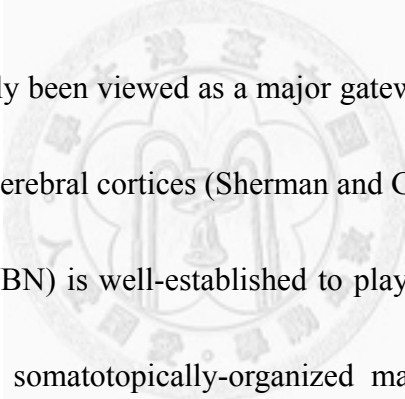
Abstract

The somatosensory thalamus, ventrobasal nucleus (VBN), is the relay station transmitting somatosensory information from spinal cord to cerebral cortex; it also receives reciprocal cortical feedback. Subcortical somatosensory system as a widely used model for research in the field of sensory physiology, in which basic properties of synaptic transmission and plasticity are surprisingly limited in detailed characterization. Here we started with comparing fast excitatory synaptic transmission of corticothalamic (CT) and medial lemniscal (ML) inputs onto relay neurons in the VBN of rat thalamus. Whole-cell recordings were made on VBN relay cells from thalamic slices of SD rats aged postnatal 13-24 days (P13-24), with most of them P13-17. Best efforts were made to recruit CT and ML pathways simultaneously in the same neuron for characterization of input-specific synaptic properties. CT EPSCs showed larger rise time, linear stimulus-response curve, paired-pulse facilitation

(PPF), inward-rectifying I-V relationship, a larger peak current ratio of NMDAR- / non-NMDAR-mediated response, and preferential sensitivity to philanthotoxin-433 (PhTx-433) and NAS, both selective antagonist for calcium-permeable AMPA receptors (CaP-AMPARs). In contrast, ML EPSCs showed all-or-none responses in response to different stimulus intensity, smaller rise time, paired-pulse depression (PPD), linear I-V relationship, a smaller peak current ratio of NMDAR- / non-NMDAR-mediated response, and insensitivity to NAS and PhTx-433. In addition, PPR of CT EPSCs at the $V_h < 0$ mV is higher than at the $V_h > 0$ mV, which did not hold for ML EPSCs, suggesting that activity-dependent relief of polyamine block was selectively occurred at CT synapses. Complementary peaked-scaled nonstationary noise analysis was also applied to evoked responses of CT and ML synapses to compare their weighted mean single-channel conductances of synaptic non-NMDARs. Despite the dramatic difference in the amplitude of evoked unitary EPSCs between CT and ML pathways, the latter of which was typically minimally stimulated with the stimulus intensity range we normally used, the result showed that the trend of the difference in single-channel conductance was, however, opposite to that of the difference in unitary EPSC amplitide: compared to ML responses, CT responses composed of smaller unitary events were contributed by non-NMDARs with larger single-channel conductance, which supported the experimental interpretation that

CaP-AMPARs are preferentially expressed at CT, but not ML, synapses. Taken together, these results illustrate fundamental differences of synaptic transmission between CT and ML synapses, especially the composition of ionotropic glutamate receptors.

Introduction

Thalamus has generally been viewed as a major gateway for sensory information relayed from periphery to cerebral cortices (Sherman and Guillery, 2004). In particular, the ventrobasal nucleus (VBN) is well-established to play a pivotal role for relaying somatosensory input in a somatotopically-organized manner (Jones, 2007). VBN receives primary sensory information carried by medual lemniscus (*ml*) as well as reciprocal cortical feedback from higher cortices (Liu et al. 1995; Sherman and Guillery, 2002). It was suggested that, in the dorsal lateral geniculate nucleus (dLGN), sensory inputs account for only 10% of synapses onto relay neurons, whereas cortical inputs more than 50% (Erisir et al. 1997; Latawiec et al. 2000), although this difference has been argued to be an overestimate (Jones, 2007). There are two types of corticothalamic fibers (Deschênes et al., 1998; Landisman and Connors, 2007;

Reichova and Sherman, 2004; Rouiller and Welker, 2000), namely, those arising from cortical layer V and layer VI pyramidal neurons; the corticothalamic projections to the VBN in rodents were found to originate mainly from the layer VI (Deschênes et al., 1998; Killackey and Sherman, 2003; Reichova and Sherman, 2004; Rouiller and Welker, 2000; Van Horn and Sherman, 2004), and was regarded as an essential modulator for the properties of thalamic spike transfer (Destexhe, 2000; Ergenzinger et al., 1998; Jones, 2007; Krupa et al., 1999; Murphy and Sillito, 1987; Sherman, 2005), especially considering the predominance in the number of corticothalamic synaptic contacts onto relay neurons (Jones, 2007; Sherman and Koch, 1986). The landmark firing duality of mammalian thalamic neurons, continuous (tonic / regular) versus burst spiking, is dependent on the voltage-dependent inactivation property of T-type voltage-gated calcium channels (VGCCs) (Jahnsen and Llinás, 1984; Suzuki and Rogawski, 1989) and proposed to be a key determinant for the functional state of thalamic information transfer (Jones, 2007; McCormick and Bal, 1997; McCormick and Feeser, 1990; Sherman, 2001; Sherman, 2005).

Pioneering efforts have been made to elucidate the cellular basis underlying the thalamic information processing and transfer (Bal and McCormick, 1993; Jahnsen and Llinás, 1984; Kao and Coulter; 1997; Le Masson et al., 2002; Leamey and Ho, 1998;

Miyata and Imoto, 2006; Reichova and Sherman, 2004; Turner and Salt, 1998).

Nevertheless, many basic properties of major synaptic inputs to somatosensory

thalamus have not been investigated in a systematic and comparative way, not to

mention the properties and conditions required for induction of long-term synaptic

plasticity (see Castro-Alamancos and Calcagnotto, 1999). Even though the importance

of CT feedback in thalamic function has been widely appreciated, the factors known

to modulate the efficacy of CT transmission are limited (see Alexander and Godwin,

2005; Castro-Alamancos, 2002; Miyata and Imoto, 2009; Ulrich et al., 2007), and, in

particular, whether natural firing patterns of relay neurons play any parts remains

elusive.
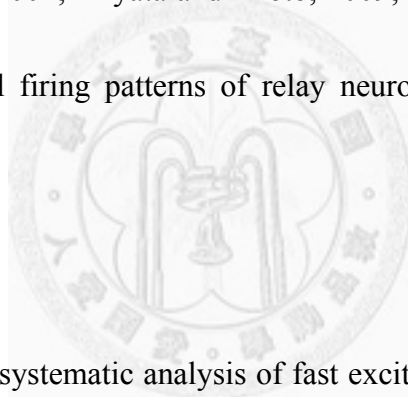
Here we started with systematic analysis of fast excitatory synaptic transmission

from cortex (CT pathway) and medial lemniscus (ML pathway) onto the VBN of rat

thalamus. Our results demonstrated the significant differences of synaptic

transmission between these two pathways, especially in the composition of ionotropic

glutamate receptors, which was carefully examined by multiple experimental and

analytical approaches.

Methods

Preparation of acute slices

The use of animals in this study was in accordance with the guidelines of the local ethical committee for animal research of National Taiwan University. Sprague-Dawley (SD) rats of both sexes aged 13-24 postnatal days (P13-24) were used, but most were aged P13-16. The animals at these ages were chosen because the intrinsic and firing properties of rat VBN neurons reach developmental steady-state after P12, including the resting membrane potential (V_m), input resistance (R_N), ability to fire full-blown LTS-driven bursting, width of action potential (AP) and after-hyperpolarization (AHP) (Velazquez and Carlen, 1996). Possibly attributible to less extent of myelinated fibers, the success rate in obtaining good seal and recording quality was also significantly higher from animals of this age window, which is especially critical for the purpose of simultaneous recruitment of CT and ML synapses.

The rats were anaesthetized with isoflurane and decapitated with a small-animal guillotine, and the brain was quickly removed and placed in ice-cold artificial

cerebrospinal fluid (ACSF). Coronal slices were used for initial experiments. We then discovered that, in horizontal slices, it was easier to recruit CT and ML EPSCs simultaneously in the same relay neuron, horizontal preparation was adopted for the most part of this study. For horizontal preparation, the two halves of the brain were first separated, and their ventral portions were trimmed in parallel to the ventral surfaces of brainstem to ensure standard horizontal cutting orientation in accordance with traditional stereotaxic coordinates. A block of agar was glued behind the medial surface of a half-brain to provide physical support during slicing. Horizontal brain slices (300 μm) containing the ventrobasal nucleus (VBN), internal capsule (*ic*) and medial lemniscus (*ml*) fibers were prepared, using the patterns of *ic* and the fibers in the ventral posterolateral nucleus (VPL) as landmarks (Fig. 2.1). For coronal preparation, intact coronal slices were cut and the two halves were separated by blade. Coronal brain slices (300 μm) containing the VBN, *ic* and *ml* were prepared, using the patterns of VBN and its fiber patterns as landmarks (Fig. 2.1).
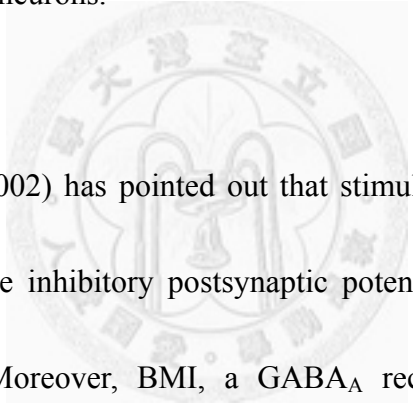
The slices were cut with a vibroslicer (752M, Campden, Loughborough, England or ZERO 1, D.S.K., Osaka, Japan). The ACSF contained (in mM): 119 NaCl, 2.5 KCl, 1.3 MgSO$_4$, 26.2 NaHCO$_3$, 1 NaH$_2$PO$_4$, 2.5 CaCl$_2$, and 11 glucose; pH adjusted to 7.4 by gassing with carbogen consisted of of 95 % O$_2$ / 5 % CO$_2$. The slices were kept in

oxygenated ACSF (95% O_2 / 5% CO_2) at room temperature (24-25°C) to allow

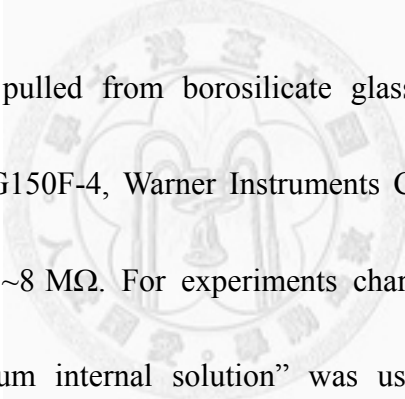recovery for at least 90 minutes before recording was started.

Electrophysiology

Slices were transferred to an immersion-type recording chamber mounted to an

upright microscope (BX50WI, Olympus Optical, Tokyo, Japan), equipped with

water-immersion objectives, a Normaski optic system, an infrared filter and a CCD

camera (XC-E150, Sony, Tokyo, Japan) (IR-DIC system). In horizontal slices, the

VBN, *ic* and *ml* were clearly identifiable under low-magnification light microscopy.

In some cases, we noticed that there was a small heterogeneous zone locating in the

border of VPL medial to *ic*, which indicated a lower density of myelinated fibers (Fig.

2.1A$_3$). Recordings made from this zone was avoided to prevent potential

confounding factors which may originate from functional or biochemical

heterogeneities within VBN (see introduction from more descriptions). Neurons in the

VBN were recorded under visual guidance. The typical number of fast spikes of a

LTS-burst firing is 4~9 as depolarizing current pulses were injected at the V_m <

-75mV. Occasionally, some neurons had a spike number of LTS-burst < 3 and were

discarded.

According to Arcelli et al. (1997), GABAergic interneurons were less than 1 %

in almost all the thalamic relay nuclei of rats, except for the dorsal lateral geniculate

nucleus (dLGN) (for the lack of inhibitory interneurons in the VBN of rodents, see

Ohara and Lieberman, 1993; Špacek and Lieberman 1974). In the dorsal thalamus of

rodents, virtually all inhibitory influences originate in the reticular nucleus (Rt) (Jones,

2007). Thus, all recorded VBN neurons in this study presumably belong to excitatory

thalamocortical projecting neurons.

Castro-Alamancos (2002) has pointed out that stimulation of medial lemniscus

(*ml*) usually did not evoke inhibitory postsynaptic potentials (IPSPs) in horizontal

slices of mouse VBN. Moreover, BMI, a $GABA_A$ receptor antagonist, had no

significant effects on evoked lemniscal responses or te characteristics of

frequency-dependent depression. This is expected because lemniscal pathway does

not produce feed-forward inhibition due to the lack of inhibitory interneurons in the

VBN of rodents. Rt interneurons can be activated by collaterals of thalamocortical

fibers on their way to neocortex (Jones, 2007). In the experiments of horizontal

preparation, the only source of inhibition is the feedback from Rt interneurons

following firing of sufficient thalamocortical relay neurons. Alternatively, Rt

interneurons can be activated via sufficient excitation of collaterals of corticothalamic fibers. The IPSPs were, however, rarely observed in horizontal VBN slices of mice (Castros-Alamancos, 2002), which could be attributed to the orientation of the slice preparation so the fibers were not well preserved. Nevertheless, all experiments carried out in this study were performed in the presence of 0.1 mM picrotoxin and 1 µM strychnine to avoid any potential confounding effects of GABAergic and glycinergic IPSPs.

Patch pipettes were pulled from borosilicate glass (1.5 mm outer diameter, 0.32 mm wall thickness; G150F-4, Warner Instruments Corp., Hamden, CT, USA), and had a resistance of 3~8 MΩ. For experiments characterizing basic excitatory synaptic properties, "cesium internal solution" was used to avoid metabotropic receptor-dependent potassium conductances (for evoked $GABA_B$ IPSC in the VBN of rats, see Kao and Coulter, 1997). The cesium internal solution contained (in mM): 114.7 CsOH, 17.5 CsCl, 117.6 gluconic acid, 10 HEPES, 2 EGTA, 8 NaCl, 2 ATP, 0.3 GTP, and 6.7 biocytin; pH was titrated to 7.2 by CsOH and osmolarity to 300-305 mOsm. For experiments on the synaptic plasticity, "normal internal solution" was used, which contained (in mM): 131 K-gluconate, 20 KCl, 10 HEPES, 2 EGTA, 8 NaCl, 2 ATP, 0.3 GTP, and 6.7 biocytin; pH was titrated to 7.2 by KOH and

osmolarity to 300-305 mOsm. In all experiments in which depolarizing step commands were used, 5 mM QX-314 was included in the internal solution to block voltage-gated Na^+ channels and enhance the voltage control. Signals were obtained by Axopatch 1D amplifier (Axon Instruments, Union City, CA, USA). Slices were continuously perfused with oxygenated solutions at 1~2 ml / min under room temperature. For voltage-clamp recordings, whole-cell conductance (Gw) and series resistance (Rs) were continuously monitored by a test voltage pulse of 3 mV; Rs was typically < 20 MΩ and was not left uncompensated. For current-clamp recordings, the input resistance (R_N) was continuously monitored by a test current pulse of +30 pA, and the bridge was balanced by adjusting the Rs compensation of the amplifier. Data were discarded when Rs or R_N varied by more than 20% from its baseline value during the recording. All signals were low-pass-filtered at a corner frequency of 2 kHz, then digitized at 10 kHz using a Micro 1401 interface (Cambridge Electronic Design, Cambridge, UK). Data were collected using Signal (Cambridge Electronic Design, Cambridge, UK) or Spike 5 (Cambridge Electronic Design, Cambridge, UK) by episode-based capture. The liquid junction potential was measured to be ~ +10 mV and left uncorrected (following the method by Neher, 1992).

Stimulation of CT and ML synapses

The best efforts were made to recruit CT and ML synapses at the same relay neurons in most experiments for a reliable comparison of input-specificity of the properties examined (Fig. 2.4A). A bipolar stainless steel electrode (PK/12, FHC, St Bowdoin, ME, USA) was placed locally within 150 μm away from the recorded cell or in *ic* for evoking CT EPSCs, and another electrode was placed in *ml* for evoking CT EPSCs. No significant differences were observed between the CT EPSCs evoked by these two conditions (Table 2.1). In some cases, however, only CT EPSCs or ML EPSCs were evoked, and these data were also pooled for statistical comparison. In occasion, stimulation of *ic* antidromically discharged relay neurons; however, antidromic responses showed apparent all-or-none behavior and no short-term plasticity normally displayed by synaptic responses, therefore easily identifiable. Antidromic activation of relay cells cannot contribute to monosynaptic EPSCs because of the lack of recurrent connections between thalamic relay neurons in VBN (Castro-Alamacos, 1999).

In high-magnification IR-DIC images of horizontal slices, we observed a large number of fiber bundles projecting from the direction of *ic*, traversing the reticular nucleus (Rt) and the small heterogeneous zone in the border of VPL (described above)

into VBN. We traced along the fiber bundles proximal to the recorded neuron, back to

their origin in *ic*, and placed the stimulating electrode accordingly to facilitate the

success rate of recruiting measurable CT EPSCs. A typical stimulus consisted of a

4~100 μs square pulse with the amplitude ranged in 30~800 μA. In some cases, the

stimulating artifact was relatively large, and the synaptic responses were analyzed

after the artifact waveform obtained in 10 μM DNQX, a selective non-NMDARs

antagonist, was subtracted.

For recording the excitatory postsynaptic currents (EPSCs) or excitatory

postsynaptic potentials (EPSPs), V_m was clamped (voltage-clamp) or held

(current-clamp) at -70 mV, with 100 μM picrotoxin (PTX) and 1 μM strychnine were

added to the bath ACSF solution to block ionotropic $GABA_A$ receptors and glycine

receptors (for the glycinergic transmission in the VBN, see Ghavanini et al., 2005;

Ghavanini et al., 2006), respectively. After the experiments were finished, 10 μM

DNQX were applied in the bath in most cases to confirm the identity of recorded

activities as a non-*N*-methyl-D-aspartate receptor (non-NMDAR)-mediated

component. EPSCs were evoked at 0.067–0.125 Hz; in experiments in which CT

EPSCs and ML EPSCs were simultaneously recruited, alternate stimulations were

made to the IC (or locally) and ML tracts, with the stimulation rate to both inputs

being 0.067–0.125 Hz. For recording of EPSPs in current-clamp mode, data were accepted only if the EPSP activity had smooth rising and exponentially decaying phases. If EPSP had signs of NMDAR-mediated activities on the decaying phase, (Landisman and Connors, 2007), characterized by a slow component on top of the fast decay phase of EPSPs, or an abnormally fast rising phase (maybe indicative of the occurrence of antidromic excitation or fast dendritic spike), the data were discarded.

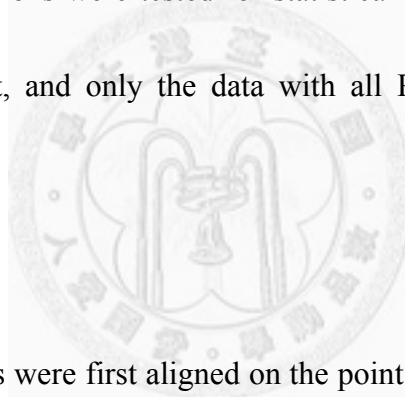*Characterization of basic properties of synaptic transmission*

The weighted decay time constant was calculated from the time constants obtained from double exponential fit to the decay phase of EPSC. The paired-pulse EPSCs used to measure paired-pulse ratio (PPR) were elicited every 10-18 seconds. To estimate NMDAR- to non-NMDAR-mediated peak current ratios, non-NMDAR components were first evoked at -90 mV, which was then blocked by 10 μM DNQX, and NMDAR components were evoked at +60 mV. Finally, 100 μM APV was applied to confirm the recorded activity was mediated by NMDARs. NMDAR- and non-NMDAR-mediated currents were averaged over 10–40 sweeps of recordings. To measure rectification index (RI) of non-NMDAR-mediated EPSC, 100 μM APV was added to the bath to block NMDARs, and EPSCs were evoked with the V_m clamped at

multiple levels, ranging from −90 to +60 mV in an increment of 30 mV. At each V_h, EPSCs were were averaged over 10 sweeps of recordings. RI was defined as the ratio of the measured current amplitude to the predicted one at +60 mV (extrapolated from a linear fit to the I–V relationship from −90 to 0mV).

Peaked-scaled nonstationary noise analysis

In order to identify fundamental differences of ionotropic glutamate receptors between CT and ML synapses, we used peak-scaled nonstationary noise analysis to compare single-channel conductance of synaptic non-NMDARs (Benke et al., 1998; Hartveit and Veruki, 2007; Heinemann and Conti, 1992; Lei et al., 2003; Robinson et al., 1991; Silver et al., 1996; Traynelis and Jaramillo, 1998; Traynelis et al., 1993) mostly following Traynelis et al. (1993) and Hartveit and Veruki (2007). ML EPSC amplitude is much bigger than CT EPSC; to prevent amplifier from being saturated, ML ESPCs were normally recorded at a smaller gain (1/2 or 1/4 of that used for CT EPSC). Only the data with good signal-to-noise ratio and almost perfectly stable recording quality (series resistance) were chosen for analysis. Their EPSC waveforms were then visually examined to exclude those contaminated by spontaneous synaptic activities or sudden changes of the holding current; only the waveforms showing

smooth rising and decaying phases were selected, with the total of 18-63 EPSC

waveforms for each analysis. To evaluate potential time-dependent drift / run-down,

and the presence of differential electrotonic filtering of the EPSCs, they were tested

for time stability and correlations between waveform parameters (Hartveit and Veruki,

2007); that is: (1) the time stability of 10-90% rise time, decay time constant obtained

by mono-exponential curve fitting, and peak amplitude (2) the correlations between

the data of each pair among 10-90% rise time, decay time constant, and peak

amplitude. All the correlations were tested for statistical significance by Spearman's

rank-order correlation test, and only the data with all $P > 0.05$ were selected for

further analysis.

The EPSC waveforms were first aligned on the point of the steepest rise, and the

results of alignment were visually inspected to check the adequacy. Among the 5 data

sets of CT EPSCs from the selected neurons, one of them seemed to be aligned more

poorly after the alignment procedure compared with that without alignment. For the

evoked EPSCs, responses are presumably aligned by the stimulus (Hartveit and

Veruki, 2007), and we therefore cancelled the alignment procedure for this case. All

ML EPSCs were aligned very well after the alignment procedure. To isolate the

current fluctuation associated with stochastic channel gating, the averaged EPSC

waveform was scaled to set its peak to the value of individual EPSC waveforms at the corresponding time point, and the ensemble variances were calculated for each point in the decay period of 10 times the decay time constant of the averaged waveform. The amplitude of the averaged EPSC waveform was then divided into 30 equally-sized bins, and the ensemble variances were pooled according to their corresponding ones. The binned variances were plotted against the binned currents, and the postsynaptic parameters were estimated by the least-squared fitting of the variance-current relationship according to $\sigma^2 = i\,I - I^2 / N^P + \sigma_b^2$ (Sigworth, 1980) with the σ_b^2 constrained, where σ^2 is the variance, I is the current, i is the weighted-mean single channel current, N^P is the average number of channels open at the peak of the EPSC, and σ_b^2 is the variance of the background noise, which was estimated from the pre-stimulus period. The weighted mean single-channel conductance, γ, was determined by $\gamma = i / V$, where V is the driving force (the holding potential minus the measured reversal potential of +2 mV and +14 mV at CT and ML synapses, respectively). All mathematical manipulations were implemented with MATLAB (The MathWorks, Natick, MA, USA).

One of the most important concerns for applying this method to our system is that CT synapses are morphologically distal to recording site (Liu et al., 1995), which

could severely compromise the space clamp. However, it has been reported that the

estimated electrotonic length of relay neurons in dorsal and ventral lateral geniculate

nucleus (dLGN and vLGN) of rats (Crunelli et al., 1987) is ~ 0.7, suggesting that

thalamic relay neurons may be relatively electrotonically compact. In most analyzed

cases, especially CT EPSCs, the variance-current relationships were skewed to the

right (Fig. 2.12A), which was independent of the situations of alignment and existed

even in the case of almost perfect alignment; therefore, that may be attributable to the

kinetic properties of the non-NMDARs or asynchronous release (Hartveit and Veruki,

2006; Momiyama et al., 2003; Traynelis et al., 1993). Although the estimates of N^P

would be unreliable under this condition (Hartveit and Veruki, 2007; Heinemann and

Conti, 1992; Robinson et al., 1991; Silver et al., 1996; Traynelis and Jaramillo, 1998;

Traynelis et al., 1993), we fitted the initial 33% of the variance-current relationships

linearly to give estimates of weighted mean single-channel currents, which were

proposed to be relatively insensitive to the skewness of the relationships and the

electrotonic distance between the recording and synaptic sites (Benke et al., 2001;

Hartveit and Veruki, 2006; Robinson et al., 1991; Traynelis and Jaramillo, 1998;

Traynelis et al., 1993). N^P was calculated from I^P / i, where I^P is peak amplitude of

averaged EPSCs (Silver et al., 1996).

Histochemistry

In all experiments, 6.7 mM biocytin (Sigma) was routinely included in the internal solution. Neurons were filled by passive diffusion of biocytin from the patch pipette during the recording period, without the need of current application. After recording, pipettes were withdrawn and the brain slices were fixed overnight in 4% paraformaldehyde (Sigma) in 0.1 M phosphate buffer (PB, pH 7.4) at 4 °C. Slices were rinsed with PB several times after fixation and were subjected to histochemical staining procedures without further sectioning. They were treated with 3% H_2O_2 in 0.1 M PB for 30 minutes, rinsed in 0.03% Triton X-100 in phosphate- buffered saline (PBST), and then incubated for 1 hour at room temperature in PBST containing 2% bovine serum albumin (BSA) and 10% normal goat serum (NGS). The slices were then incubated overnight at 4 °C in PBST containing a 1 / 100 dilution of Avidin-Biotin Complex (ABC; Vector laboratories, Burlingame, CA). Finally, the cell was visualized with 3,3'-diaminobenzidine (DAB) as the chromogen. The staining results for the biocytin-filled neurons were examined and photographed under bright-field microscopy.

Drugs

Chemicals used for ACSF and internal solution were purchased from Merck (Damstadt, Germany). *N*-2,6-Dimethylphenylcarbamoylmethyl triethylammonium bromide (QX-314) was purchased from Alomone Laboratories (Jerusalem, Israel). DL-2-Amino-5-phosphonopentanoic acid (APV), 6,7-dinitroquinoxaline-2,3-dione (DNQX), nimodipine (Nim), spermine tetrahydrochloride, tetrodotoxin (TTX), and mibefradil were purchased from Tocris Cookson (Bristol, UK). MgATP, NaGTP, BAPTA, picrotoxin, strychnine, philanthotoxin-433 tris(trifluoroacetate) salt (PhTx-433), 1-naphthylacetyl spermine (NAS), and nickel chloride were purchased from Sigma (St. Louis, MO, USA). All drugs were made as stock solutions, stored at -20°C, and diluted to working concentration immediately before use. The experiments using nimodipine and PhTx-433 were performed in the dark to avoid drug deterioration.

Statistics

All data are presented as the mean ± S.E.M. The nonparametric Mann-Whitney-Wilcoxon U test was used for statistical comparison between unpaired data and Wilcoxon matched-pairs sign-ranks test was used for paired data. The

correlation analysis was performed by non-parametric Spearman's rank-order correlation test. The criterion for significance was $P < 0.05$ for all statistical tests. Origin (Microcal, Northhampton, MA, USA) and SAS (SAS, Cary, NC, USA) software were used for data analysis.

Results

Morphological and electrophysiological features of the ventrobasal nucleus (VBN) of rat thalamus
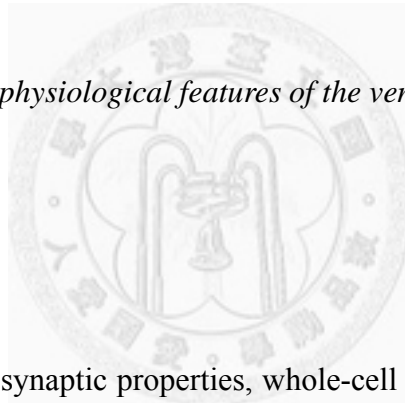
To characterize basic synaptic properties, whole-cell recordings were made from the VBN neurons in the horizontal slices (300 μm) prepared from young SD rats (Fig. 2.1). After the recordings, the biocytin-filled VBN neurons were stained by the *post hoc* ABC histochemistry, and the morphology of the recorded cells was revealed (Fig. 2.2). Typically, these recorded cells have polygonal soma shape with 6-10 large primary dendrites. These first-order dendrites usually coursed to visible swellings called whorls (Peschanski et al., 1984), from which they branched to the second-order dendrites; these second-order dendrites were thinner but exhibited similar patterns of

terminal branching, therefore giving a tufted, bushy appearance of dendritic

arborization. Moreover, most cells had easily identifiable axons (arrows in Fig. 2.2)

projecting toward cerebral cortex. These observations were consistent with the

descriptions of the relay neurons in rat VBN by Peschanski et al. (1984).

All the VBN neurons showed membrane-potential (V_m)-dependent dual firing

modes — continuous (tonic / regular) and burst spiking with the watershed for mode

switch at $V_m \sim$ -60 mV (Fig. 2.3A), which comes from the inactivation property of the

T-type voltage-gated calcium channels (VGCCs). At $V_m >$ -60 mV, depolarizing

current injection led to continuous firing of the VBN neurons, and a prominent delay

of the 1st action potential (AP) firing could be observed at $V_m =$ -60 ~ -50 mV (Fig.

2.3A$_1$); at $V_m <$ -60 mV, however, similar current injection led to high-frequency burst

firing of APs induced by the low-threshold spike (LTS) (Fig. 2.3A$_2$). In addition, clear

sag (Fig. 2.3A$_2$, star) and rebound burst firings (Fig. 2.3A, arrows) could be induced

by the injection of large hyperpolarizing currents.

After intracellular dialysis of QX-314 (5mM) into the VBN neurons, they fired

spikes with distinct kinetic properties: compared with the APs observed in

QX-314-free normal internal solution, these spikes had larger half-width, smaller

amplitude, and smaller slope of the rising phase, which could be blocked by specific L-type VGCC blocker nimodipine (10 µM) applied in the bath (Fig. 2.3B), implying that VBN neurons were endowed with a considerable number of L-type VGCCs to sustain this form of regenerative calcium spikes.

Basic properties of corticothalamic (CT) and lemniscal (ML) EPSCs

Whole-cell voltage clamp recordings (V_h = -70 mV) were made from the VBN neurons of horizontal slices, and a bipolar electrode was placed in internal capsule (*ic*) or medial lemniscus (*ml*) for corticothalamic (CT) or lemniscal (ML) pathway-specific stimulation, respectively (Fig. 2.4A).

The electrophysiological criteria for identifying these two pathways was established in the brain slices of mice as following (Castro-Alamancos, 2002a; Castro-Alamancos and Calcagnotto, 1999; Miyata and Imoto, 2006): first, CT EPSCs increased monotonically with increasing stimulus intensity; in contrast, ML EPSCs in most of VBN neurons showed all-or-none responses, while a few displayed two readily identifiable steps upon increasing stimulus intensity (Miyata and Imoto, 2006). In our horizontal VBN slices prepared from rats, similar pathway-specific differences
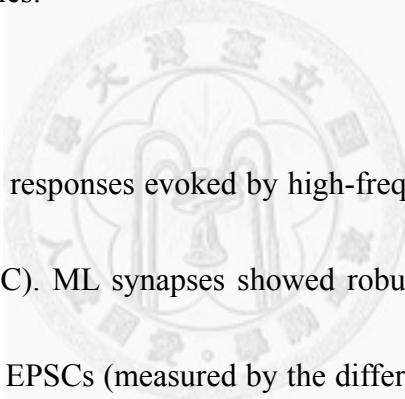
69

could be observed (Fig. 2.4B~C): CT EPSCs showed linear stimulus-response

relationship; however, EPSCs evoked by stimulating medial lemniscus (*ml*) consisted

of not only all-or-none, but also linear responses. Out of 662 VBN neurons tested,

only 122 neurons (18 %) showed clear all-or-none responses, which might reflect

native heterogeneity in the properties of ML synapses in rats. In this study, only the

EPSCs showing typical all-or-none characteristics were considered medial lemniscal

(ML) response, in accordance with the conventional criteria for ML EPSCs.

Occasionally, all-or-none responses were evoked with the electrode positioned locally

around the patched cell, in which cases their identities as from *ml* fibers or fibers from

layer V cortical neurons was not distinguishable (Reichova and Sherman, 2004;

Landisman and Connors, 2007); these data were discarded without further analysis.

Both the CT and ML EPSCs displayed short, constant latency, and followed

high-frequency (50 Hz) stimulation reliably (Fig. 2.5C), suggesting they are

monosynaptic in nature. Significant differences were observed in the onset latency,

10–90% rise time, and decay time constant (Table 2.2; see Discussion).

Second, the two pathways were different in short-term plasticity. The ML EPSCs

/ EPSPs showed paired-pulse depression (PPD), whereas the CT EPSCs / EPSPs

showed paired-pulse facilitation (PPF) in mouse VBN slices (Castro-Alamancos,

2002a; Castro-Alamancos and Calcagnotto, 1999; Miyata and Imoto, 2006). This prominent difference was also observed in our preparation of rat horizontal VBN slices (Fig. 2.5A~B, Table 2.2). Moreover, the differences in these two properties could be clearly observed from CT and ML EPSCs obtained from the same neurons (n = 5, data not shown). We also noted that, in response to paired-pulse stimulation (PPS), while the latency of the first EPSC was shorter than that of the second one for ML EPSCs, the latency of the first was longer than that of the second for CT EPSCs (Table 2.2); in other words, CT EPSCs showed conduction supernormality, while ML EPSCs showed conduction subnormality (Landisman and Connors, 2007). Taken together, according to these physiological criteria, the CT and ML pathways in the rat VBN slices could be successfully identified and recruited, and their basic properties were consistent to those from the studies conducted in mice.

We found that locally-evoked EPSCs showed similar rise time, decay time constant, latency shift, small unitary evoked event (i.e. minimally-stimulated response, as compared to ML EPSCs), linear characteristics, and PPF (Table 2.1), all consistent with the properties of EPSCs evoked by stimulation of internal capsule (*ic*). Locally-evoked EPSPs also share similar characteristics with EPSPs evoked from *ic* in many aspects (Fig. 2.6). Also considering the dominant number of corticothalamic

synapses onto VBN neurons (Jones, 2007; Sherman and Koch, 1986), we postulated

that the locally-evoked responses virtually originated from the corticothalamic inputs.

Because of the very low success rate of obtaining CT and ML EPSCs simultaneously

from the same neuron (6 %; out of 88 VBN neurons tested, we simultaneously

recruited CT and ML EPSCs only from 5 neurons), especially under the long physical

distance between internal capsule (*ic*) and medial lemniscal fibers (*ml*), this working

hypothesis was of great practical importance, especially for investigating the input

specificity of many properties.

We also compared the responses evoked by high-frequency stimulations (50 Hz)

at both pathways (Fig. 2.5C). ML synapses showed robust short-term depression in

that peak amplitude of ML EPSCs (measured by the difference of peak EPSC and the

current just before the stimulating artifact) reached maximal depression at the 3rd

stimulation (n = 4), while CT EPSC showed short-term facilitation but only strong

enough to overcome the saturation and desensitization of postsynaptic receptors (Sun

and Beierlein, 2011) and the depletion of presynaptic vesicles at the 2nd stimulation

(n = 3). It is noteworthy that the postsynaptic summation of CT EPSC was much

better than ML EPSC, as indicated by the continual increase of the inward current

measured just before every successive stimulus artifact, even after the maximal

change of EPSC had been achieved.

The peak current ratio of the NMDAR- to non-NMDAR-mediated EPSCs was higher

at CT synapses than ML synapses

We next investigated the relative composition of NMDAR-mediated and

non-NMDAR-mediated components of CT and ML EPSCs. CT and ML EPSCs were

completely blocked by 10 μM DNQX applied in the bath, indicating EPSCs of both

pathways were mainly contributed by the non-NMDA ionotropic glutamate receptors

at V_h = -70 (Fig. 2.7A). Non-NMDAR-mediated components were first evoked at -90

mV, which was then blocked by 10 μM DNQX, and then EPSCs were evoked at +60

mV to relieve the voltage-dependent Mg^{2+} block of the NMDA receptors (Fig. 2.7B,

obtained from the same neuron); the outward currents recorded at +60 mV could be

blocked by 100 μM DL-APV in all cases, indicating they were indeed mediated by

NMDA receptors. The peak current ratios of NMDAR- to non-NMDAR-mediated

EPSCs were similar for synapses recruited by stimulating internal capsule (3.83 $\pm$

1.20, n = 6) and by local stimulation (1.70 $\pm$ 0.39, n = 8) (P > 0.05,

Mann-Whitney-Wilcoxon test) and thus pooled together (2.62 $\pm$ 0.61, n = 14), which

was significantly higher than that of the ML synapses (0.43 $\pm$ 0.05, n = 10; P < 0.0001,

Mann-Whitney-Wilcoxon test) (Fig. 2.7C). These results implied that the relative contribution of the NMDAR-mediated component was greater at CT than ML synapses, conferring distinct potential of synaptic transmission and plasticity on these two synapses.

The evidence for the differential expression of calcium-permeable AMPA receptors (CP-AMPARs) at CT and ML synapses

Characterization of the I-V relationships of the non-NMDAR-mediated EPSCs could provide basic information of fast excitatory synaptic transmission such as reversal potential and rectification index. The I-V curve of ML EPSCs showed clear linearity with the rectification index (RI) of 0.96 ± 0.15 (n = 9) and the reversal potential of 17.71 ± 4.88 mV (n = 9), comparable to the properties of non-NMDA receptors at typical synapses of mammalian central nervous system (CNS) (Golshani et al., 1998); the I-V curve of CT EPSCs was inward-rectifying with the RI of 0.50 ± 0.05 (n = 9) and the reversal potential of 4.14 ± 3.24 mV (n = 9). Polyamine-mediated inward rectification is a landmark property of the calcium-permeable non-NMDA receptors (Bowie and Mayer, 1995; Donevan and Rogawski, 1995; Iino et al., 1990); to examine the effects of polyamines on the

inward rectification, we further characterized the I-V relationship using the internal solution supplemented with 0.1 mM spermine. The new I-V curves of CT EPSCs (RI = 0.74 $\pm$ 0.09, reversal potential = -1.67 $\pm$ 4.79 mV; n = 7) and ML EPSCs (RI = 0.89 $\pm$ 0.08, reversal potential = 8.57 $\pm$ 2.29 mV; n = 7) were similar to those obtained without spermine (see Fig. 2.8B; all P > 0.05, Mann-Whitney-Wilcoxon test) and thus pooled together, respectively (CT EPSCs: RI = 0.61 $\pm$ 0.05, reversal potential = 1.60 $\pm$ 2.78 mV, n = 16, Fig. 7A$_2$; ML EPSCs: RI = 0.93 $\pm$ 0.09, reversal potential = 13.71 $\pm$ 3.07 mV, n = 16; junction potential was estimated to be ~ + 10 mV and left uncorrected) (Fig. 2.8A, C). Taken together, the RI of the non-NMDAR-mediated EPSCs at CT synapses was significantly smaller than that at ML synapses, indicating the CT EPSCs showed inward rectification.

To further examine the relationship between inward-rectification and expression of calcium-permeable AMPA receptors (CP-AMPARs), we tested the sensitivity of EPSCs to polyamine toxins which selectively block CP-AMPARs. After a 5-min stable baseline, 10 μM philanthotoxin-433 (PhTx-433), a wasp polyamine toxin (Andersen et al., 2006; Washburn and Dingledine, 1996), was applied in the bath, which reduced the amplitude of locally-evoked EPSCs (55.4 $\pm$ 15.4 % compared with baseline, n = 6) but not ML EPSCs (99.4 $\pm$ 6.0 % compared with baseline; n = 6)

(Fig. 2.9; CT and ML EPSCs obtained from the same neurons). Similarly, 250 μM

1-naphthylacetyl spermine (NAS), a synthetic analog of Joro spider toxin (JSTX)

(Blakemore et al., 2006; Koike et al., 1997; Ma and Lowe, 2007), also reduced the

amplitude of CT EPSCs (53.7 $\pm$ 5.5 % compared with baseline; n = 6) but not ML

EPSCs (95.5 $\pm$ 4.9 % compared with baseline; n = 4) (Fig. 2.10). It has been shown

that, at synapses containing CaP-AMPARs, paired-pulse ratio (PPR) of evoked EPSCs

is enhanced by activity-dependent relief of polyamine block, a mechanism dependent

on V_h at which paired pulses are applied (Rozov et al., 1998; Rozov and Burnashev,

1999). For every relay neuron tested, PPR of CT EPSC at the $V_h < 0$ mV is higher

than that at the $V_h > 0$ mV, whereas it was not the case for ML EPSC, consistent with

the selective expression of CaP-AMPARs at CT synapses (Fig. 2.11). It has also been

reported that calcium-permeable AMPAR has higher single-channel conductance than

calcium-impermeable AMPAR (Guire et al., 2008; Oh and Derkach, 2005; Smith et al.,

1999; Swanson et al., 1996; Swanson et al., 1997). Therefore, peak-scaled

nonstationary noise analysis was applied to compare the weighted mean conductance

of single synaptic non-NMDARs at CT and ML synapses (Fig. 2.12). The results

showed that non-NMDARs at CT synapses had a significantly higher mean

single-channel conductance than at ML synapses (7.5 $\pm$ 1.1 pS, n = 5 and 3.1 $\pm$ 0.3

pS, n = 7 for CT and ML synapses, respectively; P < 0.01, Mann-Whitney-Wilcoxon

test). Considering the significantly higher peak amplitude of ML EPSC than CT EPSC under our experimental condition, the average number of non-NMDARs open at the peak of EPSC was very much larger at ML synapses than CT synapses (CT synaspes: 95 $\pm$ 20, n = 5; ML synapses: 1732 $\pm$ 417, n = 7; P < 0.01, Mann-Whitney-Wilcoxon test). However, it is noteworthy that the stimulus intensity normally used in our experiments was presumably close to minimal stimulation for ML synapses, but not CT synapses, since stimulus intensity was always adjusted to recruit ML EPSC at its first step (e.g. Fig. 2.4B), which had small CV and quantal variability (e.g. Fig. 2.9, Fig. 2.10); in contrast, because of the linearity of stimulus-response relationship of CT EPSCs (Fig. 2.4B~C), it was difficult to identify an optimal intensity for minimal stimulation, and stimulus intensity was always adjusted to recruit CT EPSC that was readily measurable, in which case EPSCs were accompanied by a higher quantal variability (e.g. Fig. 2.9, Fig. 2.10). Therefore, under this condition, the number of unitary events recruited at CT and ML synapses might be different. To summarize, we found that CP-AMPARs are preferentially expressed at CT synapses, rather than ML synapses.

Discussion

As one of the most important animal model for studying the electrophysiology of somatosensory system, the *rat* VBN system was mostly studied *in vivo* (ex., Mishima, 1992; Salt, 1986); in those studies conducted *in vitro* (Kao and Coulter; 1997; Landisman and Connors, 2007; Leamey and Ho, 1998), the analyses of the properties of CT and ML synapses were basically not carried out in a systematic and comparative manner, although valuable information is still available in several studies (Landisman and Connors, 2007; Miyata and Imoto, 2006; Reichova and Sherman, 2004). In this study, several pathway-specific properties showed great consistency with those described in previous literature, demonstrating the successful identification of CT and ML pathways in our system.

First, the latency of EPSC was shorter at ML synapses than CT synapses (Castro-Alamancos, 2002a; Landisman and Connors, 2007). We also observed the "supernormality" of conduction (Landisman and Connors, 2007; Swadlow and Waxman; 1975) at CT inputs: that is, during the paired-pulse stimulations, the onset latency of the second CT EPSC decreased relative to that of the first one, which was proposed to be specific to the CT axons originated from the layer VI neurons of

cerebral cortex (Li et al., 2003; Kelly et al., 2001); in our system, the decrease in the

onset latency of the second EPSC was ~ 0.3 ms, consistent with that observed in rat

thalamocortical slice system (Landisman and Connors, 2007). There are two types of

corticothalamic fibers (Deschênes et al., 1998; Landisman and Connors, 2007;

Reichova and Sherman, 2004; Rouiller and Welker, 2000), namely, those arising from

layer V and layer VI pyramidal neurons, with the former ones showing

electrophysiological and ultrastructural similarities to the primary sensory inputs

(such as lemniscal and retinal inputs). Because the corticothalamic projections to the

somatosensory thalamus of rodents were found to originate mainly from the layer VI

(Deschênes et al., 1998; Killackey and Sherman, 2003; Reichova and Sherman, 2004;

Rouiller and Welker, 2000; Van Horn and Sherman, 2004), the similarities of the

EPSCs evoked both by stimulating internal capsule and local stimulation to those

coming from layer VI neurons (i.e., linear EPSCs and PPF; Landisman and Connors,

2007; Reichova and Sherman, 2004; Li et al., 2003) further validate our pathway

identifications. Second, the rise time of ML EPSCs was significantly shorter than that

of CT EPSCs (Miyata and Imoto, 2006). In principle, this difference could result from

differential cable filtering introduced by different electrotonic distances these two

synapses away from the recording site (soma), as CT synapses contact the dendrites

more distally than ML synapses (Bourassa et al., 1995; Liu et al., 1995). However,

this explanation is not consistent with the observation that the difference of weighted decay time constants between CT and ML EPSCs was relatively much smaller (Table 2.1), since the cable filtering effect, in theory, can be reflected more unambiguously in the decay phase of EPSC than the rising phase, especially in that the dynamics of glutamate release and non-NMDAR channel gating can have dominant influences over rising kinetics. Consistent with this argument, it was reported that in the dorsal and ventral lateral geniculate nucleus (dLGN and vLGN) of rat, the estimated electrotonic length of relay neurons is ~ 0.7, suggesting that thalamic relay neurons are electronotically compact (Crunelli et al., 1987). If this is true, alternative explanations for the discrepancy in the rise times of CT and ML EPSCs could be differential expression of kainite type ionotropic glutamate receptors (Miyata and Imoto, 2006) or differential asynchrony of presynaptic glutamate release. Third, CT EPSCs showed different behaviors in stimulus-relationships and short-term plasticity (Arsenault and Zhang, 2006; Castro-Alamancos, 2002a; Castro-Alamancos and Calcagnotto, 1999; Kao and Coulter, 1997; Landisman and Connors, 2007; Mishama, 1992; Miyata and Imoto, 2006; Reichova and Sherman, 2004), which have been correlated with dintinct ultrastructural characteristics of their fiber terminals (Bourassa et al., 1995; Li et al., 2003; Mineff and Weinberg, 2000; Špacek and Lieberman, 1974) and may, coupled to the state-dependent neuromodulation

(Castro-Alamancos 2002; Castro-Alamancos and Calcagnotto, 2001), confer distinct properties of temporal filtering on these two synapses (Fortune and Rose, 2001; Miyata and Imoto, 2006). For the synapses expressing CP-AMPARs, the use-dependent relief of CP-AMPARs from polyamine block can contribute to an increase of PPR at Vm < 0 mV (Bowie et al., 1998; McBain, 1998; Rozov and Burnashev, 1999), which could also be observed at CT synapses instead of ML synapses. The molecular composition of vesicular glutamate transporters was also shown to be different between corticothalamic and primary sensory pathways to the mouse VBN, suggesting another possible determinant for the PPR at these two synapses (Graziano et al., 2008). Fourth, the peak current ratio of NMDAR- to non-NMDAR-mediated EPSCs of CT synapses was significantly higher (Arsenault and Zhang, 2006; Miyata and Imoto, 2006). The properties of kinetics, short-term plasticity, and postsynaptic integration of synaptic inputs were proposed to shape the neuronal outputs in response to high-frequency inputs (Zucker, 1989); together with all the pathway-specific properties described above, different composition of glutamate receptors at the two synapses can also serve to underlie those NMDAR- and CT-dependent priming and modulation of sensory information relay through VBN thalamus described *in vivo* (Eaton and Salt, 1996; Salt, 1986; Steriade, 1993; Temereanca and Simons, 2004; Krupa et al., 1999; Fanselow et al., 2001).

The evidence for the differential expression of CP-AMPARs at CT and ML synapses

Our experimental results imply that CP-AMPARs may be differentially expressed at CT and ML synapses. More than AMPARs, kainate receptors (KARs) have been reported to contribute to the fast EPSCs at CT synapses (Miyata and Imoto, 2006) and, therefore, may also contribute to the rectification behavior, weighted mean conductance, and sensitivity to polyamine toxins depending on their conditions of molecular composition and RNA editing at the synapses (Kamboj et al., 1995; Herb et al., 1992; Howe et al., 1996; Sommer et al., 1991; Swanson et al., 1996; Burnashev et al., 1995).

Complementary peaked-scaled nonstationary noise analysis was applied to evoked responses of CT and ML synapses to compare their weighted mean single-channel conductances of synaptic non-NMDARs. Despite the dramatic difference in the amplitude of evoked unitary EPSCs between CT and ML pathways, the latter of which was typically minimally stimulated with the stimulus intensity range we normally used, the result showed that the trend of the difference in

single-channel conductance was, however, opposite to that of the difference in unitary EPSC amplitide: compared to ML responses, CT responses composed of smaller unitary events were contributed by non-NMDARs with larger single-channel conductance, which supported the experimental interpretation that CaP-AMPARs are preferentially expressed at CT, but not ML, synapses.

The peaked-scaled nonstationary noise analysis yielded the weighted mean conductance of 7.47 ± 1.15 pS for the non-NMDARs of CT synapses, which is much higher than calcium-impermeable non-NMDARs (Guire et al., 2008; Oh and Derkach, 2005; Smith et al., 1999; Swanson et al., 1996; Swanson et al., 1997) but at the same level with calcium-permeable non-NMDARs (or synaptic populations containing them) estimated in several other systems, such as 7-8 pS (Swanson et al., 1997), 5.4 pS (Swanson et al., 1996), 5.4 pS (Smith et al., 1999), 4.9 pS (Guire et al., 2008), and 11.5 pS (Derkach et al., 1999); although higher estimates were also reported (Lei et al., 2003; Mameli et al., 2007; Soto et al., 2007), reasonable variations should be acceptable, which may result from the diversity of native accessory proteins like transmembrane AMPAR regulatory proteins (TARPs) (Soto et al., 2007), molecular biophysics, developmental regulations (Ho et al., 2007; Kumar et al., 2002; Monyer et al., 1991; Shin et al., 2005; Smith et al., 1999; Smith et al., 2000; Wisden and Seeburg,

1993), receptor occupancy (Gebhardt and Cull-Candy, 2006), or can be explained by

possible overestimation introduced by asynchronous release (Guire et al., 2008). In

our experiments, the rectification indices (RIs) obtained without and with spermine

supplementation were similar, which is also the case in olfactory nerve-external tufted

cell synapses in the olfactory glomerular circuitry of rats (Ma and Lowe, 2007) and

may be explained by: (1) the existence of diffusion barriers coming from fine

dendritic geometry, which can hinder the washout of endogenous polyamines and the

loading of spermine (Ma and Lowe, 2007), (2) the usage of MgATP in the internal

solution, possibly offering too low intracellular $[ATP^{2-}]$ to chelate the native

polyamines (Meksuriyen et al., 1998; Soto et al., 2007; Watanabe et al., 1991) in the

spermine-free case, (3) the properties of native regulatory proteins like TARPs, which

can attenuate the intracellular polyamine block of CP-AMPARs, therefore obscuring

the sensitivity of spermine-loading experiments and markedly reducing the inward

rectification (Soto et al., 2007), compatible with the relatively higher RI of the EPSCs

at CT synapses, and (4) the unknown identity and native concentration of the

polyamines in local dendrites for effective channel block (Ma and Lowe, 2007). In the

VPM slices of juvenile *mouse* aged 11-13 and 20-24 days, Arsenault and Zhang (2006)

reported that lemniscal EPSCs showed age-independent inward-rectifying I-V curves,

by which they proposed GluR2-lacking AMPARs were expressed at lemniscal

synapses. One possible explanation for this difference is species difference. They further cited two electron microscopy (EM) studies comparing the GluR2/3 immunolabelling of corticothalamic and lemniscal synapses onto VPM or VPL of *adult* rats (Liu, 1997; Mineff and Weinberg, 2000) to support their argument. The citation of Mineff and Weinberg (2000) is, however, not appropriate due to the statistical insignificance of GluR2/3 labeling between corticothalamic and lemniscal synapses, and the animal age used in both studies (instead of juvenile animals) is another critical difference. Besides, functional glutamate receptors are tetramers with the subunit composition very critical to the biophysics like rectification, and by EM approach one can only detect the expression level of receptor subunits without knowing the assembly and composition of functional receptors *in situ*. Quantitative inconsistency also occurs between the GluR2/3 immunolabelling data of the two EM studies, and different staining techniques, small sample number (n = 1 in Liu, 1997), as well as the antibody specificity may also concern in the discrepancy between electrophysiological and morphological data.

CP-AMPARs have been proposed to play a great variety of roles in the input-specific synaptic transmission and dynamic information processing, such as precise control of spike timing (Geiger et al., 1995; Geiger et al., 1997; Lawrence et

al., 2004; Walker et al., 2002), induction / expression / consolidation / maintenance of activity-dependent, homeostatic, or drug-induced long-term synaptic plasticity (Asrar et al., 2009; Bellone and Lüscher, 2005; Bellone and Lüscher, 2006; Clem and Barth, 2006; Derkach et al., 1999; Desai et al., 2002; Goel et al., 2006; Guire et al., 2008; Ju et al. 2004; Kakegawa et al., 2004; Laezza et al., 1999; Liu and Cull-Candy, 2000; Mahanty and Sah, 1998; Mameli et al., 2007; Oh and Derkach, 2005; Pelkey et al., 2005; Plant et al., 2006; Sutton et al., 2006; Thiagarajan et al., 2005; Toth et al., 2000; Watt et al., 2000), a postsynaptic form of short-term plasticity (Bowie et al., 1998; McBain, 1998; Rozov et al., 1998; Rozov and Burnashev, 1999), developmental synaptic function (Ho et al., 2007; Kumar et al., 2002; Monyer et al., 1991; Shin et al., 2005; Smith et al., 1999; Smith et al., 2000; Wisden and Seeburg, 1993), and activity- and pathophysiology-dependent synaptic modulation through the regulation of endogenous polyamines (Aizenman et al., 2002; Aizenman et al., 2003; Hayashi et al., 1993; Shin et al., 2005); whether the specific targeting of CA-AMPARs to thalamic CT synapses underlies these functions is unknown. Moreover, corticothalamic inputs are periodically activated under many normal (like some stages of non-rapid eye movement sleep) and abnormal (like absence seizures) physiological conditions (Crunelli et al., 2006; Jones, 2007; Kostopoulos, 2001; McCormick, 2002; McCormick and Bal, 1997; Meeren et al., 2005; Sanchez-Vives and McCormick,

2000; Steriade et al., 1993; Steriade and Contreas, 1995; Timofeev and Steriade, 1996), and it is therefore very interesting to know whether repetitive activations of the additional calcium pathways mediated by calcium-permeable non-NMDARs at thalamic CT synapses have any functional impacts.

Figures

Figure 2.1 Anatomical features of the ventrobasal nucleus (VBN, including VPM and VPL) of rat thalamus

Acute horizontal (**A**) and coronal (**B**) brain slices were prepared from SD rats (P13-P24). EPSCs were evoked by stimulating either medial lemniscus (*ml*) or internal capsule (*ic*), and then the recorded cells were stained with ABC histochemistry. $A_1 \sim A_2$, Comparison of the rat brain atlas (Paxinos & Watson, 2007) and bright field microscopy of horizontal slice. A_3, Enlarged view of the dashed box in A_2. In some cases, we observed a small heterogeneous zone locating in the border of VPL (arrows). $B_1 \sim B_2$, Comparison of the rat brain atlas and bright field microscopy of coronal slice. Rt, reticulat nucleus.
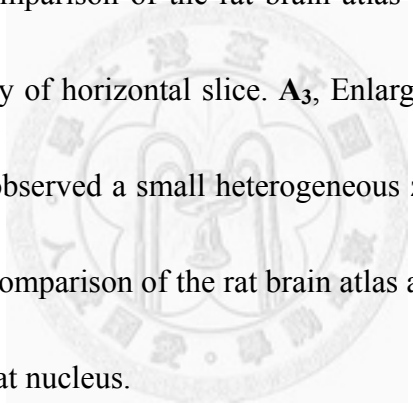
Figure 2.1
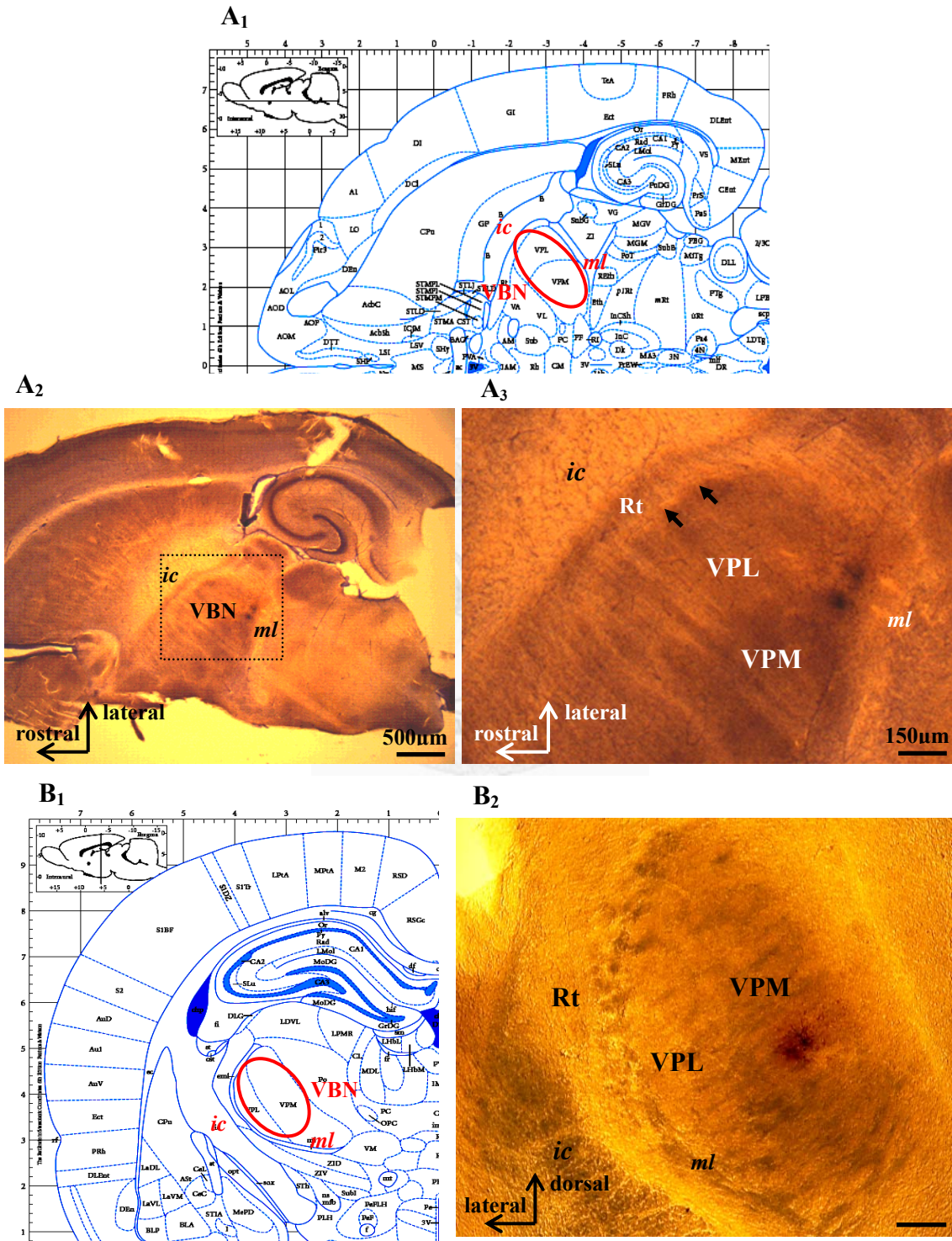
Figure 2.2 Morphology of the VBN relay neurons of rat thalamus

A~C, Typical examples of biocytin-filled cells stained with ABC histochemistry after whole-cell recording. The polygonal shape of soma, "whorl" of the primary dendrites, and the tufted, bushy patterns of dendritic arborization were consistent with those described in the previous literature (**D**, from Peschanski et al., 1984; see also Jones, 2007). Most cells had easily identifiable axons (arrows) projecting toward cerebral cortex.

Figure 2.2
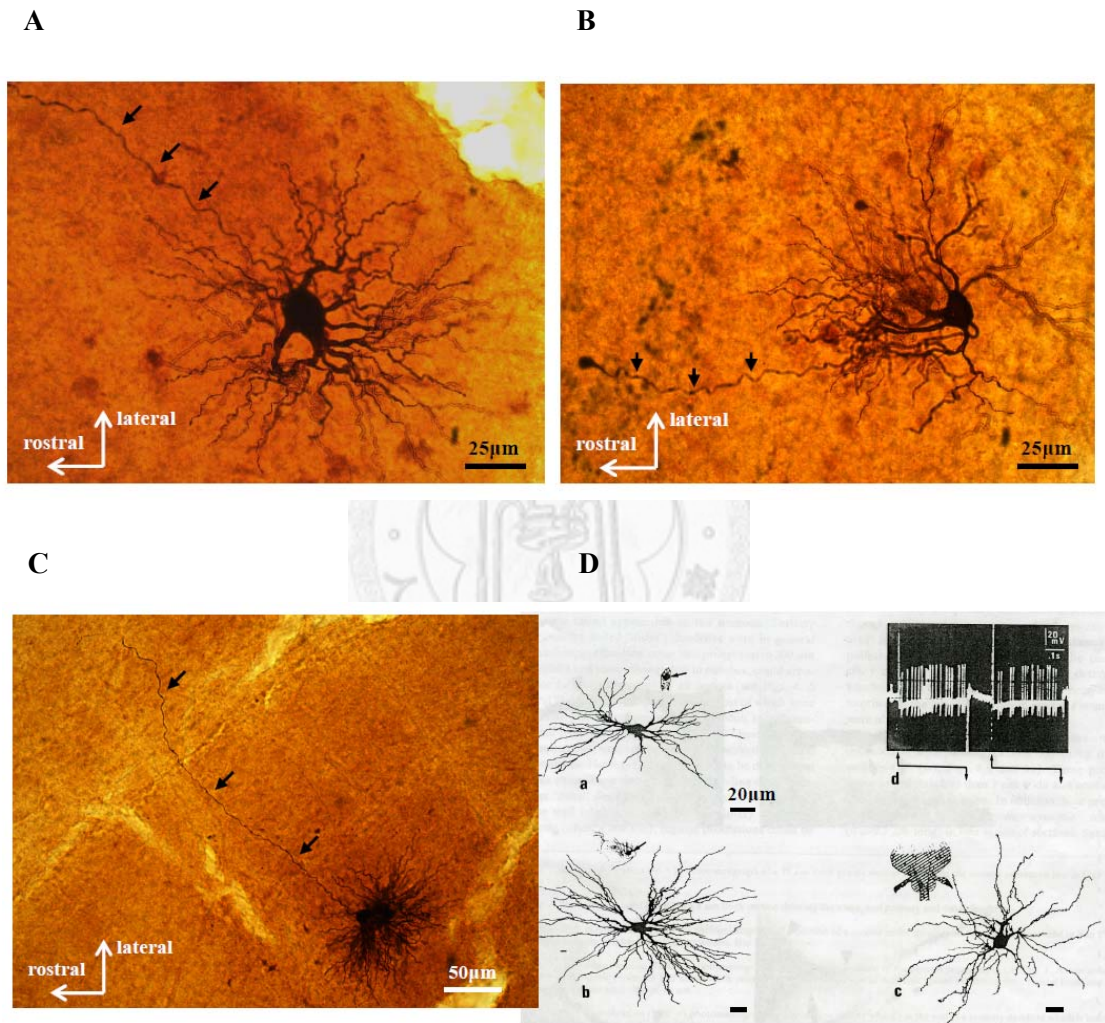
Figure 2.3 Firing modes of VBN relay neurons

VBN relay neurons showed membrane potential (V_m)-dependent firing properties. **A,** In response to steady depolarizing current injection, VBN cells fired in continuous (tonic / regular) spiking mode at $V_m \sim$ -55 mV (**A₁**) while in burst spiking mode at $V_m \sim$ -55 mV (**A₂**). It has been well characterized that the burst, high-frequency Na^+ spiking is triggered by the underlying low-threshold spike (LTS), which is dependent on the activation of T-type voltage-gated calcium channels (VGCCs). Steady hyperpolarizing current injection induced a sag at hyperpolarized V_m (star in **A₂**), termination of which triggered rebound burst spiking (arrows), which can be explained by the de-inactivation, and thus the increase in the availability of T-type VGCCs during the hyperpolarized phase. **B**, VBN neurons can fire broaden spikes (half-width $\sim$ 35 ms) with significantly slower rising kinetics and smaller amplitude after intracellular dialysis of QX-314 (5 mM), which was blocked by selective L-type VGCC blocker nimodipine (10μM) applied in the bath, indicating that their ionic basis is calcium.

Figure 2.3

A₁   **A₂**

-55 mV

+100 pA
-190 pA

-70 mV

+100 pA
-190 pA

*

30 mV

200 ms

B

QX-314 (5 mM)   **+   Nimodipine (10 μM)**
(internal solution)

-40 mV

-40 mV

10 mV

250 ms
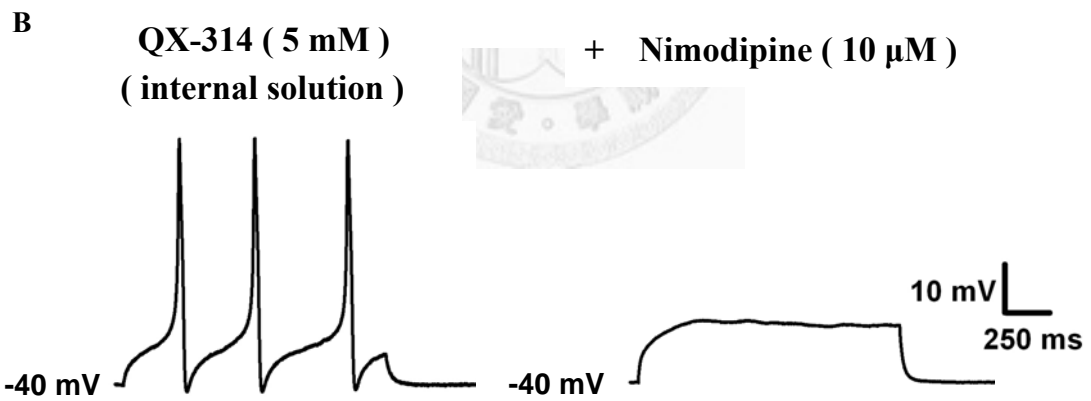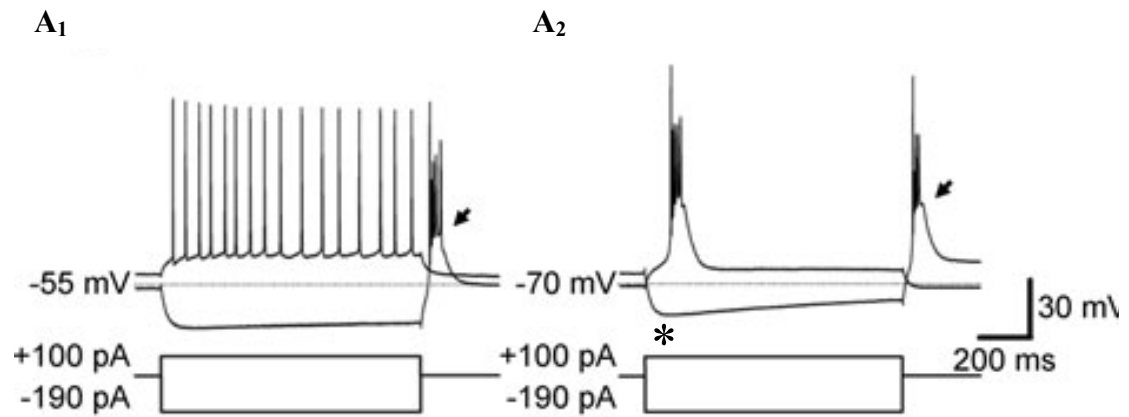
Figure 2.4 Stimulus-response relationships of the EPSCs elicited by stimulation of corticothalamic (CT) and lemniscal (ML) fibers

A, Schematic illustration of experimental configuration. Reproduced from Min (unpublished). **B~C,** Representative examples of EPSC traces elicited by stimulation of internal capsule (*ic*) (CT EPSC) and medial lemniscus (*ml*) (ML EPSC) (**B**) and summary of the peak synaptic responses upon increasing stimulus intensity (**C**). ML EPSCs had significantly smaller 10-90% rise time and relatively larger peak amplitude than CT EPSCs. Typically, ML EPSCs responded to different stimulus intensity in an all-or-none fashion, while CT EPSCs increased in peak amplitude monotonically with increasing stimulus intensity, showing a linear relationship. Please see text for detailed description of pathway characterization. The V_m of VBN neurons was held at -70 mV.
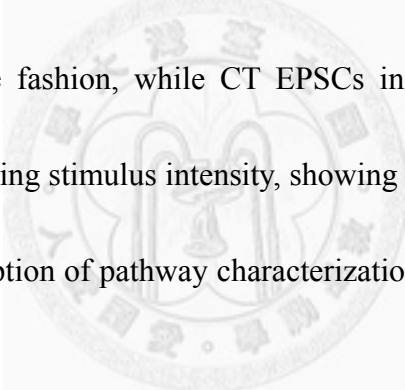
Figure 2.4
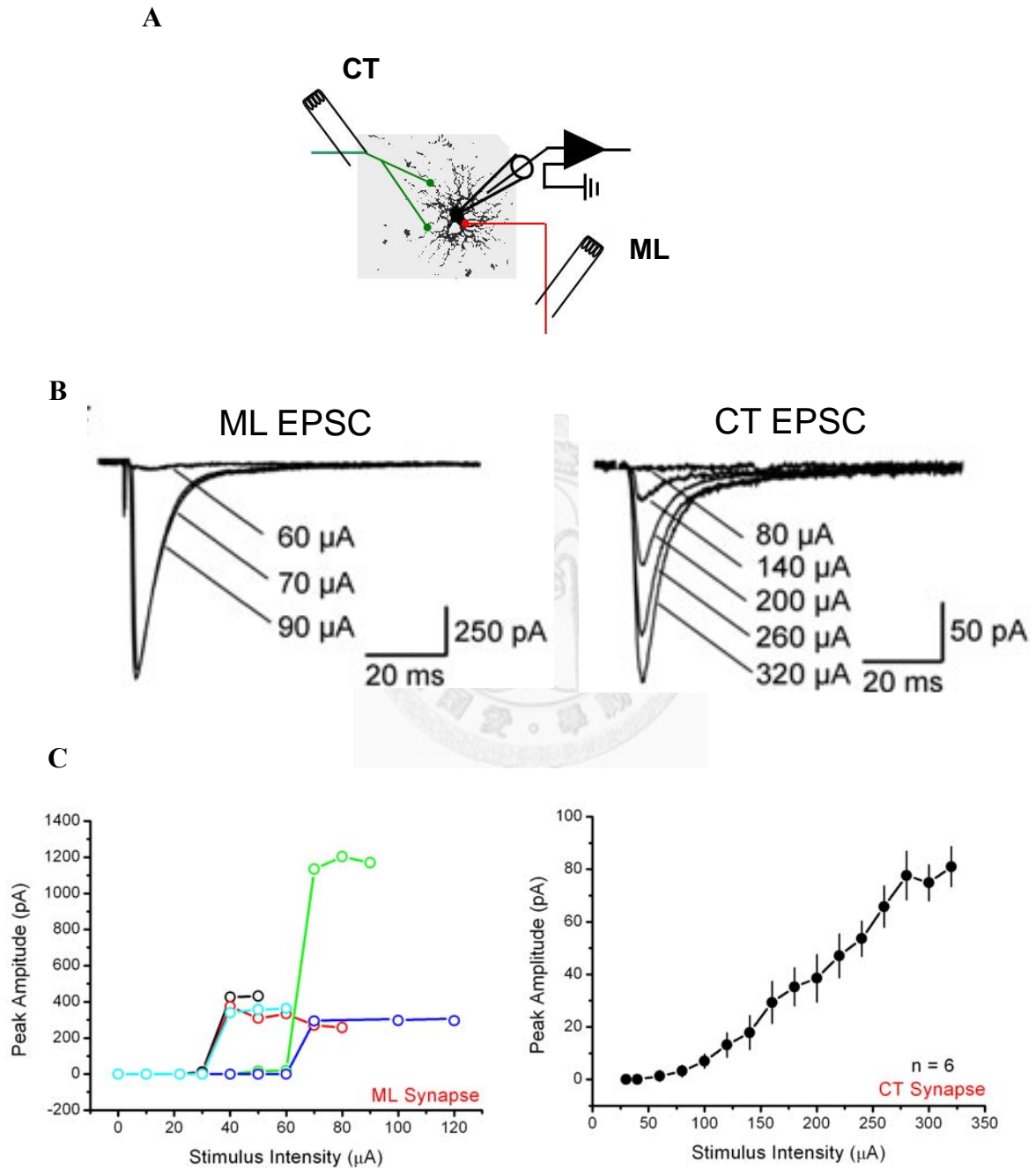
Figure 2.5 Short-term plasticity of corticothalamic (CT) and lemniscal (ML) EPSCs

A, Representative synaptic responses elicited by paired-pulse stimulation of CT and ML fibers. ML EPSCs showed paired-pulse depression (PPD), whereas CT EPSCs showed paired-pulse facilitation (PPF). These responses were evoked from the same relay neuron. **B**, Summary of paired-pulse ratio plotted as a function of inter-pulse interval. Short-term plasticity of CT and ML EPSCs was still observed at the interval of up to 1000 ms. **C**, Representative responses to high-frequency stimulations (50 Hz) of CT and ML synapses. ML synapses showed robust short-term depression in that peak amplitude of ML EPSCs (measured by the difference of peak EPSC and the current just before the stimulating artifact) reached maximal depression at the 3rd stimulation (n = 4), while CT EPSC showed short-term facilitation but only strong enough to overcome the saturation and desensitization of postsynaptic receptors (Sun and Beierlein, 2011) and the depletion of presynaptic vesicles at the 2nd stimulation (n = 3). It is noteworthy that the postsynaptic summation of CT EPSC was much better than ML EPSC, as indicated by the continual increase of the inward current measured just before every successive stimulus artifact, even after the maximal change of EPSC had been achieved. These traces were averaged from 3 waveforms.
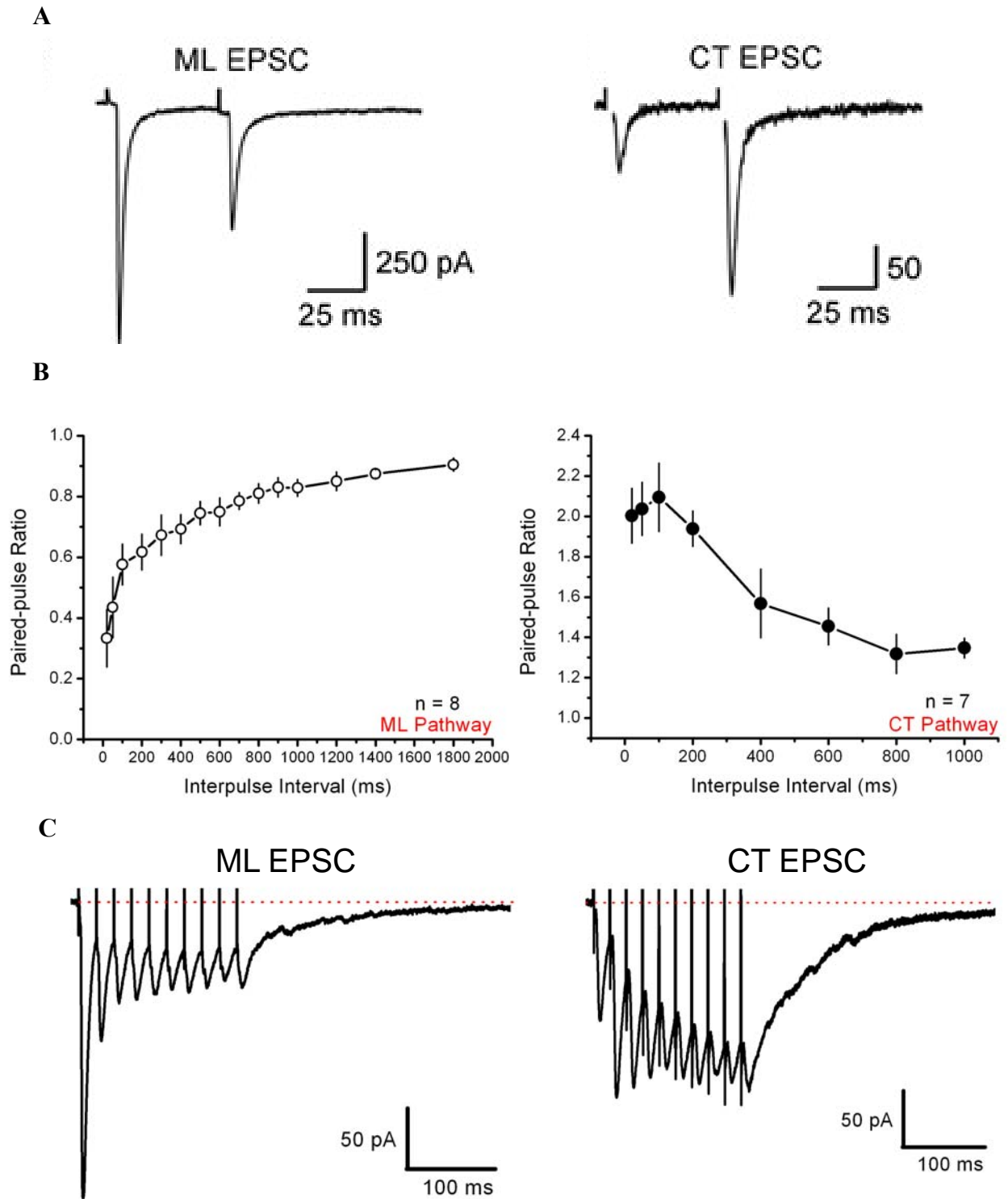
Figure 2.5

Figure 2.6 Comparison of EPSPs elicited by stimulation of internal capsule and local stimulation

Internal capsule (*ic*)-evoked EPSPs and locally-evoked EPSPs have similar kinetics and short-term plasticity, suggesting their common cortical origin.
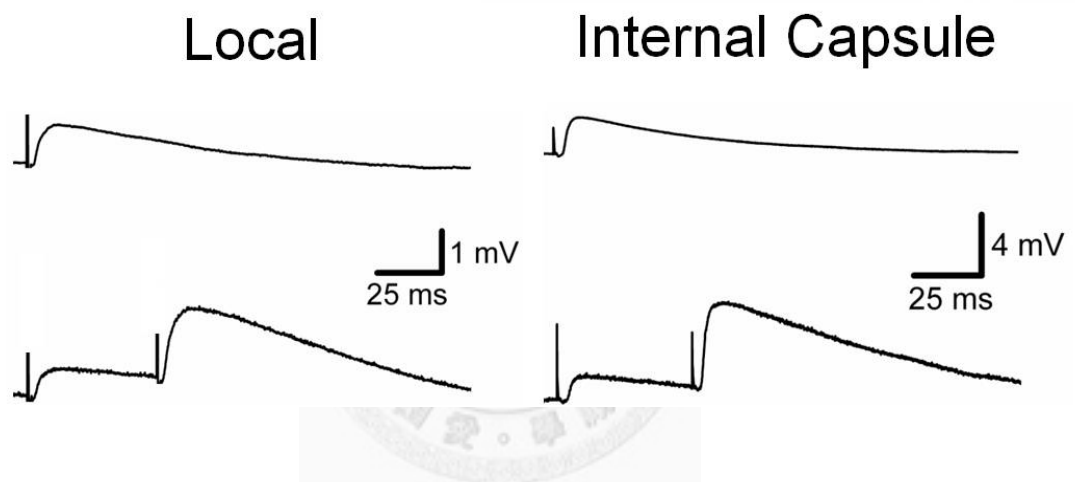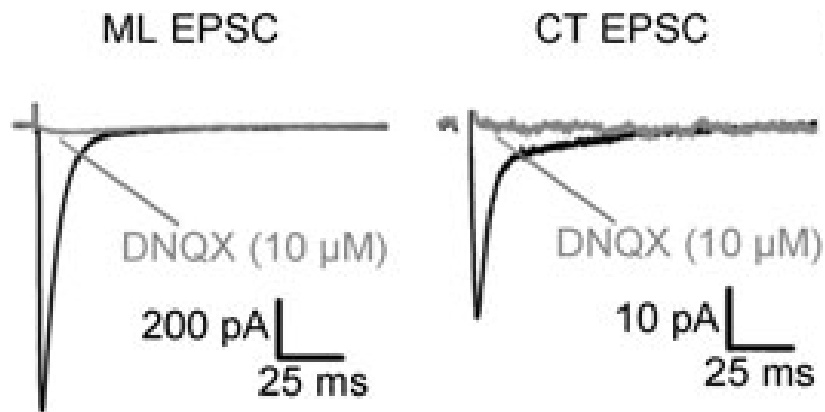
Figure 2.6

Local   Internal Capsule

1 mV
25 ms

4 mV
25 ms

Figure 2.7 Peak current ratio of NMDAR- to non-NMDAR-mediated EPSC at CT and ML synapses

A, At the V_m held ~ -70 mV, both CT and ML EPSC were completely blocked by 10μM DNQX applied in the bath. All traces were averaged from 10~15 consecutive sweeps. **B~C,** Representative example (**B**) of NMDAR- and non-NMDAR-mediated EPSCs obtained from the same relay neuron, and the summary of data (**C**), showing a larger peak current ratio of NMDAR- to non-NMDAR-mediated EPSC at CT than ML synapses. The non-NMDAR-mediated EPSCs (inward current traces) were recorded at -90 mV, and then the NMDAR-mediated EPSCs (outward current traces) were obtained at +60 mV in the presence of 10μM DNQX, which in turn can be blocked with 100 μM DL-APV. For comparison, the peak current amplitude of NMDAR-mediated EPSC at ML synapses was scaled to match that at CT synapses. The summarized data include one experiment in which the CT EPSCs and ML EPSCs were evoked in the same relay neuron.
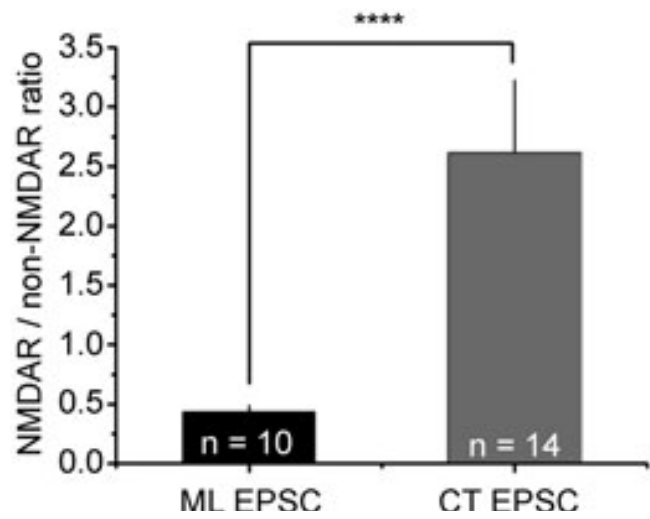
Figure 2.7

A

B

C
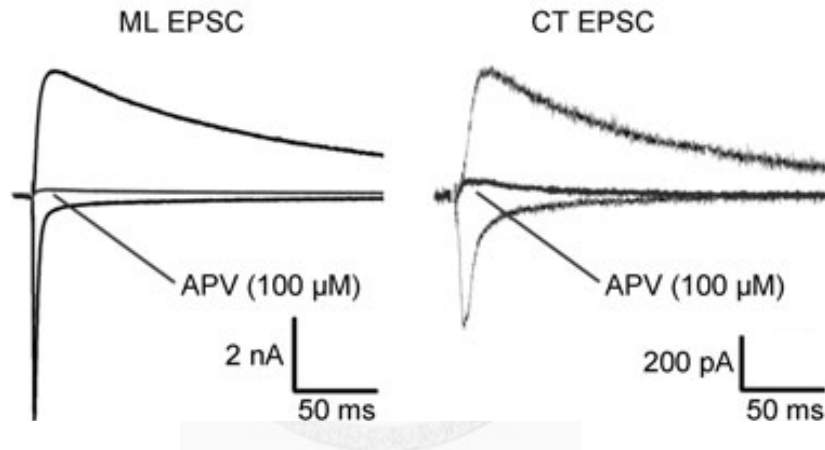
Mann-Whitney-Wilcoxon test
**** P < 0.0001

101

Figure 2.8 Current-voltage (I-V) relationship and rectification property of non-NMDAR-mediated EPSC at CT and ML synapses

A, The I-V relationship of non-NMDAR-mediated EPSC. The dotted lines represent the linear fit to the data points recorded at the holding potentials from -90 to 0 mV. The ML EPSC showed linear I-V relationship; CT EPSC, however, had the I-V relationship which significantly deviated from linearity (out of the 16 cells tested, 7 were patched with internal solution containing 0.1mM spermine and 9 were patched without spermine). The traces are averaged from 10 waveforms at each holding potential. **B**, The rectification index (RI) of CT EPSC was not significantly different after 0.1 mM spermine was supplemented in the pipette internal solution. **C**, Summary of the RIs of CT and ML EPSCs, showing the inward rectification of CT EPSC, but not ML EPSC.
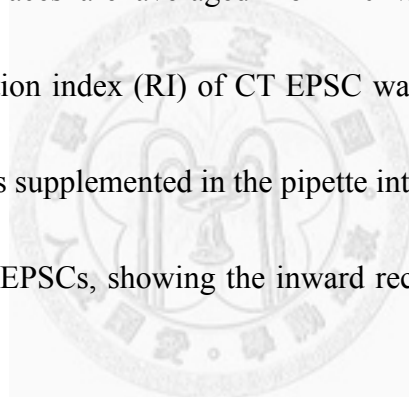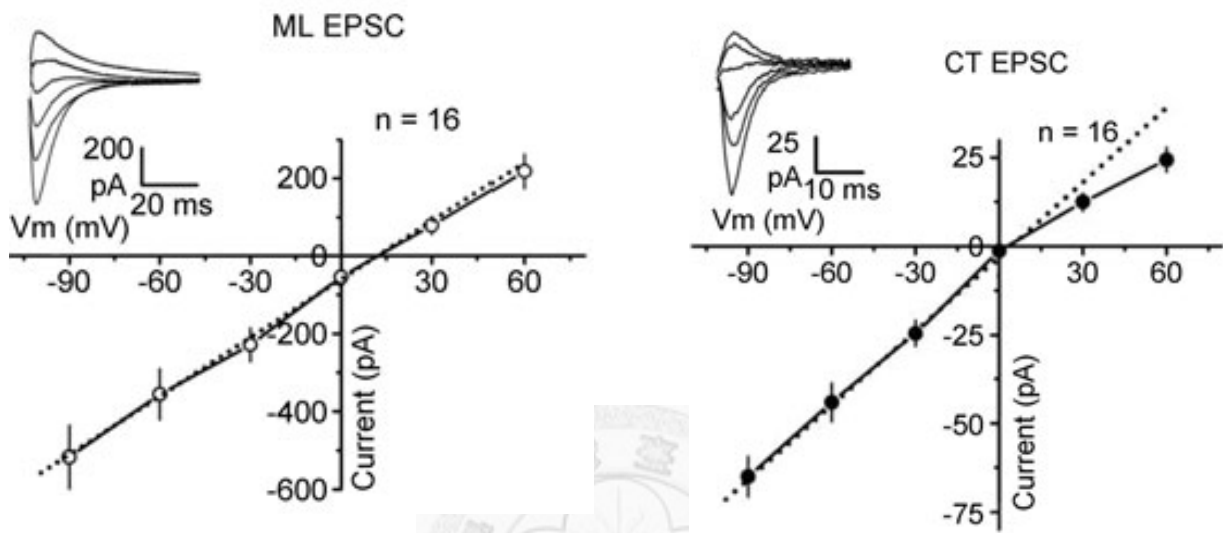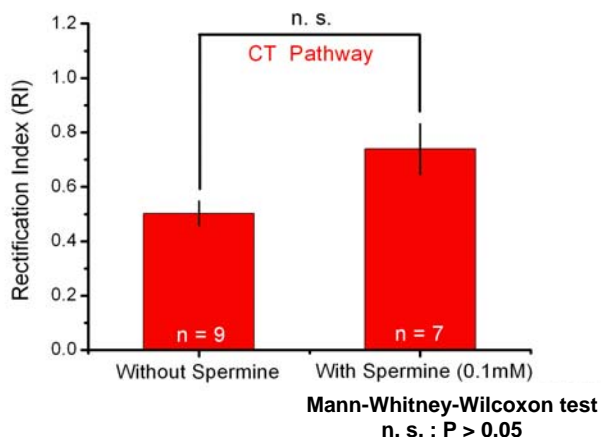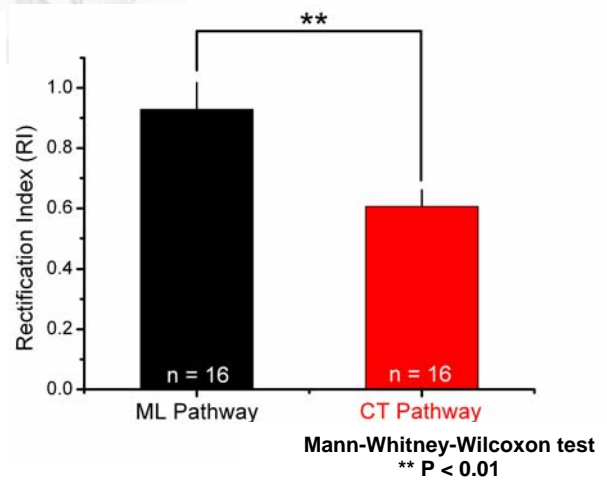
Figure 2.8

Figure 2.9 The sensitivity of the non-NMDAR-mediated EPSC to philanthotoxin-433 (PhTx-433) at CT and ML synapses

A representative example (**A**) and the summary (**B**) of the effects of 10 μM Philanthotoxin-433 (PhTx-433), a selective CaP-AMPAR blocker, on the ML and CT EPSCs recorded from the same relay neurons. After a 5-min stable baseline, PhTx was applied in the bath, which significantly attenuated the amplitude of CT EPSC but not ML EPSC. At the bottom are representative traces before (control), during (PhTx), and after washout of the drug application (wash). Each trace was averaged from 6 sweeps. EPSC Decr., decrease in EPSC amplitude.
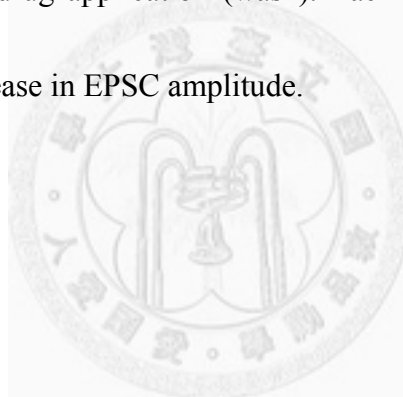
Figure 2.9

A

B

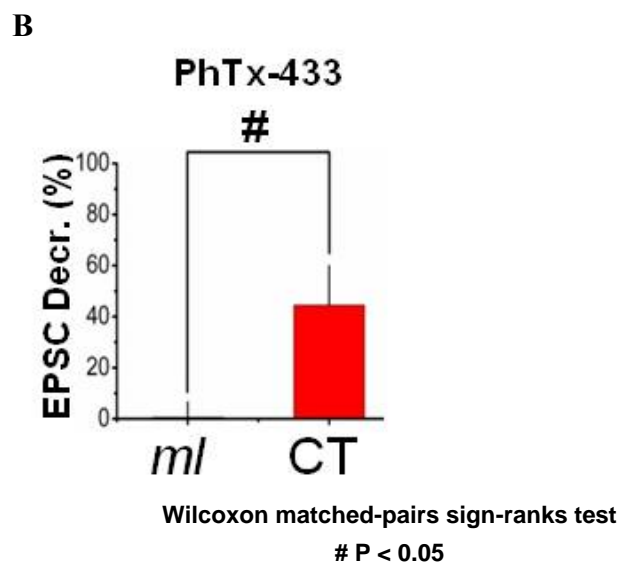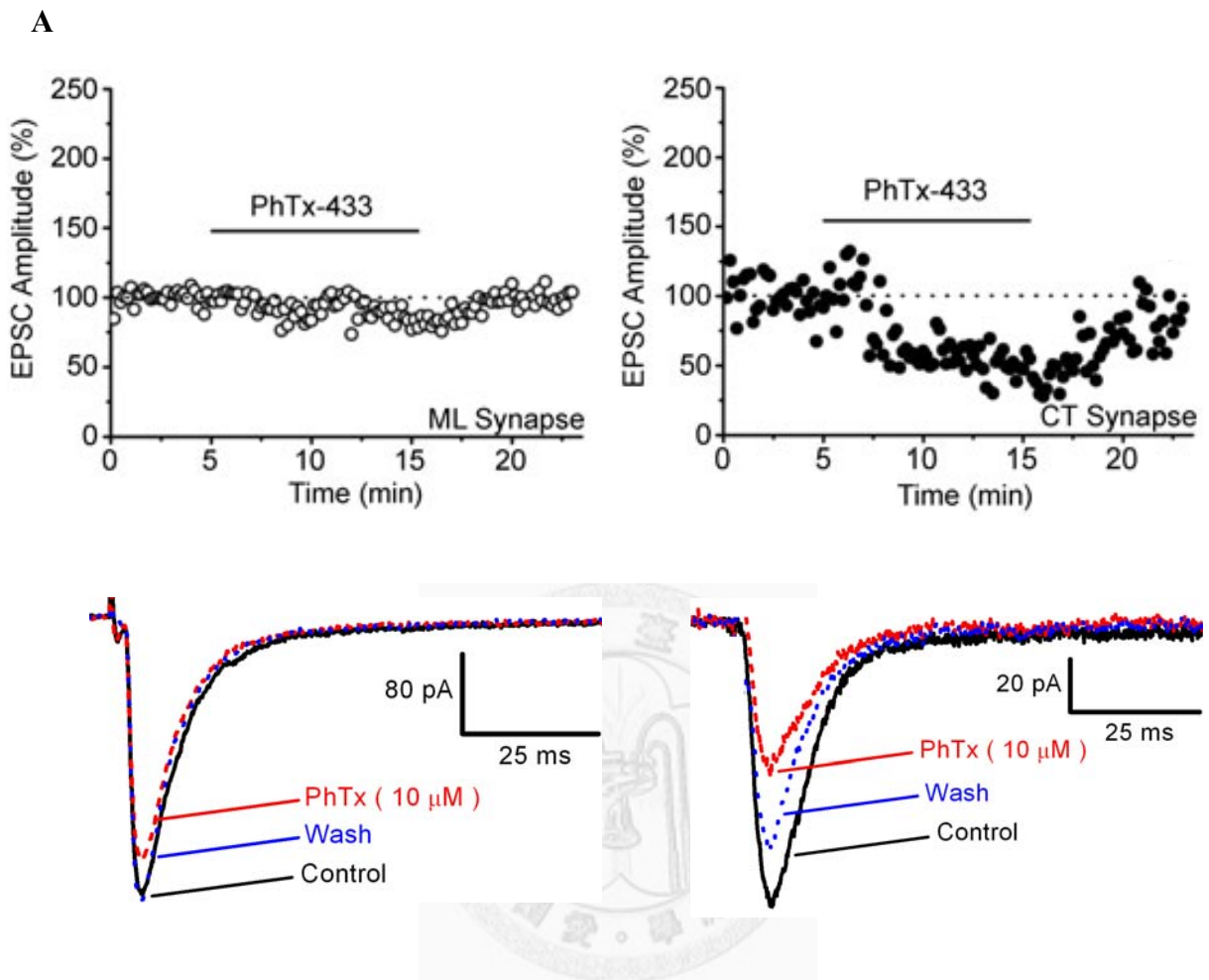Wilcoxon matched-pairs sign-ranks test
# P < 0.05

105

Figure 2.10 The sensitivity of the non-NMDAR-mediated EPSC to 1-naphthylacetyl spermine (NAS) at CT and ML synapses

A representative example (**A**) and the summary (**B**) of the effects of 250μM NAS, a polyamine toxin which selectively blocks CP-AMPARs, on the ML and CT EPSCs. After a 5-min stable baseline, NAS was applied in the bath, which significantly attenuated the amplitude of CT EPSC but not ML EPSC. At the bottom are representative traces before (control) and during (NAS) the drug application. Each trace was averaged from 10 sweeps. EPSC Decr., decrease in EPSC amplitude.

Figure 2.10

A

B

NAS
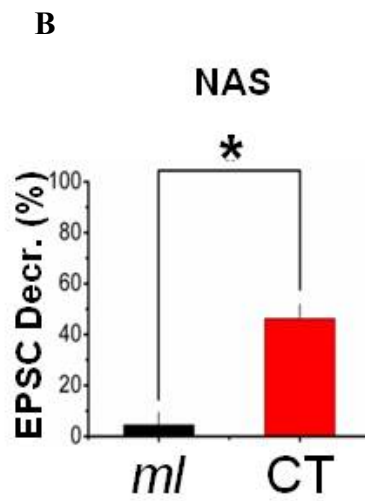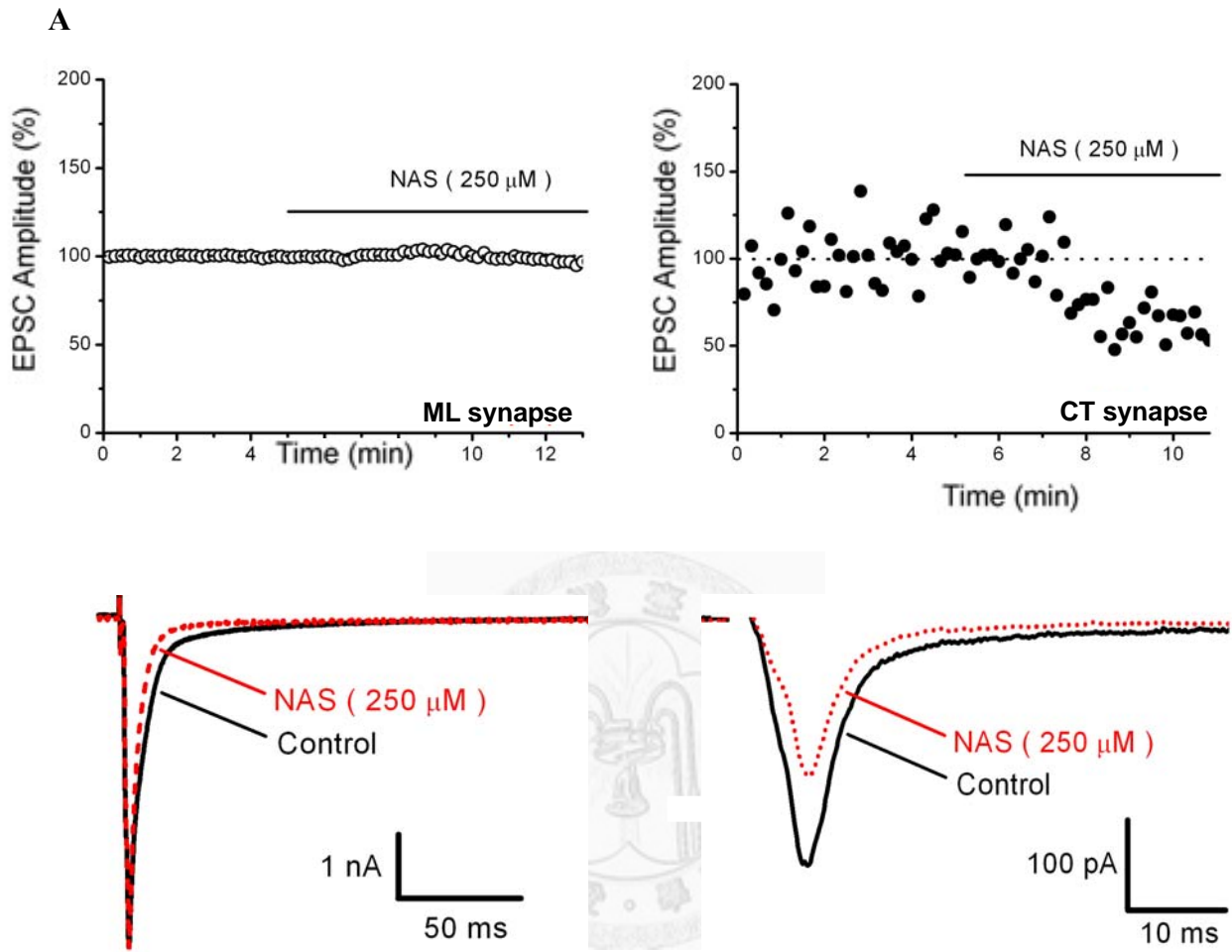
Mann-Whitney-Wilcoxon test
* P < 0.05

107

Figure 2.11 Paired-pulse ratios (PPRs) of CT and ML EPSCs at different holding voltage (V_h)

Representative responses evoked by paired pulses with the inter-pulse interval of 50 ms (A), and summary (B) of paired-pulse ratios of CT and ML EPSCs at two different holding voltage (V_h). For every cell tested, PPR of CT EPSC at the $V_h < 0$ mV is higher than at the $V_h > 0$ mV, whereas it was not the case for ML EPSC, suggesting that activity-dependent relief of polyamine block was selectively occurred at CT synapses (Rozov et al., 1998; Rozov and Burnashev, 1999). The summarized data include one experiment in which the CT EPSCs and ML EPSCs were evoked in the same relay neuron.

Figure 2.11

A

CT EPSC   ML EPSC

+60 mV

-90 mV

40 pA
25 ms

120 pA
25 ms

40 pA
25 ms

120 pA
25 ms

B

Paired-pulse ratio (PPR)

2.8
2.6
2.4
2.2
2.0

-70 / -90 mV   +60 mV

CT Synapse

Paired-pulse ratio (PPR)
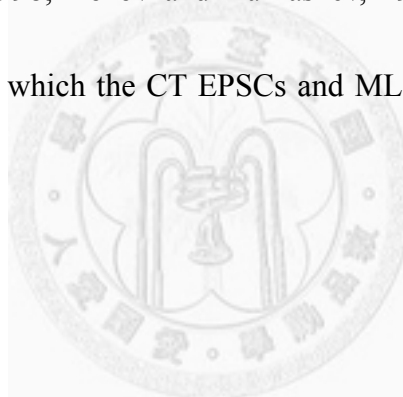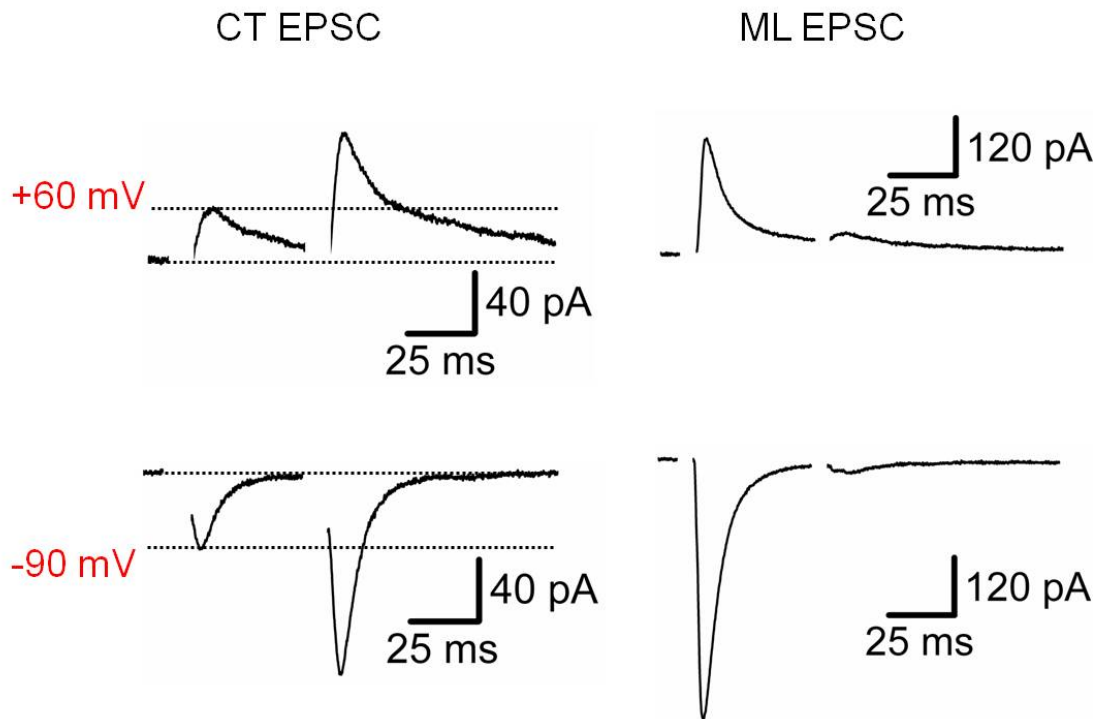
1.0

0.5

0.0

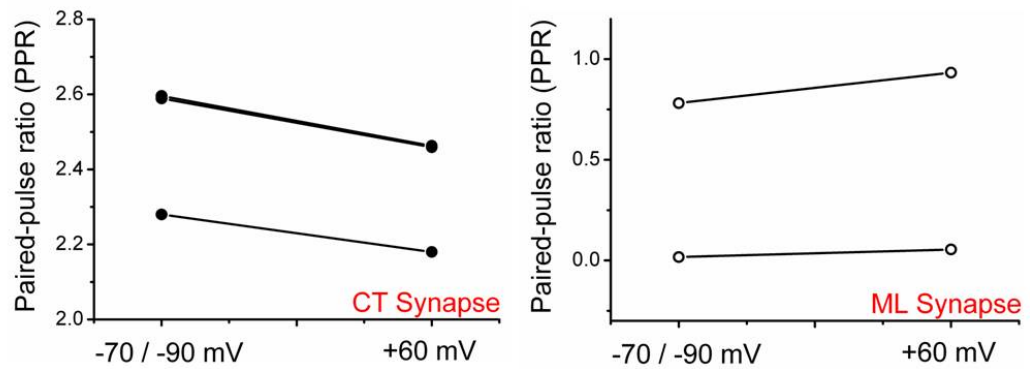-70 / -90 mV   +60 mV

ML Synapse

Figure 2.12 Peaked-scaled nonstationary noise analysis of non-NMDAR-mediated EPSCs at CT and ML synapses

A, Peak-scaled nonstationary noise analysis was applied to compare the weighted mean single-channel conductance of non-NMDARs at CT and ML synapses. The mean waveform (black line) of evoked EPSC traces was peak-scaled to individual EPSCs (gray lines) for calculating the ensemble variance and variance-mean relationship of EPSC decay phase, in order to isolate the variance associated with stochastic gating behaviors of single synaptic channels. 26 and 19 EPSCs were selected (see Methods) for analysis of single-channel conductance at CT and ML synapses, respectively. At the bottom are the variance-mean relationships; linear fitting (red dashed lines) was applied to the initial 33% of variance-mean relationship, yielding the weighted mean single-channel conductance of 5.41 and 3.08 pS at CT and ML synapses, respectively. Dotted lines denote the variance originating from background noise, which was constrained during the fitting process. Note the ML EPSC amplitude is much bigger than CT EPSC; to prevent amplifier from being saturated, ML ESPCs were normally recorded at a smaller gain (1/2 or 1/4 of that used for CT EPSCs), as evidenced by the larger variance of background noise. Lines with different thickness were used for CT and ML EPSCs for proper visualization of noise.

B, Summary of the weighted mean single-channel conductance of non-NMDARs.

Mean conductance of single non-NMDARs is significantly larger at CT synapses than

ML synapses (7.3 ± 1.1 pS, n = 5 and 3.1 ± 0.3 pS, n = 7 for CT and ML synapses,

respectively), which is consistent with our experimental results (**Fig. 2.8~2.11**) that

CaP-AMPARs are preferentially expressed at CT synapses. The average number of

non-NMDARs open at the peak of EPSC is 95 ± 20 (n = 5) and 1732 ± 417 (n = 7)

for CT and ML synapses, respectively.

Figure 2.12

A

ML EPSC

CT EPSC
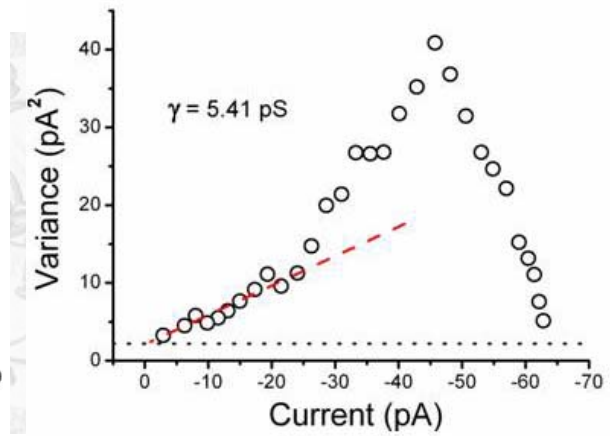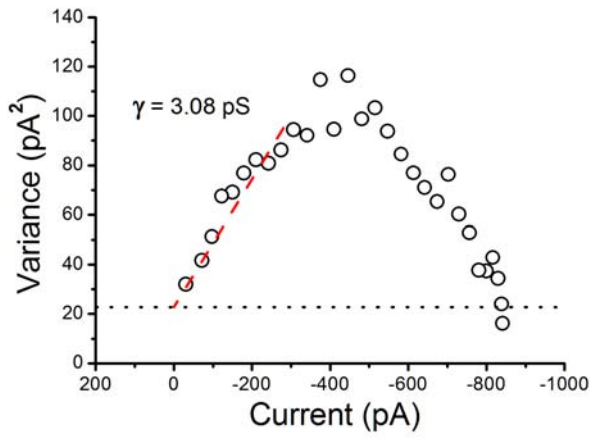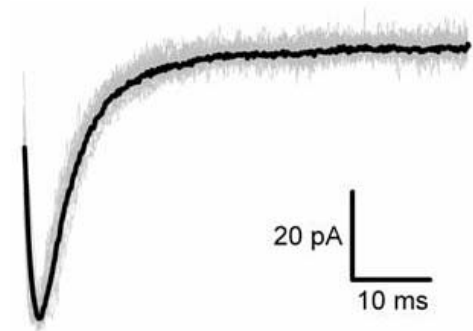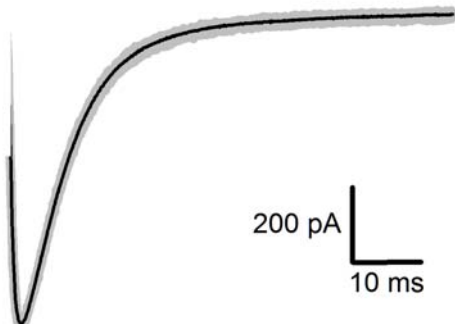
B
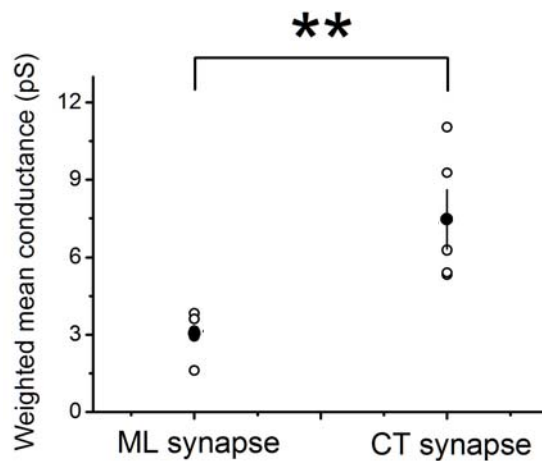
Mann-Whitney-Wilcoxon test

** P < 0.01

112

Tables

Table 2.1 Comparison of dynamic characteristics, short- and long term plasticity between corticothalamic (CT)-excitatory postsynaptic currents (EPSCs) evoked by internal capsule (*ic*) or local stimulations

LS, latency shift (defined as the latency of the 1st EPSC minus the latency of the 2nd EPSC); LTD, long-term depression; LTP, long-term potentiation. The data are expressed as the mean ± S.E.M.

[ns] Not significant, by non-parametric Mann-Whitney-Wilcoxon test
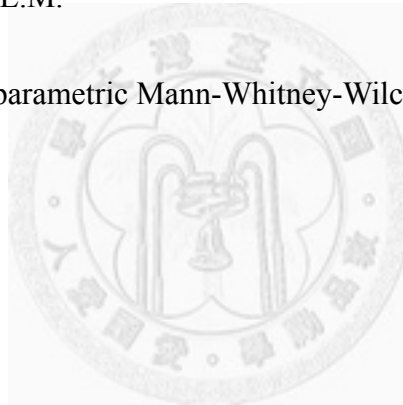
Table 2.1

	Internal capsule		Local		
10 ~ 90% rise time (ms)	2.67 ± 0.21	(*n* = 11)	2.82 ± 0.44	(*n* = 5) [ns]	
Weighted decay τ (ms)	10.25 ± 0.57	(*n* = 11)	11.69 ± 1.96	(*n* = 5) [ns]	
EPSC onset latency (ms)	3.80 ± 0.48	(*n* = 12)	4.41 ± 0.42	(*n* = 6) [ns]	
LS (μs)	208 ± 86	(*n* = 10)	423 ± 126	(*n* = 5) [ns]	
Paired-pulse ratio	2.32 ± 0.22	(*n* = 14)	2.61 ± 0.37	(*n* = 6) [ns]	
NMDAR/ non-NMDAR ratio	3.83 ± 1.20	(*n* = 6)	1.70 ± 0.39	(*n* = 8) [ns]	
LTP (%)	131.9 ± 13.2	(*n* = 10)	160.0 ± 18.1	(*n* = 10) [ns]	
LTD (%)	68.3 ± 3.6	(*n* = 4)	74.3 ± 5.2	(*n* = 22) [ns]	
LTD + nimodipine (%)	99.7 ± 10.1	(*n* = 4)	100.1 ± 3.9	(*n* = 7) [ns]	
LTD (stepping from -50mV) (%)	69.1 ± 9.3	(*n* = 4)	59.7 ± 7.1	(*n* = 8) [ns]	
LTP by modified pairing protocol + nimodipine (%)	118.9 ± 10.0	(*n* = 9)	117.3 ± 10.9	(*n* = 5) [ns]	
LTD of CT EPSPs by continuous spiking (%)	74.9± 12.2	(*n* = 3)	85.5± 8.5	(*n* =6) [ns]	

Table 2.2 Comparison of the dynamic characteristics and short-term plasticity of corticothalamic (CT) excitatory postsynaptic currents (EPSCs) and medial lemniscal (ML) EPSCs

OL, onset latency; RT, 10%-90% rise time; Dτ, weighted decay time constant; PPR, paired-pulse ratio; LS, latency shift (defined as the latency of the 1st EPSC minus the latency of the 2nd EPSC). The data are expressed as the mean ± S.E.M.

[#] SR, number of experiments in which CT EPSCs and ML EPSCs were simultaneously recruited in a thalamocortical relay neuron.

* Nonparametric Mann-Whitney-Wilcoxon test.

Table 2.2

	CT EPSCs	ML EPSCs	SR[#]	Statistics*
OL (ms)	4.0 ± 0.4 $n = 18$	2.7 ± 0.2 $n = 26$	7	$p < 0.001$
RT (ms)	2.7 ± 0.2 $n = 16$	1.0 ± 0.1 $n = 15$	6	$p < 10^{-5}$
Dτ (ms)	10.7 ± 0.7 $n = 16$	8.1 ± 0.7 $n = 15$	6	$p < 0.05$
PPR	2.4 ± 0.2 $n = 20$	0.4 ± 0.1 $n = 26$	8	$p < 10^{-8}$
LS (ms)	0.28 ± 0.07 $n = 15$	$- 0.21 \pm 0.08$ $n = 17$	5	$p < 10^{-4}$
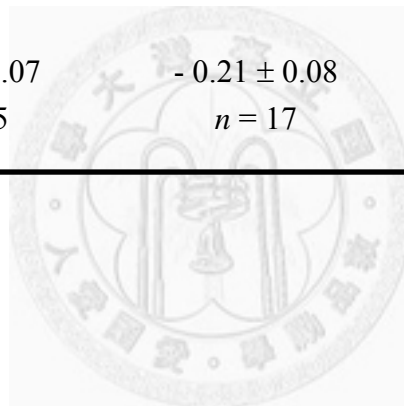
Chapter 3

Differential induction of synaptic plasticity

between corticothalamic and medial lemniscal synapses

Abstract

Our experimental results indicated that the composition of iontropic glutamate receptors at CT and ML synapses are very different. In particular, NMDARs have a higher contribution to synaptic responses (as relative to non-NMDARs) at CT than ML synapses; moreover, CaP-AMPARs are preferentially expressed at CT synapses. It has been widely appreciated that these two types of glutamate receptors, as gateways for calcium influx into neurons, serve to play multiple roles in the induction and expression of long-term synaptic plasticity. Therefore, it is of particular interest to know whether synaptic plasticity of CT and ML pathways is also very different. We found that an NMDAR-dependent long-term potentiation (LTP) could be induced by pairing 1-Hz presynaptic stimulation with postsynaptic depolarization to 0 mV at CT synapses, but not ML synapses. Interestingly, this LTP was impaired with the pairing protocol modified in such a way that a phase with $V_h = -70$ mV was retained prior to

each presynaptic stimulation, which spares activation of NMDARs but de-inactivates voltage-dependent inactivating conductances. This phenomenon could be explained by a concomitant expression of an long-term depression (LTD) that was previously unknown at CT synapses, which could be induced by the same modified protocol without presynaptic stimulation (thus equivalent to postsynaptic depolarizing pulses), but depolarizing pulses could not induce long-term plasticity at ML synapses. Induction of CT LTD is dependent on activation of L-type voltage-gated calcium channels (VGCCs), but not T-type VGCCs, NMDARs, and CaP-AMPARs. An additional attempt was made to examine the potential role of CaP-AMPARs in induction of long-term plasticity at CT synapses. To sum up, under our experimental paradigms, synaptic strength of CT pathway is more flexible than ML pathway, which may have profound functional implications for the physiological operation of somatosensory thalamocortical system.

Introduction

The ventrobasal nucleus (VBN) of the thalamus serves as a major gateway for relaying somatosensory information to the cerebral cortex (Jones, 2007).

Thalamocortical relay neurons fire action potentials either in continuous or burst mode, depending on membrane potential (Vm). In early studies, continuous spiking is commonly recorded in sensory thalamus when animals are awake and alert, and the sensory information is faithfully represented in response to peripheral stimuli, while rhythmic burst spiking is normally recorded when animals are in non-REM sleep or inattentive, and sensory information is not linearly represented by thalamic activities, therefore neuronal firing mode is believed to underlie the functional connectivity between relay neurons and the afferent input (McCormick and Feeser, 1990; Le Masson et al. 2002; Sherman, 2005; Sherman and Guillery, 2004).

Physiological mechanisms of firing mode switch in relay neurons and thus transfer of sensory information has been intensively studied, despite most efforts made on intrinsic membrane properties that govern the activation of T-type VGCCs and other active conductances. Considering the predominant number of CT synaptic contacts on relay neurons, cortical feedback signals are generally regarded as an essential modulator for the properties of thalamic spike transfer (Murphy and Sillito, 1987; Ergenzinger et al. 1998; Krupa et al. 1999; Sillito and Jones, 2002; Sherman, 2005). Following this line, significant roles for synaptic drive in firing mode regulation has been suggested since recently (Ergenzinger et al. 1998;

119

Castro-Alamancos and Calcagnotto, 2001; Hughes et al. 2002; Sillito and Jones, 2002).

Since there are intense reciprocal interactions between cerebral cortex and somatosensory thalamus, which is critical for sensory processing, use-dependent modification of synaptic efficacy in the VBN may provide a means by which the extent of thalamocortico-corticothalamic interactions underlying somatosensory processes are dynamically regulated. Here, we studied the input-specific competence of bi-directional synaptic plasticity in the VBN, and found that long-term plasticity are differentially manifested between these two synapses. A novel form of LTD at CT synapses is described, which is L-type VGCC-dependent, and synaptic strength of CT pathway can integrate different induction signals and adapts accordingly in a dynamic way.

Methods

Preparation of acute slices

The use of animals in this study was in accordance with the guidelines of the local ethical committee for animal research of National Taiwan University. Sprague-Dawley (SD) rats of both sexes aged 13-24 postnatal days (P13-24) were used, but most were aged P13-16. The animals at these ages were chosen because the intrinsic and firing properties of rat VBN neurons reach developmental steady-state after P12, including the resting membrane potential (Vm), input resistance (R_N), ability to fire full-blown LTS-driven bursting, width of action potential (AP) and after-hyperpolarization (AHP) (Velazquez and Carlen, 1996). Possibly attributible to less extent of myelinated fibers, the success rate in obtaining good seal and recording quality was also significantly higher from animals of this age window, which is especially critical for the purpose of simultaneous recruitment of CT and ML synapses.

The rats were anaesthetized with isoflurane and decapitated with a small-animal guillotine, and the brain was quickly removed and placed in ice-cold artificial cerebrospinal fluid (ACSF). Coronal slices were used for initial experiments. We then discovered that, in horizontal slices, it was easier to recruit CT and ML EPSCs simultaneously in the same relay neuron, horizontal preparation was adopted for the most part of this study. For horizontal preparation, the two halves of the brain were

first separated, and their ventral portions were trimmed in parallel to the ventral surfaces of brainstem to ensure standard horizontal cutting orientation in accordance with traditional stereotaxic coordinates. A block of agar was glued behind the medial surface of a half-brain to provide physical support during slicing. Horizontal brain slices (300 μm) containing the ventrobasal nucleus (VBN), internal capsule (*ic*) and medial lemniscus (*ml*) fibers were prepared, using the patterns of *ic* and the fibers in the ventral posterolateral nucleus (VPL) as landmarks (Fig. 2.1). For coronal preparation, intact coronal slices were cut and the two halves were separated by blade. Coronal brain slices (300 μm) containing the VBN, *ic* and *ml* were prepared, using the patterns of VBN and its fiber patterns as landmarks (Fig. 2.1).

The slices were cut with a vibroslicer (752M, Campden, Loughborough, England or ZERO 1, D.S.K., Osaka, Japan). The ACSF contained (in mM): 119 NaCl, 2.5 KCl, 1.3 $MgSO_4$, 26.2 $NaHCO_3$, 1 NaH_2PO_4, 2.5 $CaCl_2$, and 11 glucose; pH adjusted to 7.4 by gassing with carbogen consisted of of 95 % O_2 / 5 % CO_2. The slices were kept in oxygenated ACSF (95% O_2 / 5% CO_2) at room temperature (24-25°C) to allow recovery for at least 90 minutes before recording was started.

Electrophysiology

Slices were transferred to an immersion-type recording chamber mounted to an

upright microscope (BX50WI, Olympus Optical, Tokyo, Japan), equipped with

water-immersion objectives, a Normaski optic system, an infrared filter and a CCD

camera (XC-E150, Sony, Tokyo, Japan) (IR-DIC system). In horizontal slices, the

VBN, *ic* and *ml* were clearly identifiable under low-magnification light microscopy.

In some cases, we noticed that there was a small heterogeneous zone locating in the

border of VPL medial to *ic*, which indicated a lower density of myelinated fibers (Fig.

2.1A$_3$). Recordings made from this zone was avoided to prevent potential

confounding factors which may originate from functional or biochemical

heterogeneities within VBN (see introduction from more descriptions). Neurons in the

VBN were recorded under visual guidance. The typical number of fast spikes of a

LTS-burst firing is 4~9 as depolarizing current pulses were injected at the V_m <

-75mV. Occasionally, some neurons had a spike number of LTS-burst < 3 and were

discarded.

IPSPs were rarely observed in horizontal VBN slices of mice

(Castros-Alamancos, 2002), which could be attributed to the orientation of the slice

preparation so the fibers were not well preserved. Nevertheless, all experiments

carried out in this study were performed in the presence of 0.1 mM picrotoxin and 1 μM strychnine to avoid any potential confounding effects of GABAergic and glycinergic IPSPs.

Patch pipettes were pulled from borosilicate glass (1.5 mm outer diameter, 0.32 mm wall thickness; G150F-4, Warner Instruments Corp., Hamden, CT, USA), and had a resistance of 3~8 MΩ. For experiments characterizing basic excitatory synaptic properties, "cesium internal solution" was used to avoid metabotropic receptor-dependent potassium conductances (for evoked $GABA_B$ IPSC in the VBN of rats, see Kao and Coulter, 1997). The cesium internal solution contained (in mM): 114.7 CsOH, 17.5 CsCl, 117.6 gluconic acid, 10 HEPES, 2 EGTA, 8 NaCl, 2 ATP, 0.3 GTP, and 6.7 biocytin; pH was titrated to 7.2 by CsOH and osmolarity to 300-305 mOsm. For experiments on the synaptic plasticity, "normal internal solution" was used, which contained (in mM): 131 K-gluconate, 20 KCl, 10 HEPES, 2 EGTA, 8 NaCl, 2 ATP, 0.3 GTP, and 6.7 biocytin; pH was titrated to 7.2 by KOH and osmolarity to 300-305 mOsm. In all experiments in which depolarizing step commands were used, 5 mM QX-314 was included in the internal solution to block voltage-gated Na^+ channels and enhance the voltage control. Signals were obtained by Axopatch 1D amplifier (Axon Instruments, Union City, CA, USA). Slices were

continuously perfused with oxygenated solutions at 1~2 ml / min under room temperature. For voltage-clamp recordings, whole-cell conductance (Gw) and series resistance (Rs) were continuously monitored by a test voltage pulse of 3 mV; Rs was typically < 20 MΩ and was not left uncompensated. For current-clamp recordings, the input resistance (R_N) was continuously monitored by a test current pulse of +30 pA, and the bridge was balanced by adjusting the Rs compensation of the amplifier. Data were discarded when Rs or R_N varied by more than 20% from its baseline value during the recording. All signals were low-pass-filtered at a corner frequency of 2 kHz, then digitized at 10 kHz using a Micro 1401 interface (Cambridge Electronic Design, Cambridge, UK). Data were collected using Signal (Cambridge Electronic Design, Cambridge, UK) or Spike 5 (Cambridge Electronic Design, Cambridge, UK) by episode-based capture. The liquid junction potential was measured to be ~ +10 mV and left uncorrected (following the method by Neher, 1992).

Stimulation of CT and ML synapses

The best efforts were made to recruit CT and ML synapses at the same relay neurons in most experiments for a reliable comparison of input-specificity of the properties examined (Fig. 2.4A). A bipolar stainless steel electrode (PK/12, FHC, St

Bowdoin, ME, USA) was placed locally within 150 μm away from the recorded cell

or in *ic* for evoking CT EPSCs, and another electrode was placed in *ml* for evoking

CT EPSCs. No significant differences were observed between the CT EPSCs evoked

by these two conditions (Table 2.1). In some cases, however, only CT EPSCs or ML

EPSCs were evoked, and these data were also pooled for statistical comparison.

In high-magnification IR-DIC images of horizontal slices, we observed a large

number of fiber bundles projecting from the direction of *ic*, traversing the reticular

nucleus (Rt) and the small heterogeneous zone in the border of VPL (described above)

into VBN. We traced along the fiber bundles proximal to the recorded neuron, back to

their origin in *ic*, and placed the stimulating electrode accordingly to facilitate the

success rate of recruiting measurable CT EPSCs. A typical stimulus consisted of a

4~100 μs square pulse with the amplitude ranged in 30~800 μA. In some cases, the

stimulating artifact was relatively large, and the synaptic responses were analyzed

after the artifact waveform obtained in 10 μM DNQX, a selective non-NMDARs

antagonist, was subtracted.

For recording the excitatory postsynaptic currents (EPSCs), V_m was

voltage-clamped at -70 mV, with 100 μM picrotoxin (PTX) and 1 μM strychnine

added to the bath ACSF solution to block ionotropic GABA$_A$ receptors and glycine

receptors (for the glycinergic transmission in the VBN, see Ghavanini et al., 2005;

Ghavanini et al., 2006), respectively. After the experiments were finished, 10 μM

DNQX were applied in the bath in most cases to confirm the identity of recorded

activities as a non-N-methyl-D-aspartate receptor (non-NMDAR)-mediated

component. EPSCs were evoked at 0.1 Hz; in experiments in which CT EPSCs and

ML EPSCs were simultaneously recruited, alternate stimulations were made to the IC

(or locally) and ML tracts, with the stimulation rate to both inputs being 0.1 Hz.

Long-term synaptic plasticity

For synaptic plasticity experiments, a stable baseline was recorded for at least 5

min, followed by an additional ~ 25 min of recording after induction protocol was

applied. To prevent potential washout of cell content required for induction of

synaptic plasticity, data were discarded if the time of recording after "break-in" into

whole-cell configuration was over 12 min but the induction protocol had not been

applied yet. Amplitude of individual EPSC was normalized with respect to the mean

measurement of all baseline responses before induction, and the normalized

measurements recorded in 18.5~23.5 min after induction were averaged and used for

statistical comparison.

Drugs

Chemicals used for ACSF and internal solution were purchased from Merck (Damstadt, Germany). *N*-2,6-Dimethylphenylcarbamoylmethyl triethylammonium bromide (QX-314) was purchased from Alomone Laboratories (Jerusalem, Israel). DL-2-Amino-5-phosphonopentanoic acid (APV), 6,7-dinitroquinoxaline-2,3-dione (DNQX), nimodipine (Nim), spermine tetrahydrochloride, tetrodotoxin (TTX), and mibefradil were purchased from Tocris Cookson (Bristol, UK). MgATP, NaGTP, BAPTA, picrotoxin, strychnine, and nickel chloride were purchased from Sigma (St. Louis, MO, USA). All drugs were made as stock solutions, stored at -20°C, and diluted to working concentration immediately before use. The experiments using nimodipine were performed in darkness to avoid drug deterioration.
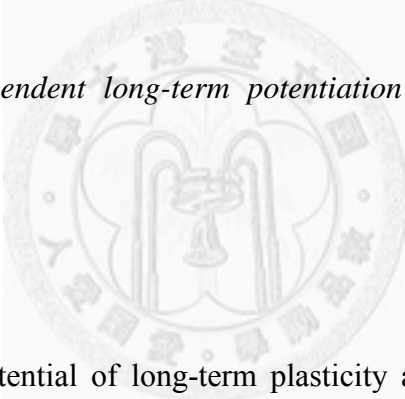
Statistics

All data are presented as the mean ± S.E.M. The nonparametric Mann-Whitney-Wilcoxon U test was used for statistical comparison between unpaired

data and Wilcoxon matched-pairs sign-ranks test was used for paired data. The criterion for significance was P < 0.05 for all statistical tests. Origin (Microcal, Northhampton, MA, USA) and SAS (SAS, Cary, NC, USA) software were used for data analysis.

Results

Induction of NMDAR-dependent long-term potentiation (LTP) specifically at CT synapses

To investigate the potential of long-term plasticity at these two pathways, we used a brief induction protocol by conjunctive pairing postsynaptic depolarization to 0 mV with 1 Hz extracellular stimulation (Gustaffson et al., 1987; Wang et al., 1997a). Similar long-term potentiation (LTP) was induced by this protocol for the EPSCs evoked by stimulating internal capsule (131.9 $\pm$ 13.2 % compared with baseline, n = 10) and by local stimulation (160.0 $\pm$ 18.1 % compared with baseline, n = 10) (P > 0.05, Mann-Whitney-Wilcoxon test) and thus pooled together (Fig. 3.1A; LTP = 146.0 $\pm$ 11.3 % compared with baseline, n = 20). This LTP could be blocked by 50 μM

bath-applied APV (locally-evoked EPSCs: 96.6 $\pm$ 7.7 % compared with baseline, n = 9), a specific NMDA receptor antagonist (Fig. 3.1B). These findings suggested that the induction of LTP at CT synapses was NMDAR-dependent. The same conjunctive pairing protocol, however, failed to induce LTP at the ML synapses (Fig. 3.1A; 95 $\pm$ 9 % compared with baseline, n = 7; P > 0.05, Wilcoxon matched-pairs sign-ranks test), indicating the NMDAR-dependent LTP was input-specific. Interestingly, accompanying LTP induction at CT synapses, there was a parallel long-lasting increase in GW (141 $\pm$ 12 % compared with baseline, P < 10^{-4}, Wilcoxon matched-pairs sign-ranks test), which was blocked by APV, and not induced when pairing was applied to ML pathway (110 $\pm$ 6 % compared with baseline; P > 0.05, Wilcoxon matched-pairs sign-ranks test), indicating such a increase is also NMDAR-dependent and has the property of input specificity, similar to the case in CA1 pyramidal neurons of hippocampus and could be attributed to a local upregulation of dendritic hyperpolarization-activated cyclic nucleotide-gated cationic channels (HCNs) (Campanac et al., 2008; Fan et al., 2005).

Associativity, input specificity, and cooperativity are typical characteristics of LTP (Bliss and Collingridge, 1993). To test if the LTP was associative, the pairing protocol was applied without postsynaptic depolarization or 1 Hz stimulation; both

these protocols failed to induce LTP at CT synapses (Fig. 3.2; without depolarization, 101.2 ± 10.4 % compared with baseline, n = 5; without stimulation, 110.2 ± 7.6 % compared with baseline, n = 4; both locally-evoked EPSCs; both P > 0.05, Wilcoxon matched-pairs sign-ranks test). Pairing depolarization to -45 mV with 1 Hz stimulation, a protocol presumably activating NMDA receptors in a relatively moderate manner, could not induce any synaptic plasticity at CT synapses, either (Fig. 3.3A; locally-evoked EPSCs: 102.5 ± 10.4 % compared with baseline, n = 12; P > 0.05, Wilcoxon matched-pairs sign-ranks test), consistent with the requirement of strong postsynaptic depolarization, and thus sufficient activation of NMDAR, for the induction of LTP. For a weak test pathway, the requirement of sufficient depolarization may underlie the dependence of LTP induction on the number of coincident inputs recruited or synchronized tetanization of a strong pathway, which was termed "cooperativity" in early studies (Barrionuevo and Brown 1983; Levy and Steward 1979; Markram et al., 1997; McNaughton et al. 1978). In our horizontal preparations, stimulation of medial lemniscus (ml) recruited not only all-or-none responses but also linear responses. In contrast to those all-or-none responses, these linear EPSCs showed slower rising kinetics, smaller amplitude, and PPF. Despite the similarity between these EPSCs and CT EPSCs, pairing depolarization to 0 mV with 1 Hz stimulation was unable to induce LTP at this "undefined pathway" (95.9 ± 4.4 %

compared with baseline, n = 10; P > 0.05, Wilcoxon matched-pairs sign-ranks test) (Fig. 3.3B). This result indicated the input specificity of the LTP at CT synapses. Accordingly, locally-recruited synapses showed the competence of expressing NMDAR-dependent LTP, therefore supporting our postulation that the locally-evoked responses had their corticothalamic origin.

Taken together, the pairing protocol could induce the NMDAR-dependent LTP specifically at CT synapses, which showed the canonical properties of LTP (Fig. 3.3C).
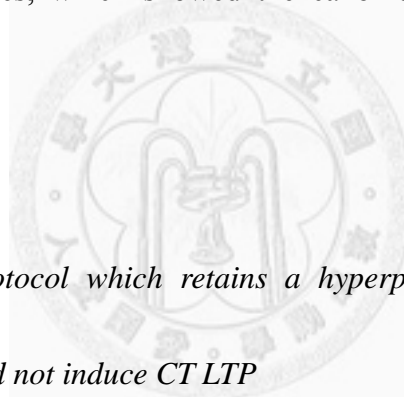
The modified pairing protocol which retains a hyperpolarized phase prior each presynaptic stimulation did not induce CT LTP
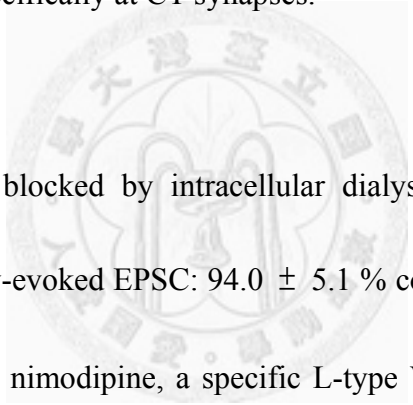
To further determine whether involvement of voltage-gated channels can play any roles in the synaptic plasticity of CT synapses, we used **a modified pairing protocol in** which the holding voltage (V_h) returns to -70 mV for 500 ms prior to each presynaptic stimulation, which presumably de-inactivates and recruits inactivating conductances more effectively. Intriguing, this protocol did not induce long-term plasticity at the CT synapses (Fig. 3.4; locally-evoked EPSCs: 97.6 ± 13.6 %

compared with baseline, n = 11; P > 0.05, Wilcoxon matched-pairs sign-ranks test), despite the activation of NMDARs were putatively spared since the requirements of glutamate release and properly-timed postsynaptic depolarization were still satisfied.

Depolarizing steps induced L-type VGCC-dependent LTD specifically at CT synapses

The mask of CT LTP could be attributed to the direct crosstalk between signaling mediated by NMDA receptors and unknown voltage-gated processes, or a net effect caused by a parallel expression of unknown synaptic plasticity. In order to distinguish between the possibilities that inclusion of a modified hyperpolarized phase interferes with either the induction process of LTP, i.e. the signaling downstream to NMDAR activation is disrupted, or the expression of LTP, by means of the concomitant expression of long-term plasticity at CT synapses that was previously unknown, 1-Hz repetitive postsynaptic depolarizing pulses alone were applied to the recorded cell. Surprisingly, applying the depolarizing steps alone induced long-term depression (LTD) for the EPSCs evoked by stimulating internal capsule (68.3 ± 3.6 % compared with baseline, n = 4) and by local stimulation (74.3 ± 5.2 % compared with baseline, n = 22), which were similar (P > 0.05, Mann-Whitney-Wilcoxon test) and thus pooled together (Fig. 3.5A; 73.4 ± 4.4 % compared with baseline, n = 26); the same protocol,

however, failed to induced significant plasticity at ML synapses (109.0 ± 5.2 % compared with baseline, n = 10; P > 0.05, Wilcoxon matched-pairs sign-ranks test). Moreover, from the cases in which CT and ML EPSCs were recruited in the same neurons, this LTD could also be induced specifically at CT synapses (Fig. 3.5A$_1$; locally-evoked EPSCs: 67.4 ± 10.4 % compared with baseline, n = 6; ML EPSCs: 113.6 ± 8.2 % compared with baseline, n = 6; P < 0.05, Wilcoxon matched-pairs sign-ranks test). These results indicated that the depolarizing steps can induce long-term modification specifically at CT synapses.

This LTD could be blocked by intracellular dialysis of BAPTA, a calcium chelator (Fig. 3.5B; locally-evoked EPSC: 94.0 ± 5.1 % compared with baseline, n = 4), or 10 µM bath-applied nimodipine, a specific L-type VGCC blocker (Fig. 3.5C; internal capsule stimulation: 99.7 ± 10.1 % compared with baseline, n = 4; local stimulation: 100.1 ± 3.9 % compared with baseline, n = 7; P > 0.05, Mann-Whitney-Wilcoxon test; pooled: 100.0 ± 4.1 % compared with baseline, n = 11), indicating its dependence on the rise of intracellular calcium concentration and activation of L-type VGCCs. It also suggests that local network activities, potentially driven by repetitive, powerful excitation of the recorded neuron was not sufficient to this form of LTD.

The mask of LTP at CT synapses could be partly explained by a concomitant expression of L-type VGCC-dependent LTD induced by depolarizing steps

The finding of the L-type VGCC-dependent LTD provides a possible explanation for the mask of LTP by inclusion of the hyperpolarized phases. To directly test this hypothesis, we applied the modified pairing protocol in presence of 10 μM bath-applied nimodipine. Upon blockade of L-type VGCCs, an LTP was uncovered for EPSCs evoked by stimulating internal capsule (118.9 ± 10.0 % compared with baseline, n = 9) and by local stimulation (117.3 ± 10.9 % compared with baseline, n = 5) ($P > 0.05$, Mann-Whitney-Wilcoxon test) and thus pooled together (Fig. 3.6; 118.3 ± 7.3 % compared with baseline; n = 14). These results supported our hypothesis, implying the mask of LTP could be explained by the concomitant expression of L-type VGCC-dependent LTD at CT synapses. However, the magnitude of the uncovered LTP was smaller (despite not significantly); therefore, a potentially more complex scenario may need to be considered.

Role of T-type VGCCs and NMDARs in the induction of LTD at CT synapses

To assess the role of T-type VGCCs in the induction of LTD at CT synapses, we looked for specific pharmacological tools. Unfortunately, in our system, nickel (Ni^{2+}) had the concentration of the half-maximal effect on blockade of LTS to be ~ 600 μM (n = 4, Fig. 3.7A), a concentration much higher than that selectively blocking low-threshold T-type VGCCs (Avery and Johnston, 1996; Lee et al., 1999; Magee and Johnston, 1995); mibefradil, a VGCC blocker with moderate selectivity for T-type channels (IC_{50} ~ 2.7 μM and 18.6 μM for T-type and L-type channels respectively, as specified from data sheet provided by the provider), could not block the LTS effectively at the concentration of less than 20 ~ 50 μM (Fig. 3.7B). Therefore, we adopted an alternative approach: modifying the protocol to set the holding potential (V_h) of the hyperpolarized phase to -50mV, at which LTS was completely absent (Fig. 2.3A). This new protocol, however, did not impared expression of LTD at CT synapses (Fig. 3.7C; internal capsule stimulation: 69.1 ± 9.3 % compared with baseline, n = 4; local stimulation: 59.7 ± 7.1 % compared with baseline, n = 8; P > 0.05, Mann-Whitney-Wilcoxon test; pooled: 62.9 ± 5.6 % compared with baseline, n = 12). We also tested if activation of NMDARs or CaP-AMPARs contributes CT LTD, since both of which can function as channels for calcium influx, and CaP-AMPARs have been especially emphasized for their roles in synaptic plasicity. Neither of them is required for CT LTD, however, as evidenced by the fully expressed LTD induced

even in presence of APV or PhTx-433 (Fig. 3.8A, B). Taken together, these results

suggested the induction of LTD at CT synapses is dependent on activation of L-type,

but not T-type VGCCs or NMDARs   (Fig. 3.8C).

Role of CaP-AMPARs in induction of synaptic plasticity of CT pathway

The lack of a role of CaP-AMPARs in induction of CT LTD deepened our

curiosity to their physiological function at CT synapses. Based on the idea that

CaP-AMPARs are also responsible for induction of synaptic plasticity in some

systems (Lamsa et al., 2007; Liu and Cull-Candy, 2000), we tested the effect of an

"anti-Hebbian" protocol on CT EPSCs. This protocol is composed of 2 cycles of

pairing 100-Hz presynaptic stimulation for 1 s with postsynaptic hyperpolarization to

-90 mV, with an interval of 10 s, which potentially maximizes activation of

CaP-AMPARs. The results showed that no long-term plasticity of CT synapses was

significantly induced by this protocol (Fig. 3.9; 110 $\pm$ 16 % compared to the baseline,

n = 7; P > 0.05, Wilcoxon matched-pairs sign-ranks test). However, some other factor,

such as a simultaneous activation of mGluRs expressed postsynaptically to CT

synapses (Golshani et al., 1998; Hughes et al., 2002; Reichova and Sherman, 2004;

Sherman and Guillery, 2004) during high-frequency stimulation, should be taken into

consideration for interpreting this result.

Discussion

In this study, we discovered novel long-term plasticity at corticothalamic feedback in that, LTP induction is NMDAR-dependent and associative, and LTD induction is L-type VGCC-dependent and non-Hebbian. Our results uphold the emerging viewpoint that thalamus does not merely serve as a passive channel for signal relay, emphasizing and providing plausible neuronal basis for active contribution of thalamus to state-dependent information processing.

Despite the historical importance of thalamus in research of sensory physiology, only a few studies addressed the issue of long-term synaptic plasticity in thalamus. The early study of rat dLGN only briefly described the phenomenon of change in synaptic responses following high-frequency stimulation (Turner and Salt, 1998). A long-lasting increase in the frequency of spontaneous inhibitory postsynaptic currents (sIPSCs) in mouse dLGN was also reported (Bright and Brickley, 2008).

In line with the observation made in thalamic slices of mice (Miyata and Imoto, 2006), we found that the peak current ratio of NMDAR- to non-NMDAR-mediated EPSCs at CT synapses was significantly higher than that at ML synapses. This difference could explain the readily inducible NMDAR-dependent associative LTP at CT synapses, but not at ML synapses. Castro-Alamancos and Calcagnotto (1999) reported that a homosynaptic LTP at CT synapses induced by presynaptic stimulation at 10 Hz is NMDAR-independent. The discrepancy of LTP induction between their report and our results may stem from the difference in induction protocol (homosynaptic v.s. associative) and / or different species of animals used (mice v.s. rats).
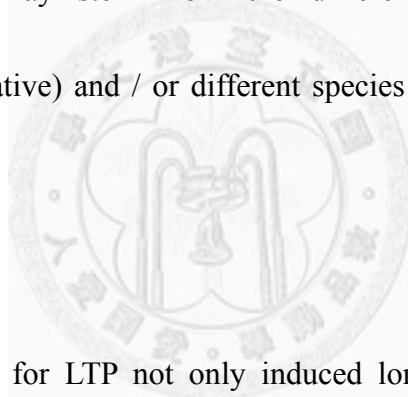
The pairing protocol for LTP not only induced long-term change in synaptc strength of CT pathway, but also induced a parallel increase in Gw, which was not observed when NMDARs were blocked, when depolarization or presynaptic stimulation was applied alone, or when postsynaptic depolarization was weaker (-45 mV). Furthermore, it was not observed when pairing was applied to ML pathway. These observations suggest the increase in G_W share similar cellular mechanism and properties with LTP of CT synapses, i.e. dependence on NMDARs, associativity, input specificity, and requirement for strong depolarization. In pyramidal neurons of

hippocampal CA1 area, in parallel with LTP, activation of NMDARs by paired pre- and postsynaptic activities upregulates local dendritic HCN1 channels, and thus reduce overall neuronal excitability (Fan et al. 2005). Since such a reduction in cellular excitability, together with synaptic potentiation at specific synapses, can provide a feedback mechanism for normalizing neuronal output firing and enhancing specificity of synaptic effectiveness (Fan et al. 2005), it will be very important to determine whether a similar mechanism underlie the intrinsic plasticity of VBN relay neurons. Unlike LTP, the induction of LTD of CT EPSC was not associated with a significant change in *Gw*.
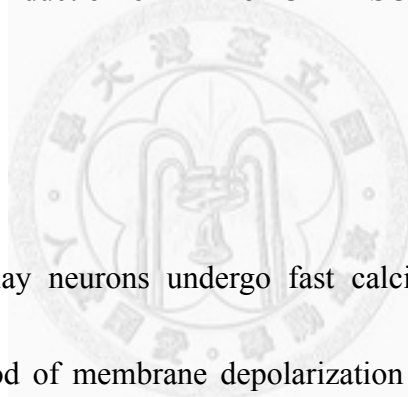
L-VGCCs in TC relay neurons undergo fast calcium-dependent inactivation (CDI) during a long period of membrane depolarization (Kammermeier and Jones, 1998; Meuth et al. 2002). This may explain why L-VGCCs appeared to be more efficiently activated by repeated depolarizing voltage pulses than by steady-state depolarization, as application of steady-state depolarization to postsynaptic relay neurons alone did not induce significant LTD (Fig. 3.2A).
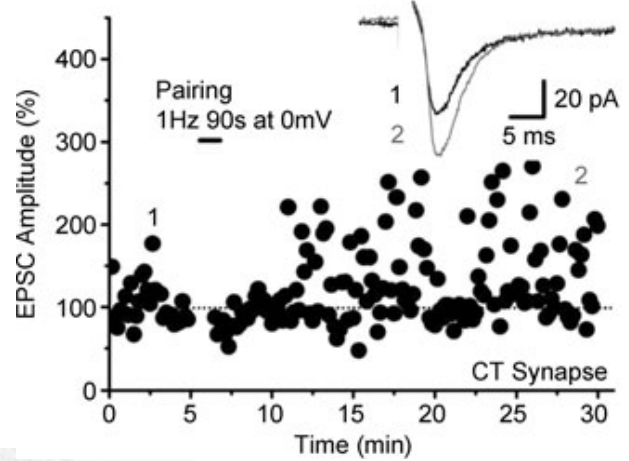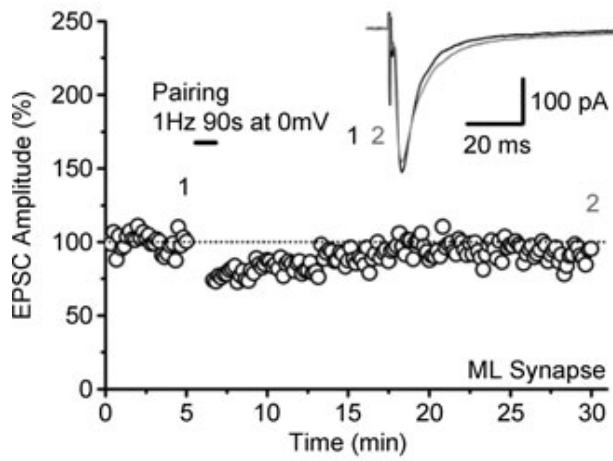
Figures

Figure 3.1 Induction of NMDAR-dependent long-term potentiation (LTP) at CT, but not ML synapses

Representative example (A_1) and summary (A_2) of the induction of LTP at CT synapses, but not ML synapses, by conjunctive pairing postsynaptic depolarization to 0 mV with 1 Hz stimulation for 90 s, which was blocked with 50μM APV, a selective NMDA receptor antagonist, applying in the bath (**B**). The upper and lower panels of A_2 and **B** show the time courses of synaptic responses and input conductance (G_W), respectively, of the cell tested. Accompanying LTP induction at CT synapses, there was a parallel long-lasting increase in G_W, which was blocked by APV, and not induced when pairing was applied to ML pathway, indicating such a increase is also NMDAR-dependent and has the property of input specificity, similar to the case in CA1 pyramidal neurons of hippocampus and could be attributed to a local upregulation of dendritic hyperpolarization-activated cyclic nucleotide-gated cationic channels (HCNs) (Campanac et al., 2008; Fan et al., 2005). Traces are averaged from 10 consecutive sweeps of recording. The pairing protocol is shown in the inset of A_2. In A_2 and **B**, each point is a 5-point average.

Figure 3.1
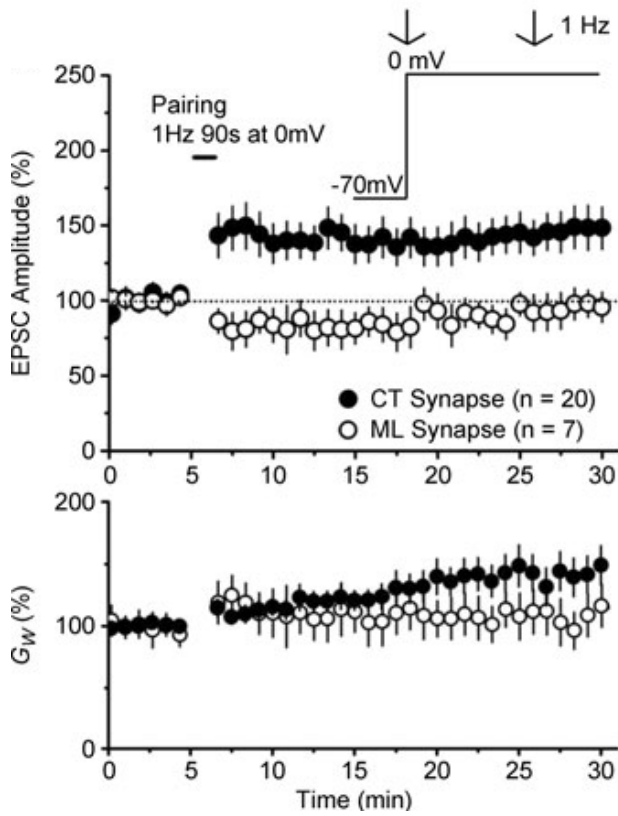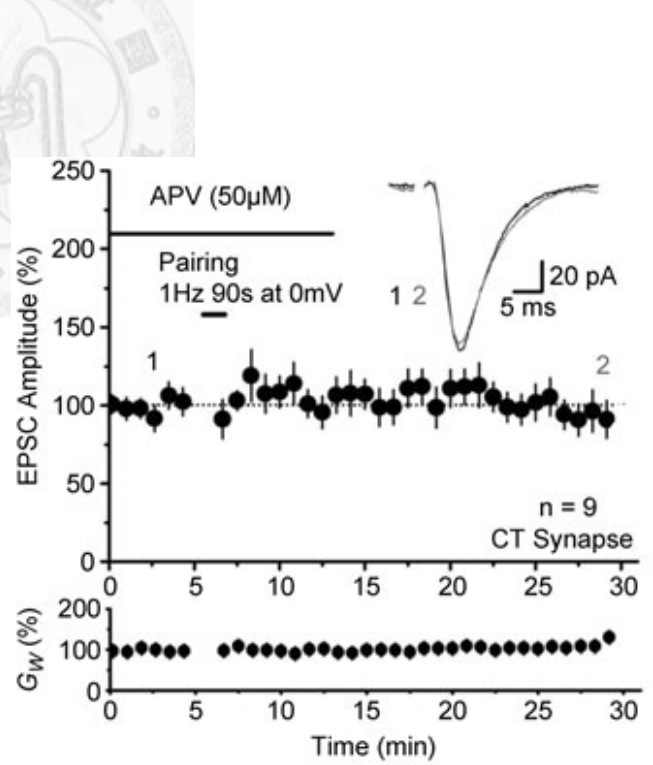
Figure 3.2 Associativity of the LTP at CT synapses

A~B, As control experiments, the pairing protocol was applied without 1-Hz presynaptic stimulation (**A**) or postsynaptic depolarization (**B**). Neither postsynaptic depolarization alone nor presynaptic stimulation alone induced long-term synaptic plasticity at the CT synapses, showing associativity of LTP induction at CT synapses. Note that the long-lasting increase in *Gw* was induced in neither cases, indicating a parallel associativity of induction of such an intrinsic plasticity. The traces are averaged responses over 10 sweeps of recordings. All conventions are similar to Fig. 3.1.

Figure 3.2

Figure 3.3 Input specificity and depolarization requirement of the LTP at CT synapses

A, A pairing protocol with the postsynaptic depolarization to -45 mV did not induce long-term synaptic plasticity at CT synapses, consistent with the requirement of strong postsynaptic depolarization, and thus sufficient activation of NMDAR, for the induction of LTP. For a weak test pathway, the requirement of sufficient depolarization may underlie the dependence of LTP induction on the number of coincident inputs recruited or synchronized tetanization of a strong pathway, which was termed "cooperativity" in early studies (Barrionuevo and Brown 1983; Levy and Steward 1979; Markram et al., 1997; McNaughton et al. 1978). **B,** In some cases, EPSCs evoked by stimulating medial lemniscus (*ml*) showing linearity and paired-pulse facilitation ("undefined pathway"), which reflects the potential heterogeneity of *ml* fibers; please see text for detailed discussion of pathway characterization. For these cases, the pairing protocol for LTP induction at CT synapses did not induce long-term plasticity, supporting the input specificity of LTP at CT synapses. All conventions are similar to Fig. 3.1. **C**, Summary of all experiments described in **Fig. 3.1 ~ 3.3**, showing the associativity, requirement of strong depolarization, and input specificity of the induction of NMDAR-dependent LTP at CT synapses.

Figure 3.3

Figure 3.4 A modified pairing protocol in which the holding voltage (V_h) returns to -70 mV for 500 ms prior to each presynaptic stimulation did not induce LTP at CT synapses

Representative example (**A**) and summary (**B**) of time courses of CT EPSCs in response to a modified pairing protocol. To de-inactivate the voltage- or calcium-dependent inactivating conductances, so their role in the induction of long-term plasticity at CT synapses can be tested while the activation of NMDARs is presumably spared, the pairing protocol was modified to retain a 500-ms-long phase with the V_h = -70 mV prior each presynaptic stimulation, and the new protocol is thus equivalent to a conjunctive pairing of 1Hz presynaptic stimulation with postsynaptic depolarizing pulses. However, this protocol did not induce long-term plasticity at CT synapses. Note that long-lasting increase in *Gw* was not induced, either. The traces are averaged responses over 10 sweeps of recordings. All conventions are similar to Fig. 3.1.
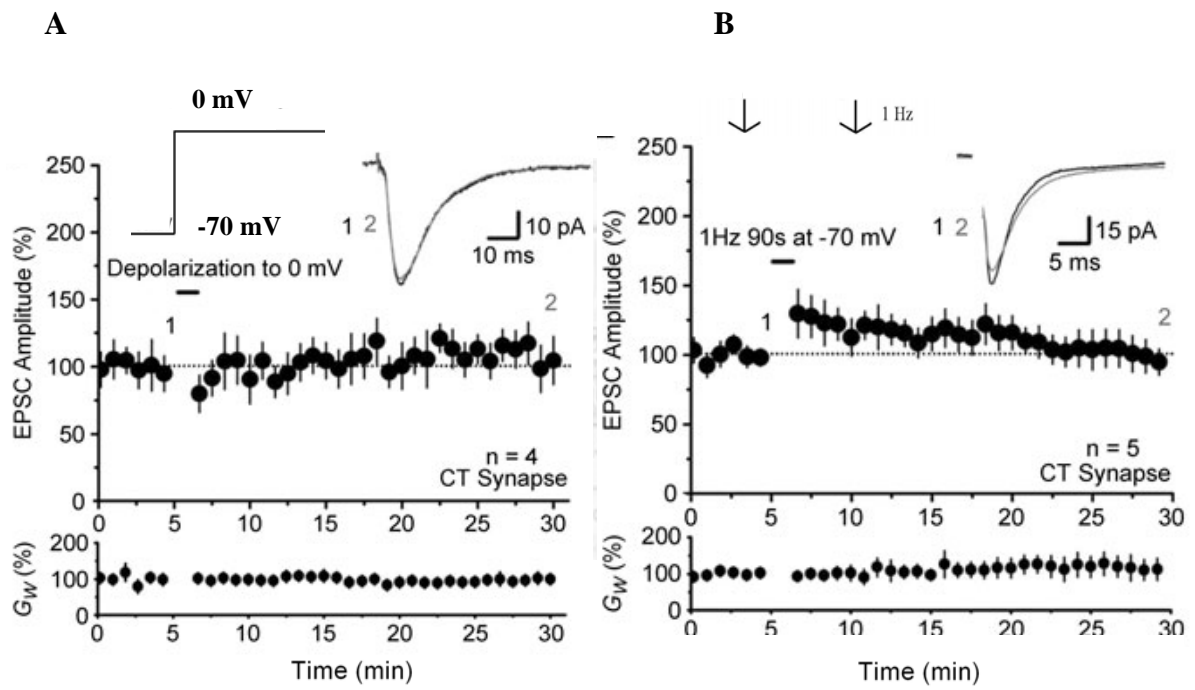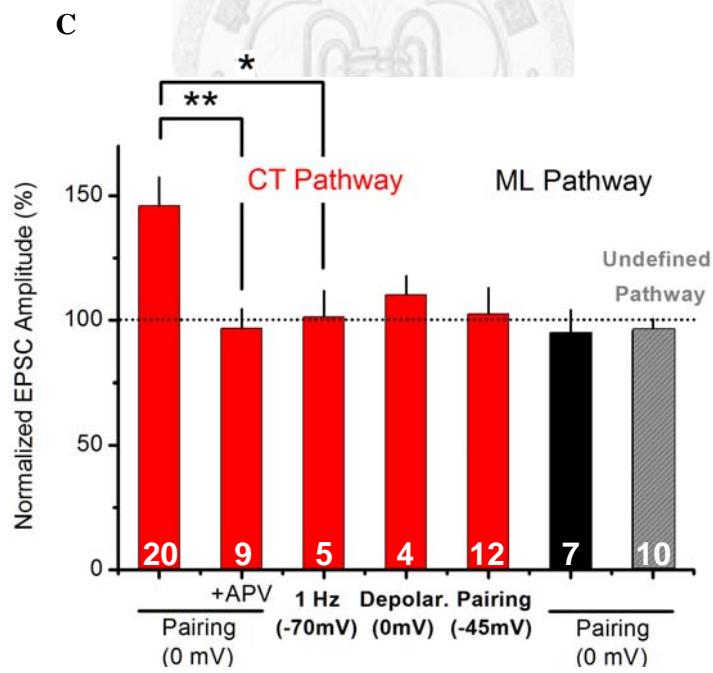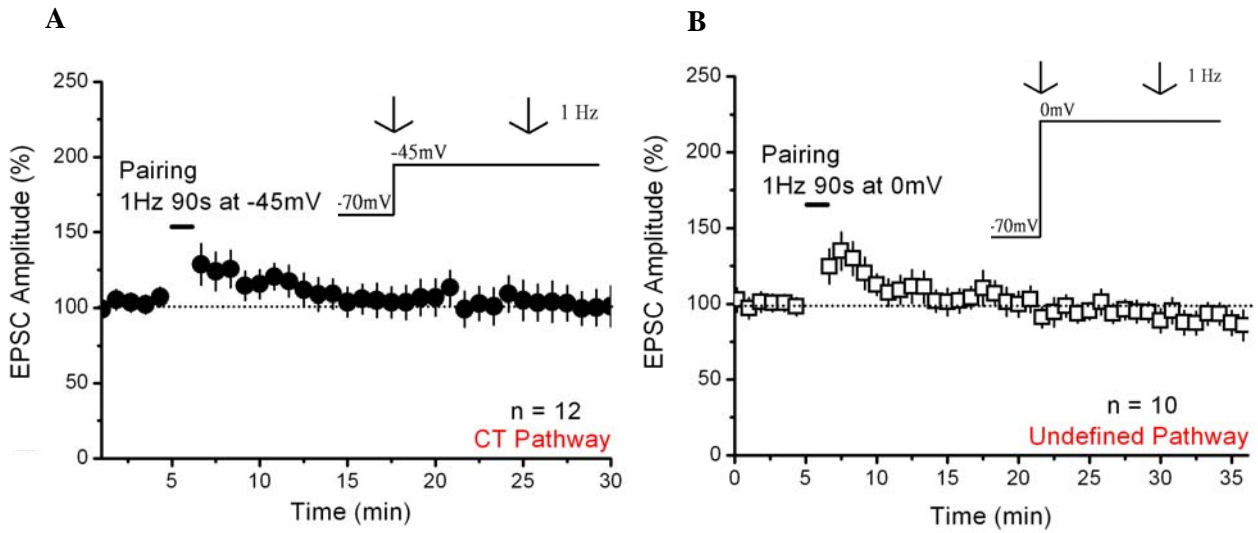
Figure 3.4
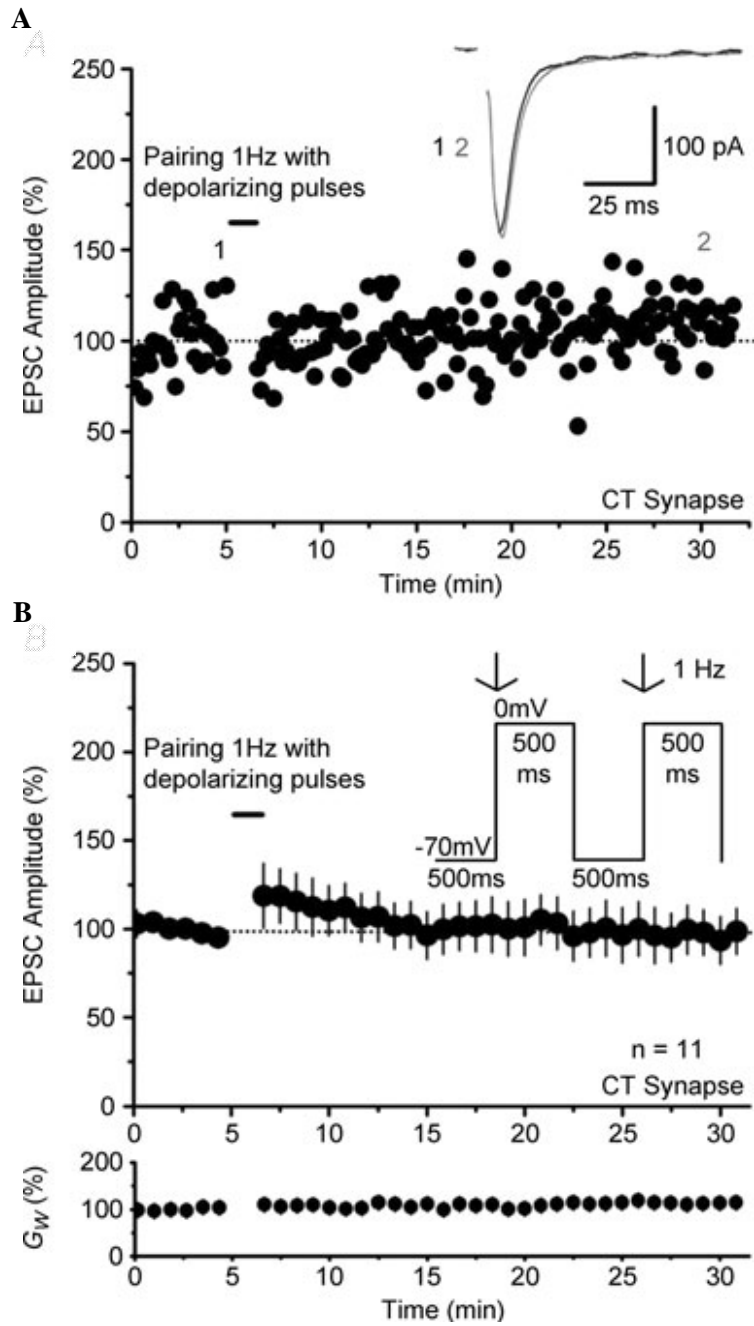
Figure 3.5 Repetitive depolarizing pulses induced L-type VGCC-dependent LTD at CT synapses, but not ML synapses

A, Representative example of time courses of CT and ML EPSCs, evoked from the same neuron, in response to repeated depolarizing pulses (A_1) and the corresponding summary (A_2). In order to distinguish between the possibilities that inclusion of a modified phase prior to each stimulation interferes with either the induction process of LTP, i.e. the signaling downstream to NMDAR activation is disrupted, or the expression of LTP, by means of the concomitant expression of long-term plasticity at CT synapses that was previously unknown, 1-Hz repetitive postsynaptic depolarizing pulses alone were applied to the recorded cell. A novel LTD was induced selectively at CT synapses, but not ML synapses; in contrast to LTP, there was no significant change in G_W paralleling expression of LTD at CT synapses. The data include 6 experiments in which CT and ML EPSCs were simultaneously recruited in the same relay neuron. All traces were averaged from 7 consecutive sweeps of recording. **B**, This LTD was blocked by intracellular dialysis of BAPTA, a fast calcium chelator, indicating that LTD was dependent on the rise of intracellular calcium concentration. It also suggests that local network activities, potentially driven by repetitive, powerful excitation of the recorded neuron was not sufficient to this form of LTD. **C**, This LTD was blocked by nimodipine, a selective L-type VGCC blocker, applied in the bath,

showing that LTD was dependent on activation of L-type VGCCs. All conventions are

similar to Fig. 3.1.

Figure 3.5
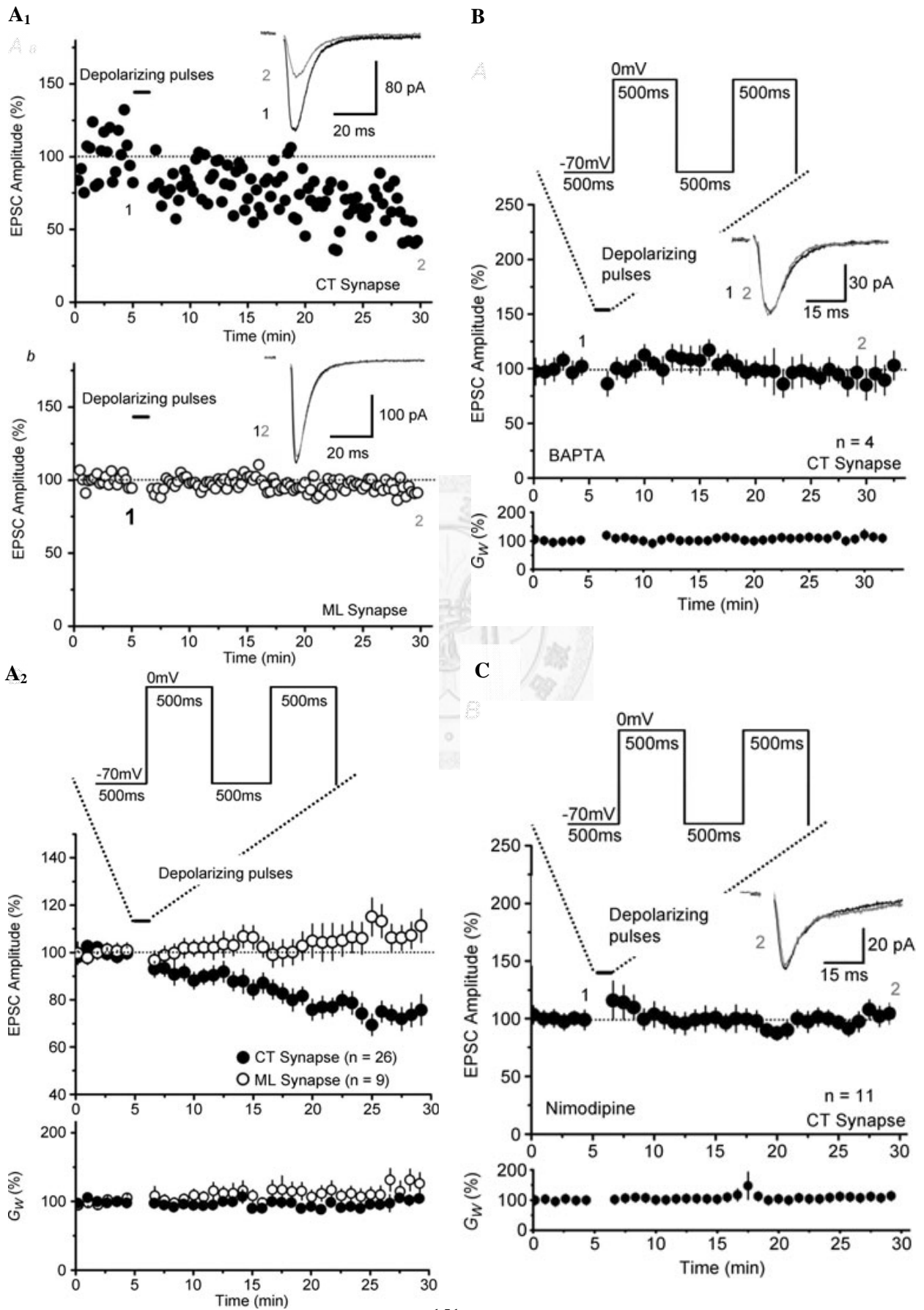
Figure 3.6 The blocking effect on LTP by retaining a hyperpolarized phase prior to presynaptic stimulation can be partly explained by a concomitant expression of L-type VGCC-dependent LTD at CT synapses

Representative example (**A**) and summary (**B**) of time courses of CT EPSC in response to the modified pairing protocol in the presence of nimodipine applied in the bath. Blockade of L-type VGCCs uncovered LTP expression at CT synapses, supporting the hypothesis that absence of LTP in response to returning V_h back to -70 mV in the pairing protocol reflects a concomitant counteracting expression of LTD at CT synapses induced by activation of L-type VGCCs. It is, however, worth noting that no long-lasting increase in *Gw* accompanied CT LTP expression in this condition, which might be due to the effect made by activation of inactivating conductances other than L-type VGCCs or some unknown voltage-dependent cellular process. This hypothesis can potentially explain the similar absence of increase in *Gw* in **Fig. 3.4**, as our results suggest LTP at CT synapses had occurred (despite masked by simultaneous expression of LTD). Traces are averaged from 10 consecutive sweeps of recordings. Conventions are similar to those in Fig. 3.1.

Figure 3.6

A

B

153
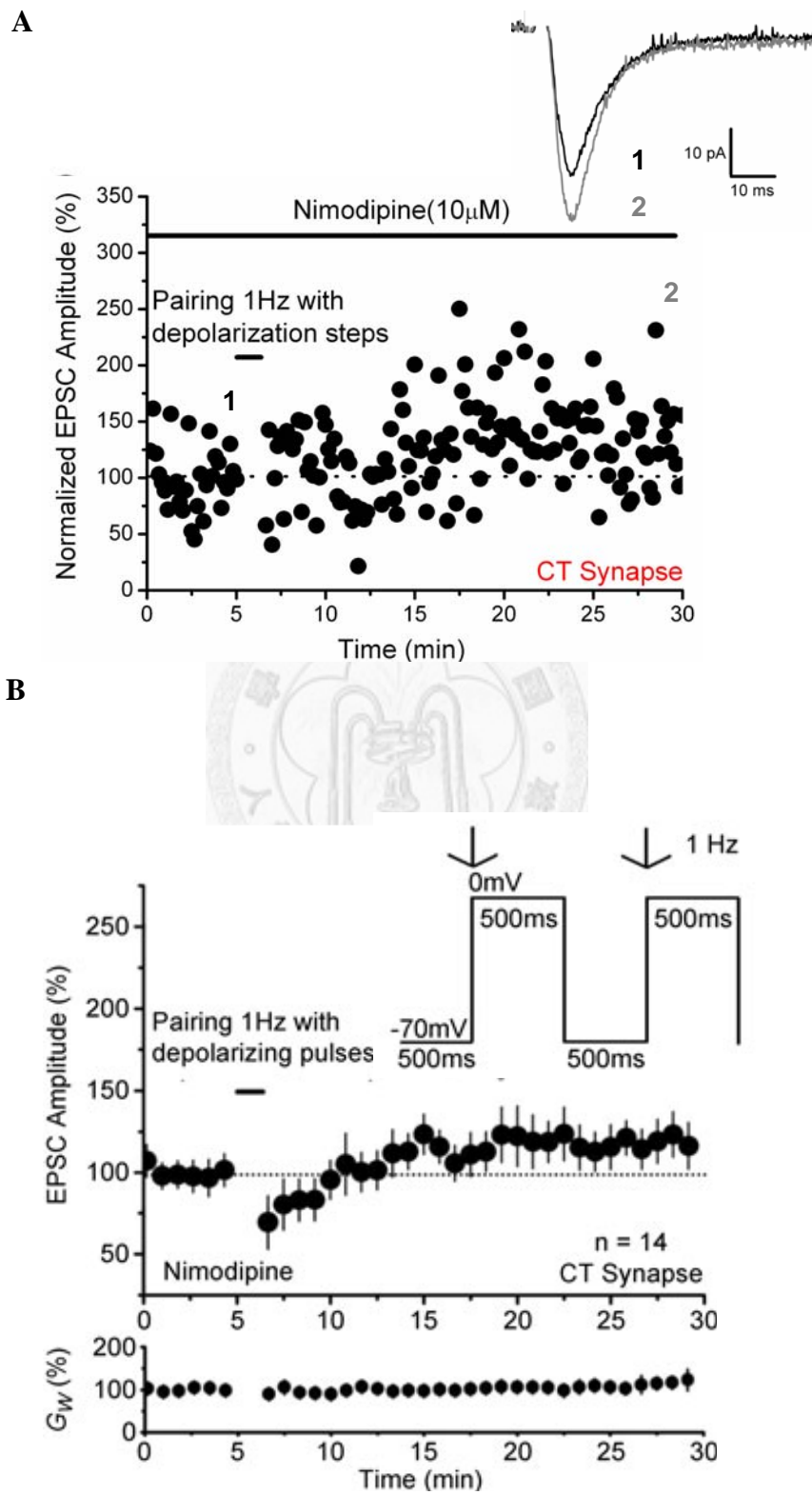
Figure 3.7 LTD induced by depolarizing pulses at CT synapses was not dependent on activation of T-type VGCCs

Repetitve switches of the V_h back to -70 mV during depolarizing pulses can de-inactivate multiple inactivating conductances. To assay the role of T-type VGCCs in induction of CT LTD, we quantified the blocking effects of Ni^{2+} and mibefradil, two of the most widely used pharmacological agents for T-type VGCC blockade, on LTS of VBN relay nenrons so as to assess their specificity and reliability. LTS was isolated by postivie current injection at Vm ~ -70 mV in the presence of 5 mM QX-314 (internally-applied) and 10 μM nimodipine (bath-applied) to block Na^+ spikes and $Ca2^+$ spikes, and the drug to be tested was applied to the bath. **A,** Ni^{2+} had a concentration of half-maximal blocking effect on LTS to be ~ 600 μM, which is far beyond its working range for selective blockade of T-type VGCCs (Avery and Johnston, 1996; Lee et al., 1999; Magee and Johnston, 1995). **B,** Mibefradil could not significantly reduce the amplitude of LTS at the concentration which permits moderate selectivity for the blockade of T-type VGCCs, as specified by its commercial provider (IC_{50} is ~ 2.7 μM and 18.6 μM for blocking T-type and L-type channels, respectively; from Tocris). Taken together, neither of them could block LTS effectively at low micromolar concentrations. **C,** To avoid confounding side effects by using these pharmacological tools, we adopted a substitutive strategy to prevent

activation of T-type VGCCs during depolarizing pulses by means of voltage-dependent inactivation. The hyperpolarized phase of depolarizing pulses was changed to -50 mV, a voltage at which LTS was completely absent in current-clamp mode (**Fig. 2.3A**). Induction and expression of LTD was not affected by this modification, suggesting the lack of involvement of T-type channels in CT LTD. The traces were averaged over 10 consecutive sweeps of recordings. Conventions are similar to **Fig. 3.1**.

Figure 3.7

A

B

C

156
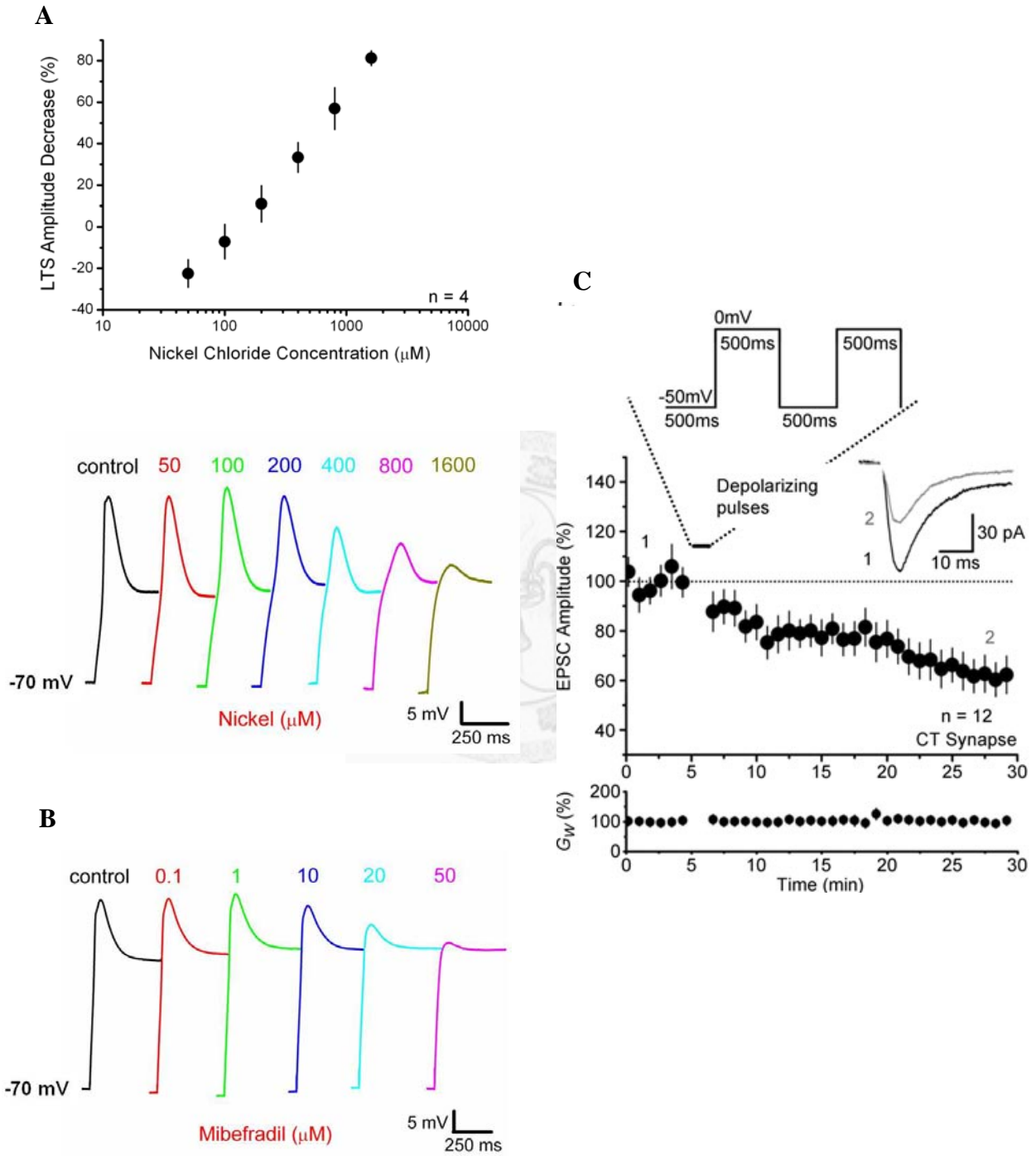
Figure 3.8 LTD induced by depolarizing pulses at CT synapses was not dependent on activation of NMDARs and CaP-AMPARs

A~B, Summary of time courses of CT EPSC in response to depolarizing pulses in the presence of APV (**A**) and PhTx-433 (**B**) applied in the bath to block NMDARs and CaP-AMPARs, respectively. The results showed that neither receptors contribute to LTD at CT synapses. All Conventions are similar to **Fig. 3.1**. **C**, Summary of all experiments described in **Fig. 3.4 ~ 3.8**, with a comparison of the magnitude of LTP (**Fig. 3.1A**). L-type VGCC-dependent LTD was selectively expressed at CT synapses, which does not require activation of T-type VGCCs, NMDARs, and CaP-AMPARs, and can at least partly explain the masked expression of CT LTP in the case of modified pairing protocol.
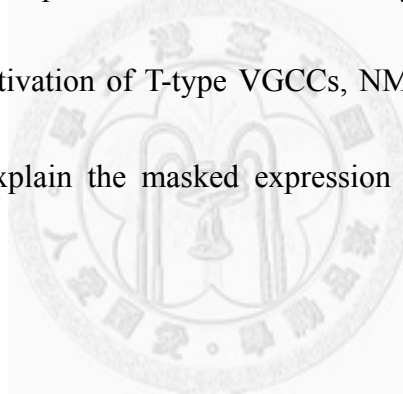
Figure 3.8
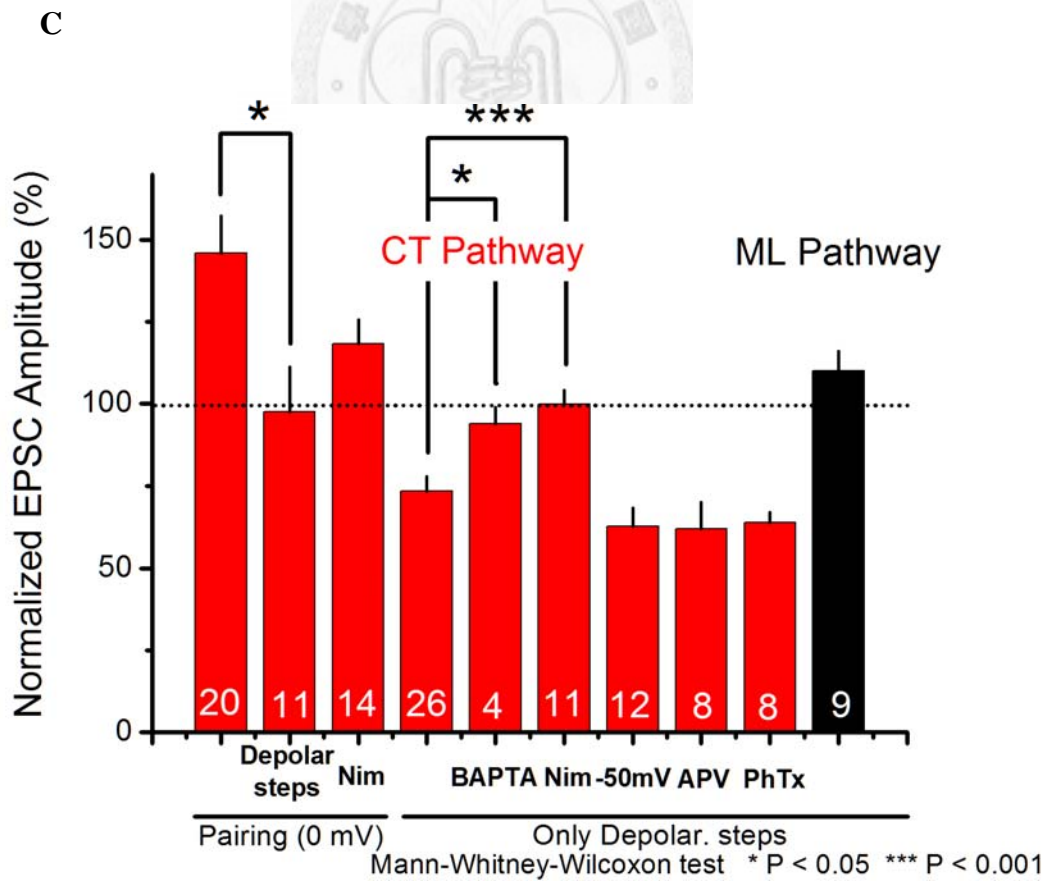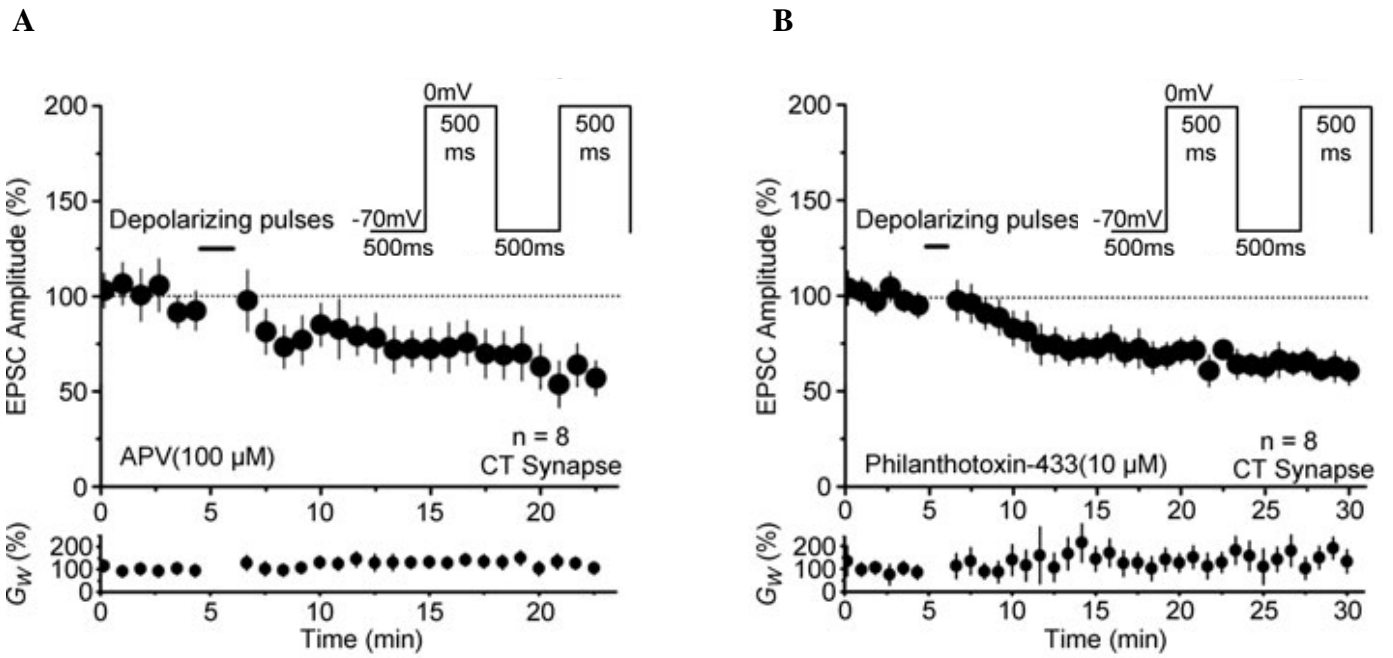
Figure 3.9 "Anti-Hebbian" pairing protocol could not induce long-term plasticity at CT synapses.

Representative example (A) and summary (B) of time courses of CT EPSC in response to an "anti-Hebbian" protocol, which is composed of 2 cycles of pairing 100-Hz presynaptic stimulation for 1 s with postsynaptic hyperpolarization to -90 mV, with an interval of 10 s, which potentially maximizes activation of CaP-AMPARs (Lamsa et al., 2007; Liu and Cull-Candy, 2000). The internal solution was supplemented with spermine. The results showed that no long-term plasticity of CT synapses was significantly induced by this protocol (110 ± 16 %). However, some other factor, such as a simultaneous activation of mGluRs expressed postsynaptically to CT synapses (Golshani et al., 1998; Hughes et al., 2002; Reichova and Sherman, 2004; Sherman and Guillery, 2004) during high-frequency stimulation, should be taken into consideration for interpreting this result. All Conventions are similar to **Fig. 3.1**.

Figure 3.9

A
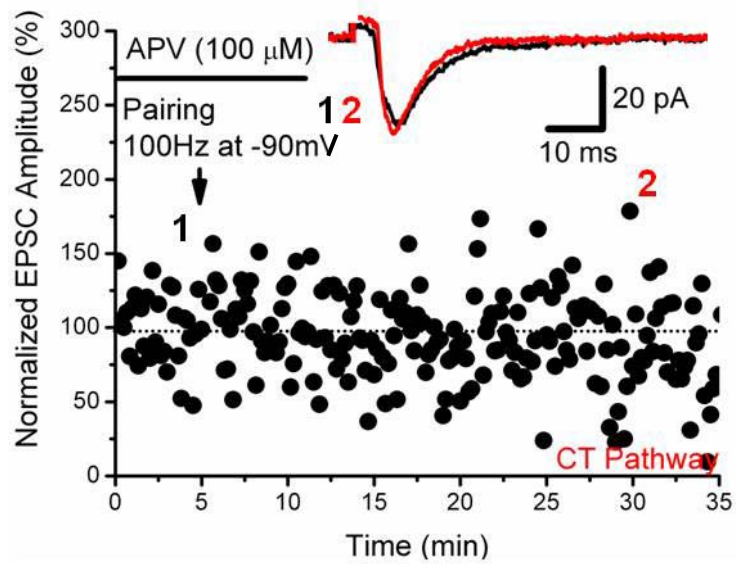
B
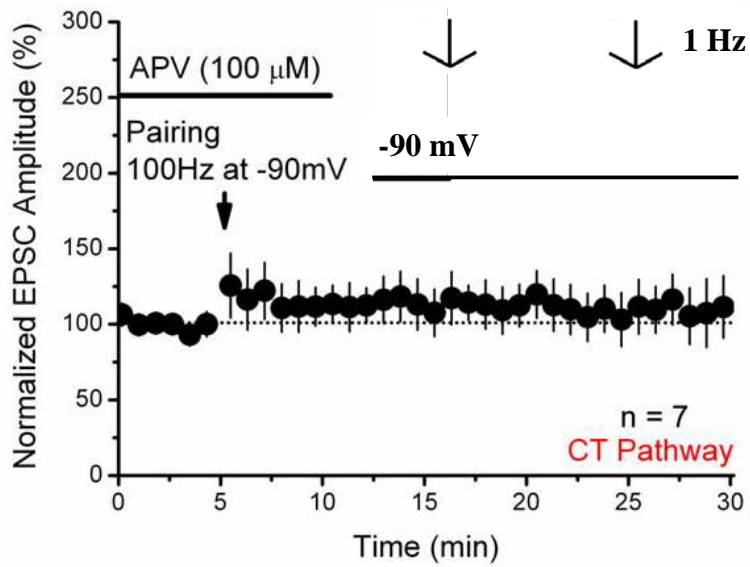
Chapter 4

The role of ionotropic glutamate receptors

in long-term plasticity of corticothalamic synapses

Abstract

Our findings concerning the differences between CT and ML synapses in the ability to expressing long-term plasticity are interesting. In view of the coincidences of higher functional expression of NMDARs, selective expression of CaP-AMPARs, and bidirectional long-term plasticity of CT pathway, fundamental questions with regard to the role of these ionotropic gluramate receptors in the synaptic plasticity of CT pathway were addressed in this chapter. We showed that induction and expression of LTD are not dependent on NMDARs and calcium-permeable non-NMDARs by pharmacological experiments. In particular, comparisons of rectification index (RI) of I-V relationship and weighted mean single-channel conductance before and after LTD suggested that LTD induction is not accompanied by a significant preferential downregulation of calcium-permeable non-NMDARs. Our peak-scaled nonstationary noise analysis also indicated that average number of synaptic non-NMDARs open at

the peak of EPSC does not change following LTD, together with coefficient of variation (CV) analysis of EPSC amplitude, implying the expression mechanisms mainly involve presynaptic modification. To summarize, these results suggested that expression of L-type VGCC-dependent LTD at CT synapses is independent to NMDARs and calcium-permeable non-NMDARs, and potentially involve presynaptic mechanism.

Introduction

Our findings regarding the differences between CT and ML synapses in the ability to expressing long-term plasticity are interesting, and the induction mechanisms for the bi-directional synaptic plasticity of CT pathway had been identified (chapter 3). The intriguing coincidences of selective expression of CaP-AMPARs, higher NMDAR content, and synaptic plasticity of CT pathway motivates us to pursue the fundamental question: what is the functional significance of these ionotropic glutamate receptors to long-term plasticity of CT synapses? Recent research have demonstrated the functional relationships between CaP-AMPARs and long-term synaptic plasticity. CaP-AMPARs were reported to

162

involve the induction (Lamsa et al., 2007; Liu and Cull-Candy, 2000), expression (Ho et al., 2007), and consolidation (Plant et al., 2006) of synaptic plasticity. At parallel fiber-stellate cells synapses of cerebellum, it was shown that CaP-AMPARs contribute to the subtype switch of synaptic AMPA receptors in a self-regulated manner (Liu and Cull-Candy, 2000). Ho et al. (2007) reported that a time-dependent, input-specific CaP-AMPARs expression at developing mossy fiber-CA3 synapses of hippocampus coincides with the developmental window only within which an L-type VGCC-dependent LTD can be induced by a strong depolarizing command in voltage-clamp recording, and express by means of a preferential downregulation of synaptic CaP-AMPARs. These findings arouse our curiosity over the parallelism of CaP-AMPAR and LTD expression. We have touched this question by a preliminary experiment to test the possibility that they contribute to induction of long-term synaptic plasticity by an "anti-Hebbian" mechanism (chapter 3). In this chapter, we continue applying multiple approaches to investigate the relationships between ionotropic glutamate receptors and long-term plasticity of CT synapses.

Methods

Preparation of acute slices

The use of animals in this study was in accordance with the guidelines of the local ethical committee for animal research of National Taiwan University. Sprague-Dawley (SD) rats of both sexes aged 13-24 postnatal days (P13-24) were used, but most were aged P13-16. The animals at these ages were chosen because the intrinsic and firing properties of rat VBN neurons reach developmental steady-state after P12, including the resting membrane potential (Vm), input resistance (R_N), ability to fire full-blown LTS-driven bursting, width of action potential (AP) and after-hyperpolarization (AHP) (Velazquez and Carlen, 1996). Possibly attributible to less extent of myelinated fibers, the success rate in obtaining good seal and recording quality was also significantly higher from animals of this age window, which is especially critical for the purpose of simultaneous recruitment of CT and ML synapses.

The rats were anaesthetized with isoflurane and decapitated with a small-animal guillotine, and the brain was quickly removed and placed in ice-cold artificial

cerebrospinal fluid (ACSF). Coronal slices were used for initial experiments. We then

discovered that, in horizontal slices, it was easier to recruit CT and ML EPSCs

simultaneously in the same relay neuron, horizontal preparation was adopted for the

most part of this study. For horizontal preparation, the two halves of the brain were

first separated, and their ventral portions were trimmed in parallel to the ventral

surfaces of brainstem to ensure standard horizontal cutting orientation in accordance

with traditional stereotaxic coordinates. A block of agar was glued behind the medial

surface of a half-brain to provide physical support during slicing. Horizontal brain

slices (300 μm) containing the ventrobasal nucleus (VBN), internal capsule (*ic*) and

medial lemniscus (*ml*) fibers were prepared, using the patterns of *ic* and the fibers in

the ventral posterolateral nucleus (VPL) as landmarks (Fig. 2.1). For coronal

preparation, intact coronal slices were cut and the two halves were separated by blade.

Coronal brain slices (300 μm) containing the VBN, *ic* and *ml* were prepared, using the

patterns of VBN and its fiber patterns as landmarks (Fig. 2.1).

The slices were cut with a vibroslicer (752M, Campden, Loughborough, England

or ZERO 1, D.S.K., Osaka, Japan). The ACSF contained (in mM): 119 NaCl, 2.5 KCl,

1.3 $MgSO_4$, 26.2 $NaHCO_3$, 1 NaH_2PO_4, 2.5 $CaCl_2$, and 11 glucose; pH adjusted to 7.4

by gassing with carbogen consisted of of 95 % O_2 / 5 % CO_2. The slices were kept in

oxygenated ACSF (95% O_2 / 5% CO_2) at room temperature (24-25°C) to allow

recovery for at least 90 minutes before recording was started.

Electrophysiology

Slices were transferred to an immersion-type recording chamber mounted to an

upright microscope (BX50WI, Olympus Optical, Tokyo, Japan), equipped with

water-immersion objectives, a Normaski optic system, an infrared filter and a CCD

camera (XC-E150, Sony, Tokyo, Japan) (IR-DIC system). In horizontal slices, the

VBN, *ic* and *ml* were clearly identifiable under low-magnification light microscopy.

In some cases, we noticed that there was a small heterogeneous zone locating in the

border of VPL medial to *ic*, which indicated a lower density of myelinated fibers (Fig.

2.1A$_3$). Recordings made from this zone was avoided to prevent potential

confounding factors which may originate from functional or biochemical

heterogeneities within VBN (see chapter 1 for detailed descriptions). Neurons in the

VBN were recorded under visual guidance. The typical number of fast spikes of a

LTS-burst firing is 4~9 as depolarizing current pulses were injected at the V_m <

-75mV. Occasionally, some neurons had a spike number of LTS-burst < 3 and were

discarded.

IPSPs were rarely observed in horizontal VBN slices of mice (Castros-Alamancos, 2002), which could be attributed to the orientation of the slice preparation so the fibers were not well preserved. Nevertheless, all experiments carried out in this study were performed in the presence of 0.1 mM picrotoxin and 1 μM strychnine to avoid any potential confounding effects of GABAergic and glycinergic IPSPs.

Patch pipettes were pulled from borosilicate glass (1.5 mm outer diameter, 0.32 mm wall thickness; G150F-4, Warner Instruments Corp., Hamden, CT, USA), and had a resistance of 3~8 MΩ. For experiments characterizing basic excitatory synaptic properties such as rectification index (RI) of I-V relationship (Fig. 4.2 A~B), "cesium internal solution" was used to avoid metabotropic receptor-dependent potassium conductances (for evoked $GABA_B$ IPSC in the VBN of rats, see Kao and Coulter, 1997). The cesium internal solution contained (in mM): 114.7 CsOH, 17.5 CsCl, 117.6 gluconic acid, 10 HEPES, 2 EGTA, 8 NaCl, 2 ATP, 0.3 GTP, and 6.7 biocytin; pH was titrated to 7.2 by CsOH and osmolarity to 300-305 mOsm. For experiments on the synaptic plasticity, "normal internal solution" was used, which contained (in mM): 131 K-gluconate, 20 KCl, 10 HEPES, 2 EGTA, 8 NaCl, 2 ATP,

0.3 GTP, and 6.7 biocytin; pH was titrated to 7.2 by KOH and osmolarity to 300-305

mOsm. In all experiments in which depolarizing step commands were used, 5 mM

QX-314 was included in the internal solution to block voltage-gated Na^+ channels and

enhance the voltage control. Signals were obtained by Axopatch 1D amplifier (Axon

Instruments, Union City, CA, USA). Slices were continuously perfused with

oxygenated solutions at 1~2 ml / min under room temperature. For voltage-clamp

recordings, whole-cell conductance (Gw) and series resistance (Rs) were continuously

monitored by a test voltage pulse of 3 mV; Rs was typically < 20 MΩ and was not left

uncompensated. Data were discarded when Rs varied by more than 20% from its

baseline value during the recording. All signals were low-pass-filtered at a corner

frequency of 2 kHz, then digitized at 10 kHz using a Micro 1401 interface

(Cambridge Electronic Design, Cambridge, UK). Data were collected using Signal

(Cambridge Electronic Design, Cambridge, UK) or Spike 5 (Cambridge Electronic

Design, Cambridge, UK) by episode-based capture. The liquid junction potential was

measured to be ~ +10 mV and left uncorrected (following the method by Neher,

1992).

Stimulation of CT and ML synapses

A bipolar stainless steel electrode (PK/12, FHC, St Bowdoin, ME, USA) was placed locally within 150 μm away from the recorded cell or in *ic* for evoking CT EPSCs. No significant differences were observed between the CT EPSCs evoked by these two conditions (Table 2.1). In occasion, stimulation of *ic* antidromically discharged relay neurons; however, antidromic responses showed apparent all-or-none behavior and no short-term plasticity normally displayed by synaptic responses, therefore easily identifiable.

In high-magnification IR-DIC images of horizontal slices, we observed a large number of fiber bundles projecting from the direction of *ic*, traversing the reticular nucleus (Rt) and the small heterogeneous zone in the border of VPL (described above) into VBN. We traced along the fiber bundles proximal to the recorded neuron, back to their origin in *ic*, and placed the stimulating electrode accordingly to facilitate the success rate of recruiting measurable CT EPSCs. A typical stimulus consisted of a 4~100 μs square pulse with the amplitude ranged in 30~800 μA. In some cases, the stimulating artifact was relatively large, and the synaptic responses were analyzed after the artifact waveform obtained in 10 μM DNQX, a selective non-NMDARs antagonist, was subtracted.

For recording the excitatory postsynaptic currents (EPSCs), V_m was voltage-clamped at -70 mV, with 100 μM picrotoxin (PTX) and 1 μM strychnine added to the bath ACSF solution to block ionotropic GABA$_A$ receptors and glycine receptors (for the glycinergic transmission in the VBN, see Ghavanini et al., 2005; Ghavanini et al., 2006), respectively. After the experiments were finished, 10 μM DNQX were applied in the bath in most cases to confirm the identity of recorded activities as a non-N-methyl-D-aspartate receptor (non-NMDAR)-mediated component. EPSCs were evoked at 0.1 Hz.

Long-term synaptic plasticity

For synaptic plasticity experiments, a stable baseline was recorded for at least 5 min, followed by an additional ~ 25 min of recording after induction protocol was applied. To prevent potential washout of cell content required for induction of synaptic plasticity, data were discarded if the time of recording after "break-in" into whole-cell configuration was over 12 min but the induction protocol had not been applied yet. Amplitude of individual EPSC was normalized with respect to the mean measurement of all baseline responses before induction, and the normalized measurements recorded in 18.5~23.5 min after induction (16.5~21.5 min after

induction for LTD induction in the presence of APV) were averaged and used for statistical comparison.

Peaked-scaled nonstationary noise analysis

In order to investigate the expression mechanism of synaptic plasticity, we used peak-scaled nonstationary noise analysis to compare the postsynaptic parameters before and after the plasticity induction (Benke et al., 1998; Hartveit and Veruki, 2007; Heinemann and Conti, 1992; Lei et al., 2003; Robinson et al., 1991; Silver et al., 1996; Traynelis and Jaramillo, 1998; Traynelis et al., 1993) mostly following Traynelis et al. (1993) and Hartveit and Veruki (2007). Only the data which were sufficiently amplified before digitization with good signal-to-noise ratio and almost perfectly stable recording quality (series resistance) were chosen for analysis. Their EPSC waveforms were then visually examined to exclude those contaminated by spontaneous synaptic activities or sudden changes of the holding current; only the waveforms showing smooth rising and decaying phases were selected, with the total of 18-63 EPSC waveforms for each analysis. To evaluate potential time-dependent drift / run-down, and the presence of differential electrotonic filtering of the EPSCs, they were tested for time stability and correlations between waveform parameters

(Hartveit and Veruki, 2007); that is: (1) the time stability of 10-90% rise time, decay time constant obtained by mono-exponential curve fitting, and peak amplitude (2) the correlations between the data of each pair among 10-90% rise time, decay time constant, and peak amplitude. All the correlations were tested for statistical significance by Spearman's rank-order correlation test, and only the data with all P > 0.05 were selected for further analysis.

The EPSC waveforms were first aligned on the point of the steepest rise, and the results of alignment were visually inspected to check the adequacy. Among the 5 data sets from the selected neurons, one of them seemed to be aligned more poorly after the alignment procedure compared with that without alignment. For the evoked EPSCs, responses are presumably aligned by the stimulus (Hartveit and Veruki, 2007), and we therefore cancelled the alignment procedure for this case. To isolate the current fluctuation associated with stochastic channel gating, the averaged EPSC waveform was scaled to set its peak to the value of individual EPSC waveforms at the corresponding time point, and the ensemble variances were calculated for each point in the decay period of 10 times the decay time constant of the averaged waveform. The amplitude of the averaged EPSC waveform was then divided into 30 equally-sized bins, and the ensemble variances were pooled according to their

corresponding ones. The binned variances were plotted against the binned currents, and the postsynaptic parameters were estimated by the least-squared fitting of the variance-current relationship according to $\sigma^2 = i\,I - I^2 / N^P + \sigma_b^2$ (Sigworth, 1980) with the σ_b^2 constrained, where σ^2 is the variance, I is the current, i is the weighted-mean single channel current, N^P is the average number of channels open at the peak of the EPSC (not the total number of channels exposed to neurotransmitters), and σ_b^2 is the variance of the background noise, which was estimated from the pre-stimulus period. The weighted mean single-channel conductance, γ, was determined by $\gamma = i / V$, where V is the driving force (the holding potential minus the measured reversal potential of +2 mV at CT synapses). All mathematical manipulations were implemented with MATLAB (The MathWorks, Natick, MA, USA).

One of the most important concerns for applying this method to our system is that CT synapses are morphologically distal to recording site (Liu et al., 1995), which could severely compromise the space clamp. However, it has been reported that the estimated electrotonic length of relay neurons in dorsal and ventral lateral geniculate nucleus (dLGN and vLGN) of rats (Crunelli et al., 1987) is ~ 0.7, suggesting that thalamic relay neurons may be relatively electrotonically compact. In all analyzed
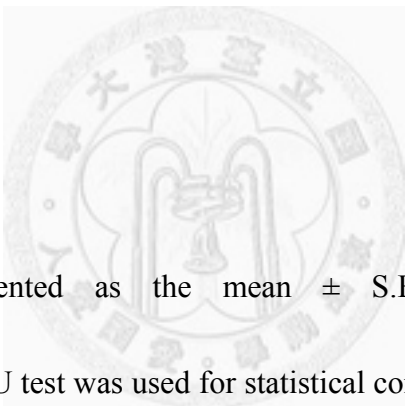
cases of CT pathway, the variance-current relationships were skewed to the right (Fig. 4.3), which was independent of the situations of alignment and existed even in the case of almost perfect alignment; therefore, that may be attributable to the kinetic properties of the non-NMDARs or asynchronous release (Hartveit and Veruki, 2006; Momiyama et al., 2003; Traynelis et al., 1993). Although the estimates of N^P would be unreliable under this condition (Hartveit and Veruki, 2007; Heinemann and Conti, 1992; Robinson et al., 1991; Silver et al., 1996; Traynelis and Jaramillo, 1998; Traynelis et al., 1993), we fitted the initial 33% of the variance-current relationships linearly to give estimates of weighted mean single-channel currents, which were proposed to be relatively insensitive to the skewness of the relationships and the electrotonic distance between the recording and synaptic sites (Benke et al., 2001; Hartveit and Veruki, 2006; Robinson et al., 1991; Traynelis and Jaramillo, 1998; Traynelis et al., 1993). N^P was calculated from I^P / i, where I^P is peak amplitude of averaged EPSCs (Silver et al., 1996).

Drugs

Chemicals used for ACSF and internal solution were purchased from Merck (Damstadt, Germany). *N*-2,6-Dimethylphenylcarbamoylmethyl triethylammonium

bromide (QX-314) was purchased from Alomone Laboratories (Jerusalem, Israel).

DL-2-Amino-5-phosphonopentanoic acid (APV), 6,7-dinitroquinoxaline-2,3-dione

(DNQX), and spermine tetrahydrochloride were purchased from Tocris Cookson

(Bristol, UK). MgATP, NaGTP, picrotoxin, strychnine, and philanthotoxin-433

tris(trifluoroacetate) salt (PhTx-433) were purchased from Sigma (St. Louis, MO,

USA). All drugs were made as stock solutions, stored at -20°C, and diluted to working

concentration immediately before use.

Statistics

All data are presented as the mean ± S.E.M. The nonparametric

Mann-Whitney-Wilcoxon U test was used for statistical comparison between unpaired

data and Wilcoxon matched-pairs sign-ranks test was used for paired data. The

correlation analysis was performed by non-parametric Spearman's rank-order

correlation test. The criterion for significance was $P < 0.05$ for all statistical tests.

Origin (Microcal, Northhampton, MA, USA) and SAS (SAS, Cary, NC, USA)

software were used for data analysis.

Induction and expression of LTD at CT synapses is not dependent on NMDARs and

calcium-permeable non-NMDARs

In order to understand the role of ionotropic glutamate receptors in long-term

plasticity and the expression mechanism of LTD at CT synapses, multiple approaches

were applied. We have found that LTP induction at CT synapses is dependent on

activation of NMDARs (Fig. 3.1). On the contrary, LTD could be induced with APV

applied in the bath throughout the whole experiment ($62 \pm 8\%$ of the baseline, n = 8;

Fig. 4.1B), indicating that neither induction nor expression requires activation of

NMDARs.

To clarify the functional relationship between calcium-permeable non-NMDARs

and LTD expression at CT synapses, we started with the induction of LTD upon

blockade of CaP-AMPARs. LTD was induced in the presence of 10 μM bath-applied

PhTx-433 throughout the whole experiment ($64 \pm 3\%$ of the baseline, n = 8; Fig.

4.1A), suggesting that neither induction nor expression of LTD depends on

CaP-AMPARs. The independence of LTD expression to the preferential regulation of

calcium-permeable non-NMDARs is further supported by the following experiments:

first, rectification index (RI) of I–V relationship of non-NMDAR-mediated EPSC

before and after LTD induction was compared. As shown in Fig. 4.1B and C, the RI

during baseline was 0.56 ± 0.08 (n = 6), which was not significantly different from

that after LTD induction (RI = 0.61 ± 0.06).

Second, peak-scaled nonstationary noise analysis was applied to compare

postsynaptic single-channel conductances before and after LTD induction (Fig. 4.2)

(Benke et al., 1998; Hartveit and Veruki, 2007; Heinemann and Conti, 1992; Lei et al.,

2003; Robinson et al., 1991; Silver et al., 1996; Traynelis and Jaramillo, 1998;

Traynelis et al., 1993). To isolate current fluctuation associated with stochastic

channel gating, the averaged EPSC waveform has to be peak-scaled to individual

EPSC waveforms for calculating ensemble variances. Although the estimates of N^P

(average number of channels open at the peak of EPSC) was unreliable by fitting due

to the skewness (Hartveit and Veruki, 2007; Heinemann and Conti, 1992; Robinson et

al., 1991; Silver et al., 1996; Traynelis and Jaramillo, 1998; Traynelis et al., 1993), we

linearly fitted the initial 33% of the variance-current relationships to estimate

weighted mean single-channel current (Fig. 4.2A), which were proposed to be

relatively insensitive to the skewness of the relationship (Hartveit and Veruki, 2006;

Robinson et al., 1991; Traynelis and Jaramillo, 1998; Traynelis et al., 1993). After

LTD induction, the fitting yielded the weighted mean conductance of 6.2 ± 1.3 pS (n

= 5), which was not significantly different from that under baseline condition, 7.3 ±

1.1 pS (n = 5) (Fig. 4.2B; all locally-evoked EPSCs; P > 0.05, Wilcoxon

matched-pairs sign-ranks test). Therefore, the expression of LTD at CT synapses was

not accompanied by a significant change of mean conductance of synaptic

non-NMDARs. Average number of channels open at the peak of EPSC was also

calculated (see Methods). Theoretically, the results that the RI of I-V relationship (Fig.

4.1B) and the *weighted* mean single-channel conductance (Fig. 4.2B$_1$) did not change

following LTD induction could also be explained by a *proportionate* downregulation

of calcium-permeable and -impermeable non-NMDARs. This may not be the case,

however, because the average number of open synaptic non-NMDARs was not

reduced (baseline: 95 ± 20; LTD: 91 ± 29; P > 0.05, Wilcoxon matched-pairs

sign-ranks test). This result is also consistent with the implication of the CV analysis

(Fig. 4.3B) that expression of LTD mainly involves presynaptic modification (see

following). Taken together, our experiments showed that both induction and

expression of LTD do not depend on NMDARs and calcium-permeable

non-NMDARs, and LTD expression is not accompanied by alteration of

non-NMDAR content at CT synapses.

Analysis of coefficient of variation (CV)

Assuming that releasing behavior of presynaptic releasable quanta is a Bernoulli process, and the probability of the number of quanta released upon each presynaptic action potential is binomial, coefficient of variation (CV) of EPSC amplitude can reflect presynaptic quantal content (Malinow and Tsien, 1990). CV analysis showed that $1 / CV^2$ of EPSC amplitude increased after LTP induction (Fig. 4.3A; normalized $1 / CV^2 = 3.10 \pm 1.21$, n = 20; P < 0.001, Wilcoxon matched-pairs sign-ranks test; the figure does not include one case in which EPSC failed before but did not fail after LTP induction, giving the normalized $1 / CV^2$ as high as 25.59); in contrast, $1 / CV^2$ of EPSC amplitude decreased after LTD induction (Fig. 4.3B; normalized $1 / CV^2 = 0.70 \pm 0.07$, n = 26; P < 0.001, Wilcoxon matched-pairs sign-ranks test). Change in $1 / CV^2$ may reflect the modifications of presynaptic quantal content, which is consistent with the implications from Fig. 4.2 that expression of LTD at CT synapses may mainly involve presynaptic mechanisms.

Interpretation of CV analysis should be made carefully, especially in a system whose synaptic plasticity can be mediated by the activation of silent synapses

(Malenka and Nicoll, 1997). In some cases, no measurable synaptic response was evoked by stimulation of internal capsule (*ic*) fibers at the holding voltage (V_h) of -70 mV, while a clear outward current with slow kinetics comparable to that of NMDAR-mediated EPSC (c.f. Fig. 2.7B) could be revealed simply by switching the V_h to +60 mV without changing the stimulus intensity (Fig. 4.3C). CT EPSCs at $V_h =$ -70 mV are mediated by non-NMDARs; the lack of non-NMDAR responses in the presence of NMDAR responses implies the existence of "silent synapse" among certain population of CT synapses (Isaac et al., 1995; Issac et al., 1997). If postsynaptically silent synapses exist in CT pathway in our system, it opens the possibility that a change of $1 / CV^2$ following LTP induction might be contributed by the conversion of silent synapse (with functional NMDARs only) into active one (with both functional NMDARs and non-NMDARs) (Isaac et al., 1996; Liao et al., 1995; Malenka and Nicoll, 1997). On the other hand, whether a reverse process can underlies LTD expression in physiological systems remains uncertain (Feldman and Knudsen, 1998; Feldman et al., 1999).

Discussion

Interpretation of results

Our experimental and analytical attempts described in this chapter did not support a causal relationship between regulation of CaP-AMPARs and the expression of LTD at CT synapses, making the question of how input specificity of this plasticity to be achieved open. However, several lines of information were revealed related to these analyses. First, preferential downregulation is not a possible mechanism for LTD expression (Fig. 4.2). Second, weighted mean single-channel conductance of non-NMDARs did not change following LTD (Fig. 4.3), keeping an equal downregulation of calcium-permeable and calcium-impermeable non-NMDAR possible. However, the pharmacological experiments using PhTx-433 seemed to exclude any possible involvement of Ca-AMPAR downregulation. It should be kept in mind that practically, noise analysis has limitation in resolution. Ho et al. (2007) reported that preferential downregulation of CaP-AMPARs underlies L-type VGCC-dependent LTD at developing mossy fiber-CA3 synapses. Even then, the results of peak-scaled nonstationary noise analysis from the same research team yielded the single-channel conductance unchanged following LTD (Lei et al., 2003),

possibly reflecting the limitation of this technique as well as insufficient resolution for this particular question. In our system, the similarity of mean single-channel conductance before and after LTD induction at CT synapses does not necessarily exclude postsynaptic involvement in LTD expression, such as a downregulation of calcium-impermeable AMPARs. Caution should be taken in interpretation of this result, and more supportive experimental approaches will be very helpful to untangle this mystery. Third, CV analyses suggest presynaptic modification accompanying synaptic plasticity, but the possible existence of silent synapses reminds us of the potential complexity of a real biological system. Furthermore, $1 / CV^2$ provides only presynaptic information of the number of releasable quanta and release probability, while some lines of studies have suggested that certain presynaptic parameter not traditionally appreciated, such as "postfusional" regulation of released glutamate concentration and profile, may also contribute to expression of LTP at slilent synapses (Choi et al., 2000).

Other candidate mechanisms underlying LTD expression at CT synapses

One main finding in this study is that depolarizing steps can induce LTD at CT synapses. Depolarization-induced long-term synaptic modification has been reported

in other systems, dependent on L-type VGCCs (Cummings et al., 1996; Lei et al., 2003) or NMDARs (Bright and Brickley, 2008). The earliest discovery of synaptic modification induced by postsynaptic depolarization is depolarization-induced suppression of inhibition (DSI) (Llano et al., 1991; Pitler and Alger, 1992), which has been well-linked with cannabinoid systems (Wilson and Nicoll, 2001); besides, this retrograde signaling can also mediate LTD (Auclair et al., 2000). The LTD induction at CT synapses depends on postsynaptic depolarization and calcium influx, similar to the requirements for endocannabinoid release (Auclair et al., 2000; Diana and Marty, 2004; Wilson and Nicoll, 2001), and CV analysis also implies presynaptic involvement in expression. For the above reasons, cannabinoid is a reasonable candidate for downstream signaling to mediate LTD expression, though other retrograde signals for long-term modification cannot be excluded, such as nitric oxide (NO) (Bright and Brickley, 2008) or endocannabinoids (Sun et al., 2011). It was also reported that some LTD can be induced by the co-activation of L-VGCCs and either group I metabotropic glutamate receptors (Lin et al. 2006; Adermark and Lovinger, 2007; Naie et al. 2007) or type 1 cannabinoid receptors (Auclair et al., 2000; Diana and Marty, 2004; Chevaleyre et al. 2006), and the differential expression of these receptors may account for the selective expression of L-VGCC-dependent LTD at CT, but nor at ML, synapses.

Figures

Figure 4.1 Induction and expression of L-VGCC-dependent LTD at CT synaspes do not involve CaP-AMPARs and NMDARs

A, Representative example (**A₁**) and summary (**A₂**) showing the induction of LTD at CT synapses in the presence of bath-applied PhTx-433 to block CaP-AMPARs. LTD was spared, suggesting that neither induction nor expression of LTD involves CaP-AMPARs. The traces are averaged over 10 sweeps of recordings. **B**, Representative example (**B₁**) and summary (**B₂**) showing the induction of LTD at CT synapses in the presence of bath-applied APV, and demonstrating the measurement of RI of the I–V relationship of non-NMDAR-mediated EPSC before and after induction of LTD at CT synapses. The outward and inward currents were recorded with the V_m clamped at +50 and −70 mV, respectively. The traces are averaged over 5–8 sweeps of recordings. **C**, summarized results showing that expression of LTP at CT synapses was not accompanied by a significant change of RI. The data include results from 6 cells, with each pair of open circles connected by dotted lines indicating the RI measured before (baseline) and after (LTD) LTD was induced. The filled circles represent the mean ± S.E.M. of these data. All conventions are similar to **Fig. 3.1**.

Figure 4.1
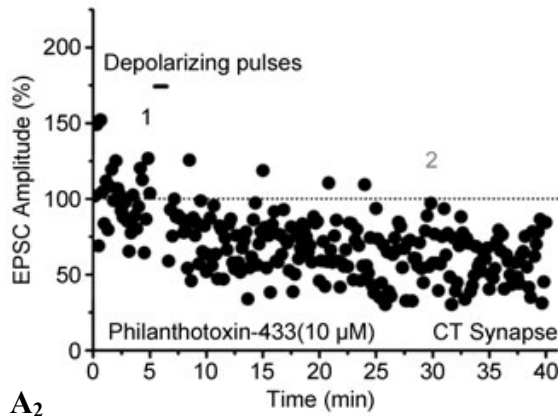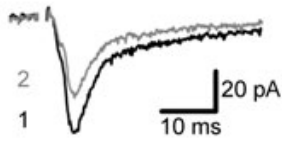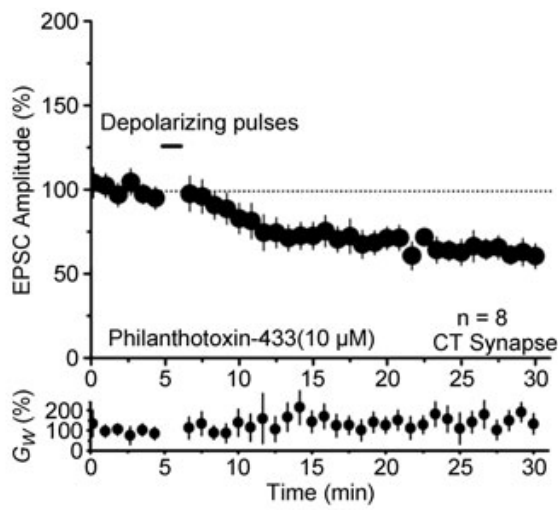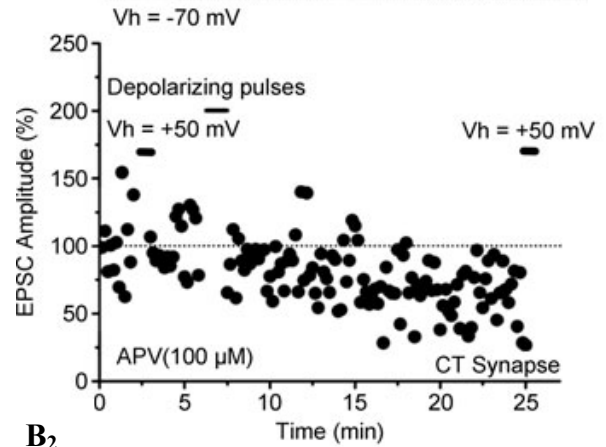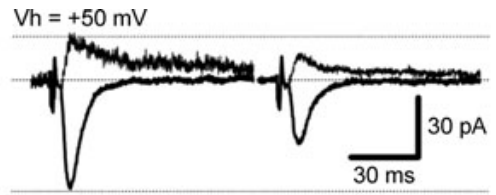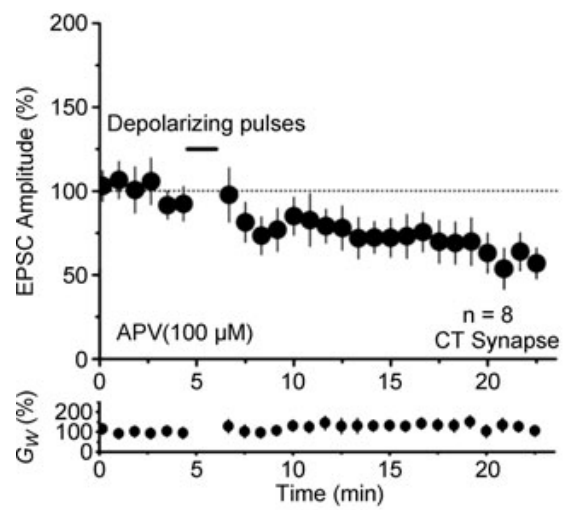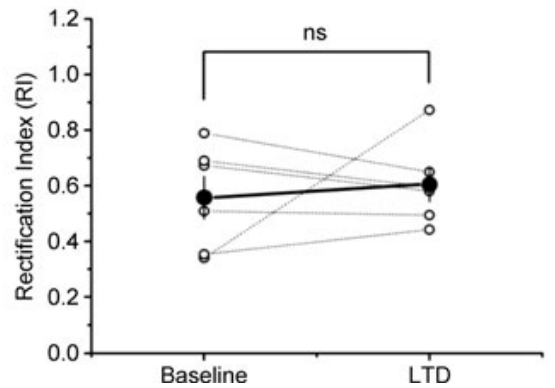
Figure 4.2 Expression of the LTD at CT synapses was not accompanied by a significant change of weighted mean single-channel conductance of non-NMDAR and average number of non-NMDAR open at the peak of EPSC

A, Peak-scaled nonstationary noise analysis was applied to compare the weighted mean single-channel conductance of non-NMDARs at CT synapses before and after induction of the LTD. The mean waveform (black line) of evoked EPSC traces was peak-scaled to individual EPSCs (gray lines) for calculation of ensemble variance and the variance-mean relationship of EPSC decay phase, in order to isolate the variance associated with stochastic gating behaviors of single synaptic channels. 26 and 63 EPSCs were selected (see methods and materials) for analysis of single-channel conductance at CT synapses before (baseline) and after (LTD) LTD was induced. At the bottom are the variance-mean relationships; linear fitting (red dashed lines) was applied to the initial 33% of variance-mean relationship, yielding the weighted mean single-channel conductance of 5.3 and 4.0 pS before and after the LTD induction, respectively. Dotted lines denote the variance originating from background noise, which was constrained during the fitting process. **B**, Summary of the weighted mean single-channel conductance (**B₁**) and average number of channels open at the peak of EPSC (**B₂**) before (baseline) and after (LTD) LTD induction at CT synapses. **B₁**, No significant change of single synaptic conductance following LTD induction is

consistent with the implication of **Fig. 4.1** that expression of LTD does not involve subtype switch of synaptic non-NMDARs (e.g. preferential downregulation of CaP-AMPARs) at CT synapses. **B$_2$**, The average number of non-NMDAR open at the peak of EPSC did not change following LTD induction. Theoretically, if calcium-permeable and -impermeable non-NMDARs are downregulated by the same proportion, i.e. their percentages keep the same, the RI of I-V relationship (**Fig. 4.1B**) and the *weighted* mean single-channel conductance (**Fig. 4.2B$_1$**) will not change. This may not be the case, however, because the average number of open non-NMDARs was not reduced, consistent with the implication of **Fig. 4.3B** that expression of LTD mainly involves presynaptic modification. Each pair of open circles connected by dotted lines indicates data from the same neuron. The filled circles represent the mean ± S.E.M. of these data.

Figure 4.2
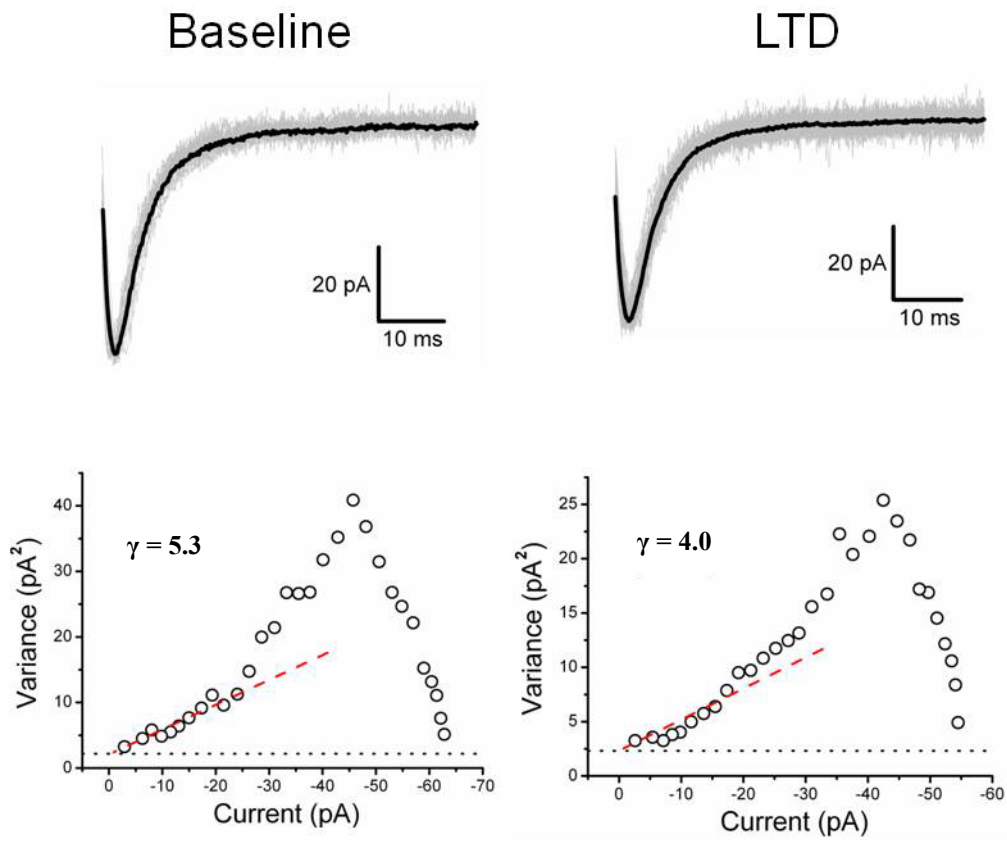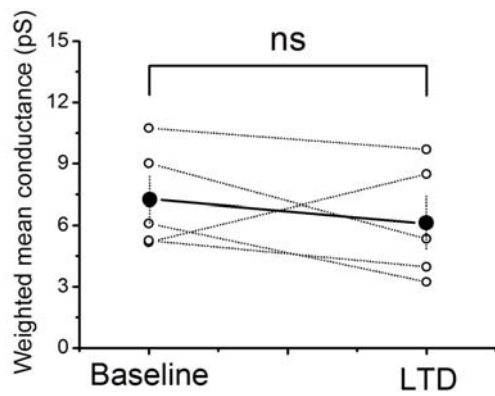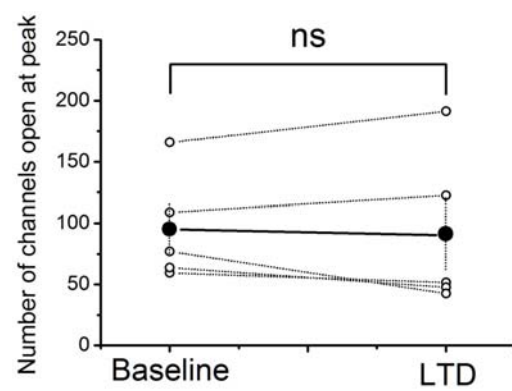
Figure 4.3 Analysis of coefficient of variation (CV) of EPSC amplitude before and after induction of long-term synaptic plasticity at CT synapses

A~B, Summary of normalized $1/CV^2$ of EPSC amplitude before (filed circle) and after (square) induction of NMDAR-dependent LTP (**A**) and L-VGCC-dependent LTD (**B**) at CT synapses ($1/CV^2$ after induction was normalized with respect to that before induction for each cell tested). The increase of EPSC amplitude for LTP was accompanied by an increase of $1/CV^2$; on the contrary, the decrease of EPSC amplitude for LTD was accompanied by an decrease of $1/CV^2$. Change in $1/CV^2$ may reflect the modification of quantal content following induction of long-term plasticity at CT synapses, implying potential presynaptic involvement of plasticity expression.

C, In some cases, no measurable synaptic response was evoked by stimulation of internal capsule (*ic*) fibers at the holding voltage (V_h) of -70 mV, while a clear outward current with slow kinetics comparable to that of NMDAR-mediated EPSC (c.f. **Fig. 2.7B**) could be revealed simply by switching the V_h to +60 mV without changing the stimulus intensity. The arrows indicated stimulating artifacts. CT EPSCs at V_h = -70 mV are mediated by non-NMDARs (**Fig. 2.7A**); the lack of non-NMDAR responses in the presence of NMDAR responses implies the existence of "silent synapse" among the population of CT synapses (Isaac et al., 1995; Issac et al., 1997). If postsynaptically silent synapses exist in CT pathway in our system, it will open the

possibility that the one potential mechanism contributing to the change of $1/CV^2$

following LTP induction (**A**) is the conversion of silent synapse (with functional

NMDARs only) into active one (with both functional NMDARs and non-NMDARs)

(Isaac et al., 1996; Liao et al., 1995; Malenka and Nicoll, 1997); however, whether a

reverse process can underlies LTD expression in physiological systems remains

uncertain (Feldman and Knudsen, 1998; Feldman et al., 1999). The age of animal for

this case is P14.

Figure 4.3

A   **NMDAR-dependent LTP**   **B**   **L-VGCC-dependent LTD**

CT Pathway

CT Synapse

C

$V_h = +60$ mV

80 pA

20 ms

$V_h = -70$ mV

CT synapse

Animal age: P14

191
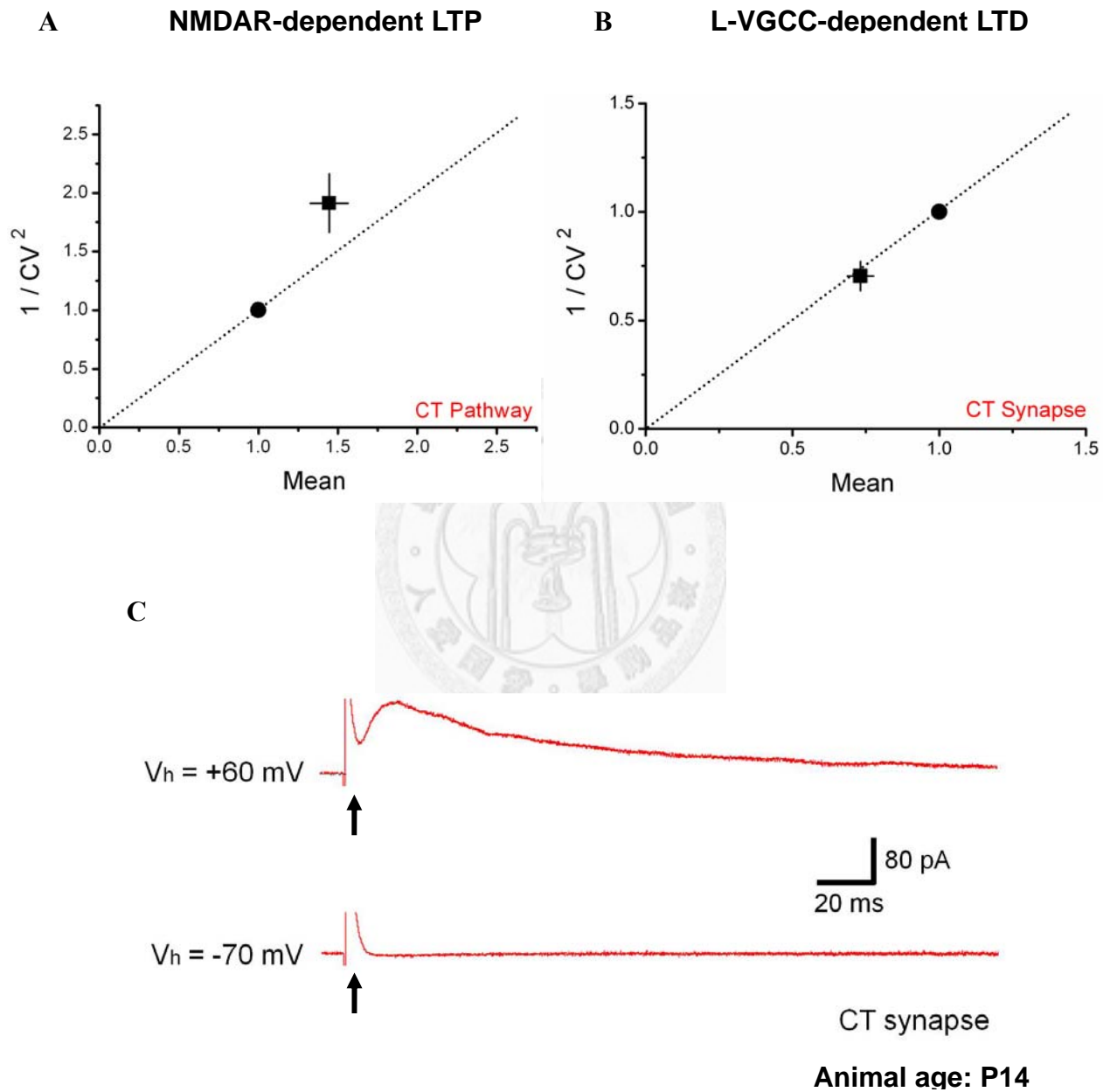
Chapter 5

Induction of long-term synaptic plasticity at corticothalamic synapses by physiologically-relevant spiking patterns

Abstract

Relay neurons in the somatosensory thalamus transmit somatosensory information to cerebral cortices and receive sensory (ML) and feedback corticothalamic (CT) synaptic inputs. A fundamental question of thalamus physiology is that how the thalamic information relay is dynamically tuned in response to internal states of the system and external stimuli. The duality of firing modes of relay neurons, burst and continuous, was thought to underlie state dependence of thalamic information transfer, but the impact of different firing patterns on synaptic weights was rarely explored. In relay neurons of the ventrobasal nucleus (VBN) of rat thalamus, we addressed this question by two sets of experiments. In light of the experimental paradigms used to induce LTP and LTD at CT synapses (chapter 3), we tried to induce long-term synaptic plasticity by similar physiological firing patterns in current-clamp mode. In the first series of experiments, 1-Hz periodic groups of

neuronal spiking, which mimics the repetitive depolarizing pulses used in their voltage-clamp counterpart, were triggered by current injection at depolarized (~ -55 mV) or hyperpolarized (~ -70 mV) V_m for 90 s, therefore resulting in cycles of continuous spiking or burst spiking driven by low threshold spike (LTS), respectively. Interestingly, the results showed that continuous spiking, but not LTS-burst spiking, induced L-type-VGCC dependent LTD at CT synapses. To further investigate the role of burst spiking in long-term synaptic plasticity, CT EPSP was paired with LTS-burst spiking triggered at V_m ~ -70 mV repetitively at low frequency (0.167 Hz) for 100 times. This protocol induced LTP at CT synapses, which was dependent on the timing of EPSP and postsynaptic burst spiking, and was blocked by a combination of NMDAR antagonist APV and calcium chelator BAPTA. However, pairing EPSP with high-frequency spiking, which was triggered at V_m ~ -55 mV by short pulses (1~2 ms) of current injection, mimicking the fast Na^+ spikes of natural burst spiking of relay neurons but without underlying LTS, could not induce long-term plasticity at CT synaspes. This is consistent with the proposition that backpropagating action potentials (bAPs) are not sufficient for induction of LTP, and LTS initiated by T-type VGCCs fulfills the requirement of postsynaptic depolarization (a form of cooperativity) for LTP induction at CT synapses. In conclusion, our results showed that synaptic strength of CT pathway can be modified differently according to specific

physiological spiking patterns of relay neurons, and the biophysical properties of L-type and T-type VGCCs enriches the mechanistic arrays of synaptic plasticity induction in response to complex internal and external statuses. Given our current understanding that CT input is essential to modulation of information relay and receptive filed properties of thalamic relay neurons, the effectiveness of ML sensory input on cortical activities may be dynamically tuned, jointly by specific spiking patterns driven by powerful ML synapses and global states, in a self-regulated manner.

Introduction

The ventrobasal nucleus (VBN) of thalamus serves as a major gateway for relaying sensory information from periphery to cerebral cortex (Jones, 2007). VBN relay neurons receive primary sensory information conveyed by medial lemniscal (ML) synapses and corticothalamic (CT) feedback from higher cortical areas (Jones, 2007; Liu et al., 1995; Sherman and Guillery, 2004; Špaček and Lieberman, 1974). There are two types of CT fibers (Deschênes et al., 1998; Landisman and Connors, 2007; Li et al., 2003; Reichova and Sherman, 2004; Rouiller and Welker, 2000),

namely, those arising from cortical layer V and layer VI pyramidal neurons; the corticothalamic projections to the VBN of rodents were found to originate mainly from layer VI (Deschênes et al., 1998; Killackey and Sherman, 2003; Reichova and Sherman, 2004; Rouiller and Welker, 2000; Van Horn and Sherman, 2004). Considering the predominant number of CT synaptic contacts onto relay neurons (Jones, 2007; Sherman and Koch, 1986), many studies proposed that CT input plays an essential modulatory role in controlling thalamic spike transfer (Destexhe, 2000; Destexhe and Sejnowski, 2002; Ergenzinger et al., 1998; Fanselow et al., 2001; Jones, 2007; Krupa et al., 1999; Murphy and Sillito, 1987; Sherman, 2005; Wolfart et al., 2005).
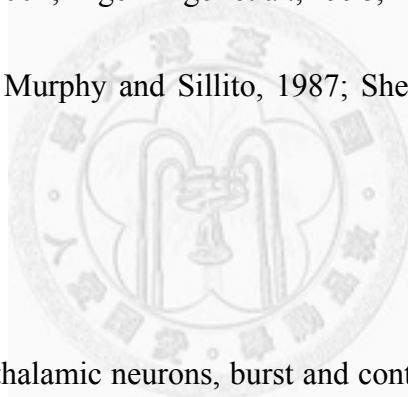
The firing duality of thalamic neurons, burst and continuous spiking, is critically dependent on the voltage-dependent inactivation property of T-type voltage-gated calcium channels (VGCCs): at depolarization, T-type channels are inactivated and the neurons fire continuously and regularly; at hyperpolarization, in contrast, T-type channels are de-inactivated and available for activation, which initiate a low threshold spike (LTS) and drive the neurons to fire a high-frequency burst of action potentials (APs) (Deschênes, 1982; Jahnsen and Llinás, 1984a, 1984b; Llinás and Jahnsen, 1982; Suzuki and Rogawski, 1989). Continuous spiking is typically observed in the

thalamus of awake and vigilant animals, while burst spiking is mostly associated with

inattentive, drowsy, anesthetized states or slow-wave sleep, which prompted the

suggestion that, in the burst mode, thalamus is functionally disconnected from cortex

(Jones, 2007; Le Masson et al., 2002; Livingstone and Hubel, 1981; McCormick and

Bal, 1997; McCormick and Feeser, 1990); emerging evidence has, however, indicated

that bursting also occurs in awake animals and can serve as a powerful mode of

thalamocortical information transfer (Crick, 1984; Fanselow et al., 2001; Guido et al.,

1992; Guido et al., 1995; Guido and Weyand, 1995; Lu et al., 1992; Mukherjee and

Kaplan, 1995; Ramcharan et al., 2000; Reinagel et al., 1999; Swadlow and Gusev,

2001; Weyand et al., 2001).
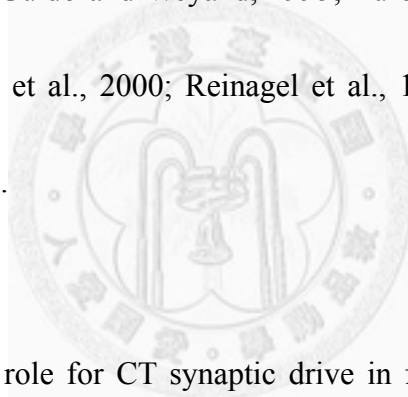
Despite a significant role for CT synaptic drive in firing mode switching, and

thus state-dependent information processing, of thalamus has been proposed

(Castro-Alamancos and Calcagnotto, 2001; Ergenzinger et al., 1998; Fanselow et al.,

2001; Godwin et al., 1996; Hughes et al., 2002; McCormick and Von Krosigk, 1992;

Sherman, 2001; Sillito and Jones, 2002; Wolfart et al., 2005), factors capable of

modulating the efficacy of CT input onto relay neurons were relatively less

investigated (see Alexander and Godwin, 2005; Castro-Alamancos, 2002;

Castro-Alamancos and Calcagnotto, 1999; Miyata and Imoto, 2009; Ulrich et al.,

2007); in particular, little is known regarding the impact of physiologically relevant firing patterns on the strength of CT synapses, which may provide a firing mode-dependent mechanism for self-regulation of thalamic transfer function.

Here, these questions were approached first by analyzing the functional outcomes of physiological spiking patterns in current-clamp mode, which mirror the voltage-clamp experiments (chapter 3), to strength of CT EPSP. We extended our findings to spike-timing-dependent plasticity (STDP), a cellular correlate of timing-based Hebbian learning (Dan and Poo, 2004; Markram et al., 1997). We paired CT EPSP with LTS-burst spiking, and identified a novel spike-timing-dependent LTP at CT synapses. Intriguingly, pairing CT EPSP with high-frequency spiking of APs alone failed to induce synaptic plasticity, suggesting LTS initiated by T-type VGCCs is critical to LTP induction at CT synapses. Our results support the view that backpropagating APs are not sufficient for induction of LTP (Lisman and Spruston, 2005).

Methods

Preparation of thalamic slices

The use of animals in this study was in accordance with guidelines of the Ethical

Committee for Animal Research of National Taiwan University. Sprague-Dawley rats

aged 13~24 days were used. The rats were anaesthetized with isoflurane and

decapitated with a small-animal guillotine, and their brains were quickly removed and

placed in ice-cold artificial cerebrospinal fluid (ACSF). The ACSF contained (in mM):

119 NaCl, 2.5 KCl, 1.3 $MgSO_4$, 26.2 $NaHCO_3$, 1 NaH_2PO_4, 2.5 $CaCl_2$, and 11 glucose;

the pH was adjusted to 7.4 by gassing with 95% O_2 / 5% CO_2. For horizontal slices,

the two halves of the brain were first separated, and their ventral portions were

trimmed in parallel to the ventral surfaces of brainstem to ensure standard horizontal

cutting orientation in accordance with traditional stereotaxic coordinates. A block of

agar was glued behind the brain tissue to provide physical support during slicing.

Horizontal brain slices (300 μm) containing the ventrobasal nucleus (VBN), internal

capsule (*ic*) and medial lemniscus (*ml*) fibers were prepared (Fig. 2.1). Coronal slices

of 300 μm thickness containing the VBN and internal capsule were cut using a

vibroslicer (ZERO 1, D.S.K., Osaka, Japan) (Fig. 2.1). The slices were kept in

oxygenated ACSF (95% O_2 / 5% CO_2) at room temperature (24-25 °C) to allow

recovery for 60~ 90 min before recording commenced.

Electrophysiology

Slices were transferred to an immersion-type recording chamber mounted to an

upright microscope (BX50WI, Olympus Optical, Tokyo, Japan), equipped with an

infrared-differential interference contrast microscopic video. The VBN and *ic* were

clearly identified under low magnification in coronal slices (see Fig. 2.1B). Neurons

in the VBN were recorded under visual guidance with patch pipettes pulled from

borosilicate glass (1.5-mm outer diameter, 0.32-mm wall thickness; G150F-4, Warner

Instruments, Hamden, CT, USA). The patch electrodes had a resistance of 3~8 MΩ

when filled with a solution consisting of (in mM): 131 K-gluconate, 20 KCl, 10

HEPES, 2 EGTA, 8 NaCl, 2 ATP, 0.3 GTP, and 6.7 biocytin; the pH was adjusted to

7.2 by KOH and osmolarity to 300~305 mOsm. Recordings were made with an

Axopatch 1D amplifier (Axon Instruments, Union City, CA, USA) at room

temperature. For current-clamp recordings, the input resistance (R_N) was constantly

monitored by applying a current pulse of -10 ~ -30 pA, and the bridge was balanced

by adjusting the R_S compensation of the amplifier. Data were discarded when R_N

varied by > 20% of its original value during the recording. All signals were low-pass-filtered at the corner frequency of 2 kHz and then digitized at 10 kHz using a Micro 1401 interface (Cambridge Electronic Design, Cambridge, UK). Data were collected using Signal software (Cambridge Electronic Design).

The slices were constantly perfused with ACSF containing 0.1 mM picrotoxin (PTX) and 1 μM strychnine to isolate pure excitatory activity after they were transferred to a recording chamber. After the experiments were finished, 10 μM DNQX were applied in the bath in most cases to confirm the identity of recorded activities as a non-N-methyl-D-aspartate receptor (non-NMDAR)-mediated component. A bipolar stainless steel electrode (FHC, St. Bowdoin, ME, USA) was placed locally in the VBN or in the *ic* (in horizontal slices) for CT EPSP recruitment; no significant differences were observed between the responses evoked by these two conditions (see chapter 2). In high-magnification IR-DIC images of horizontal slices, we observed a large number of fiber bundles projecting from the direction of ic, traversing the reticular nucleus (Rt) and the small heterogeneous zone in the border of VPL (described above) into VBN. We traced along the fiber bundles proximal to the recorded neuron, back to their origin in ic, and placed the stimulating electrode accordingly to facilitate the success rate of recruiting measurable CT EPSCs. Unless

specified, the V_m values of the recorded TC relay neurons were held (or clamped) at -70 mV. The estimated liquid junction potential was ~ +10 mV and was left uncorrected (following the method by Neher, 1992). For recording of EPSP activity in current-clamp mode, data were accepted if the EPSP had a smooth rising phase and an exponentially decaying phase; the data in which the EPSPs had any signs of NMDAR-mediated activities on the decaying phase (characterized by the appearance of a slow component; see Landisman and Connors, 2007) or an abnormally fast rising phase (maybe indicative of the occurrence of antidromic excitation or fast dendritic spike), were discarded.
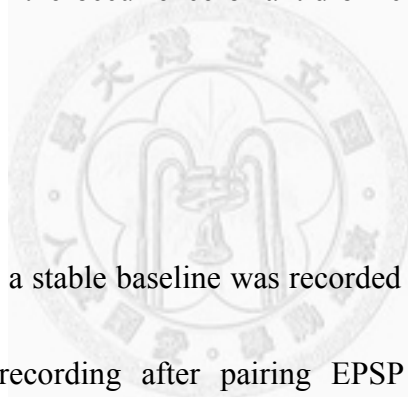
For LTP experiments, a stable baseline was recorded for at least 5 min, followed by at least 30 min of recording after pairing EPSP with LTS (low-threshold spike)-burst spiking or high-frequency spiking at 0.167 Hz for 100 times. EPSPs were evoked at 0.1 Hz. Time interval of pairing (Δt) was defined by the average difference in time between the onset of EPSP and the peak of the 1st action potential (AP). We referred to "positive" (Δt > 0) pairing as the EPSP onset leads the 1st AP, whereas the "negative" (Δt < 0) pairing as the EPSP onset lags the 1st AP. LTS-burst spiking was induced by 1~2-ms or 200-ms somatic current injections with Vm held at ~ -70 mV, and the data showed no significant differences for synaptic plasticity between these

two conditions (for $\Delta t = 0 \sim 30$ ms, 1~2 ms: 141 ± 17%, n = 5; 200 ms: 144 ± 13%, n

= 6; P > 0.05; for $\Delta t = 0 \sim -30$ ms, 1~2 ms: 115 ± 11%, n = 9; 200ms: 109 ± 18%, n =

5; P > 0.05) and thus were pooled together. High-frequency spiking was induced by

five 1-ms somatic current injections at 125 Hz (the average number and frequency of

AP spiking of a typical LTS-burst) with Vm held at ~ -55 mV.

Drugs

The chemicals used for the ACSF and internal solution were purchased from

Merck (Darmstadt, Germany). DL-APV and nimodipine (Nim) was purchased from

Tocris Cookson (Bristol, UK). MgATP, NaGTP, BAPTA, picrotoxin, strychnine were

purchased from Sigma (St. Louis, MO, USA).

Data analysis and statistics

Weighted decay time constant was calculated from the time constants of double

exponential fit to the decay phase of EPSCs. For LTP experiments, the initial slope of

EPSP was monitored and normalized to that of baseline average response, and the

average EPSP slope recorded 25~30 min after pairing was used for statistical

comparison. LTS depolarization (Fig. 5.3B$_3$) was measured as the difference between

the membrane potential of the baseline and that just after the last AP of LTS-burst

spiking, typically at ~ 40 ms after the 1st AP. Sometimes the plateau potential

following the last AP reached the threshold and evoked an additional AP; however, it

was included for analysis as long as the additional AP firing did not affect the

measurement. For residual depolarization following high-frequency spiking, the

difference between the membrane potential of the baseline and that just after the 5th

somatic current injection (also at ~ 40 ms after the 1st AP) was measured. AP

attenuation (Fig. 5.3B$_4$) was calculated as the ratio of the amplitude of the 1st AP to

that of the last AP of the LTS-burst spiking, both of which were measured from the

membrane potential of the baseline.
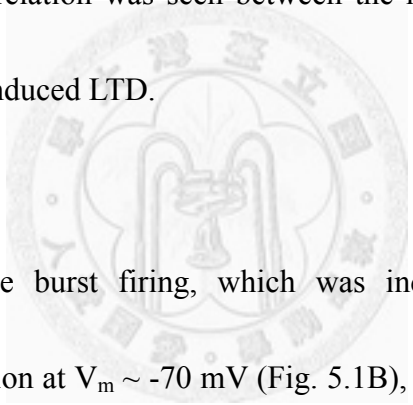
All data are presented as mean ± S.E.M. Statistical significance was assessed

with nonparametric Mann-Whitney-Wilcoxon U test or Wilcoxon matched-pairs

sign-ranked test. For correlation analysis, statistical significance was assessed by

nonparametric Spearman's rank-order correlation test. The criterion for significance

was $P < 0.05$.

Results

L-type VGCC-dependent LTD at CT synapses could be induced by repetitive tonic firing

In current-clamp mode, sufficient calcium influx via L-type VGCCs could probably be induced by repetitive activity patterns; in order to investigate the appropriate conditions for the induction of the LTD at CT synapses in a relatively physiological context, we tested the effects of the repetition of two distinct physiologically relevant firing patterns of VBN neurons on the CT EPSCs. After a 5-min stable baseline, repetitive continuous spiking was induced by 1Hz, 500pA, 500ms-long depolarizing current injection at $V_m \sim -55$ mV (Fig. 5.1A). The averaged rate of continuous spiking gradually declined presumably caused by the accumulative inactivation of voltage-gated sodium channels, with that induced by the first current injection of 68.4 ± 4.9 Hz (n = 12). After repetitive continuous spiking, similar LTD was induced for the EPSCs evoked by stimulating internal capsule and by local stimulation (P > 0.05, Mann-Whitney-Wilcoxon test) and thus pooled together (Fig. 5.1C; 82 ± 7 % compared with baseline; n = 9), which was to the same level of CT LTD induced by depolarizing pulses (P > 0.05, Mann-Whitney-Wilcoxon test). In

addition, this LTD was also blocked by 10μM bath-applied nimodipine (Fig. 5.1C; internal capsule stimulation: 114.1 ± 4.9 % compared with baseline, n = 10), showing L-type VGCC-dependent LTD could also be induced by natural firing pattern. Note that as shown in Fig. 5.1C (the lower panel), the averaged Rn for recordings at 20–25 min after LTD induction in control ACSF or in the presence of nimodipine was 94 ± 3% or 97 ± 4% of corresponding baseline, respectively; the difference was not significant. The range of the mean spiking frequency of the relay neurons was 35–85 Hz and no significant correlation was seen between the mean frequency of spiking and the magnitude of the induced LTD.

In contrast, repetitive burst firing, which was induced by 1Hz, 1ms-long depolarizing current injection at V_m ~ -70 mV (Fig. 5.1B), failed to induce significant synaptic plasticity at CT synapses (Fig. 5.1D; local stimulation: 115.8 ± 17.7 % compared with baseline, n = 8; P > 0.05, Wilcoxon matched-pairs sign-ranks test). Taken together, these results suggested that the induction of synaptic plasticity at CT synapses was dependent on specific activity patterns of VBN neurons, conferring the dynamic flexibility on CT inputs according to recent firing history of VBN neurons.

Spike-timing-dependent plasticity of CT EPSP induced by pairing EPSP with

The burst firing of TC relay neurons mediated by T-type VGCCs was considered to be critical to conscious states and information relay (Bal and McCormick, 1993; Jones, 2007; Le Masson et al., 2002; McCormick and Feeser, 1990; Sherman, 2001; Sherman, 2005); however, the impact of this firing pattern on synaptic plasticity in thalamus is currently unknown, which may contribute to the understanding of thalamic information processing. To address this question, we paired CT EPSP with LTS-burst spiking, which was induced by somatic current injections with V_m held at ~ -70mV, at 0.167 Hz for 100 times (Fig. 5.2A_2, 5.2B_2). By changing the time interval of pairing (Δt), we found that LTP could be induced by positive pairing conditions ($\Delta t = 0 \sim 30$ ms: 143 ± 10 % of the baseline, n = 11; $P < 0.01$), but not by negative ones ($\Delta t = 0 \sim -30$ ms: 113 ± 9 % of the baseline, n = 14; $P > 0.05$) (Fig. 5.2).

The spiking-timing-dependent LTP of CT EPSP could be blocked by the combination of including NMDA receptor (NMDAR) antagonist APV (50 μM) in the bath and calcium chelator BAPTA (10 mM) in the internal solution ($\Delta t = 0 \sim 30$ ms: 84 ± 5 % of the baseline, n = 2; $P < 0.05$ compared with $\Delta t = 0 \sim 30$ ms without APV and BAPTA; Fig. 5.3A), indicating the LTP is NMDAR- or / and calcium- dependent,

can be blocked pharmacologically, and therefore is not an artifact of system drift.

Intrinsic variability of LTS-burst spiking

During the pairing, we observed trial-to-trial variability of LTS-burst spiking, especially in the number (range of average AP number: 3.5 ~ 8) and timing of APs. The variability may be attributable to the intrinsic variability of neuronal properties, such as biophysical states of active conductances, which can lead to the variability of pairing conditions (variability in total AP number and temporal relationships of EPSP and APs during the pairing). In order to examine if such kinds of variability obscure the relation between Δt and synaptic plasticity, we further tested the correlation between these factors and synaptic plasticity. The results showed that plasticity was correlated to neither the average spike number of LTS-burst spiking (Fig. $5.3B_1$, $P > 0.05$ for $\Delta t > 0$ and $\Delta t > 0$ separately or together) nor the timing of APs in terms of the (average) EPSP onset positions relative to AP spike number (Fig. $5.3B_2$, $P > 0.05$ for $\Delta t > 0$ and $\Delta t > 0$ separately or together), suggesting the failure of plasticity induction by negative pairing could not be accounted for by the confounding effect of these variables.

It has been shown that spike-timing-dependent LTP is correlated with postsynaptic depolarization (Clark and Normann, 2008; Sjöström et al., 2001). Our results is consistent with this observation: within a similar time window, LTP could be induced by pairing EPSP *with* burst spiking with LTS (Fig. 5.2A; LTS depolarization: 32.8 ± 1.7 mV); on the contrary, no significant LTP could be induced by pairing EPSP with high-frequency spiking which mimics the AP spiking of LTS-burst *without* the underlying LTS (see below, Fig. 5.4A; residual depolarization following high-frequency spiking: 6.1 ± 0.6 mV). A closer examination revealed that intrinsic variability of LTS depolarization and attenuation of APs within a LTS-burst spiking exists, which were inversely correlated with each other (LTS depolarization v. s. AP attenuation, $P < 0.001$); nevertheless, this variability did not confound the results of synaptic plasticity, either, since none were correlated with plasticity (Fig. 5.3B$_3$, 5.3B$_4$; $P > 0.05$ for $\Delta t > 0$ and$\Delta t > 0$ separately or together). Taken together, these analyses showed that despite the existence of the variability of LTS-burst spiking, it did not confound the results of synaptic plasticity. Furthermore, any single factors discussed above failed to account for the failure of plasticity induction in the negative-pairing experiments (Fig. 5.2B).

Spike-timing-dependent LTP of CT EPSP is dependent on LTS

Is the high-frequency spiking of APs alone sufficient to induce the LTP of CT EPSP? Alternatively, the LTS might be necessary for the induction. To investigate the induction mechanism of spike-timing-dependent LTP, we paired CT EPSP with high-frequency spiking, which was induced by five brief somatic current injections at 125 Hz (the average number and frequency of AP spiking of a typical LTS-burst) with Vm held at ~ -55 mV, at 0.167 Hz for 100 times (see materials and methods; Fig. 5.4A$_2$, B$_2$). In this way, the high-frequency spiking mimics the AP spiking but lacks the LTS of a single LTS-burst. In contrast with the case of pairing EPSP with LTS-burst spiking, we found that no plasticity could be induced neither by positive pairing conditions (Δt = 0 ~ 50 ms: 121 ± 23 % of the baseline, n = 6; P > 0.05) nor by negative ones (Δt = 0 ~ -55 ms: 112 ± 19 % of the baseline, n = 4; P > 0.05) (Fig. 5.4). Our results indicated that, for the spike-timing-dependent LTP of CT EPSP, bursts of APs are not sufficient, and it require the involvement of LTS during the pairing.

Discussion

Synaptic plasticity of CT synapses induced by physiological spiking patterns

In the current-clamp recordings, sufficient calcium influx can occur during this continuous spiking activity, leading to LTD of CT pathway. In contrast, only a small number of overshooting spikes were generated when TC relay neurons were driven to fire in burst mode. Under this condition, the influx of calcium might have been insufficient to induce significant change in the strength of CT pathway. This spiking-pattern-dependent modification of synaptic inputs of cortical origin is functionally intriguing. Provided cortical feedback can change the status of spiking of relay neurons (Murphy and Sillito, 1987; Ergenzinger et al. 1998; Krupa et al. 1999; Sillito and Jones, 2002), particular physiological spiking of relay neurons would modify the strength of cortical inputs onto themselves. In other words, this LTD of cortical inputs provides a means by which cortical modulation of the transfer of somatosensory information can be dynamically tuned (see chapter 6).

Many efforts have been made to elucidate the functional significance of different firing modes in thalamus. As to thalamic relay neurons, bursting activity is also

intrinsic to many other systems such as hippocampal pyramidal neurons (O'Keefe and

Recce, 1993; Ranck, 1973) and neocortical pyramidal neurons (Connors et al., 1982;

Llinás, 1988; McCormick et al., 1985; Williams and Stuart, 1999), which is often

considered as a qualitatively distinct signaling unit with various functional impacts,

such as reliable synaptic activation / improved stimulus detectability (Babadi, 2005;

Beierlein et al., 2002; Fanselow et al., 2001; Guido et al., 1995; Guido and Weyand,

1995; Lisman, 1997; Sherman, 2001; Swadlow and Gusev, 2001; Williams and Stuart,

1999), learning-related associative plasticity, reorganization of cortical circuits,

synaptic downscaling, memory consolidation, and gene expression (Birtoli and Ulrich,

2004; Clark and Normann, 2008; Fields et al., 1997; Frank et al., 2001; Paulsen and

Sejnowski, 2000; Pick et al., 1999; Remy and Spruston, 2007; Steriade, 2006; Thomas

et al., 1998); on the contrary, the functional importance of the other

mode—continuous spiking—to synaptic physiology of thalamus draws little attention.

Our results show the first evidence that repetitive tonic firing can induce LTD at

corticothalamic synapses, and suggested that corticothalamic modulation can be

bi-directional modified according to recent history of neuronal activities as well.

Multiplicative gain modulation of neuronal transfer function has been theoretically

proved to be necessary for as well as occurs in several *in vivo* behavioral tasks (Tovee

et al., 1994; Brotchie et al., 1995; Salinas and Abbott, 1995; Pouget and Sejnowski,

1997), and one important strategy to achieve this mathematical operation is to utilize synaptic background noise (Chance et al., 2002; Debay et al., 2004; Shu et al., 2003); considering the dominant number of corticothalamic synapses onto thalamic relay neurons, Wolfart et al. (2005) showed that the condition of synaptic barrages is critical to neuronal transfer function and the boundary between tonic and burst spikes. From a comparative point of view, the anatomically-distinct, secure lemniscal input is qualitatively similar to the cerebellar climbing fiber input onto Purkinje cells, known as the "instructive" pathway (Coesmans et al., 2004; Ito, 2001; Ito et al., 1982), and can provide necessary driving force for VB neuron firing. For the periods during which some assembly of relay neurons is relatively suppressed, as may happen in inattentive / drowsy states with respect to its corresponding receptive field, new somatosensory stimuli conveyed by lemniscal pathway can act as the "wake-up calls" (Sherman, 1996), leading to cortical activation, state switch of relay neurons to tonic mode, and thus enable a linear, faithful reconstruction of the sensory inputs in higher cortical areas (Sherman, 2005). If the stimuli are repetitively presented in the same receptive field, strong synaptic inputs will drive tonic firing in the relevant relay cells and, paired with corticothalamic inputs or not, as dictated by the cortical instructions like directed attention, can consequently enable the dynamic regulation of corticothalamic barrages and thus fine tuning of neuronal gain. Together with the

detailed topology of corticothalamic circuitry (Sherman, 2005; Temereanca and Simons, 2004; Tsumoto et al., 1978), spatiotemporal sensory gating originating from thalamocortical short-term depression (Aguilar and Castro-Alamancos, 2005; Castro-Alamancos, 2002b; Castro-Alamancos and Oldford, 2002; Hirata and Castro-Alamancos, 2006), and spike transfer control imposed by reticular inhibitory feedback (Le Masson et al., 2002), activity-dependent modulation of corticothalamic inputs is presumably able to dictate the spatiotemporal patterns of thalamic information relay according to the state of vigilance. The influence of neuronal activities on the synaptic background noise and input-output relationship of VB neurons, as a testable prediction of the functional hypothesis described here, can be further investigated in this system.
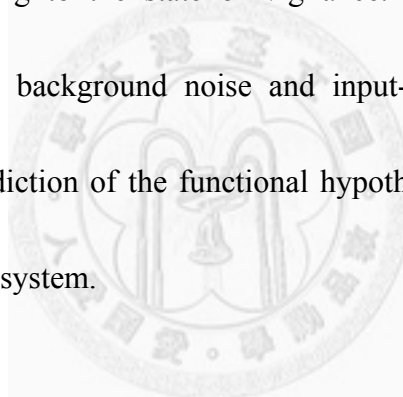
Synaptic plasticity and burst spiking pattern

The duality of firing modes of relay neurons was considered to underlie state dependence of thalamic information transfer (Deschênes, 1982; Llinás and Jahnsen, 1982; Jahnsen and Llinás, 1984a, 1984b; Jones, 2007; Le Masson et al., 2002; McCormick and Feeser, 1990; Sherman, 2001; Sherman, 2005; Weyand et al., 2001). Concerning the differences in the signal processing of thalamocortical systems

between distinct behavioral states, the impact of physiologically relevant firing patterns on the synaptic weight of sensory thalamus was, however, little studied previously (but see Hsu et al., 2010). Our preliminary study addressed this question by examining the effect of pairing EPSP with LTS-burst spiking on CT EPSP, and identified a novel form of spike-timing-dependent LTP at CT synapses, which required LTS initiated by activation of T-type voltage-gated calcium channels. Intriguingly, more than simply providing high-frequency spiking of APs, which alone failed to induce synaptic plasticity, LTS itself seemed to play an indispensable role for the LTP induction at CT synapses. Our results may support the proposition that backpropagating AP is not sufficient for induction of synaptic plasticity (Lisman and Spruston, 2005; see below for further discussions).
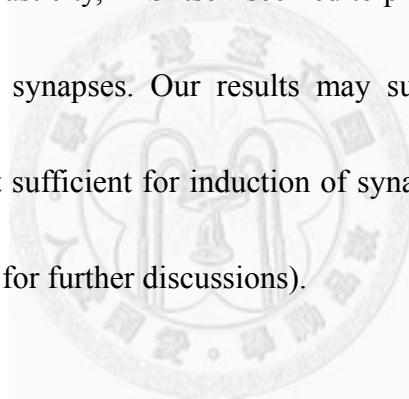
Since the discovery of long-term synaptic plasticity (Bliss and Lømo, 1973; Levy and Steward, 1983), one critical concern in this field has been to understand how natural spiking patterns dictate long-term synaptic plasticity *in vivo* (Czarnecki et al., 2007; Dobrunz and Stevens, 1999; Froemke and Dan, 2002; Hsu et al., 2010; King et al., 1999; Perrett et al., 2001; Rosanova and Ulrich, 2005). Many studies put their focus on postsynaptic burst spiking, a fundamental module of *in vivo* activities under various physiological states, such as information encoding, feature detection, active

exploration and slow-wave sleep (Crick, 1984; Guido et al., 1992; Guido and Weyand, 1995; Kandel and Spencer, 1961; Lisman, 1997; Otto et al., 1991; Paulsen and Sejnowski, 2000; Reinagel et al., 1999; Steriade et al., 2001; Weyand et al., 2001). While burst spiking can enhance LTP (Debanne et al., 1998; Froemke et al., 2006; Harnett et al., 2009; Nevian and Sakmann, 2006; Pike et al., 1999; Sjöström et al., 2001; Thomas et al., 1998; Tzounopoulos et al., 2004; Wittenberg and Wang, 2006), it can also induce LTD (Birtoli and Ulrich, 2004; Ho et al., 2009), result in variable synaptic modification (Clark and Normann, 2008), or exert no influence upon synaptic strength (Hsu et al., 2010), showing the diverse impacts of complex spike patterns on synaptic plasticity. It is noteworthy that, in contrast with the "breakdown" of spike timing dependence and the predominance of LTP under high-frequency burst spiking observed in other systems (Froemke et al., 2006; Sjöström et al., 2001), the spike timing requirement for the LTP at CT synapses was retained (Fig. 2, Fig. 3B), suggesting a different mechanism underlying spike-timing-dependent LTP at CT synapses.

Possible reasons for the requirement of LTS for LTP inudction
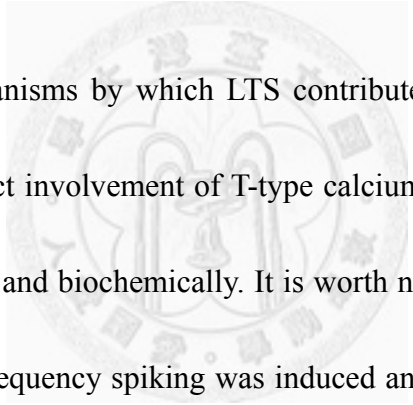
Postsynaptic LTS-burst spiking initiated by T-type calcium channels is a

signature of electrophysiological properties of thalamic relay neurons (Deschênes, 1982; Llinás and Jahnsen, 1982; Jahnsen and Llinás, 1984a, 1984b), which was correlated with information relay. In this study, we provided the first account of the LTP of thalamic relay neurons induced by pairing EPSP with LTS-burst spiking. Given the importance of high-frequency burst spiking as well as backpropagation of AP to LTP (see above; Magee and Johnston, 1997; Markram et al., 1997), the need for LTS to induce LTP could be attributed to the need for a potent driving force for triggering postsynaptic high-frequency AP spiking. This is, however, not the case, since even the high-frequency burst of APs were intact, LTP failed to be induced by pairing in the similar time window (Fig. 5.4A), suggesting LTS, and perhaps the underlying T-type calcium channels, contribute more than simply driving high-frequency AP spiking of postsynaptic neurons.

T-type voltage-gated calcium channels may play a significant role in the induction of LTP at CT synapses, which requires further investigation. In the earliest description of spike-timing-dependent plasticity, it has been reported that low-frequency pairing of presynaptic and postsynaptic neurons did not induce LTP (Markram et al., 1997), which could be rescued by prior somatic depolarization (Sjöström et al., 2001). One possible mechanism of this phenomenon is the

enhancement of the backpropagation of AP by depolarization (Lisman and Spruston, 2005; Stuart and Häusser, 2001), which, under burst-pairing condition of other experimental systems, can be provided by after-depolarization of prior AP (Sjöström et al., 2001). Of particular interest, although the high-frequency spiking protocol used to mimic burst spiking was unable to induce LTP, our finding is still explainable by this mechanism since the difference of postsynaptic depolarization between LTS-burst spiking (Fig. 5.2A) and high-frequency spiking (Fig. 5.4A) was huge, which, in this system, is caused by differential recruitment of T-type calcium channels at different membrane potentials. In thalamic relay neurons, direct patch-clamp recording, calcium imaging, modelling, and immunocytochemistry studies indicated that T-type calcium channels are expressed throughout the dendritic arbor, especially concentrated at proximal dendritic compartments, with a peak density and activation at $\sim$ 10-60 μm from the soma (McKay et al., 2006; Munsch et al., 1997; Zhou et al., 1997; Destexhe et al., 1998; Williams and Stuart, 2000). Dendritic T-type calcium channels are critical for generating and shaping the LTS response of thalamic relay neuron (Destexhe et al., 1998). It is possible that the backpropagation of AP is enhanced by dendritic T-type calcium channels, perhaps increasing the amplitude and duration of the spike arriving at synapses (Lisman and Spruston, 2005; Magee and Johnston, 1997; Stuart and Häusser, 2001), thereby facilitating the induction of LTP at

CT synapses of VBN relay neurons. The reason why high-frequency spiking alone was insufficient to induce LTP at CT synapses is unknown. Simply considering the biophysics of AP backpropagation in dendrites, this is, however, not surprising, because it has been shown that invasion of backpropagating AP to dendrites is less effective as their frequency is increased (Callaway and Ross, 1995; Spruston et al., 1995). In VBN relay neuron, the buildup of residual depolarization provided by prior APs might not enhance backpropagation of AP to activated CT synapses effectively.

Other possible mechanisms by which LTS contributes to LTP induction at CT synapses is through a direct involvement of T-type calcium channels in the induction process, biophysically or / and biochemically. It is worth noting that the experimental condition in which high-frequency spiking was induced and LTS was inactivated, the membrane potential during pairing was depolarized ($\sim$ -55 mV; Fig. 4A), possibly corresponding to a strong propagation state for AP backpropagation (Stuart and Häusser, 2001); it is unknown that to what extent the LTS (Fig. 5.2A) would be more effective than steady-state depolarization (Fig. 5.4A) in boosting the backpropagation of AP to activated synapses. In addition to generating LTS, T-type calcium channels were also shown to be instrumental to synaptic plasticity (Aizenman et al., 1998; Oliet et al., 1997). Experimental evidence has invoked the proposition that backpropagating

AP may be neither necessary nor sufficient for synaptic plasticity in many physiological conditions (Golding et al., 2002; Hardie and Spruston, 2009; Lisman and Spruston, 2005; Markram et al., 1997; Sjöström et al., 2001). Alternatively, the requirement for postsynaptic depolarization can be met by active involvement of dendritic conductance (Golding et al., 2002; Hardie and Spruston, 2009; Kampa et al., 2007; Letzkus et al., 2006; Lisman and Spruston, 2005; Thomas et al., 1998). As thalamic relay neurons, T-type calcium channels are also predominantly localized in dendrites of neocortical pyramidal neurons, and the coupling between dendritic calcium channels and axonal AP generation has been well understood. Dendritic calcium events can be activated by high-frequency burst of backpropagating APs (Larkum et al., 1999a; Letzkus et al., 2006; Williams and Stuart, 1999) or pairing distal synaptic input with AP (Larkum et al., 1999b), which can, under some circumstances, trigger and/or shape Ca^{2+}-spike-associated burst of axonal AP spiking (Kamondi et al., 1998; Larkum et al., 1999a, 1999b; Schiller et al., 1997). In thalamic relay neurons, it is also shown that dendritic calcium spike occurs as T-type calcium channels are recruited (Williams and Stuart, 2000) despite its detailed interaction with axonal AP firing is relatively less studied (but see Destexhe et al., 1998). The critical depolarization required for LTP induction might be achieved by this kind of dendritic events associated with T-type calcium channels.

Otherwise, T-type calcium channels might contribute to LTP at CT synapses biochemically, as they are coupled to specific downstream signaling mechanisms in thalamic neurons, such as adenylyl cyclase (AC) system (Pape et al., 2004) or calcium-induced calcium release (CICR) (Richter et al., 2005). The aforementioned candidate mechanisms for LTP at CT synapses are not mutually exclusive, which needs to be elucidated experimentally. Moreover, Hsu et al. (2010) showed that repetitive LTS-burst spiking (without pairing with evoked synaptic input) could not induce synaptic plasticity of CT EPSP in VBN relay neurons, which implies that glutamate-dependent processes are likely required for LTP at CT synapses, such as activation of metabotropic and/or ionotropic glutamate receptors, which can interact with high-frequency backpropagating APs and affect calcium release from internal stores (Larkum et al., 2003; Nakamura et al., 1999).

In this preliminary study, LTS-burst spiking was artificially triggered by current injection via somatic patch electrode; in realistic *in vivo* conditions, however, it can be provided or affected in a variety of ways. Provided the dendritic distribution profile of T-type calcium channels, the intrinsic bursting mechanism of thalamic relay neurons is tightly controlled by inputs onto dendrites (Antal et al., 1996; Destexhe et al., 1998;

Destexhe and Sejnowski, 2002; Krahe and Gabbiani, 2004; Zhan et al., 2000), which

may be of sensory origin or sources that exert modulatory influences regarding

conscious or physiological states (Liu et al., 1995; Sherman and Guillery, 1996). For

example, medial lemniscal (*ml*) input, which conveys primary somatosensory

information from periphery to ventrobasal thalamus, forms giant, powerful glomerular

synapses onto proximal dendrites of relay neurons (Liu et al., 1995; Špacek and

Lieberman, 1974), where T-type calcium channels are highly expressed. At

hyperpolarized membrane potentials, minimal stimulation of ml fiber secures

full-blown LTS-burst spiking (data not shown). Because the depolarization

requirement for LTP at CT synapses has been fulfilled, traditional cooperativity

(spatial summation of enough synaptic inputs) is no longer needed; therefore, minimal

sensory information carried by ml fiber can provide a reliable associative signal for

LTP induction of CT synapses. Alternatively, LTS-burst spiking can be induced or

shaped by CT input, which forms synaptic contacts onto distal dendrites of relay

neurons (Liu et al., 1995). Early studies indicated that cortex can modulate firing

mode of thalamic neurons by descending control (McCormick, 1992; McCormick et

al., 1993) or massive inhibition (through recruitment of feedforward inhibitory

reticular neurons and generation of IPSP-rebound sequence in relay neurons; see

Destexhe and Sejnowski, 2002; Jones, 2007); LTS-burst spiking can also be triggered

by excitation of CT input under some conditions (e.g., Williams and Stuart, 2000).

Despite a less expression of T-type calcium channels in the dendritic compartments

where CT synapses contact, studies still suggested that corticothalamic feedback is an

effective switch for bursting excitability control of thalamic relay neurons (Destexhe

and Sejnowski, 2002; Zhan et al., 2000). One of such switches occurs when relay

neurons receive corticothalamic bombardment (Steriade, 2001); in other systems,

correlated synaptic inputs trigger active dendritic events (Gasparini et al., 2004;

Losonczy and Magee, 2006; Williams and Stuart, 2002), which can either be in

isolation from axonal AP generation or induce bursts of AP spiking (Larkum et al.,

1999b; Schiller et al., 1997; Williams and Stuart, 2002). Together with other

CT-associated mechanisms discussed above, corticothalamic feedback and denritic

events may dictate LTP induction at CT synapses according to behavioral context.

In conclusion, the present study identified a novel form of

spike-timing-dependent LTP at CT synapses of thalamic relay neurons. Whereas

high-frequency spiking of APs alone was not sufficient, LTS mediated by T-type

voltage-gated calcium channels was necessary for LTP induction. In more

physiological conditions, T-type calcium channels, their associated burst firing of APs

and dendritic calcium spike can be activated or shaped by multiple mechanisms,

which influence synaptic plasticity at CT syanpses, and, therefore, corticothalamic bombardment onto dendrites of relay neurons. Wolfart and colleagues (2005) has shown that transfer function of thalamic relay neurons can be modulated by background synaptic noise; as a consequence, spike-timing-dependent plasticity at CT synapses can respond to various physiologically relevant variables, and dynamically fine-tune thalamocortical information relay accordingly.

Figures

Figure 5.1 L-VGCC-dependent LTD at CT synapses was induced in a spiking pattern-dependent manner

In order to characterize the natural spiking patterns ideal for induction of L-type VGCC-dependent LTD at CT synapses, two different types of repetitive physiological spiking of relay neurons were tested, as experimental counterparts mimicking the voltage-clamp experiments using depolarizing pulses (**Fig. 3.5A**). **A,** Representative example of time course of CT EPSC (top) in response to 1-Hz, 90 cycles of repetitive continuous spiking of relay neurons at $V_m \sim$ -55 mV (bottom), which were elicited by 90 depolarizing current injections of + 500 pA in magnitude with a 50 % duty cycle, as illustrated in the inset at the bottom. **B**, Representative example of time course of CT EPSC (top) in response to 1-Hz, 90 cycles of repetitive LTS-burst spiking of relay neurons at $V_m \sim$ -70 mV (bottom), which were elicited by 90 depolarizing current injections of +2 nA in magnitude with a 0.2 % duty cycle, as illustrated in the inset at the bottom. **C~D**, Summary of time courses CT EPSC in response to repetitive continuous spiking (continuous) and LTS-burst spiking (burst), showing that continuous spiking is favorable for induction of LTD at CT synapses. This LTD was also dependent on activation of L-type VGCCs (**C**), indicating it is mechanistically equivalent to the CT LTD induced in voltage-clamp experiments. Please note that

recording quality was routinely monitored by assessing the voltage response to small

current injection and the calculated input resistance (R_N), which was stable over the

whole experiment, and no difference of RN was observed between different

experimental groups. All conventions are similar to **Fig. 3.1**.

Figure 5.1
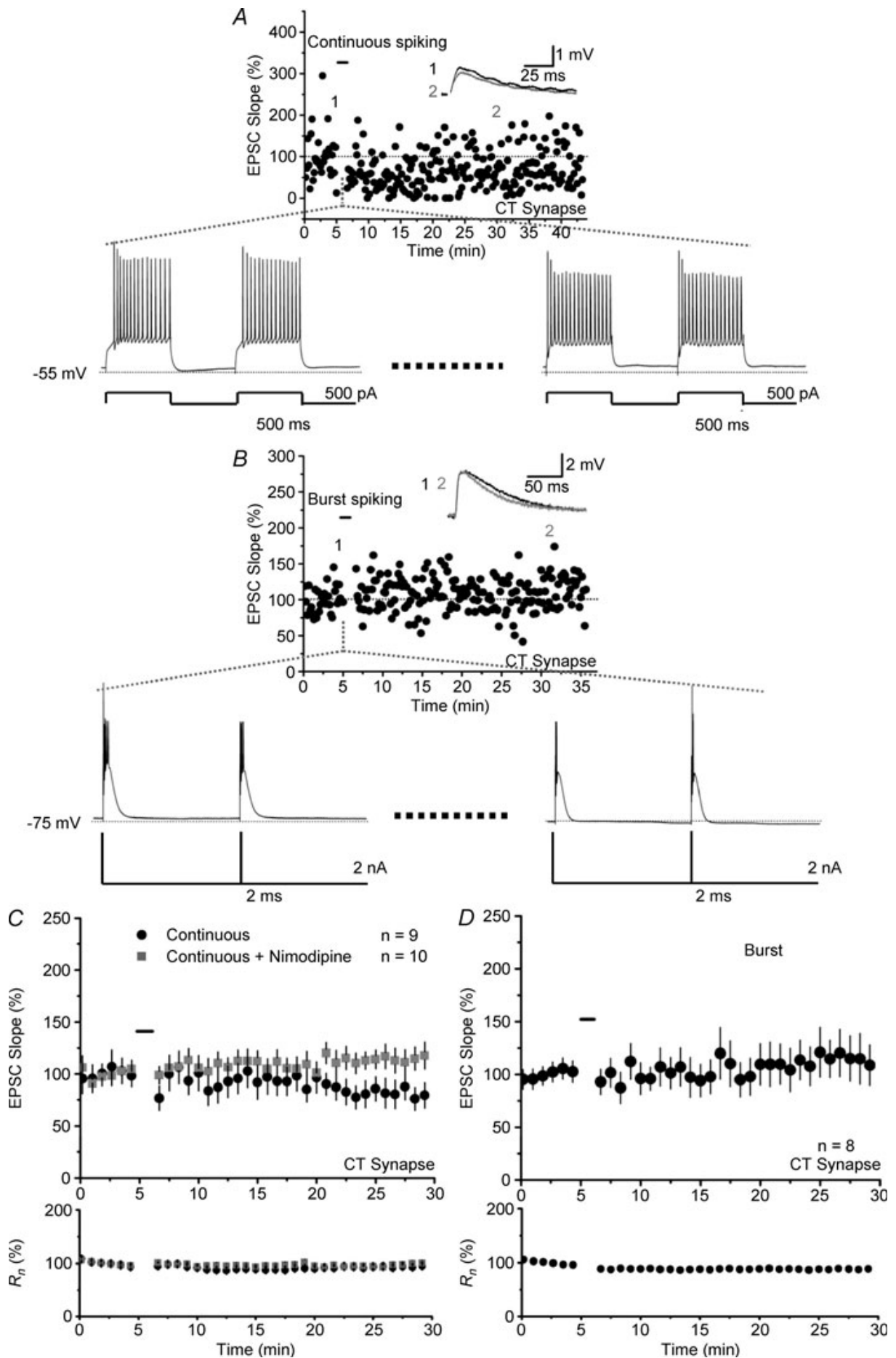
Figure 5.2 Spike-timing-dependent plasticity of CT EPSP induced by pairing EPSP with LTS-burst spiking

A, Typical example (**A₁**), representative trace during the pairing (**A₂**), and summary (**A₃**) of LTP induced by pairing CT EPSP with LTS-burst spiking at positive intervals (0 ~ +30 ms). **B**, Typical example (**B₁**), representative trace during the pairing (**B₂**), and summary (**B₃**) of the experiments with CT EPSP paired with LTS-burst spiking at negative intervals (0 ~ -30 ms). The inset traces in **A₁** and **B₁** are the responses averaged over 10 sweeps during baseline (black) and 30 min after pairing (red). The line drawings in **A₂** and **B₂** indicate the timing of extracellular stimulation ("Pre") and somatic current injection ("Post"). Note the Vm during pairing is ~ -70 mV, and a significant LTP was induced only with positive pairing.
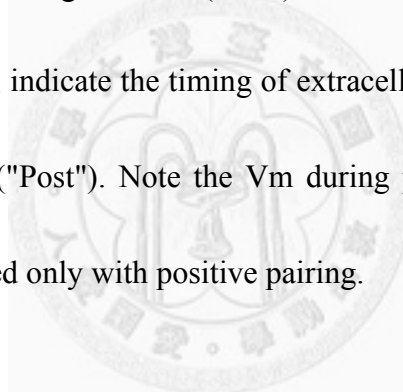
Figure 5.2
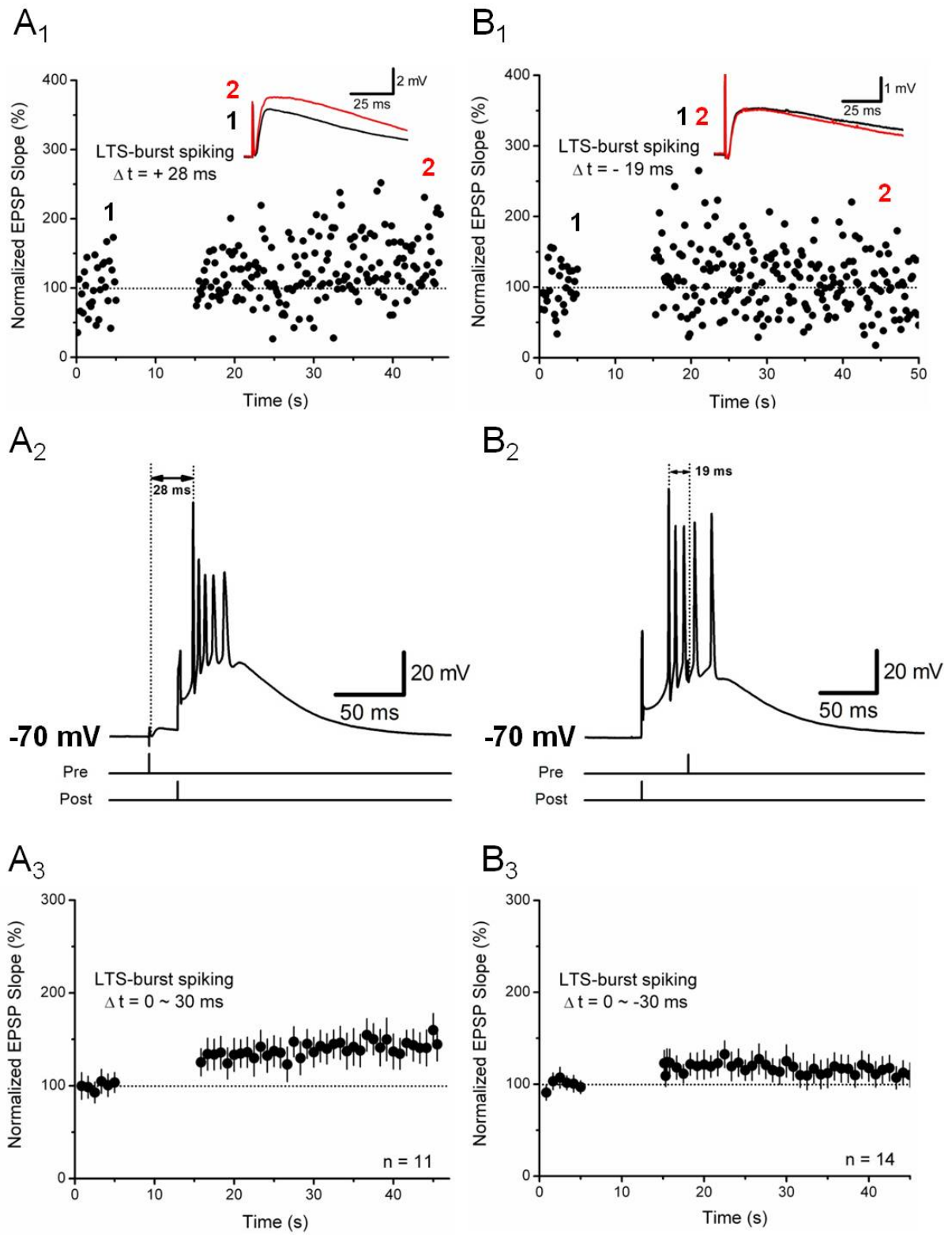
Figure 5.3 The synaptic plasticity was blocked by the combination of bath-applied APV and BAPTA included in the internal solution, and was independent of the average spike number of a single LTS-burst, relative timing of EPSP and AP spikes, LTS depolarization, and AP attenuation

A_1, Typical example of the positive-pairing experiments carried out in the presence of APV and BAPTA. The inset traces are the responses averaged over 10 sweeps during baseline (black) and 30 min after pairing (red). A_2, Summary of the experiments in **Fig. 2A** and **Fig. 3A$_1$**. **B**, The failure of plasticity induction by negative pairing (**Fig. 2B**) is not related to the average spike number (**B$_1$**), the temporal relationships of EPSP and APs (**B$_2$**), the depolarization contributed by LTS (**B$_3$**), and the AP attenuation within LTS-burst spiking (**B$_4$**) during the pairing process. "EPSP - AP" and "AP-EPSP" correspond to $\Delta t > 0$ and $\Delta t < 0$, respectively.

Figure 5.3
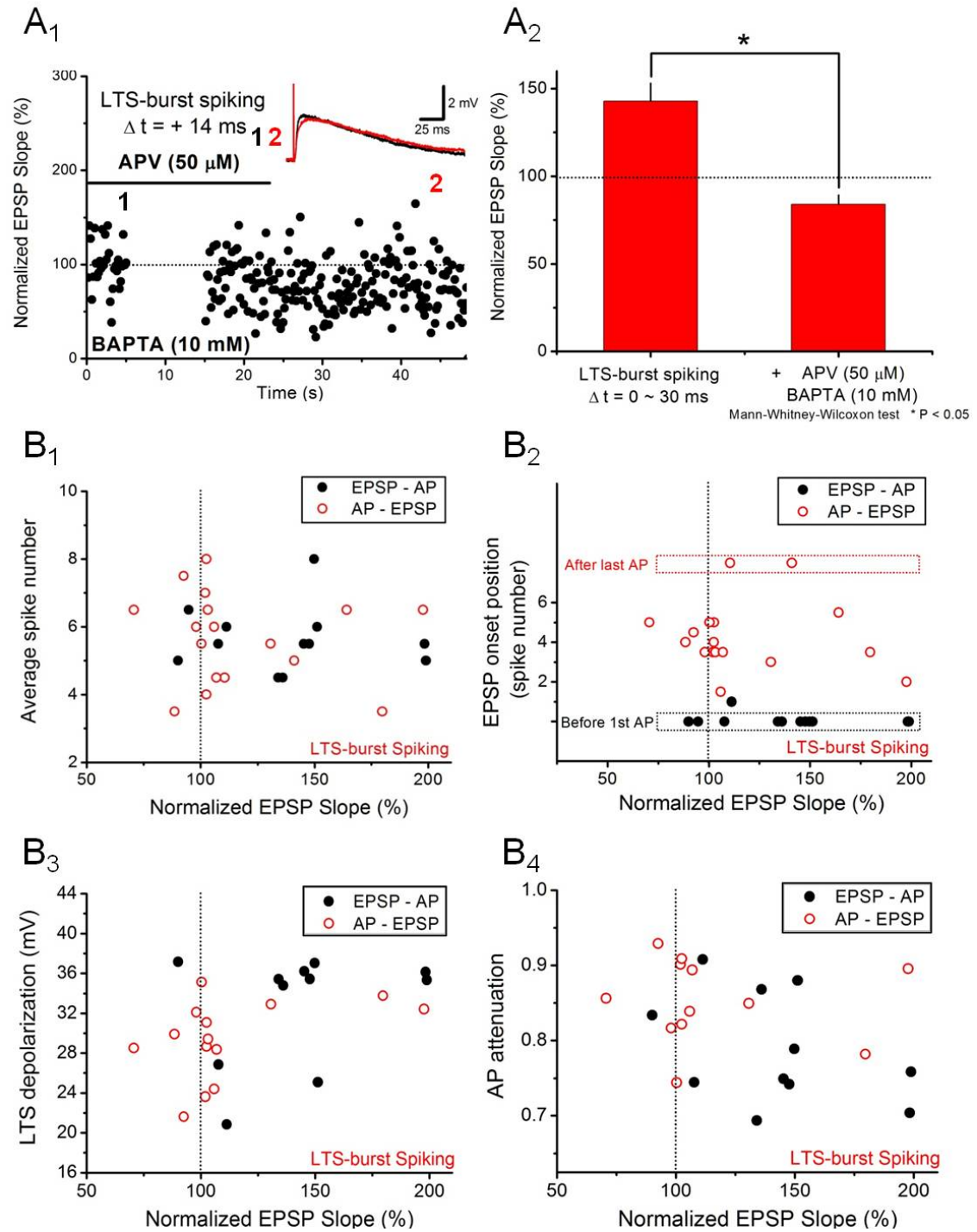
Figure 5.4 Pairing EPSP with high-frequency spiking, which mimics fast Na$^+$ spiking but lacks the underlying LTS of natural LTS-burst spiking of relay neurons, could not induce synaptic plasticity of CT EPSP

A, Typical example (**A$_1$**), representative trace during the pairing (**A$_2$**), and summary (**A$_3$**) of the experiments with CT EPSP paired with high-frequency spiking at positive intervals (0 ~ +50 ms). **B**, Typical example (**B$_1$**), representative trace during the pairing (**B$_2$**), and summary (**B$_3$**) of the experiments with CT EPSP paired with high-frequency spiking at negative intervals (0 ~ -55 ms). The inset traces in **A$_1$** and **B$_1$** are the responses averaged over 10 sweeps during baseline (black) and 30 min after pairing (red). The line drawings in **A$_2$** and **B$_2$** indicate the timing of extracellular stimulation ("Pre") and somatic current injection ("Post"). Note the Vm during pairing is held ~ -55 mV.

Figure 5.4
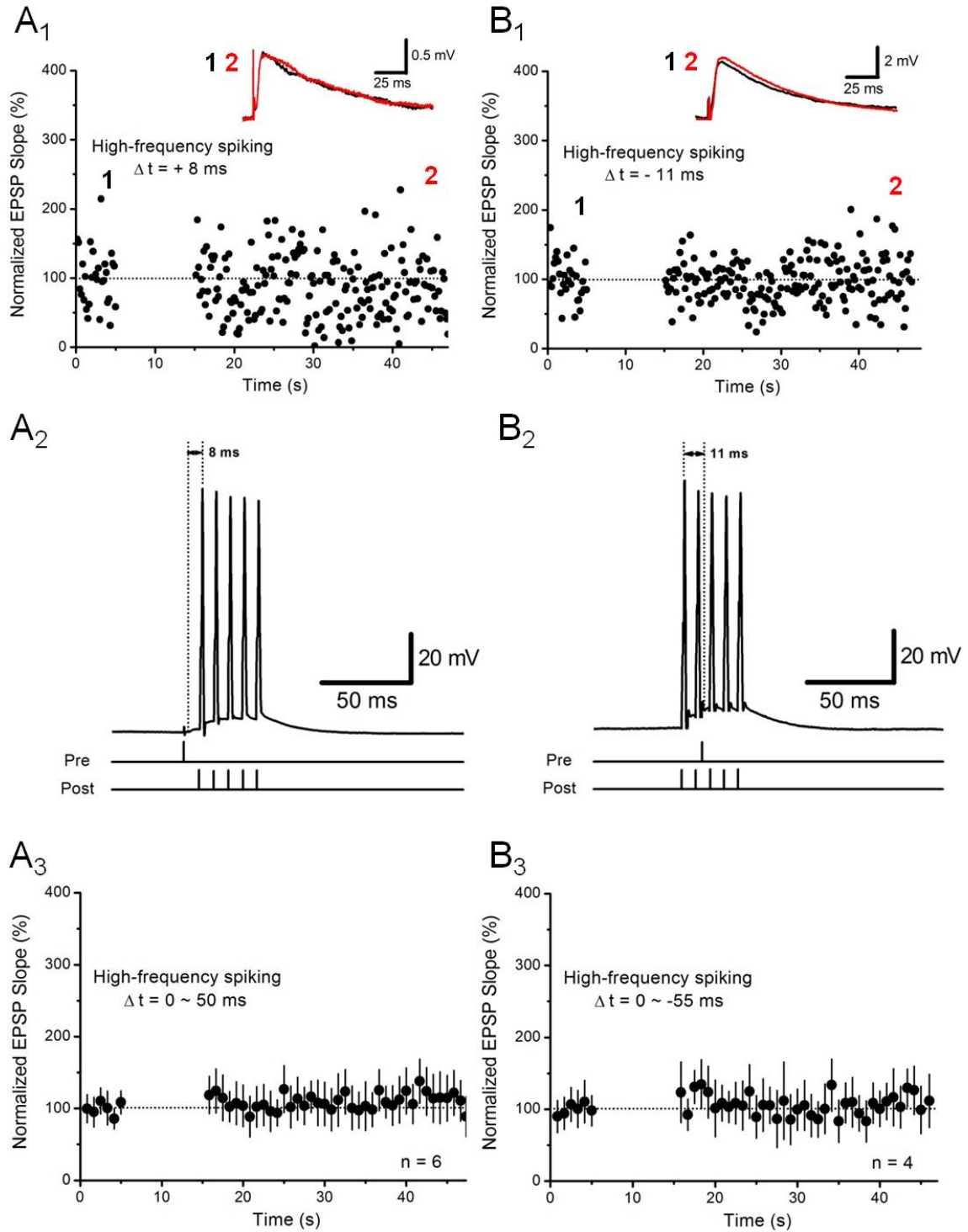
Chapter 6

Conclusions

Significance of this study

Thalamus is not only the major gateway of sensory information relay from periphery to higher cortical areas, but also serves as an important node of multiple integrated networks involved in various physiological or pathological processes, such as attention, motor function, epilepsy and central pain syndrome (Jones, 2007; Kandel et al., 2000; Sherman and Guillery, 2004). Especially, somatosensory thalamus of rodents is an invaluable and widely used model system for central sensory processing of higher mammals, and the solid knowledge of which is, therefore, critical to the in-depth understanding of the physiology of sensation / perception and also an important clue to potential targets for therapeutic interventions of related diseases.

State-dependent, top-down influences of higher cortical origins on sensory processes have been widely appreciated, especially via the actions of corticothalamic pathways (e.g. Briggs and Usrey, 2008; Fanselow et al., 2001; Krupa et al., 1999;

233

Sherman, 2005; Wolfart et al., 2005); however, one of the most important questions in this field remains: what kinds of cellular and synaptic mechanisms, and how these mechanisms, underlie the dynamic nature of corticothalamic modulation in response to variable internal and external stimuli? My work partly answered this question by systematically comparing the fundamental differences of synaptic transmission and synaptic plasticity between the two major excitatory input pathways to the ventrobasal nucleus of rat thalamus (Fig. 6.1). In particular, our data revealed their differential roles in the operation of somatosensory thalamus: ML synapses tends to act as a reliable, secure channel for information transmission, while CT synapses demonstrates impressive versatility, which renders itself ideal for reflecting and presenting the dynamic information of network status. CT synapses achieves this aim by virtue of unique glutamate receptor composition and flexibility of synaptic strength (chapter 2 and 3). We also reported that pairing-induced activation of NMDARs also resulted in a parallel long-lasting decrease of neuronal input resistance (chapter 3), which could serve as a feedback mechanism following LTP induction to normalize overall neuronal output and therefore specifically enhance effectiveness of CT input. Noteworthily, despite the negative results for our experimental attempts to elucidate the physiological function of the preferential expression of CaP-AMPARs at CT synapses (chapter 3 and 4), their roles in thalamic function and neuropathology are

very intriguing, given that CaP-AMPARs can be activated even at basal low-frequency synaptic activation of CT pathway (at the V_m held ~ -70 mV) (chapter 2), and Ca^{2+} is one of the most multifunctional and universal intracellular messengers to our knowledge; recent studies have also indicated that CaP-AMPARs are involved in diverse regulatory functions of synaptic plasticity, learning, neurodevelopment, and neurological diseases (for reviewed, see Cull-Candy et al., 2006). Most importantly, this is the first experimental account establishing the linkage between physiological spiking patterns of relay neurons and excitatory synaptic plasticity in thalamus (chapter 5), which provides a mechanistic framework for unraveling the mysterious parallelism of state-dependent neuronal firing properties and thalamic functions.

Activation of T-type VGCCs is one of the most dramatic differences in thalamus during the transition from awake consciousness to inattentive or sleep state (Crunelli et al., 2006); in this study, we also proposed a critical role of T-type VGCCs in the induction of a novel-form of STDP at CT synapses (chapter 5), which not only adds to our understanding of the relations of the active conductance contingent upon global conscious states and excitatory synaptic plasticity of thalamus, but also echoes the proposition that backpropagating AP is not sufficient for induction of synaptic plasticity (Lisman and Spruston, 2005), providing insights into general principles of

synaptic physiology in the central nervous system.

One thing worth mentioned is that technical advance was also made in this study: reliable comparisons of input-specific properties require simultaneous recruitment of the two pathways in the same relay neuron; it is, however, very challenging, due to considerable distance between internal capsule (*ic*) and medial lemniscus (*ml*) and, therefore, limited preserved fibers converging onto the same cell in brain slices. Out work provides the first convincing evidence for the identity of locally-evoked EPSCs as of cortical origin (chapter 2), hence permitting the systematic analysis of input-specific properties of CT and ML pathways. Taken together, this study refines our current knowledge regarding thalamic physiology, which aids in both basic and clinical aspects of thalamus research.

A working model of dynamic thalamic information relay incorporating the synaptic plasticity of corticothalamic feedback

Corticothalamic synapses constitute the majority of synaptic contacts onto VBN relay neurons (Erisir et al. 1997; Jones, 2007; Latawiec et al. 2000; Sherman and

Koch,1986), and are believed to be responsible for the "high-conductance state" or

"synaptic barrages" of neurons observed *in vivo* (Steriade, 2001; Wolfart et al., 2005).

Multiplicative and additive gain modulations of neuronal transfer function have been

theoretically and experimentally shown to be critical for animals to perform several

behavioral tasks (Tovee et al., 1994; Brotchie et al., 1995; Salinas and Abbott, 1995;

Pouget and Sejnowski, 1997), and the biophysical implementations of both can

involve CT pathway. Multiplicative modulation (change in the slope of transfer

function) can be achieved putatively by the so-called "ceiling effect" via adjusting the

level of synaptic background noise (Chance et al., 2002; Debay et al., 2004; Shu et al.,

2003), as shown in thalamic relay neurons (Wolfart et al., 2005), while additive

modulation (shift of transfer function) can be realized via the action of balanced

excitation and inhibition, which exerts an effective influence over neuronal input

resistance, with the net effect on membrane potential only marginal (Chance et al.,

2002). In addition, a tonic GABAergic conductance has been reported in the relay

neurons of mouse dorsal lateral geniculate nucleus (dLGN) under physiological

temperature (Bright et al., 2007), which may be another molecular mechanism

underlying gain modulations, as tonic conductance provides not only a shunting effect

but also background noise by stochastic gating of ionotropic GABA receptors. An

example of how these might operate in a real thalamic system is described as follows

(cf. Sherman and Guillery, 2004): strong peripheral somatosensory input leads to powerful activation of ML fibers and thus increases firing levels of VBN relay neurons. If the input is so high that firing frequency of relay cells approaches saturation, their operational range is way beyond the linear range of the transfer function, and cells under this condition can no longer faithfully signal the input strength in terms of firing frequency. However, this robust activation of relay cells plausibly leads to increased neuronal activities in the target cortical areas, which in turn recruits massive CT feedback. CT fibers have collaterals also projecting to GABAergic neurons in thalamic reticular nucleus (Liu et al. 1995; Sherman and Guillery, 2002), and therefore the increase in feedback CT input may have two functional consequences according to the aforementioned biophysical mechanisms: the increase in background noise (glutamatergic and GABAergic) downregulates the gain of neuronal transfer function, and the concurrent recruitment of excitation (i.e. CT EPSCs) and inhibition (i.e. reticular IPSCs) reduces the input resistance of relay cells with V_m only minimally affected, both of which modulate the sensitivity of the neuronal output in response to the lemniscal input, and therefore restore the operation of relay cells into a linear scheme of transfer function.
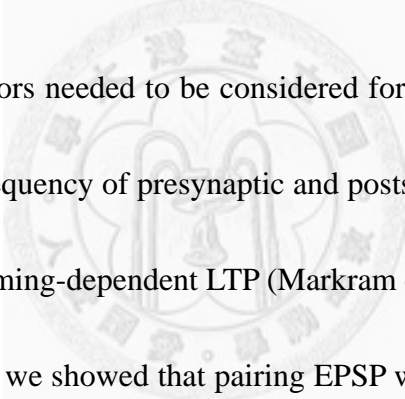
Our discovery of corticothalamic plasticity further enriches this scenario (chapter

3, 5): presumably, the pairing of feedback CT input with neuronal spiking driven by strong peripheral sensory input activates NMDARs effectively, leading to LTP of CT synapses, which in turn results in a long-lasting multiplicative downregulation of neuronal gain, aiding in the restoration of transfer linearity; the balance between excitation and inhibition delivered to relay neurons is, nevertheless, difficult to predict, due to the lack of the knowledge regarding synaptic plasticity of reticulo-thalamic GABAergic input so far. Even then, upon activation of NMDARs at CT synapses, an additive modulation can be achieved via another mechanism: intrinsic plasticity of relay neurons. A long-term decrease in input resistance reduces overall excitability of relay neurons (Fig. 3.1A); especially, considering the possibility that it is mediated by a local upregulation of dendritic I_h, so the corresponding influences on resting V_m may be spatially restricted to distal dendritic compartments, the net effect is, therefore, a long-lasting additive downregulation of neuronal information transfer, while the synaptic effectiveness of CT pathway is specifically spared given that LTP has occurred in parallel, or even enhanced if the potential local depolarizing effect (that may facilitate forward propagation of CT EPSP) introduced by upregulation of dendritic I_h is taken into account, which even boosts the multiplicative downregulation of neuron gain.

Taking a more speculative step, another condition in which such pairing and NMDAR activation at CT synapses could potentially occur is when thalamic relay neurons are in the status of slow oscillation, i.e. during deep non-REM sleep (Crunelli et al., 2006; Jones, 2007), as slow oscillatory activity is of cortical origin and may be partly contributed by corticothalamic activation of postsynaptic mGluR1a (Zhu et al., 2006; Jones, 2007), having the requirement of properly timed glutamate release at CT synapses and neuronal burst spiking to be satisfied. The resultant multiplicative downregulation of neuronal gain can suppress the responsiveness of relay neurons to sensory input, which is compatible with the view that sensory thalamus is functionally disconnected from its primary afferent during sleep.

On the other hand, depending on the intracortical interactions and specific spatiotemporal properties of lemniscal input (which may be contingent upon global conscious states and modulatory inputs from subcortical areas), insufficient CT feedback, plausibly reflecting limited excitation of the corresponding corticothalamic neurons, supplies little released glutamate for activating glutamate receptors, while L-type VGCCs can be activated in the presence of enough neuronal spiking, leading to LTD of CT synapses, which results in a long-lasting multiplicative upregulation of neuronal gain, subserving to impose the nonlinear operational scheme on relay cells

and thus "wake up" the neurons in their target cortical areas. Similarly, however, the impact of CT LTD on the long-lasting additive modulation is hard to predict. It is noteworthy that, under the condition in which LTP and LTD induction requirements are simultaneously fulfilled (chapter 3), their expression (or / and induction) can counteract each other. Therefore, CT synapses, and thus the properties of neuronal transfer function, have the "memory" of the recent activity history of thalamic system and are able to be fine-tuned in an integrative way.

There are several factors needed to be considered for this working model. It has been shown that pairing frequency of presynaptic and postsynaptic activities is critical to the induction of spike-timing-dependent LTP (Markram et al., 1997; Sjöström et al., 2001). Therefore, although we showed that pairing EPSP with high-frequency spiking (without LTS) is not effective in inducing LTP at CT synapses, particular caution must be taken to interpret it as an evidence for that no LTP can be induced by pairing with single tonic spikes usually observed under awake state. In other words, the realistic temporal profile of the lemniscal input and cortical feedback in *in-vivo* condition is an important determinant for the induction of long-term plasticity at CT synapses. It is also noteworthy that, in the dorsal lateral geniculate nucleus (dLGN) of mice, both repetitive burst spiking and tonic spiking can induce a sustained increase in the

frequency, but not amplitude, of spontaneous vesicular GABA release, which depends

on activation of NMDARs and the release of nitric oxide (Bright and Brickley, 2008).

However, the raising of spontaneous GABA release onto the recorded neuron does not

alter the tonic GABAergic current, thus imposing marginal effect on the input

resistance measured by somatic recording. This might be explained by the argument

that, compared to pharmacological methods by which ambient GABA concentration is

elevated globally across the entire slice (and thalamus), this increase of spontaneous

GABA release induced by somatic current- or voltage-clamp is relatively local (Bright

and Brickley, 2008). If this putative presynaptic GABAergic synaptic plasticity also

exists in the VBN, the scenario of the model discussed above will be more

complicated. Activity-dependent plasticity of GABA release can contribute to

multiplicative gain modulation by introducing different levels of background

fluctuation; nevertheless, its global and local influences on the input resistance of

different dendritic compartments in realistic conditions are not clear.

Perspectives and future work

The working model I propose above is critically dependent on two hypothetical

building blocks: first, the sensory information transmitted via ML synapses or slow oscillation of membrane potential drives appropriate neuronal activities as required for the induction of long-term plasticity at CT synapses; second, the long-term plasticity of CT synapses, potentially involving presynaptic expression, can modulate the transfer function of VBN relay neurons in a dynamic manner. Based on the above discussion, it is also of particular interest to know the properties of synaptic plasticity of reticular GABAergic input onto relay neurons of VBN, not only phasic but also tonic conductances. This is especially important for predicting the functional outcomes after specific activity patterns are presented to the thalamocortical system. In addition, although the efforts have been made to examine the roles of CaP-AMPARs in induction and expression of synaptic plasticity in this study, additional experiments are required for clarifying the relation of calcium-permeable non-NMDARs and LTP at CT synapses. For example, CaP-AMPARs was reported to play a significant role in consolidation of LTP (Plant et al., 2006), which is worth more investigation in this system.

From a comparative point of view, the powerful glomerular lemniscal synapse is morphologically and electrophysiologically similar to that of cerebellar climbing-fiber input onto Purkinje cells, which is known as an "instructive" pathway for its role in

dictating synaptic plasticity of parallel-fiber input in cerebellum (Coesmans et al., 2004; Han et al., 2007; Ito, 2001; Ito et al., 1982); it is worthy of further investigation that whether ML input can also serve as an instructive signal for influencing synaptic plasticity of CT pathways, especially through local interactions with proximal dendritically-located T-type VGCCs, thereby regulating information transfer and sensory processing in a complex, self-regulated manner. Moreover, it is also very interesting to know whether long-term plasticity of CT synapses can occur given that CT EPSP is paired with periodic burst spiking driven by slow oscillation, which might be induced by agonist of mGluR1a or high-frequency stimulation of CT fibers (Hughes et al., 2002; Zhu et al., 2006). More importantly, because the magnitude of synaptic plasticity is a function of pairing frequency (see above), to obtain a complete picture of the dynamic range of plasticity induction *in-vivo*, it is necessary to understand the dependence of long-term plasticity at CT synapses on pairing frequency. These works will deepen the physiological significance of our results as well as expand our horizons of how molecular, synaptic and cellular entities contribute to the emerging behaviors of sensory systems in higher mammals.

To test the second hypothesis, we can measure the basal fluctuation of membrane potential and quantify the transfer function of VBN relay neurons before and after

induction of LTP and LTD at CT synapses. Toward this end, identification of detailed

molecular mechanisms underlying synaptic plasticity of CT pathway, such as nitric

oxide (Bright and Brickley, 2008) or endocannabinoids (Sun et al., 2011), is of

particular importance, because based on our experiences, relay neurons have a very

low basal level of spontaneous background synaptic activities in the slice condition,

therefore, increase in basal activities or robust induction of long-term plasticity at

massive CT synapses, possibly by chemical means, may be critical (or at least helpful)

for the modulatory effects of CT input via change in background noise to be

measurable; another alternative experimental approach, promising but more technical

demanding, is to apply optogenetic technology for massive excitation of

genetically-defined population of synaptic inputs or neurons (Zhang et al., 2010),

which may also aid in induction of slow oscillation *in vitro* (for testing the first

hypothesis), and is especially beneficial to extend these studies to *in-vivo* whole

animal system, thus ideal for studying the functional impact of CT plasticity on the

sensory processes of awake and anesthetized animals.

Figures

Figure 6.1 Schematic summary of the properties of excitatory synaptic transmission and plasticity of corticothalamic (CT) and medial lemniscal (ML) synapses onto relay neurons in the ventrobasal nucleus (VBN) of rat thalamus

Figure 6.1
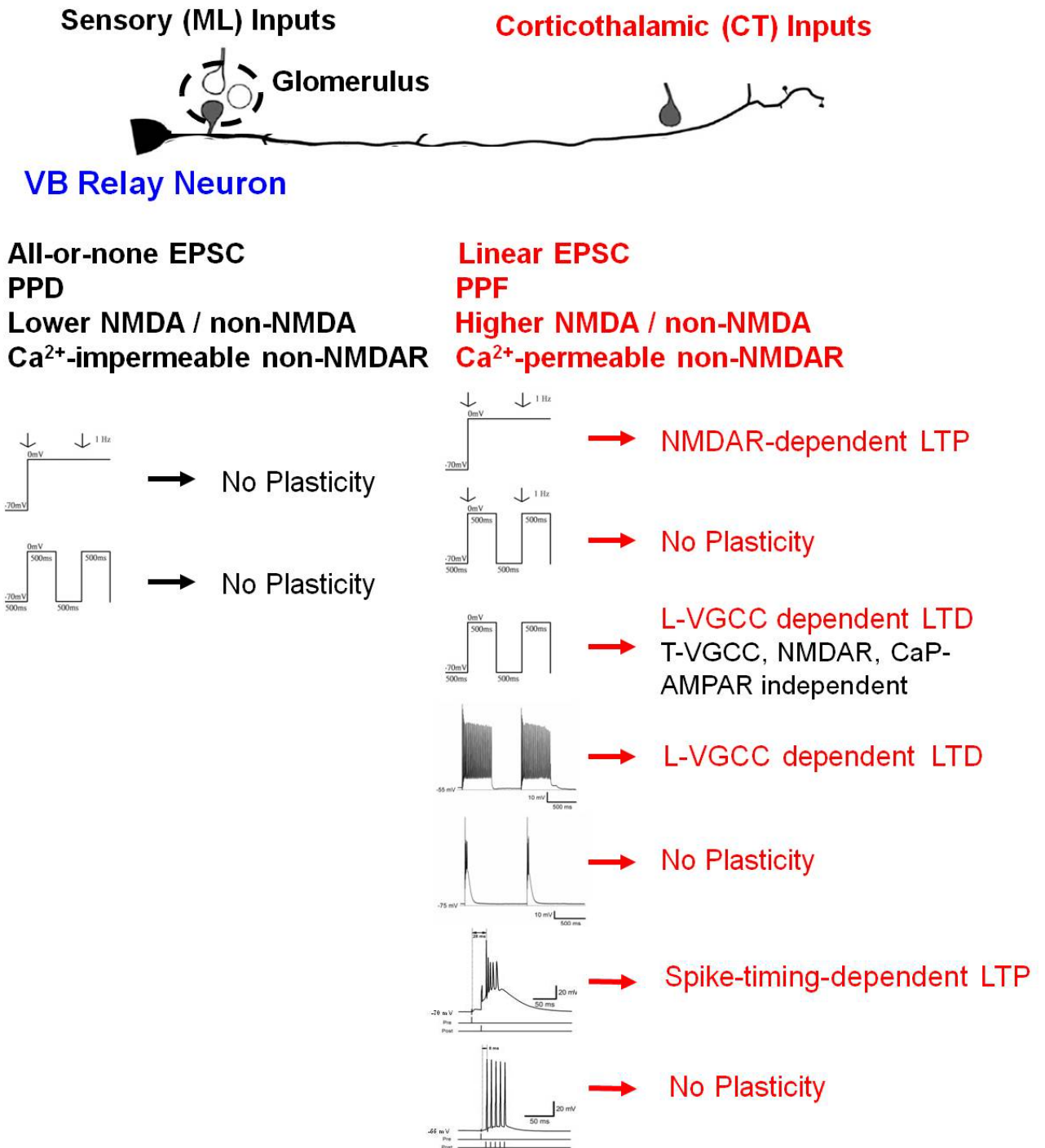
References

Adermark L, Lovinger DM (2007) Combined activation of L-type Ca^{2+} channels and synaptic transmission is sufficient to induce striatal long-term depression. *J Neurosci* **27(25)**:6781-6787

Andersen P, Morris R, Amaral D, Bliss T, O'Keefe J (2007) Historical perspective: proposed functions, biological characteristics, and neurobiological models of the hippocampus. In *The Hippocampus Book*. Oxford University Press, New York

Andersen P, Sundberg SH, Sveen O, Wigstrom H (1977) Specific long-lasting potentiation of synaptic transmission in hippocampal slices. *Nature* **266**:736-737

Andersen TF, Tikhonov DB, Bølcho U, Bolshakov K, Nelson JK, Pluteanu F, Mellor IR, Egebjerg J, Strømgaard K (2006) Uncompetitive antagonism of AMPA receptors: mechanistic insights from studies of polyamine toxin derivatives. *J Med Chem* **49**:5414-5423

Antal K, Emri Z, Tóth TI, Crunelli V (1996) Model of a thalamocortical neurone with

dendritic voltage-gated ion channels. *Neuroreport* **7**:2655-2658

Asrar S, Zhou Z, Ren W, Jia Z (2009) Ca^{2+} permeable AMPA receptor induced long-term potentiation requires PI3/MAP kinases but not Ca/CaM-dependent kinase II. *PLoS One* **4**:e4339

Auclair N, Otani S, Soubrie P, Crepel F (2000) Cannabinoids modulate synaptic strength and plasticity at glutamatergic synapses of rat prefrontal cortex pyramidal neurons. *J Neurophysiol* **83**:3287-3293

Agmon A, Connors BW (1991) Thalamocortical responses of mouse somatosensory (barrel) cortex *in vitro*. *Neuroscience* **41**:365-379

Aguilar JR, Castro-Alamancos MA (2005) Spatiotemporal gating of sensory inputs in thalamus during quiescent and activated states. *J Neurosci* **25(47)**:10990-11002

Alexander GM, Godwin DW (2005) Presynaptic inhibition of corticothalamic feedback by metabotropic glutamate receptors. *J Neurophysiol* **94**:163-175

Arcelli P, Frassoni C, Regondi MC, De Biasi S, Sprefico R (1997) GABAergic neurons in mammalian thalamus: a marker of thalamic complexity? *Brain Res Bull* **42**:27-37

Arsenault D, Zhang Z-W (2006) Developmental remodlling of the lemniscal synapse in the ventral basal thalamus of the mouse. *J Physiol* **573**:121-132

Artola A, Singer W (1993) Long-term depression of excitatory synaptic transmission and its relationship to long-term potentiation. *Trends Neurosci* **16(11)**:480-487

Avery RB, Johnston D (1996) Multiple channel types contribute to the low voltage activated calcium current in hippocampal CA3 pyramidal neurons. *J. Neurosci.* **16:**5567-5582

Aizenman CD, Akerman CJ, Jensen KR, Cline HT (2003) Visually driven regulation of intrinsic neuronal excitability improves stimulus detection in vivo. *Neuron* **39**:831–842

Aizenman CD, Munoz-Elias G, Cline HT (2002) Visually driven modulation of

glutamatergic synaptic transmission is mediated by the regulation of intracellular polyamines. *Neuron* **34**:623– 634

Babadi B (2005) Bursting as an effective relay mode in a minimal thalamic model. *Journal of Computational Neuroscience* **18**:229-243

Bain A (1855) *The Senses And The Intellect*. J.W. Parker, London

Bal T, McCormick DA (1993) Mechanisms of oscillatory activity in guinea-pig nucleus reticularis thalami in vitro: a mammalian pacemaker. *J Physiol* **468**:669-691

Banke TG, Bowie D, Lee H, Huganir RL, Schousboe A, Traynelis SF (2000) Control of GluR1 AMPA receptor function by cAMPdependent protein kinase. *J Neurosci* **20**:89–102

Barrionuevo G, Brown TH (1983) Associative long-term potentiation in hippocampal slices. *Proc Natl Acad Sci USA* **80**:7347–7351

Bear MF, Connors BW, Paradiso MA (2001) *Neuroscience: Exploring The Brain.* 2nd

ed. pp254-435, 724. Lippincott Williams & Wilkins, Baltimore and Philadelphia

Beierlein, M., Fall, C.P., Rinzel, J., Yuste, R (2002) halamocortical bursts trigger recurrent activity in neocortical networks: layer 4 as a frequencydependent gate. *J Neurosci* **22**: 9885–9894

Bell CC, Han VZ, Sugawara Y, Grant K (1997) Synaptic plasticity in a cerebellum-like structure depends on temporal order. *Nature* **387**:278-281

Bellone C, Lüscher C (2005) mGluRs induce a long-term depression in the ventral tegmental area that involves a switch of the subunit composition of AMPA receptors. *Eur J Neurosci* **21**:1280 –1288

Bekkers JM, Stevens CF (1990) Presynaptic mechanism for long-term potentiation in the hippocampus. *Nature* **346**:724--729

Bender V, Bender K, Brasier D, Feldman D (2006) Two coincidence detectors for spike timing-dependent plasticity in somatosensory cortex. *J Neurosci* **26**:4166-4177

Benke TA, Lüthi A, Isaac JT, Collingridge GL (1998) Modulation of AMPA receptor unitary conductance by synaptic activity. *Nature* **393(6687)**:793-797

Benke TA, Lüthi A, Palmer MJ, Wikström MA, Anderson WW, Isaac JT, Collingridge GL (2001) Mathematical modeling of non-stationary fluctuation analysis for studying channel properties of synaptic AMPA receptors. *J Physiol* **537.2**:407-420

Bi GQ, Poo MM (1998) Synaptic modifications in cultured hippocampal neurons: dependence on spike timing, synaptic strength, and postsynaptic cell type. *J Neurosci* **18**:10464-10472

Bienenstock EL, Cooper LN, Munro PW (1982) Theory for the development of neuron selectivity: orientation specificity and binocular interaction in visual cortex. *J Neurosci* **2(1)**:32-48

Birtoli B, Ulrich D (2004) Firing mode-dependent synaptic plasticity in rat neocortical pyramidal neurons. *J Neurosci* **24(21)**:4935-4940

Bellone C, Lüscher C (2005) mGluR induce a long-term depression in the ventral tegmental area that involves a switch of the subunit composition of AMPA receptors. *Euro J Neurosci* **21**:1280-1288
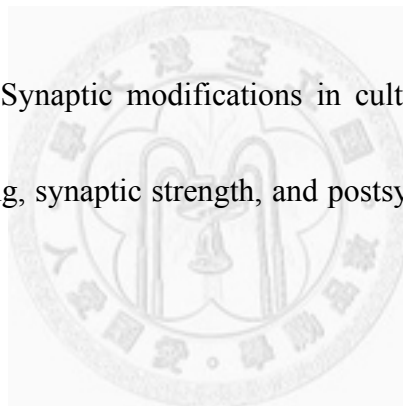
Blakemore LJ, Trombley PQ (2003) Kinetic variability of AMPA receptors among olfactory bulb neurons in culture. *Neuroreport* **14**:965-970

Blakemore LJ, Resasco M, Mercado MA, Trombley PQ (2006) Evidence for Ca^{2+}-permeable AMPA receptors in the olfactory bulb. *Am J Physiol Cell Physiol* **290**:C925-C935

Bliss TVP, Collingridge GL (1993) A synaptic model of memory: long-term potentiation in the hippocampus. *Nature* **361**:31-39

Bliss TVP, Lømo WT (1973) Long-lasting potentiation of synaptic transmission in the dentate area of the anesthetized rabbit following stimulation of the perforant path. *J Physiol* **232**:331-356

Bourassa J, Pinault D, Deschênes M (1995) Corticothalamic projections from the

cortical barrel field to the somatosensory thalamus in rats: a single-fiber study using

biocytin as an anterograde tracer *Eur J Neurosci* **7**:19-30

Bowie D, Lange GD, Mayer ML (1998) Activity-dependent modulation of glutamate

receptors by polyamines *J Neurosci* **18(20)**:8175-8185

Bowie D, Mayer ML (1995) Inward rectification of both AMPA and kainite subtypes

glutamate receptors generated by polyamine-mediated ion channel block. *Neuron*

15:453-462

Brecht M, Sakmann B (2002) Whisker maps of neuronal subclasses of the rat ventral

posterior medial thalamus, identified by whole-cell voltage recording and

morphological reconstruction. *J Physiol* **538**:495-515

Briggs F, Usrey WM. (2008) Emerging views of corticothalamic function. *Curr Opin

Neurobiol* **18(4)**:403-407

Bright DP, Brickley SG (2008) Acting locally but sensing globally: impact of

GABAergic synaptic plasticity on phasic and tonic inhibition in the thalamus. *J*

Physiol **586.21**:5091–5099

Bright DP, Aller MI, Brickley SG (2007) Synaptic release generates a tonic GABA$_A$ receptor-mediated conductance that modulates burst precision in thalamic relay neurons. *J Neurosci* **27**:2560–2569

Brotchie PR, Andersen RA, Snyder LH, Goodman SJ (1995) Head position signals used by parietal neurons to encode locations of visual stimuli. *Nature* **375**:232-235

Budde T, Munsch T, Pape H-C (1998) Distribution of L-type calcium channels in rat thalamic neurons. *Euro J Neurosci* **10**:586-597

Burnashev N, Khodorova A, Jonas P, Helm PJ, Wisden W, Monyer H, Seeburg PH, Sakmann B (1992) Calcium-permeable AMPA-kainate receptors in fusiform cerebellar glial cells. *Science* **256**:1566-1570

Burnashev N, Zhou Z, Neher JC, Sakmann B (1995) Fractional calcium currents through recombinant GluR channels of the NMDA, AMPA, and kainate receptor subtypes. *J Physiol* **485**:403-418

Caicedo A, Kungel M, Pujol R, Friauf E (1998) Glutamate-induced Co^{2+} uptake in rat auditory brainstem neurons reveals developmental changes in Ca^{2+} permeability of glutamate receptors. *Euro J Neurosci* **10**:941-954

Callaway JC, Ross WN (1995) Frequency dependent propagation of sodium action potentials in dendrites of hippocampal CA1 pyramidal neurons. *J Neurophysiol* **74**:1395–1403

Campanac E, Daoudal G, Ankri N, Debanne D (2008) Downregulation of Dendritic I_h in CA1 Pyramidal Neurons after LTP. *J Neurosci* **28(34)**: 8635-8643

Castro-Alamancos M A (1999) Neocortical synchronized oscillations induced by thalamic disinhibition in vivo. *Journal of Neuroscience* **19 RC27**:1-7

Castro-Alamancos MA (2002a) Properties of primary sensory (lemniscal) synapses in the ventrobasal thalamus and the relay of high-frequency sensory inputs. *J Neurophysiol* **87**:946-953

Castro-Alamancos MA (2002b) Role of thalamocortical sensory suppression during arousal: focusing sensory inputs in neocortex. *J Neurosci* **22(22)**:9651-9655

Castro-Alamancos MA, Calcagnotto ME (1999) Presynaptic long-term potentiation in corticothalamic synapses. *J Neuroscience* **19**:9090-9097

Castro-Alamancos MA, Calcagnotto ME (2001) High-pass filtering of corticothalamic activity by neuromodulators released in the thalamus during arousal: in vitro and in vivo *J Neurophysiol* **85**:1489-1497

Castro-Alamancos MA, Oldford E (2002) Cortical sensory suppression during arousal is due to the activity-dependent depression of thalamocortical synapses. *J Physiol* **541.1**:319-331

Catterall WA (2000) Structure and regulation of voltage-gated Ca^{2+} channels. *Annu Rev Cell Dev Biol* **16**:521-555

Chance FS, Abbott LF, Reyes A (2002) Gain modulation from background synaptic input. *Neuron* **35**:773-782

Chevaleyre V, Takahashi KA, Castillo PE (2006) Endocannabinoid-mediated synaptic plasticity in the CNS. *Annu Rev Neurosci* **29**:37–76

Choi S, Klingauf J, Tsien RW (2000) Postfusional regulation of cleft glutamate concentration during LTP at 'silent synapses'. *Nat Neurosci* **3(4)**:330-336

Christie BR, Schexnayder LK, Johnston D (1997) Contribution of voltage-gated Ca^{2+} channels to homosynaptic long-term depression in the CA1 region in vitro. *J Neurophysiol* **77(3):**1651-1655

Clark WE Le Gros (1930) The thalamus of *Tarsius*. *J Anat* **64**:371-414

Clark K, Normann C (2008) Induction mechanisms and modulation of bidirectional burst stimulation-induced synaptic plasticity in the hippocampus. *Eur J Neurosci* **28(2)**:279-287

Clem RL, Barth A (2006) Pathway-specific trafficking of native AMPARs by in vivo

experience. *Neuron* **49**:663– 670

Clem RL, Huganir RL (2010) Calcium-Permeable AMPA Receptor Dynamics Mediate Fear Memory Erasure. *Science* **330(6007)**:1108-1112

Coesmans M, Weber JT, De Zeeuw CI, Hansel C (2004) Bidirectional parallel fiber plasticity in the cerebellum under climbing fiber control. *Neuron* **44**:691-700

Collingridge GL, Kehl SJ, McLennan H (1983) Excitatory amino acids in synaptic transmission in the Schaffer collateral-commissural pathway of the rat hippocampus. *J Physiol* **334**:33– 46
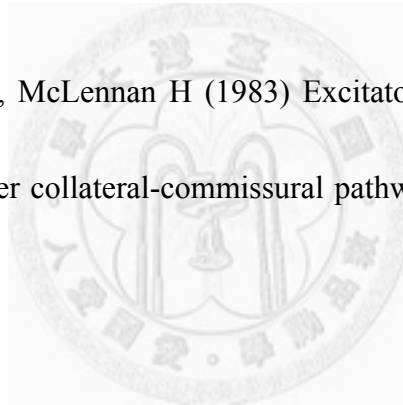
Connors BW, Gutnick MJ, Prince DA (1982) Electrophysiological properties of neocortical neurons in vitro. *J Neurophysiol* **48**:1302–1320

Contractor A, Rogers C, Maron C, Henkemeyer M, Swanson GT, Heinemann SF (2002) Trans-synaptic Eph receptor-ephrin signaling in hippocampal mossy-fiber LTP. *Science* **296**:1864–1869

Coulter DA, Huguenard JR, Prince DA (1989) Calcium currents in rat thalamocortical relay neurons: kinetic properties of the transient, low-threshold current. *J Physiol* **414**:587-604

Crair MC, Malenka RC (1995) A critical period for long-term potentiation at thalamocortical synapses. *Nature* **375**:325–328

Crepel F, Jaillard D (1991) Pairing of pre- and postsynaptic activities in cerebellar Purkinje cells induces long-term changes in synaptic efficacy in vitro. *J Physiol* **432**:123-141
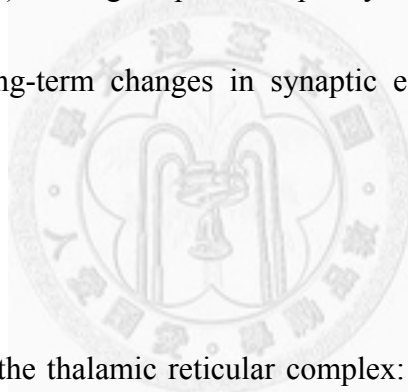
Crick (1984) Function of the thalamic reticular complex: the searchlight hypothesis. *Proc Natl Acad Sci U S A* 81(14):4586-4590

Crunelli V, Cope DW, Hughes SW (2006) Thalamic T-type Ca^{2+} Channels and NREM sleep. *Cell Calcium* **40**:175-190

Crunelli V, Kelly JS, Leresche N, Pirchiot M (1987) The ventral and dorsal lateral geniculate nucleus of the rat: intracellular recordings *in vitro*. *J Physiol* **384**:587-601

Cull-candy S, Kelly L, Farrant M (2006) Regulation of Ca^{2+}-permeable AMPA receptors: synaptic plasticity and beyond. *Curr Opin Neurobiol* **16**:288-297

Cummings JA, Mulkey RM, Nicoll RA, Malenka RC (1996) Ca^{2+} signaling requirements for long-term depression in the hippocampus *Neuron* **16**: 825-833

Czarnecki A, Birtoli B, Ulrich D. (2007) Cellular mechanisms of burst firing-mediated long-term depression in rat neocortical pyramidal cells. *J Physiol* **578.2**, 471-479

Dan Y, Poo MM (2004) Spike timing-dependent plasticity of neural circuits. *Neuron* **44**:23–30

Debay D, Wolfart J, Le Franc Y, Le Masson G, Bal T (2004) Exploring spike transfer through the thalamus using hybrid artificial-biological neuronal networks. *J Physiol (Paris)* **98**:540-558

Debanne D, Gähwiler BH, Thompson SM. (1998) Long-term synaptic plasticity

between pairs of individual CA3 pyramidal cells in rat hippocampal slice cultures. *J Physiol* **507**:237-247

Derkach V, Barria A, Soderling TR (1999) Ca^{2+}/calmodulin-kinase II enhances channel conductance of alpha-amino-3-hydroxy-5-methyl-4-isoxazolepropionate type glutamate receptors. *Proc Natl Acad Sci U S A* **96**:3269 –3274

Desai NS, Cudmore RH, Nelson SB, Turrigiano GG (2002) Critical periods for experience-dependent synaptic scaling in visual cortex. *Nat Neurosci* **5**:783–789

Deschênes M (2009) Vibrissal afferents from trigeminus to cortices. *Scholarpedia* **4(5)**:7454

Deschênes M, Roy JP, Steriade M (1982) Thalamic bursting mechanism: an inward slow current revealed by membrane hyperpolarization. *Brain Res* **239**: 289-293

Deschênes M, Veinante P, Zhang ZW (1998) The organization of corticothalamic projections: reciprocity versus parity. *Brain Res Rev* **28**:286–308

Destexhe A (2000) Modelling corticothalamic feedback and the gating of the thalamus by the cerebral cortex. *J Pysiol (Paris)* **94**:391-410

Destexhe A, Neubig M, Ulrich D, Huguenard J (1998) Dendritic low-threshold calcium currents in thalamic relay cells. *J Neurosci* **18(10)**:3574-3588

Destexhe A, Sejnowski T (2002) The initiation of bursts in thalamic neurons and the cortical control of thalamic sensitivity. *Phil Trans R Soc Lond B* **357**:1649-1657

Diamond ME (1995) Somatosensory thalamus of the rat. In *Cerebral Cortex* (ed. Jones EG, Peters A), vol. 11: *The Barrel Cortex of Rodents* (ed. Jones EG, Diamond IT). Plenum Press, New York

Diana MA, Marty A (2004) Endocannabinoid-mediated short-term synaptic plasticity: depolarization-induced suppression of inhibition (DSI) and depolarization-induced suppression of excitation (DSE) *Br J Pharmacol* **142**:9-19

Dobrunz LE, Stevens CF. (1999) Response of hippocampal synapses to natural stimulation patterns. *Neuron* **22**:157-166

Donevan SD, Rogawski MA (1995) Intracellular polyamines mediate inward rectification of Ca^{2+}-permeable α-amino-3-hydrosy-5-methyl-4isoxazolepropionic acid receptors. *Proc. Natl. Acad. Sci. USA* **92**:9298-9302

Eaton SA, Salt TE (1996) Role of N-methyl-D-aspartate and metabotropic glutamate receptors in corticothalamic excitatory postsynaptic potentials *in vivo*. *Neuroscience* **73**:1-5
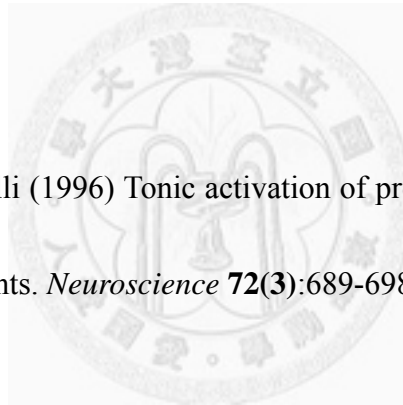
Emri Zs, Turner JP, Crunelli (1996) Tonic activation of presynaptic GABA$_B$ receptors on thalamic sensory afferents. *Neuroscience* **72(3)**:689-698

Ergenzinger ER, Glasier MM, Hahm JO, Pons TP (1998) Cortically induced thalamic plasticity in the primate somatosensory system. *Nat Neurosci* **1**:226–229

Erisir A, Van Horn SC, Sherman SM (1997) Relative numbers of cortical and brainstem inputs to the lateral geniculate nucleus. Proc Natl Acad Sci U S A **94**, 1517–1520

Fan Y, Fricker D, Brager DH, Chen X, Lu H-C, Chitwood RA, Johnston D (2005) Activity-dependent decrease of excitability in rat hippocampal nurons through increases in I$_h$. *Nat Neurosci* **8**:1542–1551

Fanselow EE, Sameshima K, Baccala LA, Nicolelis MA (2001) Thalamic bursting in rats during different awake behavioral state. *Proc Natl Acad Sci* USA **98**:15330-15335

Feldman DE, Knudsen EI (1998) Experience-dependent plasticity and the maturation of glutamatergic synapses. *Neuron* **20**:1067–1071

Feldman DE, Nicoll RA, Malenka RC (1999) Synaptic plasticity at thalamocortical synapses in developing rat somatosensory cortex: LTP, LTD, and silent synapses. *J Neurobiol* **41(1)**:92-101

Fortune ES, Rose GJ (2001) Short-term synaptic plasticity as a temporal filter. *Trends in Neuroscience* **24(7)**:381-385

Frank MG, Issa NP, Stryker MP (2001) Sleep enhances plasticity in the developing visual cortex. *Neuron* **30**:275–287

Froemke RC, Dan Y (2002) Spike-timing-dependent synaptic modification induced by natural spike trains. *Nature* **416**:433-438

Froemke RC, Tsay IA, Raad M, Long JD, Dan Y (2006) Contribution of individual spikes in burst-induced long-term synaptic modification. *J Neurophysiol* **95**:1620-1629

Garaschuk O, Schneggenburger R, Schirra C, Tempia F, Konnerth A (1996) Fractional Ca^{2+} currents through somatic and dendritic glutamate receptor channels of rat hippocampal CA1 pyramidal neurons. *J Physiol* **491**:757-772

Gasparini S, Migliore M, Magee JC. (2004) On the initiation and propagation of dendritic spikes in CA1 pyramidal neurons. *J Neurosci* **24**:11046-11056

Gebhardt C, Cull-Candy SG (2006) Influence of agonist concentration on AMPA and kainate channels in CA1 pyramidal cells in rat hippocampal slices. *J Physiol* **573.2**:371-394

Geiger JR, Lubke J, Roth A, Frotscher M, Jonas P (1997) Submillisecond AMPA receptor-mediated signaling at a principal neuron-interneuron synapse. *Neuron* **18**:1009-23

Geiger JRP, Melcher T, Koh D-S, Sakmann B, Seeburg PH, Jonas P, Monyer H (1995) Relative abundance of subunit mRNAs determines gating and Ca^{2+} permeability of AMPA receptors in principal neurons and interneurons in rat CNS. *Neuron* **15**:193–204
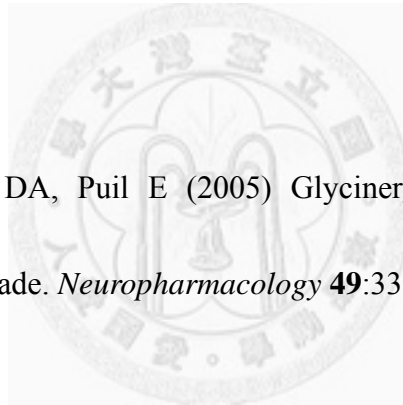
Ghavanini AA, Mathers DA, Puil E (2005) Glycinergic inhibition in thalamus revealed by synaptic blockade. *Neuropharmacology* **49**:338-349

Ghavanini AA, Mathers DA, Kim H, Puil E (2006) Distinctive glycinergic currents with fast and slow kinetics in thalamus. *J Neurophysiol* **95**:3438-3448

Goel A, Jiang B, Xu LW, Song L, Kirkwood A, Lee HK (2006) Cross-modal regulation of synaptic AMPA receptors in primary sensory cortices by visual experience. *Nat Neurosci* **9**:1001–1003

Golshani P, Warren Ra, Jones EG (1998) Progression of change in NMDA, non-NMDA, and metabotropic glutamate receptor function at the developing corticothalamic synapse. *J Neurophysiol* **80**:143-154

Golding NL, Staff NP, Spruston N. (2002). Dendritic spikes as a mechanism for cooperative long-term potentiation. *Nature* **418(6895)**: 326-331.

Graziano A, Liu X-B, Murray KD, Jones EG (2008) Vesicular glutamate transporters define two sets of glutamatergic afferents to the somatosensory thalamus and two thalamocortical projections in the mouse *J Comp Neurol* **507**:1258-1276

Guido W, Lu SM, Sherman SM (1992) Relative contributions of burst and tonic responses to the receptive field properties of lateral geniculate neurons in the cat. *J Neurophysiol* **68**:2199 –2211

Guido W, Lu SM, Vaughan JW, Godwin DW, Sherman SM (1995) Receiver operating characteristic (ROC) analysis of neurons in the cat's lateral geniculate nucleus during tonic and burst response mode. *Vis Neurosci* **12**:723–741

Guido W, Weyand T (1995) Burst responses in thalamic relay cells of the awake behaving cat. *J Neurophysiol* **74**:1782–1786

Guire ES, Oh MC, Soderling TR, Derkach VA (2008) Recruitment of calcium-permeable AMPA receptors during synaptic potentiation is regulated by CaM-kinase I. *J Neurosci* **28**:6000–6009

Gustaffson B, Wigstrom H, Abraham WC, Huang YY (1987) Long-term potentiation in the hippocampus using depolarizing current pulses as the conditioning stimulus to single volley synaptic potentials. *J Neurosci* **7**:774-780

Haack JA, Rosenberg RL (1994) Calcium-dependent inactivation of L-type calcium channels in planar lipid bilayers. *Biophysical Journal* **66**:1051-1060

Haidarliu S, Ahissar E (2001) Size gradients of barreloids in the rat thalamus. *The J Comp Neurol* **429**:372-387

Han VZ, Zhang Y, Bell CC, Hansel C (2007) Synaptic plasticity and calcium signaling in Purkinje cells of the central cerebellar lobes of mormyrid fish. *J Neurosci*

27(49):13499 −13512

Hansel C, Artola A, Singer W (1996) Different threshold levels of postsynaptic $[Ca^{2+}]_i$ have to be reached to induce LTP and LTD in neocortical pyramidal cells. *J Physiology (Paris)* **90**:317-319

Hardie J, Spruston N (2009) Synaptic depolarization is more effective than back-propagating action potentials during induction of associative long-term potentiation in hippocampal pyramidal neurons. *J Neurosci* **29(10)**: 3233-3241

Harnett MT, Bernier EB, Ahn KC, Morikawa H. (2009) Burst-timing-dependent plasticity of NMDA receptor-mediated transmission in midbrain dopamine neurons. *Neuron* **62**:826-838

Hartveit E, Veruki ML (2006) Studying properties of neurotransmitter receptors by non-stationary noise analysis of spontaneous synaptic currents. *J Physiol* **547.3**:751-785

Hartveit E, Veruki ML (2007) Studying properties of neurotransmitter receptors by

non-stationary noise analysis of spontaneous postsynaptic currents and agonist-evoked responses in outside-out patches. *Nature Protocol* **2(2)**:434-448

Hayashi Y, Momiyama A, Takahashi T, Ohishi H, Ogawa-Meguro R, Shigemoto R, Mizuno N, and Nakanishi S (1993) Role of a metabotropic glutamate receptor in synaptic modulation in the accessory olfactory bulb. *Nature* **366**:687-690

Hebb DO (1949) *The Organization of Behavior*. Wiley, New York

Heine M, Groc L, Fischknecht R, Béïque J, Lounis B, Rumbaugh G, Huganir RL, Cognet L, Choquet D (2008) Surface mobility of postsynaptic AMPARs tunes synaptic transmission. *Science* **320**:201-205

Heinemann SH, Conti F (1992) Nonstationary noise analysis and application to patch clamp recordings. *Methods in Enzymology* **207**:131-148

Herb A, Burnashev N, Werner P, Sakmann B, Wisden W, Seeburg PH (1992) The KA-2 subunit of excitatory amino acid receptors shows widespread expression in brain and forms ion channels with distantly related subunits.*Neuron* **8:**775-785

272

Hirata A, Castro-Alamancos MA (2006) Relief of synaptic depression produces long-term enhancement in thalamocortical networks. *J Neurophysiol* **95**:2479-2491

Ho MT, Ho TM, Pelkey KA, Pelletier JG, Huganir RL, Lacaille JC, McBain CJ (2009) Burst firing induces postsynaptic LTD at developing mossy fibre-CA3 pyramid synapses. *J Physiol* **587**:4441– 4454

Ho MT-W, Pelkey KA, Topolnik L, Petralia RS, Takamiya K, Xia J, Huganir RL, Lacaille J, McBain CJ (2007) Developmental expression of Ca^{2+}-permeable AMPA receptors underlies depolarization-induced long-term depression at mossy-fiber-CA3 pyramidal synapses *J Neurosci* **27(43)**:11651-11662

Hollmann M, Hartley M, Heinemann (1991) Ca^{2+} permeability of KA-AMPA-gated glutamate receptor channels depends on subunit composition. *Science* **252**:851-853

Hoogland PV, Welker E, Van der Loos H (1987) Organization of the projections from barrel cortex to thalamus in mice studied with Phaseolus vulgaris-leucoagglutinin and HRP. *Exp Brain Res* **68**:73-87

Howe JR (1996) Homomeric and heteromeric ion channels formed from the kainate-type subunits GluR6 and KA2 have very small, but different, unitary conductances. *J Neurophsiol* **76**:510-519

Hsu C-L, Yang H-W, Yen C-T, Min M-Y (2010) Comparison of synaptic transmission and plasticity between sensory and cortical synapses on relay neurons in the ventrobasal nucleus of the rat thalamus. *J Physiol* **588.22**:4347–4363

Hughes SW, Cope DW, Blethyn KL, Crunelli V (2002) Cellular mechanisms of the slow (<1 Hz) oscillation in thalamocortical neurons *in vitro*. *Neuron* **33**:947–958

Hume RI, Dingledine R, Heinemann SF (1991) Identification of a site in glutamate receptor subunits that controls calcium permeability. *Science* **253**: 1028-1031

Iino M, Ozawa S, Tsuzuki K (1990) Permeation of calcium through excitatory amino acid receptor channels in cultured rat hippocampal neurons. *Journal of Physiology* **424**:151-165

Isaac JT, Crair MC, Nicoll RA, Malenka RC (1997) Silent synapses during development of thalamocortical inputs. *Neuron* **18**:269–280

Issac JT, Hjelmstad GO, Nicoll RA, Malenka RC (1996) Long-term potentiation at single fiber inputs to hippocampal CA1 pyramidal cells. *Proc Natl Acad Sci U S A* **93**: 8710-8715

Issac JT, Nicoll RA, Malenka RC (1995) Evidence for silent synapses: implications for the expression of LTP. *Neuron* **15**:427-434

Ito M (2001) Cerebellar long-term depression: characterization, signal transduction, and functional roles. *Physiol Rev* **81**:1143-1195

Ito M, Sakurai M, Tongroach P (1982) Climbing fiber induced depression of both mossy fiber responsiveness and glutamate sensitivity of cerebellar Purkinje cells. *Journal of Physiology (London)* **324**:113-134

Jahnsen H, Llinás R (1984a) Electrophysiological properties of guinea-pig thalamic neurons: an in vitro study. *J Physiol* **349**:205-226

Jahnsen H & Llinás R. (1984b) Ionic basis for the electroresponsiveness and oscillatory properties of guinea-pig thalamic neurons *in vitro*. *J Physiol* **349:**227-247.

Jarrard LE (1993) On the role of the hippocampus in learning and memory in the rat. *Behav Neural Biol* **60**:9-26

Jones EG (2007) Thalamic neurons, synaptic organization, and functional properties. In *The Thalamus*, pp. 104-114, 171-192, 706-736. Cambridge University Press, Cambridge

Ju W, Morishita W, Tsui J, Gaietta G, Deerinck TJ, Adams SR, Garner CC, Tsien RY, Ellisman MH, Malenka RC (2004) Activity-dependent regulation of dendritic synthesis and trafficking of AMPA receptors. *Nat Neurosci* **7**:244 –253

Kakegawa W, Tsuzuki K, Yoshida Y, Kameyama K, Ozawa S (2004) Input- and subunit-specific AMPA receptor trafficking underlying long-term potentiation at hippocampal CA3 synapses. *Euro J Neurosci* **20**:101-110

Kamboj SK, Swanson GT, Cull-Candy SG (1995) Intracellular spermine confers rectification on rat calcium-permeable AMPA and kainate receptors. *J Physiol* **486**:297-303

Kammermeier PJ, Jones SW (1998) Facilitation of L-type calcium current in thalamic neurons. *J Neurophysiol* **79(1)**:410-417

Kamondi A, Acsady L, Buzsaki G. (1998) Dendritic spikes are enhanced by cooperative network activity in the intact hippocampus. *J Neurosci* **18**: 3919-3928

Kampa BM, Letzkus JJ, Stuart GJ (2007) Dendritic mechanisms controlling spike-timing-dependent synaptic plasticity. *Trends Neurosci* **30(9)**: 456-463

Kandel E, Schwartz J, Jessell T (2000) *Principles of Neural Science*, 4th Edition. pp317-998. New York: Oxford University Press

Kandel ER, Spencer WA. (1961) Electrophysiology of hippocampal neurons. II. After-potentials and repetitive firing. *J Neurophysiol* **25**:243-259

Kao C-Q, Coulter DA (1997) Physiology and pharmacology of corticothalamic stimulation-evoked responses in rat somatosensory thalamic neurons in vitro. *J Neurophysiol* **77:**2661-2676

Kelly MK, Carvell GE, Hartings JA, Simons DJ (2001) Axonal conduction properties of antidromically identified neurons in rat barrel cortex. *Somatosens Mot Res* **18**:202-210

Kelso SR, Ganong AH, Brown TH (1986) Hebbian synapses in hippocampus. *Proc Natl Acad Sci U S A* **83**:5326 –5330

Killackey HP, ShermanSM (2003) Corticothalamic projections from the rat primary somatosensory cortex. *J Neurosci* **23**:7381–7384

King C, Henze DA, Leinekugel X, Buzsaki G. (1999) Hebbian modification of a hippocampal population pattern in the rat. *J Physiol* **521**: 159-167

Kirischuk S, Clements JD, Grantyn R (2002) Presynaptic and postsynaptic mechanisms underlie paired pulse depression at single GABAergic boutons in rat

collicular cultures *J Physiol* **543.1**:99-116

Koike M, Iino M, Ozawa S (1997) Blocking effect of 1-naphthyl acetyl spermine on Ca^{2+}-permeable AMPA receptors in cultured rat hippocampal neurons. *Neuroscience Research* **29**:27-36

Kostopoulos GK (2001) Involvement of the thalamocortical system in epileptic loss of consciousness. *Epilepsia* **42 Suppl 3**:13-19

Krahe R, Gabbiani F (2004) Burst firing in sensory systems. *Nat Rev Neurosci* **5**:13-23
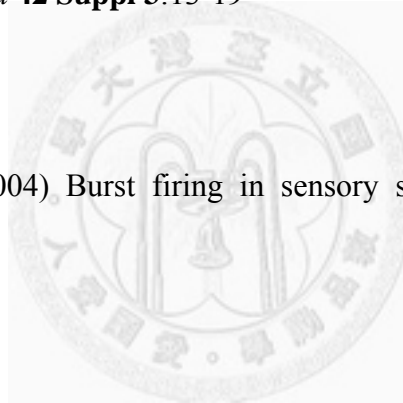
Kreitzer AC, Regehr WG (2001) Retrograde inhibition of presynaptic calcium influx by endogenous cannabinoids at excitatory synapses onto Purkinje cells. *Neuron* **29:**717-727

Krupa DJ, Ghazanfar AA, Nicolelis MA (1999) Immediate thalamic sensory plasticity depends on corticothalamic feedback. *Proc Natl Acad sci U S A* **96**:8200-8205

Kullmann DM (1996) Long-term potentiation of NMDA and AMPA receptor-mediated signals in CA1 pyramidal cells: Qualitatively similar but quantitatively different. *J Physiol* **491P**:137-138

Kullmann DM, Erdemli G, Asztély F (1996) LTP of AMPA and NMDA receptor-mediated signals: evidence for presynaptic expression and extrasynaptic glutamate spill-over. *Neuron* **17(3)**:461-474

Kullmann DM, Nicoll RA (1992) Long-term potentiation is associated with increases in quantal content and quantal amplitude. *Nature* **357**:240–244

Kumar SS, Bacci A, Kharazia V, Huguenard JR (2002) A developmental switch of AMPA receptor subunits in neocortical pyramidal neurons. *J Neurosci* **22**:3005-3015

Kuo C-C, Yang S (2001) Recovery from inactivation of T-type Ca^{2+} channels in rat thalamic neurons. *J Neurosci* **21(6)**:1884-1892

Lamsa KP, Heeroma lH, Somogyi P, Rusakov DA, Kullmann DM (2007) Anti-Hebbian long-term potentiation in the hippocampal feedback inhibitory circuit.

Science **315**:262-266

Land PW, Buffer SA, Yaskosky JD (1995) Barreloids in adult rat thalamus: three-dimensional architecture and relationship to somatosensory cortical barrels. *J Comp Neurol* **355**:573-588

Landisman CR, Connors BW (2007) VPM and PoM nuclei of the rat somatosensory thalamus: intrinsic neuronal properties and corticothalamic feedback *Cerebral Cortex* **17**:2853-2865

Lanté F, Toledo-Salas J-C, Ondrejcak T, Rowan MJ, Ulrich D (2011) Removal of Synaptic Ca^{2+}-Permeable AMPA Receptors during Sleep. *J Neurosci* **31(11)**:3953–3961

Larkum ME, Kaiser KMM, Sakmann B (1999a) Calcium electrogenesis in distal apical dendrites of layer 5 pyramidal cells at a critical frequency of back-propagating action potentials. *Proc Natl Acad Sci USA* **96**:14600-14604

Larkum ME, Watanabe S, Nakamura T, Lasser-Ross N, Ross WN (2003) Synaptically

activated Ca^{2+} waves in layer 2/3 and layer 5 rat neocortical pyramidal neurons. *J Physiol* **549**:471-488

Larkum ME, Zhu JJ, Sakmann B (1999b) A new cellular mechanism for coupling inputs arriving at different cortical layers. *Nature* **398**:338-341

Laroche S, Jay TM, Thierry AM (1990) Long-term potentiation in the prefrontal cortex following stimulation of the hippocampal CA1/subicular region. *Neurosci Lett* **114**:184-190

Laroche S, Lynch G (1986) Induction of synaptic potentiation in hippocampus by patterned stimulation involves two events. *Science* **232**:985-988

Latawiec D, Martin KA, Meskenaite V (2000) Termination of the geniculocortical projection in the striate cortex of macaque monkey: a quantitative immunoelectron microscopic study. *J Comp Neurol* **419**, 306–319

Lavallée P, Urbain N, Dufresne C, Bokor H, Acsády L, Deschênes M (2005) Feedforward inhibitory control of sensory information in higher-order thalamic nuclei.

J Neurosci **25**:7489-7498

Le Masson G, Renaus-Le Masson S, Debay D, Bal T (2002) Feedback inhibition controls spike transfer in hybrid thalamic circuit. *Nature* **417**:854-858

Leamey CA, Ho SM (1998) Afferent arrival and onset of functional activity in the trigeminothalamic pathway of the rat *Dev Brain Res* **105**:195-207

Lee J-H, Gomora JC, Cribbs LL, Perez-Reyes E (1999) Nickle block of three cloned T-type calcium channels: low concentrations selectively block α1H *Biophysical Journal* **77**:3034-3042
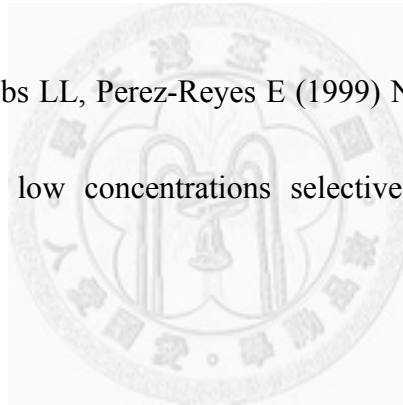
Lee HK, Barbarosie M, Kameyama K, Bear MF, Huganir RL (2000) Regulation of distinct AMPA receptor phosphorylation sites during bidirectional synaptic plasticity. *Nature* **405**:955–959

Lei S, Pelkey KA, Topolnik L, Congar P, Lacaille J, McBain CJ (2003) Depolarization-induced long-term depression at hippocampal mossy fiber-CA3 pyramidal neuron synapses. *J Nuerosci* **23(30):**9786-9795

Lerma J, Paternain AV, Naranjo JR, Mellstrom B (1993) Functional kainite-selective glutamate receptors in cultured hippocampal neurons. *Proc Natl Acad Sci USA* **90**:11688-11692

Letzkus JJ, Kampa BM, Stuart G (2006) Learning rule for spike timing-dependent plasticity depend on synapse location. *J Neurosci* **26(41)**: 10420-10429

Levy WB, Steward O (1979) Synapses as associative memory elements in the hippocampal formation. *Brain Res* **175**: 233–245

Levy WB, Steward O (1983) Temporal contiguity requirements for long-term associative potentiation / depression in the hippocampus. *Neuroscience* **8**:791-797

Laezza F, Doherty JJ, and Dingledine R (1999) Long-term depression in hippocampal interneurons: joint requirement for pre- and postsynaptic events. *Science* **285**: 1411–1414

Li J, Guido W, Bickford ME (2003) Two distinct types of corticothalamic EPSPs and

their contribution to short-term plasticity. *J Neurophysiol* **90**:3429-3440

Liao D, Hessler NA, Malinow R (1995) Activation of postsynaptically silent synapses during pairing-induced LTP in CA1 region of hippocampal slice. *Nature* **375**: 400-404

Liao CC, Chen RF, Lai WS, Lin RC, Yen CT (2010) Distribution of large terminal inputs from the primary and secondary somatosensory cortices to the dorsal thalamus in the rodent. *J Comp Neurol* **518(13)**:2592-2611

Lisman JE (1997) Burst as a unit of neural information: making unreliable synapses reliable. *Trends Neurosci* **20**:38–43
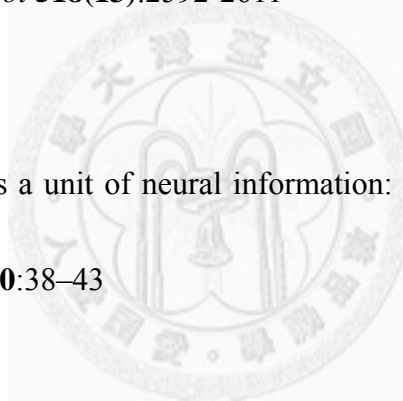
Lisman J, Spruston N (2005) Postsynaptic depolarization requirements for LTP and LTD: a critique of spike timing-dependent plasticity. *Nat. Neurosci* **8**: 839–841

Liu X-B (1997) Subcellular distribution of AMPA and NMDA receptor subunit immunoreactivity in ventral posterior and reticular nuclei of rat and cat thalamus. *The J Comp Neurol* **388**:587-602

Liu S-Q J, Cull-Candy S (2000) Synaptic activity at calcium-permeable AMPA receptors induces a switch in receptor subtype. *Nature* **405**:454-458

Liu X-B, Honda CN, Jones EG (1995) Distribution of four types of synapse on physiologically identified relay neurons in the ventral posterior thalamic nucleus of the cat. *J Comp Neurol* **352**:69–91

Livingstone MS, Hubel DH (1981) Effects of sleep and arousal on the processing of visual information in the cat. *Nature* **291**: 554 - 561
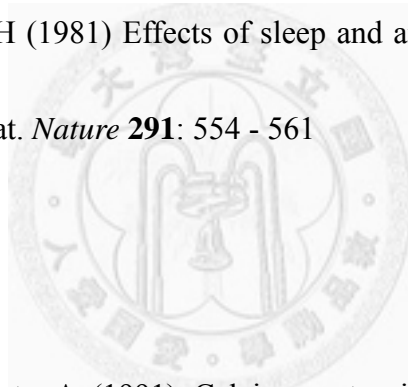
Llano I, Leresche N, Marty A (1991) Calcium entry increases the sensitivity of cerebellar Purkinje cells to applied GABA and decreases inhibitory synaptic currents. *Neuron* **6**:565-574

Llano DA, Sherman SM (2009) Differences in intrinsic properties and local network connectivity of identified layer 5 and layer 6 adult mouse auditory corticothalamic neurons support a dual corticothalamic projection hypothesis. *Cereb Cortex* **19**:2810-2826

Llinás R (1988) The intrinsic electrophysiological properties of mammalian neurons: insights into central nervous system function. *Science* **242**:1654-1664

Llinás R, Jahnsen H (1982) Electrophysiology of mammalian thalamic neurons in vitro. *Nature* **297**:406-408, 1982

Lo F-S, Mize RR (2000) Synaptic regulation of L-type Ca^{2+} channel activity and long-term depression during refinement of the retinocollicular pathway in developing rodent superior colliculus. *J Neurosci* **20**:RC58 (1-6)

Lo F-S, Mize RR (2002) Properties of LTD and LTP of retinocollicular synaptic transmission in the developing rat superior colliculus. *Euro J Neurosci* **15**:1421-1432

Losonczy A, Magee JC (2006) Integrative properties of radial oblique dendrites in hippocampal CA1 pyramidal neurons. *Neuron* **50**:291-307

Lu SM, Guido W, Sherman SM (1992) Effects of membrane voltage on receptive field properties of lateral geniculate neurons in the cat: contributions of the

low-threshold Ca2 conductance. *J Neurophysiol* **68**:1285–1298

Lu W-Y, Man H-Y, Ju W, Trimble WS, MacDonald JF, Wang YT (2001) Activation of synaptic NMDA receptors induces membrane insertion of new AMPA receptors and LTP in cultured hippocampal neurons. *Neuron* **29**:243–254.

Luthi A, McCormick DA (1998a) Periodicity of thalamic synchronized oscillations: the role of Ca^{2+}-mediated upregulation oh I_h. *Neuron* **20**:553-563

Luthi A, McCormick DA (1998b) H-current: properties of a neuronal and network pacemaker. *Neuron* **21**:9-12
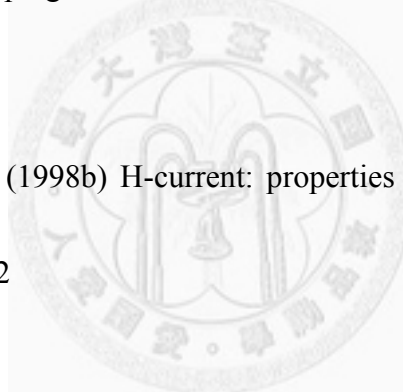
Lynch GS, Dunwiddie T, Gribkoff V (1977) Heterosynaptic depression: a postsynaptic correlate of long-term potentiation. *Nature* **266**:737-739

Lynch C, Larson I, Kelso S, Barrionuevo C, Schonler F (1983) Intracellular injections of ECTA block induction of hippocampal long-term potentiation. *Nature* **305**: 719-721

Ma J, Lowe G (2007) Calcium permeable AMPA receptors and autoreceptors in external tufted cells of rat olfactory bulb. *Neuroscience* **144**:1094-1108

Ma W, Peschanski M, Ralston J-M (1986) The overlap of spinothalamic and dorsal column nuclei projections in the ventrobasal complex of the rat thalamus: A double anterograde labeling study using light microscopy analysis. *J Comp Neurol* **245(4)**:531-540
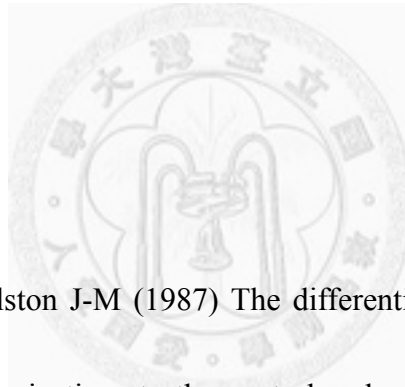
Ma W, Peschanski M, Ralston J-M (1987) The differential synaptic organization of the spinal and lemniscal projections to the ventrobasal complex of the rat thalamus. Evidence for convergence of the two systems upon single thalamic neurons. *Neuroscience* **22(3)**:925-934

Ma PM, Woolsey TA (1984) Cytoarchitectonic correlates of the vibrissae in the medullary trigeminal complex of the mouse. *Brain Res* **306**:374-379

Ma J, Lowe G (2007) Calcium permeable APMA receptors and autoreceptors in

external tufted cells of rat olfactory bulb. *Neuroscience* **144**:1094-1108

MacDermott AB, Mayer ML, Westbrook GL, Smith SJ, Barker JL (1986) NMDA-receptor activation increases cytoplasmic calcium concentration in cultured spinal cord neurones. *Nature* **321**: 519–522

Magee JC, Johnston D. (1995) Characterization of single voltage-gated Na and Ca channels in apical dendrites of rat CA1 pyramidal neurons. *J Physiol. (Lond.)* **487**:67-90

Magee JC, Johnston D. (1997) A synaptically controlled, associative signal for Hebbian plasticity in hippocampal neurons. *Science* **275**: 209-213

Malenka RC, Bear MF (2004) LTP and LTD: an embarrassment of riches. *Neuron* **44**:5-21

Malenka RC, Nicoll RA (1993) NMDA-receptor-dependent synaptic plasticity: multiple forms and mechanisms. *Trends Neurosci* **16(12)**:521-527

Malenka RC, Nicoll RA (1997) Silent synapses speak up. *Neuron* **19**:473-476.

Malinow R, Tsien RW (1990) Presynaptic enhancement shown by whole-cell recordings of long-term potentiation in hippocampal slices *Nature* **346**:177-180

Mameli M, Balland B, Lujan R, Lüscher C (2007). Rapid synthesis and synaptic insertion of GluR2 for mGluR-LTD in the ventral tegmental area. *Science* **317**: 530–533
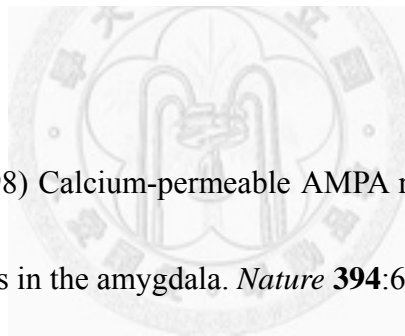
Manhanty NK, Sah P (1998) Calcium-permeable AMPA receptors mediate long-term potentiation in interneurons in the amygdala. *Nature* **394**:683–687

Maren S, Baudry M (1995) Properties and mechanisms of long-term synaptic plasticity in the mammalian brain: relationships to learning and memory. *Neurobiology of Learning And Memory* **63**:1-18

Markram H, Lübke J, Frotscher M, Roth A, Sakmann B (1997) Physiology and anatomy of synaptic connections between thick tufted pyramidal neurones in the developing rat neocortex. *J Physiol* **500:**409–440

Martin SJ, Morris RGM (2002) New life in an old idea: the synaptic plasticity and memory hypothesis revisited. *Hippocampus* **12(5)**:609-636

Massey PV, Bashir ZI (2007) Long-term depression: multiple forms and implications for brain function. *TRENDS in Neuriscience* **30(4)**:176-184

Mayer ML, Westbrook GL, Guthrie PB (1984) Voltage dependent block by Mg21 of NMDA responses in spinal cord neurones. *Nature* **309**:261–263

McBain CJ (1998) A short-term mechanism of plasticity for interneurons? *J Physiol* **511**:331

McCormick DA (1992) Neurotransmitter actions in the thalamus and cerebral cortex and their role in neuromodulation of thalamocortical activity. *Prog Neurobiol* **39**:337-388

McCormick DA. (1993) Corticothalamic activation modulates thalamic firing through

glutamate 'metabotropic' receptors. *Proc Natl Acad Sci USA* **89**:2774-2778

McCormick DA (2002) Cortical and subcortical generators of normal and abnormal rhythmicity. *Int Rev Neurobiol* **49**:99-114

McCormick DA, Bal T (1997) Sleep and arousal: thalamocortical mechanisms. *Annu Rev Neurosci* **20**:185-215

McCormick DA, Connors BW, Lighthall JW, Prince DA (1985) Comparative electrophysiology of pyramidal and sparsely spiny stellate neurons of the neocortex. *J Neurophysiol* **54(4)**:782-806

McCormick DA, Feeser HR (1990) Functional implication of burst firing and single spike activity in lateral geniculate relay neurons. *Neurosci* **39**: 103-113

Mckay BE, McRory JE, Molineux ML, Hamid J, Snutch TP, Zamponi GW, Turner RW (2006) Ca_v3 T-type calcium channel isoforms differentially distribute to somatic and dendritic compartments in rat central neurons. *Eur J Neurosci* **24**:2581-2594

McNaughton BL, Douglas RM, Goddard GV (1978) Synaptic enhancement in fascia dentata: cooperativity among coactive afferents. *Brain Res* **157**:277–293

Meeren H, van Luijtelaar G, Lopes da Silva F, Coenen A (2005) Evolving concepts on the pathophysiology of absence seizures. *Arch Neurol* **62**:371-376

Meksuriyen D, Fukuchi-Shimogori T, Tomitori H, Kashiwagi K, Toida T, Imanari T, Kawai G, Igarashi K (1998) Formation of a complex containing ATP, Mg^{2+}, and spermine. Structure evidence and biological significance. *J Biol Chem* **273(47)**:30939-30944
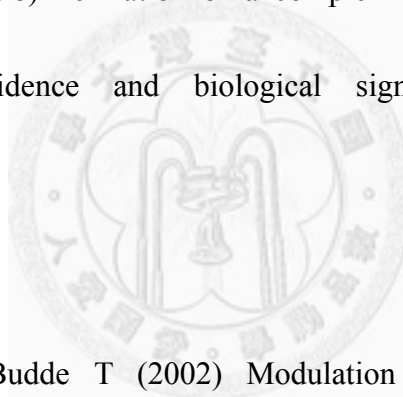
Meuth S, Pape H-C, Budde T (2002) Modulation of Ca^{2+} currents in rat thalamocortical relay neurons by activity and phosphorylation. *Euro J Neurosci* **15**:1603-1614

Mineff EM, Weinberg RJ (2000) Differential synaptic distribution of AMPA receptor subunits in the ventral posterior and reticular thalamic nuclei of the rat. *Neuroscience* **101(4)**:969-982

Mishima K (1992) Facilitatory and inhibitory processes in the thalamic vnetrobasal nucleus of the rat. *Japanese Journal of Physiology* **42**:193-210

Miyata M, Imoto K (2006) Different composition of glutamate receptors in corticothalamic and lemniscal synaptic responses and their roles in the firing responses of ventrobasal thalamic neurons in juvenile mice. *J Physiol* **575**:161-174

Miyata M, Imoto K (2009) Contrary roles of kainate receptors in transmitter release at corticothalamic synapses onto thalamic relay and reticular neurons. *J Physiol* **587.5**:999-1012
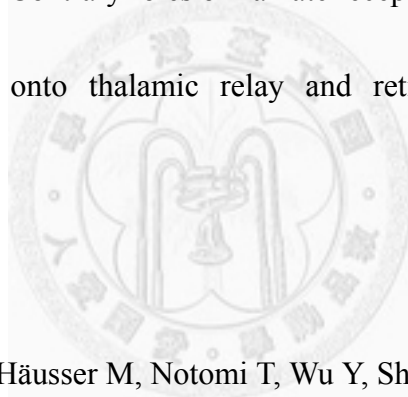
Momiyama A, Silver RA, Häusser M, Notomi T, Wu Y, Shigemoto R, and Cull-Candy SG (2003) The density of AMPA receptors activated by a transmitter quantum at the climbing fibre–Purkinje cell synapse in immature rats. *J Physiol* **549.1**, 75-92

Monyer H, Seeburg PH, Wisden W (1991) Glutamate-operated channels: developmentally early and mature forms arise by alternative splicing. *Neuron* **6**:799–810

Mukherjee P, Kaplan E. (1995) Dynamics of neurons in the cat lateral geniculate nucleus: in vivo electrophysiology and computational modeling. J Neurophysiol **74(3)**:1222-1243

Munsch T, Budde T, Pape HC (1997) Voltage-activated intracellular calcium transients in thalamic relay cells and interneurons. *Neuroreport* **8**:2411-2418

Murphy PC, Sillito AM (1987) Corticofugal feedback influences the generation of length tuning in the visual pathway. *Nature* **329**:727–729

Naie K, Tsanov M, Manahan-Vaughan D (2007) Group I metabotropic glutamate receptors enable two distinct forms of long-term depression in the rat dentate gyrus in vivo. *Eur J Neurosci* **25**: 3264–3275

Nakamura T, Barbara J-G, Nakamura K, Ross WN (1999) Synergistic release of Ca^{2+} from IP_3-sensitive stores evoked by synaptic activation of mGluRs paired with backpropagating action potentials. *Neuron* **24**:272-737

Neher E (1992) Correction for liquid junction potentials in patch clamp experiments.

Methods in Enzymology **207**:123-131

Nevian T, Sakmann B (2006) Spine Ca^{2+} signaling in spike-timing-dependent plasticity. **26(43)**: 11001-11013

Ngezahayo A, Schachner M, Artola A (2000) Synaptic activity modulates the induction of bidirectional synaptic changes in adult mouse hippocampus. *J Neurosci* **20(7)**:2451-2458

Nicolelis MA, Chapin JK (1994) Spatiotemporal structure of somatosensory responses of many-neuron ensembles in the rat ventral posterior medial nucleus of the thalamus *J Neurosci* **14(6)**:3511-3532

Nicolelis MA, Fanselow EE (2002) Thalamocortical optimization of tactile processing according to behavioral state. *Nat Neurosci* **5**:517-523

Nicolelis MA (2005) Computing with thalamocortical ensembles during different behavioural states. *J Physiol* **566.1**: 37-47

Nicolelis MA, Lin RCS, Woodward DJ, Chapin JK (1993) Dynamic and distributed properties of many-neuron ensembles in the ventral posterior medial thalamus of awake rats. *Proc Natl Acad Sci USA* **90:**2212-2216

Normann C, Peckys D, Schulze CH, Walden J, Jonas P, Bischofberger J (2000) Associative long-term depression in the hippocampus is dependent on postsynaptic N-type Ca^{2+} channels. *J Neurosci* **20(22)**:8290-8297

Nowak L, Bregetovski P, Ascher P, Herbet A, Prochiantz A (1984) Magnesium gates glutamate activated channels in mouse central neurones. *Nature* **307**:462–465

Oh MC, Derkach VA (2005) Dominant role of the GluR2 subunit in regulation of AMPA receptors by CaMKII. *Nat Neurosci* **8**:853– 854

Ohara PT, Lieberman AR (1993) Some aspects of the synaptic circuitry underlying inhibition in the ventrobasal thalamus. *J Neurocytol* **22**:815-825

O'Keefe J, Recce ML (1993) Phase relationship between hippocampal place units and the EEG theta rhythm. *Hippocampus* **3(3)**:317-30

Oliet SH, Malenka RC, Nicoll RA (1997) Two distinct forms of long-term depression coexist in CA1 hippocampal pyramidal cells. *Neuron* **18**:969-982

Otto T, Eichenbaum H, Wiener SI, Wible CG. (1991) Learning-related patterns of CA1 spike trains parallel stimulation parameters optimal for inducing hippocampal long-term potentiation. *Hippocampus* **1**, 181-192

Pape HC, Munsch T, Budde T (2004) Novel vistas of calcium-mediated signalling in the thalamus. *Pflügers Arch* **448(2)**:131-138

Paulsen O, Sejnowski TJ (2000) Natural patterns of activity and long-term synaptic plasticity. *Curr Opin Neurobiol* **10**:172-179

Paxinos G, Watson C (2007) *The Rat Brain in Stereotaxic Coordinates.* Elsevier, London

Pelkey KA, Lavezzari G, Racca C, Roche KW, McBain CJ (2005) mGluR7 is a metaplastic switch controlling bidirectional plasticity of feedforward inhibition.

Neuron **46**:89 –102

Perrett SP, Dudek SM, Eagleman D, Montague PR, Friedlander MJ. (2001) LTD induction in adult visual cortex: role of stimulus timing and inhibition. *J Neurosci* **21**, 2308-2319

Peschanski M, Lee CL, Ralston HJ (1984) The structural organization of the ventrobasal complex of the rat as revealed by the analysis of physiologically characterized neurons injected intracellularly with horseradish peroxidase. *Brain Research* **297**:63-74
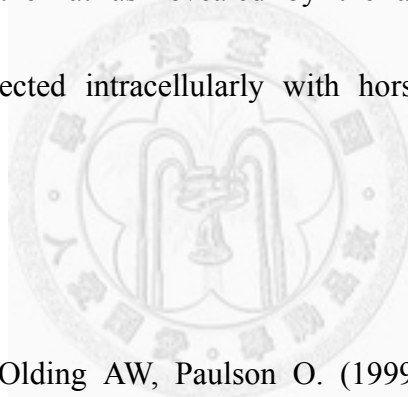
Pike FG, Meredith RM, Olding AW, Paulson O. (1999) Postsynaptic bursting is essential for 'Hebbian' induction of associative long-term potentiation at excitatory synapses in rat hippocampus. *J Physiol* **518**: 571-576

Pickard L, Noel J, Duckworth JK, Fitzjohn SM, Henley JM, Collingridge GL, Molnar E (2001) Transient synaptic activation of NMDA receptors leads to the insertion of native AMPA receptors at hippocampal neuronal plasma membranes. *Neuropharmacology* **41**:700–713

Pierret T, Lavallée P, Deschênes M (2000) Parrallel streams for the relay of vibrissal information through thalamic barreloids. *J Neurosci* **20(19)**:7455-7462

Pitler TA, Alger BE (1992) Postsynaptic spike firing reduces synaptic GABA$_A$ responses in hippocampal pyramidal cells. *J Neurosci* **12**:4122-4132

Plant K, Pelkey KA, Bortolotto ZA, Morita D, Terashima A, McBain CJ, Collingridge GL, Isaac JTR (2006) Transient incorporation of native GluR2-lacking AMPA receptors during hippocampal long-term potentiation. *Nat Neurosci* **9(5)**:602-604

Pouget A, Sejnowski TJ (1997) Spatial transformatons in the parietal cortex using basis functions. *J Cogn Neurosci* **9**:222-237

Ramcharan EJ, Gnadt JW, Sherman SM (2000) Burst and tonic firing in thalamic cells of unanesthetized, behaving monkeys. *Vis Neurosci* **17**:55– 62

Ranck J B (1973) Studies on single neurons in dorsal hippocampal formation and septum in unrestrained rats. I. Behavioral correlates and firing repertoires. *Exp Neurol*

41:461—531

Raymond CR, Redman SJ (2005) Spatial segregation of neuronal calcium signals encodes different forms of LTP in rat hippocampus. *J Physiol* **570**:97-111

Reichova I, Sherman SM (2004) Somatosensory corticothalamic projections: distinguishing drivers from modulators *J Neurophysiol* **92**:2185-2197

Reid CA, Dixon DB, Takahashi M, Bliss TVP, Fine A (2004) Optical quantal analysis indicates that long-term potentiation at single hippocampal mossy fiber synapses is expressed through increased release probability, recruitment of new release sites, and activation of silent synapses. *J Neurosci* **24**:3618–3626

Reinagel P, Godwin D, Sherman SM, Koch C (1999) Encoding of visual information by LGN bursts. *J Neurophysiol* **81**:2558 –2569

Remy S, Spruston N (2007) Dendritic spikes induce single-burst long-term potentiation. *Proc Natl Acad Sci U S A* **104**:17192–17197

Richter TA, Kolaj M, Renaud LP (2005) Low voltage-activated Ca^{2+} channels are coupled to Ca^{2+}-induced Ca^{2+} release in rat thalamic midline neurons. *J Neurosci* **25**:8267-8271

Robinson HPC, Sahara Y, Kawai N (1991) Nonstationary fluctuation analysis and direct resolution of single channel currents at postsynaptic sites. *Biophys J* **59**:295-304

Ronesi J, Lovinger DM (2005) Induction of striatal long-term synaptic depression by moderate frequency activation of cortical afferents in rat. *J Physiol* **562.1**:245-256

Rosanova M, Timofeev I (2005) Neuronal mechanism mediating the variability of somatosensory evoked potentials during sleep oscillation in cats. *J Physiol* **562.2**:569-582

Rosanova M, Ulrich D (2005) Pattern-specific associative long-term potentiation induced by a sleep spindle-related spike train. *J Neurosci* **25(41)**:9398-9405

Rose M (1935) Das Zwischenhirn des Kaninchens. *Mem Acad Pol Sci Ser B* **8**:1-108

Soto D, Coombs ID, Kelly L, Farrant M, Cull-Candy SG (2007) Stargazin attenuates intracellular polyamine block of calcium-permeable AMPA receptors. *Nat Neurosci* **10(10)**:1260-1267

Rouiller, EM, Welker E (2000) A comparative analysis of the morphology of corticothalamic projections in mammals. *Brain Res Bull* **53**:727–741

Rozov A, Burnashev N (1999) Polyamine-dependent facilitation of postsynaptic AMPA receptors counteracts paired-pulse depression. *Nature* **401**:594-598

Rozov A, Zilberter Y, Wollmuth LP, Burnashev N (1998) Facilitation of currents through rat Ca2+-permeable AMPA receptor channels by activity-dependent relief from polyamine block. *J Physiol* **511(Pt 2)**: 361–377

Rubin JE, Gerkin RC, Bi G-Q, Chow CC (2005) Calcium time course as a signal for spike-timing-dependent plasticity. *J Neurophysiol* **93**:2600-2613

Rubio-Garrido P, Pérez-de-Manzo F, Clascá F (2007) Calcium-binding proteins as markers of layer-I projecting vs. deep layer-projecting thalamocortical neurons: a

double-labeling analysis in the rat. *Neuroscience* **149**:242-250

Salinas E, Abbott LF (1995) Transfer of coded information from sensory to motor networks. *J Neurosci* **15**:6461-6474

Salt TE (1986) Mediation of thalamic sensory input by both NMDA receptors and non-NMDA receptors *Nature* **322(17)**:263-265

Sanchez-Vives MV, McCormick DA (2000) Cellular and network mechanisms of rhythmic recurrent activity in neocortex. *Nat Neurosci* **3**:1027-1034

Schiller J, Schiller Y, Stuart G, Sakmann B (1997) Calcium action potentials restricted to distal apical dendrites of rat neocortical pyramidal neurons. *J Physiol* **505**:605-616

Sherman SM (1996) Dual response modes in lateral geniculate neurons: mechanisms and functions. *Vis Neurosci* **13**:205-213

Sherman SM (2001) Tonic and burst firing: dual mode of thalamocortical relay.

Trends Neurosci **24**:122-126

Sherman SM (2005) Thalamic relays and cortical functioning. *Prog Brain Res* **149**:107-126

Sherman SM, Koch C (1986) The control of retinogeniculate transmission in the mammalian lateral geniculate nucleus. *Exp Brain Res* **63**:1-20

Sherman SM, Guillery RW (2002) The role of thalamus in the flow of information to cortex. *Philos Trans R Soc Lond (Biol)* **357**:1695–1708

Sherman S, Guillery RW (2004) Thalamus. In *"Synaptic Organization of The Brain"*. Shepherd GM., pp311-360. New York: Oxford University Press

Shin J, Shen F, and Huguenard J (2005) Polyamines modulate AMPA receptor dependent synaptic responses in immature layer V pyramidal neurons. *J Neurophysiol* **93**: 2634–2643

Shu Y, Hasenstaub A, Badoual M, Bal T, McCormick DA (2003) Barrages of synaptic activity control the gain and sensitivity of cortical neurons. *J Neurosci*

23(32):10388-10401

Sigworth FJ (1980) The variance of sodium current fluctuations at the node of Ranvier. *J Physiol* **307**:97-129

Sillito AM, Jones HE (2002) Corticothalamic interactions in the transfer of visual information. *Philos Trans R Soc Lond B Biol Sci* **357**:1739–1752

Silver RA, Cull-Candy SG, Takahashi T (1996) Non-NMDA glutamate receptor occupancy and open probability at a rat cerebellar synapse with single and multiple release sites. *J Physiol* **494.1**:231-250

Sjöström PJ, Turrigiano GG, Nelson SB (2001) Rate, timing, and cooperativity jointly determine cortical synaptic plasticity. *Neuron* **32**:1149–1164

Sjöström PJ, Turrigiano GG, Nelson SB (2003) Neocortical LTD via coincident activation of presynaptic NMDA and cannabinoid receptors. *Neuron* **39**:641-654

Smith TC, Wang L-Y, Howe JR (1999) Distinct kainate receptor phenotypes in

immature and mature mouse cerebellar granule cells. *J Physiol (Lond)* **517**:51–58

Smith TC,Wang L-Y,Howe JR (2000) Heterogeneous Conductance Levels of Native AMPA Receptors. *J Neurosci* **20(6)**:2073–2085

Sommer B, Köhler M, Sprengel R, Seeburg PH (1991) RNA editing in brain controls a determinant of ion flow in glutamate-gated channels. *Cell* **67**:11-19

Špacek J, Lieberman AR (1974) Ultrastructure and three-dimensional organization of synaptic glomeruli in rat somatosensory thalamus. *J Anat* **117**:487-516

Spruston N, Schiller Y, Stuart G, Sakmann B (1995) Activity-dependent action potential invasion and calcium influx into hippocampal CA1 dendrites. *Science* **268**:297–300

Stanton PK (1996) LTD, LTP, and the sliding threshold for long-term synaptic plasticity. *Hippocampus* **6**:35-42

Steriade (1993) Central core modulation of spontaneous oscillations and sensory

transmission in thalamocortical system. *Curr Opin Neurobiol* **3**:619-625

Steriade M. (2001) Impact of network activities on neuronal properties in corticothalamic systems. *J Neurophysiol* **86,** 1-39

Steriade (2006) Grouping of brain rhythms in corticothalamic systems. *Neuroscience* **137(4)**:1087-1106

Steriade M, Contreas D (1995) Relationship between cortical and thalamic cellular events during transition from sleep pattern to paroxysmal activity. *J Neurosci* **15**:623-642
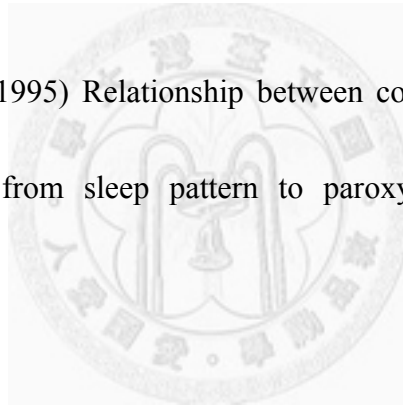
Steriade M, Datta S, Pare D, Okason G, Curro Dossi R (1990) Neuronal activity in brainstem cholinergic nuclei related to tonic activation process in thalamocortical system. *J Neurosci* **10**:2541-2559

Steriade M, Linas R (1988) The functional state of thalamus and associated neuronal interplay. *Physiol Rev* **68**:649-672

Steriade M, McCarley RW (1990) *Brainstem control of wakefulness and sleep.*

Plenum Press, New York

Steriade M, Paré D (2007) *Gating in neuronal networks*, pp. 1-26, 99-122. Cambridge

University Press, New York

Steriade M, Timofeev I (2003) Neuronal plasticity in thalamocortical networks during

sleep and waking oscillations. *Neuron* **37**:563-576

Stevens CF, Wang Y (1994) Changes in reliability of synaptic function as a

mechanism for plasticity. *Nature* **371**: 704–707
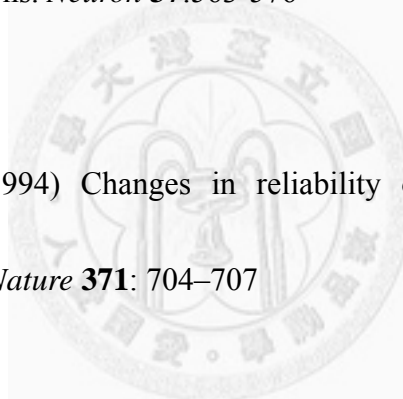
Stuart GJ, Häusser M. (2001) Dendritic coincidence detection of EPSPs and action

potentials. *Nat Neurosci* **4**:63-71

Sun YG, Beierlein M (2011) Receptor saturation controls short-term synaptic

plasticity at corticothalamic synapses. *J Neurophysiol* **105**: 2319-2329

Sun YG, Wu CS, Lu HC, Beierlein M (2011) Target-dependent control of synaptic inhibition by endocannabinoids in the thalamus. *J Neurosci* **31**: 9222-9230

Sutton MA, Ito HT, Cressy P, Kempf C, Woo JC, SchumanEM (2006) Miniature neurotransmission stabilizes synaptic function via tonic suppression of local dendritic protein synthesis. *Cell* **125**:785–799

Suzuki S, Rogawski MA (1989) T-type calcium channels mediate the transition between tonic and phasic firing in thalamic neurons. *Proc Natl Acad Sci USA* **86**:7228-7232
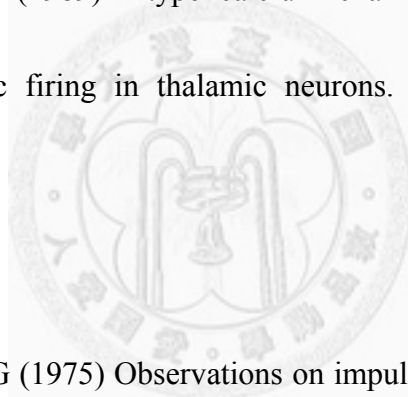
Swadlow HA, Waxman SG (1975) Observations on impulse conduction along central axons. *Proc Nat Acad Sci USA* **72(12)**:5156-5159

Swanson GT, Feldmeyer D, Kaneda M, Cull-Candy SG (1996) Effect of RNA editing and subunit co-assembly on single-channel properties of recombinant kainite receptors. *J Physiol* **492.1**:129-142

Swanson GT, Kamboj SK, Cull-Candy SG (1997) Single-channel properties of

recombinant AMPA receptors depend on RNA editing, splice variation, and subunit composition *J Neurosci* **17(1)**:58-69

Temereanca S, Simons DJ (2004) Functional topography of corticothalamic feedback enhances thalamic spatial response tuning in the somatosensory whisker/barrel system. *Neuron* **41**:639-651

Tenneigkeit F, Schwarz DWF, Puil E (1996) Mechanisms for signal transformation in lemniscal auditory thalamus. *J Neurophysiol* **76**:3597-3608

Thiagarajan TC, Lindskog M, Tsien RW (2005) Adaptation to synaptic inactivity in hippocampal neurons. *Neuron* **47**:725–737

Thomas MJ, Watabe AM, Moody TD, Makhinson M, O'Dell TJ (1998) Postsynaptic complex spike bursting enables the induction of LTP by θ frequency synaptic stimulation. *J Neurosci* **18**:7118 –7128

Timofeev I, Steriade M (1996) Low-frequency rhythms in the thalamus of intact-cortex and decorticated cats. *J Neurophysiol* **76**:4152-4168

Toth K, Suares G, Lawrence JJ, Philips-Tansey E, McBain CJ (2000) Differential mechanisms of transmission at three types of mossy fiber synapse. *J Neurosci* **20**:8279–8289

Tovee MJ, Rolls ET, Azzopardi P (1994) Translation invariance in the responses to faces of single neurons in the temporal visual cortical areas of the alert macaque. *J Neurophysiol* **72**:1049-1060

Traynelis SF, Jaramillo F (1998) Getting the most out of noise in the central nervous system. *TINS* **21(4)**:137-145
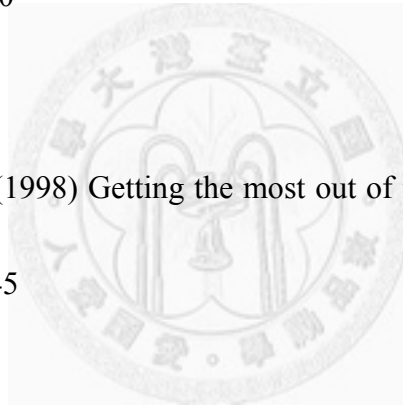
Traynelis SF, Silver RA, Cull-Candy SG (1993) Estimated conductance of glutamate receptor channels activated during EPSCs at the cerebellar mossy fiber-granule cell synapse. *Neuron* **11**:279-289

Tsumoto T, Creutzfeldt OD, Legendy CR (1978) Functional organization of the corticofugal system from visual cortex to lateral geniculate nucleus in the cat. *Exp Brain Res* **32**:345-364

Turner JP, Salt TE (1998) Characterization of sensory and corticothalamic excitatory inputs to rat thalamocortical neurons in vitro. *J Physiol* **510**:829-843

Tzounopoulos T, Kim Y, Oertel D, Trussell LO (2004) Cell-specific, spike timing-dependent plasticities in the dorsal cochlear nucleus. *Nat Neurosci* **7**:719 –725

Yu C, Derdikman D, Haidarliu S, Ahissar E (2006) Parallel thalamic pathways for whisking and touch signals in the rat. *PLoS Biology* **4(5)**:0819-0825

Ulrich D, Besseyrias V, Bettier B (2007) Functional mapping of GABA(B)-receptor subtypes in the thalamus. *J Neurophysiol* **98(6)**:3791-3795

Van der Loos H (1976) Barreloids in the mouse somatosensory. *Neurosci Lett* **2**:1-6.

Van Horn SC, Sherman SM (2004) Differences in projection patterns between large and small corticothalamic terminals. *J comp Neurol* **475**:406-415

Hartveit E, Veruki ML (2006) Studying properties of neurotransmitter receptors by

non-stationary noise analysis of spontaneous synaptic currents. *J Physiol* **547.3**:751-785

Hartveit E, Veruki ML (2007) Studying properties of neurotransmitter receptors by non-stationary noise analysis of spontaneous postsynaptic currents and agonist-evoked responses in outside-out patches. *Nat Protoc* **2(2)**:434-448

Veinante P, Deschênes M (1999) Single- and multi-whisker channels in the ascending projections from the principal trigeminal nucleus in the rat. *J Neurosci* **19**:5085-5095

Velazquez JLP, Carlen PL (1996) Development of firing patterns and electrical properties in neurons of the rat ventrobasal thalamus. *Dev Brain Res* **91:**164-170

Swadlow HA, GusevAG (2001) The impact of "bursting" thalamic impulses at a neocortical synapse. *Nat Neurosci* **4**:402– 408

Urban NN, Barrionuevo G (1996) Induction of Hebbian and non-Hebbian mossy fiber long-term potentiation by distinct patterns of high-frequency stimulation. *J Neurosci* **16**:4293– 4299

Walker HC, Lawrence JJ, McBain CJ (2002) Activation of kinetically distinct synaptic conductances on inhibitory interneurons by electrotonically overlapping afferents. *Neuron* **35**:161–171

Wang Y, Wu J, Rowan MJ, Anwyl R (1997a) Conditions for the induction of long-term potentiation and long-term depression by conjunctive pairing in the dentate gyrus in vitro. *J Neurophysiol* **78**:2569-2573

Wang Y, Wu J, Rowan MJ, Anwyl R (1997b) Induction of LTD in the dentate gyrus in vitro is NMDA receptor independent, but dependent on Ca^{2+} influx via low-threshold-activated-Ca^{2+} channels and release of Ca^{2+} from intracellular stores. *J Neurophysiol* **77**:812-825

Wang Y, Wu J, Rowan MJ, Anwyl R (1997c) LTP induction dependent on activation of Ni^{2+}-sensitive voltage-gated calcium channels, bit not NMDA receptors, in the rat dentate gyrus in vitro. *J Neurophysiol* **78**:2574-2581

Washburn MS, Dingledine R (1996) Block of

α-amino-3-hydroxy-5-methyl-4-isoxazolepropionic acid (AMPA) receptors by polyamines and polyamine toxins. *The Journal of pharmacology and experimental therapeutics* **278(2)**:669-678

Washburn MS, Numberger M, Zhang S, Dingledine R (1997) Differential dependence on GluR2 expression of three characteristic features of AMPA receptors. *J Neurosci* **17(24)**:9393-9406

Watanabe S, Kusama-Eguchi K, Kobayashi H, Igarashi K (1991) Estimation of polyamine binding to macromolecules and ATP in bovine lymphocytes and rat liver. *J Biol Chem* **266(31)**:20803-20809

Watt AJ, van Rossum MCW, MacLeod KM, Nelson SB, Turrigiano GG (2000) Activity coregulates quantal AMPA and NMDA currents at neocortical synapses. *Neuron* **26**:659–670

Weyand TG, Boudreaux M, Guido W (2001) Burst and tonic response modes in thalamic neurons during sleep and wakefulness. *J Neurophysiol* **85**:1107–1118

White G, Lovinger DM, Weight FF (1989) Transient low-threshold Ca^{2+} current triggers burst firing through an afterdepolarizing potential in an adult mammalian neuron. *Proc Natl Acad Sci USA* **86**:6802-6806

Whitney NP, Peng H, Erdmann NB, Tian C, Monaghan DT, Zheng JC (2008) Calcium-permeable AMPA receptors containing Q/R-unedited GluR2 direct human neural progenitor cell differentiation to neurons. *The FASEB Journal* **22**:2888-2900

Williams MN, Zahm DS, Jacquin MF (1994) Differential foci and synaptic organization of the principal and spinal trigeminal projections to the thalamus in the rat. *Eur J Neurosci* **6**:429–453
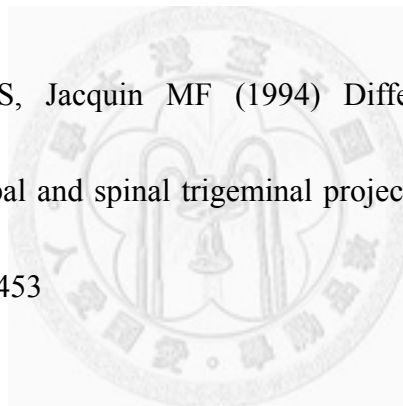
Williams SR, Stuart GJ (1999) Mechanisms and consequences of action potential burst firing in rat neocortical pyramidal neurons. *J Physiol* **521**:467–482

Williams SR, Stuart GJ (2000) Action potential backpropagation and somato-dendritic distribution of ion channels in thalamocortical neurons. *J Neurosci* **20(4)**: 1307-1317

Williams ST, Stuart GJ (2002) Dependence of EPSP efficacy on synapse location in

neocortical pyramidal neurons. *Science* **295**:1907-1910

Wilson RI, Nicoll RA (2001) Endogenous cannabinoids mediate retrograde signaling at hippocampal synapses. *Nature* **410**:588-592

Wiltgen BJ, Royle GA, Gray EE, Abdipranoto A, Thangthaeng N, Jacobs N, Saab F, Tonegawa S, Heinemann SF, O'Dell TJ, Fanselow MS, Vissel B (2010) A Role for Calcium-Permeable AMPA Receptors in Synaptic Plasticity and Learning. *PLoS ONE* **5(9)**: e12818.

Wisden W, Seeburg PH (1993) Mammalian ionotropic glutamate receptors. *Curr Opin Neurobiol* **3**:291-298

Wittenberg GM, Wang SS-H (2006) Malleability of spike-timing-dependent plasticity at the CA3-CA1 synapse. *J Neurosci* **26**:6610-6617

Wolfart J, Debay D, Le Masson G, Destexhe A, Bal T (2005) Synaptic background activity controls spike transfer from thalamus to cortex. *Nat Neurosci* **8**:1760-1767

Woolsey TA, Van der Loos H (1970) The structural organization of layer IV in the somatosensory region (SI) of mouse cerebral cortex. The description of a cortical field composed of discrete cytoarchitectonic units. *Brain Res* **17**:205-242

Wu J, Rush A, Rowan MJ, Anwyl R (2001) NMDA receptor- and metabotropic glutamate receptor-dependent synaptic plasticity induced by high frequency stimulation in the rat dentate gyrus in vitro. *J Physiol* **533:**745-755

Yu C, Derdikman D, Haidarliu S, Ahissar E (2006) Parallel thalamic pathways for whisking and touch signals in the rat. *PLoS Biology* **4(5)**:819-825

Zalutsky RT, Nicoll RA (1990) Comparison of two forms of long-term potentiation in single hippocampal neurons *Science* **248**:1619–1624

Zhan XJ, Cox CL, Sherman SM (2000) Dendritic depolarization efficiently attenuates low-threshold calcium spikes in thalamic relay cells. *J Neurosci* **20**:3909-3914

Zhang X, Davidson S, Giesler Jr GJ (2006) Thermally identified subgroups of marginal zone neurons project to distinct regions of the ventral posterior lateral

nucleus in rats *J Neurosci* **26(19):**5215-5223

Zhang F, Gradinaru V, Adamantidis AR, Durand R, Airan RD, de Lecea L, Deisseroth K (2010) Optogenetic interrogation of neural circuits: technology for probing mammalian brain structures. *Nat Protoc* **5(3)**:439-456

Zhao J-P, Phillips MA, Constantine-Paton M (2006) Long-term potentiation in the juvenile superior colliculus requires simultaneous activation of NMDA receptors and L-type Ca^{2+} channels and reflects addition of newly functional synapses. *J Neurosci* **26(49)**:12647-12655
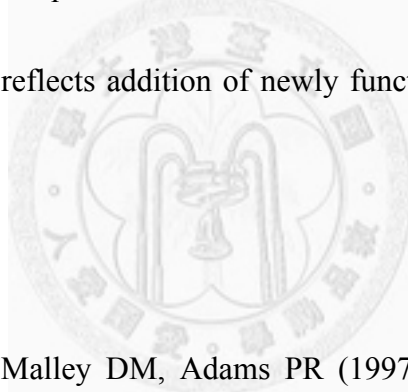
Zhou Q, Godwin DW, O'Malley DM, Adams PR (1997) Visualization of calcium influx through channels that shape the burst and tonic firing modes of thalamic relay neurons. *J Neurophysiol* **77**:2816-2825

Zhu L, Blethyn KL, Cope DW, Tsomaia V, Crunelli V, Hughes SW (2006) Nucleus- and species-specific properties of the slow (<1 Hz) sleep oscillation in thalamocortical neurons. *Neuroscience* **141**:621–636

Zucker RS (1989) Short-term synaptic plasticity. *Annu Rev Neurosci* **12**:13-31

Zucker RS (1999) Calcium- and activity-dependent synaptic plasticity. *Curr Opin Neurobiol* **9**:305-313

Appendix

List of Abbreviations

ACSF   artificial cerebrospinal fluid

ADP   afterdepolarization

AHP   after-hyperpolarization

AMPAR α-amino-3-hydroxyl-5-methyl-isoxazolepropionic acid

       receptor

bAP   back-propagating action potential

CA   Cornu Ammonis (denoting subfield of hippocampus)

CaP-AMPAR   calcium-permeable AMPA receptor

CO   cytochrome oxidase

CT   corticothalamic (as an adjective)

CV   coefficient of variation

EPSC   excitatory postsynaptic current

EPSP   excitatory postsynaptic potential

GABA γ-aminobutyric acid

HCN   hyperpolarization-activated cyclic nucleotide-gated cationic

	channel
HTB	high-threshold burst
ic	internal capsule
I$_h$	hyperpolarization-activated nonselective cationic current
IPSC	inhibitory postsynaptic current
LGN	lateral geniculate nucleus of thalamus
LTD	long-term depression
LTP	long-term potentiation
LTS	low-threshold spike
MF	mossy fiber (the fibers projecting from granule cells of
	dentate gyrus to CA3 of hippocampus)
mGluR	metabotropic glutamate receptor
ML	medial lemniscal (as an adjective)
ml	medial lemniscus (as a noun)
NMDAR	*N*-methyl-D-aspartate receptor
non-REM	non-rapid eye movement (sleep)
POm	medial portion of posterior complex of thalamus (posterior
	thalamic nuclear group)
PPD	paired-pulse depression

PPF	paired-pulse facilitation
PPR	paired-pulse ratio
PrV	principal trigeminal nucleus (pincipalis)
Rt	reticular nucleus of thalamus
S1	primary somatosensory cortex
S2	secondary somatosensory cortex
SD	Sprague- Dawley (strain name of rats)
SF	Schaefer-collateral fiber
SpV	spinal trigeminal nucleus
SpVc	caudal subnucleus of SpV (caudalis)
SpVo	oral subnucleus of SpV (oralis)
SpVi	interpolar subnucleus of SpV (interpolaris)
SpVic	interpolar subnucleus of SpV, caudal territory
SpVir	interpolar subnucleus of SpV, rostral territory
STDP	spike-timing-dependent plasticity
VBN	ventrobasal nucleus of thalamus
VGCC	voltage-gated calcium channel
VPI	ventral posterior inferior nucleus of thalamus
VPL	ventral posterior lateral nucleus of thalamus

VPM   ventral posterior medial nucleus of thalamus

VPMc   core subdivision of the barreloid in VPMdm

VPMdm   dorsal medial division of VPM ("core" compartment)

VPMvl   ventral lateral division of VPM ("tail" compartment)

VPMh   head subdivision of the barreloid in VPMdm

VPPC   parvocellular part of ventral posterior nucleus of thalamus

VMb   basal ventral medial nucleus of thalamus

List of Pharmacological Agents

APV   DL-2-Amino-5-phosphonopentanoic acid

BAPTA   1,2-bis(o-aminophenoxy)ethane-N,N,N',N'-tetraacetic acid

DAB   3,3'-diaminobenzidine

DNQX   6,7-dinitroquinoxaline-2,3-dione

glycine   glycine

PTX   picrotoxin

mibefradil   mibefradil

NAS   1-naphthylacetyl spermine

Ni^{2+} nickel (in the form of chloride salt)

Nim   nimodipine

PhTx-433   philanthotoxin-433 tris(trifluoroacetate) salt

QX-314   *N*-2,6-Dimethylphenylcarbamoylmethyl triethylammonium

                bromide

strychnine   strychnine

Trans-ACPD   (±)-1-aminocyclopentane-trans-1,3-dicarboxylic acid